

THE SPATIAL DEGREE OF CHEMICAL EQUILIBRIUM IN
SOME HIGH GRADE METAMORPHIC ROCKS

by

WILLIAM HOWARD BLACKBURN, Jr.

B.Sc. (HONORS), St. Francis Xavier University
(1964)

SUBMITTED IN PARTIAL FULFILLMENT
OF THE REQUIREMENTS FOR THE
DEGREE OF DOCTOR OF
PHILOSOPHY

at the

MASSACHUSETTS INSTITUTE OF
TECHNOLOGY

August, 1967

Signature of Author

Department of Geology and Geophysics,

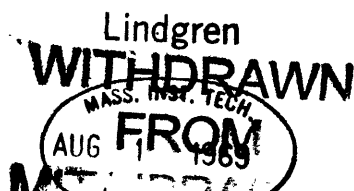
August 11, 1967

Certified by

Thesis Supervisor

Accepted by

Chairman, Departmental Committee
on Graduate Students



THE SPATIAL DEGREE OF CHEMICAL EQUILIBRIUM IN SOME HIGH
GRADE METAMORPHIC ROCKS

William Howard Blackburn, Jr.

Massachusetts Institute of Technology
Cambridge, Massachusetts

Submitted to the Department of Geology and Geophysics in August, 1967, in partial fulfillment of the requirements for the degree of Doctor of Philosophy.

ABSTRACT

Granulite facies rocks from the Grenville in the area of Ganonoque, Ontario have been studied with respect to the equilibration of several elements between garnet and biotite. These studies show that chemical equilibrium is closely approached for Mn, Co, Cr and Ni. The distribution of Fe and Mg between garnet and biotite was found to be dependent on the ratio FeO/MgO and the total CaO content of the rock. These chemical variations in the rock are reflected in the cordierite modal values.

Detailed investigations were made on the garnets of a garnet-cordierite-biotite gneiss. These investigations included grain size measurements, intergarnet distance measurements and laser microprobe determinations of Fe, Mg, Mn and Ca in the garnets. Conclusions are reached as to nucleation and growth rates of the garnets and to the volumes over which free diffusion and chemical equilibrium with respect to the elements studied took place. These volumes were found to be on the order of a few centimeters and their shapes are highly controlled by rock structures such as foliation and lineation.

A higher grade pyroxene granulite rock was also investigated with respect to garnet and biotite equilibrium. Somewhat larger volumes were noted and biotite seems to equilibrate more easily than garnet.

Thoughts are given on sampling in metamorphic rocks, the scatter in distribution diagrams and the formation of granites by large scale diffusion.

Thesis Supervisor: William H. Dennen
Title: Associate Professor of Geology

PART ONE
(Condensed from Part Two)

1. INTRODUCTION

In recent years, several workers have examined the chemical equilibration of coexisting minerals in metamorphic rocks with varying degrees of success (Kretz, 1959, 1960, 1961, 1964; Mueller, 1961, 1962; Moxham, 1965, Wynne-Edwards and Hay, 1963; Krank, 1959, 1961; Phinney, 1959, 1963; Moore, 1960). These attempts to define equilibrium relations followed two basic assumptions. First, it was assumed that the coexisting minerals were in internal equilibrium, i.e., that the minerals were not chemically or physically zoned although this may be handled in a detailed study (Hollister, 1966; Albee, Chodos and Hollister, 1966). Second, the sample from which the mineral grains were separated was in local equilibrium or the sample must be within that volume over which the same conditions of temperature and pressure have prevailed and chemical communication between grains is evident. Kretz, (1960) has summed up the second criterion:

"...it is important to consider the size of natural chemical systems (thermodynamic). Spheres of chemical communication may be different in size with reference to different elements depending on their mobility and may vary in size as a function of temperature."

It is obvious that difficulties might arise if sampling does not take place within equilibration domains, and it is proposed here that many of the problems found in the analysis of metamorphic minerals are due to sampling without regard to the dimensions of the domain of local equilibration. Phinney's study of the rocks from St. Paul Island and Money Point, Nova Scotia (Phinney, 1959, 1963) is a case in point.

The primary purpose of this study is to determine the dimensions and shapes of the volumes or domains of equilibration with respect to coexisting phases in a rock of a specific grade of metamorphism. This is a two stage

problem which may be best attacked by first ascertaining the fact of equilibrium among coexisting phases in a region where specimens are believed to have undergone the same grade of metamorphism. Next, the dimensions of the equilibrium domains may be worked out by examination of the compositions of minerals within a single specimen.

2. GEOLOGICAL AREA OF INVESTIGATION

In selecting an area for metamorphic equilibrium studies, the author has endeavored to find a regionally metamorphosed terrain of great age which has most likely been influenced by more than one regime of metamorphism. This would seem to afford the most favorable conditions for the attainment of chemical equilibrium between coexisting minerals. After searching through the literature, the area selected as being most appropriate for the present study was that of the Ganonoque-Westport region of Ontario. See Figure 4, Part Two.

The bedrock formations underlying the Ganonoque area are of Precambrian and Paleozoic ages (Wynne-Edwards, 1959, 1962; Hewitt, 1964). Approximately 80 percent of the area is Precambrian rock consisting of basic and acid volcanics and metasedimentary rocks intruded by acid and basic plutonics. Age determinations indicate that the period of orogeny, the Grenville, affected the whole of the Precambrian area (Krogh, 1964). Geologically, the region is referred to as the Frontenac Axis; being that belt which joins the Adirondack Highlands to the main Grenville body.

Garnet, garnet-cordierite, and cordierite gneisses form units varying from six inches to several hundred feet in thickness within layered quartz-biotite-feldspar gneisses. The units are continuous and have been used as marker horizons for mapping purposes (Wynne-Edwards, 1959). The mineral assemblages recorded in some of the pelitic rocks of the eastern part of the area are listed below (Wynne-Edwards, 1962; Wynne-Edwards and Hay, 1963). In all of these, Quartz and either perthite or plagioclase plus potash feldspar are also present:

1. cordierite+sillimanite+biotite
2. cordierite+garnet+sillimanite+biotite
3. cordierite+garnet+biotite
4. cordierite+biotite
5. garnet+sillimanite+biotite
6. garnet+biotite

7. biotite

In the southwestern part of the area, the rocks contain abundant hypersthene and only minor biotite (Wynne-Edwards, 1959) and have attained the pyroxene-granulite facies. The cordierite bearing gneisses described above might be classified as belonging to the cordierite-amphibolite facies of Abukuma-type metamorphism (Winkler, 1965) or transitional between amphibolite facies and granulite facies rocks (Wynne-Edwards and Hay, 1963). de Waard, however, proposes that the cordierite-garnet assemblages found in the Ganonoque region, and many other localities, should be established as the biotite-cordierite-almandite subfacies of the hornblende granulite facies. From observations made during this study, this concept seems most likely and will be retained throughout this paper.

Petrography of the samples.

From the 43 specimens collected, 30 which appeared unaltered throughout were selected for detailed examination. Thin sections were prepared for a close check on the suitability of these samples and examination of the thin sections further limited the number of specimens to 23. Figure 4, Part Two shows collection localities for the samples used in this study.

Nearly all of the thin sections showed small amounts of chlorite or sericite replacing various minerals. For the most part, however, alteration was limited to the cordierite with some local alteration of the plagioclase. Retrogression of the other minerals in the assemblages present was essentially negligible in the samples chosen for further study.

The 23 samples selected were subjected to modal analysis (See Tables 1 and 11, Part Two.) and the seven best specimens retained for the study of the spatial extent of local equilibration.

Chemical Composition of the Gneisses

Whole-rock spectrochemical analyses of the metasediments used in this study were made (Table 4, Part Two). The analytic procedure was a method of mutual standardization modified after Dennen and Fowler, (1955).

The standard rocks G-1 and W-1 (Fairbairn and others, 1951) along with GR (Roubault et al., 1966) and SR (Webber, 1965) were used as standards for the analyses. Excitation parameters are given in Table 2, Part Two. An examination of this method with respect to precision and accuracy was made by the analysis of rock standards. The data from this study is given in Table 3, Part Two.

3. ELEMENT FRACTIONATION BETWEEN COEXISTANT MINERALS

Chemical Determinations

16 specimens were selected for mineral analysis and were subjected to the following process: Each sample was cut into a cube, about 4.5 cm. on a side, which removed any weathered exterior and reduced the sample to a size over which local equilibration seems to take place (Kretz, 1959; Moxham, 1965); the sample was then fed through a jaw crusher with the second pass giving a product about one-quarter inch in size; this material was then crushed in a hand percussion mortar of the type described by Wager and Brown (1960) and the screened fractions -60, +100; -100, +200 were run through routine heavy liquid and magnetic separations.

All of the mineral separates were checked under the petrographic microscope in a liquid whose index of refraction was close to that of the mineral in question. Because of very fine inclusions of quartz and sillimanite in some of the garnets, some of these samples may contain over 2% total quartz and sillimanite. Impurities in the biotite were tiny inclusions of ilmenite, quartz and and zircon, their total not exceeding 2% in any sample.

The garnets and biotites were analyzed in at least two replicates by means of atomic absorption spectrophotometry. Partial analyses for Fe, Mg, Mn, Ca, Cr, Co, and Ni were made using, for the most part, standard techniques as described in the literature (Slavin, 1965; Trent and Slavin, 1964).

Standards for Fe, Mn, Ca, Cr, Co, and Ni were pure salt solutions made by dissolving high purity compounds of the element in 2N HCl, evaporating to dryness and and redissolving in 0.2N HCl. Standards for most elements were made in two different ways for cross-checking purposes. As a result of this, matrix effects were found to be negligible, if at all present.

Chemical and statistical data, derived from this work, on standard rocks and minerals are given in Table 6, Part

Two. Except where indicated, the following summarizes the the statistical terminology used:

- n, number of observations
- \bar{x} , arithmetic mean
- d, deviation of an observation from the mean
- s, standard deviation = $\pm \sqrt{d^2/n-1}$
- C, Coefficient of Variation = $(s/\bar{x})100$

The determination of FeO in the garnet and biotite samples was performed using the titration method of Reichen and Fahey (1962). The dissolution of the sample took place in the presence of $K_2Cr_2O_7$ with the excess dichromate being titrated with a standard solution of ferrous ammonium sulphate.

Analytic Results

As described above, 16 specimens of Grenville gneiss were selected for mineral analysis. The results of the chemical determinations made on the garnet and biotite of these samples are given in Tables 8 and 9, Part Two.

Judging from the studies of previous workers, the elements Fe, Mg, Mn, Cr, V, Ni, and Co seem to equilibrate most easily and correlate very closely to what should be expected from crystal field theory as discussed by Curtis (1964). It was decided then to use atomic ratios as the measure of concentration in this study. The calculation of these ratios is as follows:

In garnet, the measure of concentration of divalent elements is the atomic ratio, total number of atoms of the element/total number of 8-coordinated positions minus the positions occupied by Ca atoms.

In biotite, the measure of concentration of divalent elements is the total number of atoms of the element/the total number of 6-coordinated positions occupied by the divalent elements Fe^{+2} , Mg, Mn plus those positions occupied by Fe^{+3} .

Moxham points out the use of calculating the proportion of atomic sites filled by a minor element

out of the number of sites available to that element. Calculations were then performed producing the atomic ratios of the trace elements in question (Cr, Co, Ni) with the following substitutions in mind:

1. In biotite 6-coordinated positions- Cr,Co; Ni
2. In garnet 8-coordinated positions - Cr, Co, Ni

Distribution of Elements between Garnet and Biotite

Some data relating to the chemistry of the gneisses of the Ganonoque-Westport area has been published (Wynne-Edwards and Hay, 1963). For most elements, however, they had too little evidence to draw conclusions as to the extent of equilibrium in these rocks. The determinations made on the 15 samples of this study are combined with the data of Wynne-Edwards and Hay and presented graphically below. In some cases, i.e., the distribution of Ni between garnet and biotite, the combined data provides information not available in their study.

The distribution diagrams employed here are similar to those used by Kretz, (1959) and Wynne-Edwards and Hay (1963) so that a direct comparison may be made. Data taken from their paper is shown in Figure 10.

The principles involved in the application of chemical phase theory to coexisting minerals has been discussed in detail by Ramberg and Devore (1951), Kretz (1959,1961), Mueller (1960, 1961) and McIntire (1958, 1963) and need only be stated briefly here.

It has been shown that at constant temperature and pressure, the chemical potential of a component in a phase is a function of the concentration of the component, and in the case of non-ideal crystals, the chemical potential may also be a function of other chemical conditions within the crystal. If the chemical potential of a component in two coexisting phases is dependent only on concentration, then the component must be regularly partitioned between the two phases providing that equilibrium conditions exist.

The relationship between the chemical potential and the concentration of any chemical species in a phase, e.g.,

A in phase α , is

$$\mu_A^\alpha = \mu_A^{*\alpha} + RT \ln f_A^\alpha X_A^\alpha$$

where μ_A is the chemical potential of A in phase α , $\mu_A^{*\alpha}$ is the chemical potential of A in phase α in some standard state, i.e., in the pure phase AY or AZ at the same temperature and pressure, R is the gas constant ,T is the absolute temperature and f_A^α is the activity coefficient of A. The composition of the phase α with respect to A is indicated by the atomic or molecular ratio X_A^α where $X_A^\alpha = A/A+B$.

In phase β , an analogous equation may be set up,

$$\mu_A^\beta = \mu_A^{*\beta} + RT \ln f_A^\beta X_A^\beta$$

and at equilibrium

$$\mu_A^\alpha = \mu_A^\beta$$

then

$$X_A^\alpha / X_A^\beta = f_A^\beta / f_A^\alpha \exp((\mu_A^{*\beta} - \mu_A^{*\alpha}) / RT) = K_D$$

where K_D denotes the distribution coefficient. If the element in question is in ideal solution, the concentration of the element in one phase plotted against the concentration of the element in the coexisting phase will define a curve, the distribution curve. This curve will be a straight line of unit slope or will be symmetrical about such a line if the element forms ideal solutions in both phases. If the element does not form ideal mixtures, the curve will be irregular although at low concentrations the curve becomes a straight line which passes through the origin (Nernst's Law). K_D is then equal to the slope of the distribution curve.

The distribution of Fe^{+2} is shown in Figure 12, Part Two. The data , although showing a possible regular distribution, is quite scattered. This is in accordance with the observations of Wynne-Edwards and Hay (1963) and Kretz, (1959). Kretz observed a correlation between the distribution of Fe and Mg between garnet and biotite and the Mn content of the garnet and was able to assign various dis-

tribution coefficients on this basis. No such chemical chemical correlation was observed in this study. There is however, an inverse relation between the distribution coefficient $K_{Fe}^{Gar/Bio}$ and the modal ratio cordierite/cordierite+garnet+biotite. The various groupings are more easily recognized by plotting the molecular ratio FeO/MgO for garnet vs. the same ratio for biotite (Figure 12A, Part Two). Three reasonably distinct groups of distribution coefficients may then be noted according to the amount of cordierite present..

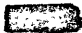
The manganese distribution between garnet and biotite is shown in Figure 14. A much greater range of atomic ratio values is present here and *altho* there is considerable scatter, a regular distribution is obvious. The distribution coefficient $K_{Mn}^{Bio/Gar} = 22$ as compared to the value of 30 obtained by Kretz. Kretz also states that the Mn distribution between garnet and biotite in the rocks of southwestern Quebec was controlled by the Fe/Mg ratio of the garnet as well as T and P. This relationship was not noted here. It is interesting to note also that there is no correlation with the distribution found by Wynne-Edwards and Hay (1963), who state that at this grade of metamorphism, garnet reaches saturation with respect to Mn at 2.3% spessartite molecule. This study finds acceptance of the spessartite molecule in garnet up to at least 5 percent.

The chromium distribution between garnet and biotite is shown in Figure 15, Part Two. The data points, although somewhat scattered, show a fairly regular distribution curve with slope of about 0.60. This would ^{indicate} an affinity of Cr for the biotite structure as opposed to garnet. In this light, it is possible that part of the chromium substitutes for aluminum in the 4-fold coordination position. This correlation might be exposed if the Al concentration in biotite and garnet were known. However, Moxham, (1965) finds, in a study of the distribution of Cr between biotite and hornblende, that data scatter is enhanced if Cr is assumed to substitute in the tetrahedral position. The

data from Wynne-Edwards and Hay, (1963) shows only one sample, (WE-4-58) with a distribution of Cr similar to that found in this study. The other samples exhibit a much stronger partition Cr to the biotite phase.

The distribution of cobalt between garnet and biotite is illustrated in Figure 16, Part Two. The distribution is quite regular and the distribution coefficient $K_{Co}^{Bio/Gar} = 0.40$ is in good agreement with data from Wynne-Edwards and Hay, (1963).

The distribution of nickel between garnet and biotite is shown in Figure 17, Part Two. Although the greater number of samples show a regular curvilinear distribution, the combination of data from Wynne-Edwards and Hay, (1963) indicate the possibility of two further distributions indicated by dashed lines in Figure 17, Part Two. An expected coherence with data for Co, Fe^{+2} and Mg, all of similar size is not observed and the reason for the various distributions is at present unknown.

The data of the this study and that of Kretz, (1959,1961) Wynne-Edwards and Hay, (1963), Phinney, (1959) and others who have attempted to define equilibrium distributions for various elements, commonly show a considerable scatter and indication of non-equilibrium. However, Zen, (1963) has shown that even  a textural and mineralogical standpoint, most metamorphic rocks are in equilibrium even at much lower grades than the rocks of this study have undergone. The following possibilities may be the cause of the distribution irregularities:

1. Lack of chemical equilibrium in the rock system
2. Poor precision and accuracy of chemical determinations
3. Lack of knowledge of all the variables in the chemical system
4. Samples taken do not reflect a single region or domain of chemical communication and equilibrium, or a statistically significant number of these domains if they are small.

The first of these possibilities may be eliminated because both texture and mineralogy are consistent with

thermodynamic equilibrium in metamorphic rocks as defined by Eskola, (1915), Fyfe, Turner and Verhoogen, (1960) and others.

The second, though still a possibility, is highly unlikely because many workers using different analytic techniques all encounter the same difficulties with respect to the equilibration of major and sometimes minor elements.

The third possibility is a serious problem for equilibration studies. Some of the parameters of metamorphism are cryptic, and to decipher many of the variables in a chemical study of metamorphic rocks, it is necessary to "plot everything against everything." It is usually possible, however, to get good chemical control on the system although this does not eliminate the scatter within the assigned ranges of variability, (Kretz, 1959; this study).

The fundamental problem may be in the fourth possibility listed above. The size of natural chemical systems in rocks is usually an unknown quantity. Local equilibrium is certainly established within a specific rock under the conditions imposed upon it. However, indication of this equilibrium may be lost by irregularities in the distribution functions if sampling is not performed with this possibility in mind.

Throughout the literature, there has been vague and sketchy mention of the size of the domains of local equilibration (Harker, 1939; Kretz, 1960; Moxham, 1965; Phinney, 1959, 1963). Workers in the field of metamorphic equilibration studies strive to collect and use small samples, 4-5 cm. in each direction, to insure "local equilibrium conditions," Moxham (1965). This attitude was taken in the present study and as in Kretz's 1959 paper, the poor quality of the distributions was still evident. In this light, Moxham (1965), in a study of element distributions between coexisting hornblendes and biotites, found that certain elements showed a definite distribution, whereas others just approached equilibrium distribution and some did not seem to approach equilibrium at all. It may be, however,

that in the investigation of the volumes of equilibration, the elements which show very little regularity on a large scale may exhibit a regularity within a small domain.

Phinney (1959, 1963) found a correlation between the FeO/MgO ratios and the garnet to staurolite ratios in the rocks from St. Paul Island and Money Point, Nova Scotia. He attributed this [REDACTED] regularity to the small scale of diffusion of Fe and Mg during metamorphism. Checking his theory, he hand-picked biotite grains from several thin sections noting the position of the grains picked. The grains exhibited a distinctive Fe/Mg ratio when analyzed spectrographically. Phinney found that the samples with a homogeneous texture showed similar compositions for all biotite grains, whereas in the less homogeneous rocks, biotite grains showed similar compositions over a distance of a few millimeters.

Similar observations have been made by Harker (1893, 1939) in thermally metamorphosed limestones, by Hagner, Leung and Dennison (1965), in mafic silicates of a single pyroxene amphibolite specimen, by Kretz (1966) in Australian biotite-muscovite-garnet gneisses and by Albee, Chodos and Hollister (1966).

Thus the problem remains of assigning a specific volume of equilibration to a particular phase with respect to a particular element under certain conditions of metamorphism.

4. A STUDY OF THE EXTENT OF LOCAL EQUILIBRATION

Description of the Samples.

Two samples were selected for the study of the shape and size of equilibration domains. The selection was made of the basis of:

1. Sufficient garnet and biotite for analytic purposes.
2. Lack of retrogression of garnet and biotite.
3. Possession of typical assemblages for the gneisses of the Ganonoque area.
4. Rocks with two different grades of metamorphism were chosen to see the effect of grade on the size of the domain of chemical communication.
5. Possession of distinct micro-structures, since it is possible that diffusion may be largely controlled by structural phenomena such as foliation and lineation.

The samples selected for this intensive study included a strongly foliated biotite-garnet-cordierite gneiss (no. 17) and a pyroxene-garnet gneiss (no. 42) with a less distinct foliation. Modal analyses for these rocks are given in Table 11, Part Two.

Sample 17 is a medium grained, highly foliated gneiss with quartz, K-feldspar, garnet, biotite and cordierite as major component minerals. Microscopically, the rock exhibits an extremely well developed foliation with foliation planes populated with biotite, sillimanite, garnet and cordierite grains for the most part. A section perpendicular to the foliation exhibits severely elongated garnets in the foliation plane. Some of these elongated garnets contain sillimanite needles which continue uninterrupted through the garnet. The elongated garnets also have local inclusions of quartz, K-feldspar and biotite; the biotite inclusions, like those of sillimanite, retain their orientation with respect to foliation and lineation. The elongated garnets are mantled by cordierite and K-feldspar.

Sample 42 exhibits a well developed layering in outcrop but foliation is not distinct in hand specimen due to the lack of platy minerals. The major phase constituents

are quartz, K-feldspar, plagioclase, orthopyroxene and garnet.

Garnet occurs as small rounded grains with sparse inclusions of quartz. Biotite is a minor constituent of the rock and occurs as small ragged, unaltered grains scattered throughout the gneiss but concentrated in pyroxene-garnet-biotite layers.

Grain Size Analysis and Intergrain Distance Measurements.

The sizes and distribution of mineral grains in metamorphic rocks are needed for a full understanding of the physico-chemical processes affecting their nucleation and growth. Data on the size distributions of garnet grains has been presented by (Galwey and Jones, 1963; Jones and Galwey, 1964 and Kretz, 1965). The distributions observed here will be compared to those works and an attempt will be made to decipher the growth of garnet grains in the rocks studied.

The original specimen of Sample 17, measuring 9.0 X 7.5 X 7.3 cm., was trimmed with a diamond saw to remove any weathered rind. Surfaces were cut, one parallel to (17II) and one perpendicular to (17I) the foliation and these thick slices were in turn cut into slabs of roughly the dimensions of a petrographic slide. The slabs thus formed were cemented to petrographic glass slides and the top surface ground parallel to the glass base. Grinding was performed on a lap using 400 mesh alumina.

A micrometer grinder, capable of allowing the accurate removal of down to $1/1000$ of an inch, was constructed as an adaptation of one used at Iowa State University for the study of oörites (Donald L. Biggs, personal communication, 1966).

With the use of a binocular microscope, the centers of all garnets exposed were traced on a transparent overlay, the coordinates of their centers determined, and the apparent grain size diameter measured by means of an ocular micrometer. Following spectrochemical analyses of the exposed garnets with a laser microprobe as described below,

the specimen was ground parallel to the initial surface to remove a layer of determined thickness (average = 0.25 m.m.) and the coordinates and apparent diameters measured again. This process was repeated until enough grains to delimit a significant population both chemical and physical, was measured (a total of 9 times). True grain diameters could thus be obtained for most grains intersected at least twice, but due to the odd shape of a great number of the garnets some size parameters has to be estimated. The sizes of about 2% of the garnets measured are by estimates on one or more axes.

Grain Size Distribution of Garnet in Specimen 17

The garnet grains range in shape from roughly spherical to ellipsoidal. Hence, it was possible to calculate the grain volume distribution using the equation,

$$\text{Volume} = \frac{d_1 d_2 d_3}{6}$$

thereby converting diameters measured to volume. A summary of grain size measurements is shown in Table 12, Part Two.

The grain size distribution was found to be bimodal as shown in Figure 20, Part Two. The volume of the garnet grains in the section perpendicular to the foliation range from 0.024 to 38.59 m.m.³ with a bimodal distribution of volumes as shown in Figure 21, Part Two. All the distributions show a strong positive skewness. In this light, it should be noted that it is possible that some of the smallest grains were not sectioned during the grinding and measuring sequence. However, this would not be expected to effect the overall distribution of garnet sizes significantly.

The distributions of the long, intermediate and short axes of the garnets in section 17 II, cut parallel to the foliation, are shown in Figure 22, Part Two. Although it might be expected, the prominent bimodal character of section 17 I does not show up here. This is possibly explained by the fact that section 17 II exhibits garnets through only one foliation surface while section 17 II affords

observation of garnets throughout the complete section of the sample. It is certainly possible that different nucleation and growth rates might have occurred in different foliation laminae.

The distribution of diameter magnitudes of garnets in section 17 II shows a positive skewness although this is not nearly as marked as in the section perpendicular to the foliation. The distribution of garnet volumes in this section, Figure 23, Part Two, however, does show a similar strong positive skewness as do the garnet volumes of section 17 I.

Intergrain Distance Measurements

The coordinates of the centers of all garnet grains were noted as a routine step in the determinations of apparent diameters. It was then possible to calculate the distance to the nearest grain and test the randomness of distribution of garnets in the two specimens.

The centers of garnet grains in the slabs may be considered points in a plane and the departure of the distribution from randomness may then be determined by measuring the distance to the nearest neighbor for each grain (Clark and Evans, 1954). The value R may range from 0 for a distribution with maximum aggregation to unity for a random distribution, to 2.1491 for a distribution as evenly and widely spaced as possible.

The values R , computed both for the grain distribution, parallel to an perpendicular to the foliation, are only slightly less than λ^{UNITY} (~ 0.93). We may then infer that the distribution of garnets in specimen 17 is very nearly random with a possible slight aggregation. This is in good agreement with macroscopic observation of these sections in which the garnets appear to locally aggregate in trains in the lineation direction.

Analysis of Garnets in Matrix

The selection of an analytic system for the investigation of the chemistry of many garnets distributed over a sizable area was of fundamental concern for this study. The electron micro-analyzer is, for many elements, a precise and accurate tool but handles only very small samples which would not be satisfactory in a program such as this where the garnets were studied with respect to size and distribution as well as chemistry. Further, an electron probe was not readily available to the author.

It was decided that the most practical tool for the job was the laser microprobe (Brech, 1962,1963,1965,1967; Goldman et al., 1964). This instrument, manufactured by the Jarrell-Ash Company, has an enormous potential as a petrographic tool.

In this study, chemically analyzed samples of silicates, already powdered and homogenized, were fused to a glass in alumina boats at 1400°C in a combustion furnace. Chemical data on the standards used are given in Table 15, Part Two.

Excitation parameters for the analyses of garnets in specimen 17 are given in Table 16, Part Two. All photometry was performed on a Hilger non-recording microphotometer.

After grinding the slabs of sample 17 and measuring the garnet apparent diameters and the coordinates of their centers, a slab was placed on the microscope stage of the laser microprobe. Each garnet exposed on the slab was then "shot" with the laser beam.

After each garnet was analyzed in duplicate in sections 17 I (perpendicular to the foliation) and 17 II (parallel to the foliation), the slabs were ground again to remove 0.25 m.m. as described above, and the apparent diameters measured. Standard glasses were "shot" on every plate.

After measurement of line densities on a microphotometer, and transformation of these densities to relative line intensities by means of the photographic calibration

curve, the following intensity ratios were calculated:

$$\frac{I_{\text{Fe } 2740}}{I_{\text{Fe } 2740} + I_{\text{Mg } 2852} + I_{\text{Mn } 4030}} \quad \frac{I_{\text{Mg } 2852}}{I_{\text{Fe } 2740} + I_{\text{Mg } 2852} + I_{\text{Mn } 4030}}$$

$$\frac{I_{\text{Mn } 4030}}{I_{\text{Fe } 2740} + I_{\text{Mg } 2852} + I_{\text{Mn } 4030}} \quad \frac{I_{\text{Ca } 3158}}{I_{\text{Fe } 2740} + I_{\text{Mg } 2852} + I_{\text{Mn } 4030} + I_{\text{Ca } 3158}}$$

All intensity ratio data, for both the garnets and standards, was converted to concentration data by means of a Fortran IV program of a least squares analysis for the IBM/360 adapted from Shaw and Bankier (1954). The program allows a least squares regression analysis of the standard data and gives average concentration values for replicate analyses plus the standard deviation and coefficient of variation for each analysis. The standard deviations of both the slope of the analytic line and its Y intercept are also calculated.

Precision and Accuracy

Table 17, Part Two presents the statistical data for the various working curves and the average of the coefficients of variation for all the grains measured in each section.

In order to evaluate the statistical data, a sample of the standard diabase W-1 (Fairbairn et al., 1951) was fused to a glass in the same manner as the standards described above. During the course of the routine determinations on the garnets, the W-1 glass was periodically "shot" following the same procedure as for the garnets. This operation was performed 5 times and the resulting mean values and statistical data are presented in Table 18, Part Two.

As may be seen from the data of Tables 17 and 18, the precision and accuracy of silicate analysis is entirely satisfactory for most petrologic investigations.

Results

In total, 365 garnet grains were measured in the above manner for Fe, Mg, Mn and Ca. Presenting an amount of data such as this in an illustrative manner is in itself a problem. It is desirable to present the data in the context of the rock, showing the concentration of an element in a grain with respect to its position in the rock section. Since tabular notation is obviously useless, it was decided that a diagrammatic presentation showing the position of each garnet grain along with the concentration of the element in question would be most lucid.

Figures 28 to 31, Part Two, show the spatial distribution of Fe, Mg, Mn and Ca in the garnets of section 17I, which is cut perpendicular to the foliation. A standard error of 10% is assumed for the analyses of all the grains and for all elements. Thus, various symbols are used to illustrate the concentration value of an element rounded off to the nearest decimal place. It is felt that this procedure is certainly a liberal estimate of the concentration since magnesium, with a coefficient of variation of 12.8 percent is, alone, significantly higher than 10 percent.

Figures 32, 33, 34 and 35, Part Two, show the spatial distribution of Fe, Mg, Mn and Ca respectively, in section 17 II cut parallel to the foliation. The same method of data presentation is employed here.

As the diagram of the sections indicate, the composition of the garnets with respect to Fe, Mg, Mn and Ca is quite variable. Groups of garnets with the same concentration of a particular element are quite small, indicating small volumes of equilibration with respect to that element. These volumes, on the average, measure only a few centimeters in their longest direction.

Looking at the figures illustrating the spatial distribution of various elements in garnets of section 17 I, it may be seen that the equilibration volumes are very small, usually measuring only a few m.m. across foliation.

However, they are more extensive in the foliation direction. Section 17 II shows more extensive domains of equilibration, and these are usually elongated in the direction of lineation.

An Investigation of Possible Zoning in the Garnets

A recent discussion of zoning in garnets by Hollister (1966) points out the problems of equilibration studies if zoning of one or more of the minerals present is observed. Hollister finds that the compositional variations in zoned garnets follows a Rayleigh fractionation model (Rayleigh, 1902) where only the extreme outermost layer of the garnet is part of the reacting chemical system at any stage of garnet growth.

It is obvious that if the garnets of the present study are zoned, most of the variation observed is probably due to poor precision of the point of analysis on each garnet. Thus, it was imperative that the garnets be inspected for compositional zoning.

Compositional variations in the garnets of this study were investigated on a Mark II Laser Microprobe at the Jarrell-Ash Company in Waltham, Massachusetts. The Mark II is the newest model of the laser microprobe and features a non-temperature sensitive neodymium laser with controlled output energy and a much improved optical system.

Four garnets were traversed at approximately 25 micron intervals and intensity ratios obtained in the same manner as discussed above. Two of the garnets examined were from sample 17 showing minor inclusions of sillimanite. One garnet was from sample 42 where inclusions in the garnets are rare and the last was from sample 8 and exhibited quartz inclusions located in a clump in the center of the garnet.

Figure 36A, Part Two, shows the Mn/Fe+Mg+Mn profile across a garnet exposed on section 17 I which is cut perpendicular to the foliation. The traverse is in the short

axis direction of one of the garnets which is elongated as described above. As is evident from Figure 36A, Part Two, no zoning with respect to manganese is apparent within the limits of analytic error. Further, there was no zoning of the garnet with respect to Fe and Mg.

A traverse across a garnet cut parallel to the foliation (section 17 II) showed no compositional zoning with respect to Mn, Fe or Mg. The profile of the compositional ratio $Mn/Fe+Mg+Mn$ in this grain is shown in Figure 36B, Part Two. The profile shows a semblance of a oscillatory zoning with respect to Mn. However, this variation is within the limits of analytic error and a proposed zoning in this grain would be purely conjectural.

Figure 37A, Part Two, illustrates the Mn profile across a garnet from section 42 II cut parallel to the foliation. No significant inhomogeneity is noted. The traverse across this grain found it homogeneous with respect to Fe and Mg as well.

The only zoning observed was along a traverse across a garnet from sample No. 8 (see Table 8, section I) which showed a distinct rise in the ratio $Mn/Fe+Mg+Mn$ from about 0.020 at the edges to 0.070 near the center. The area in which the high Mn values are located corresponds exactly with the clump of small quartz inclusions. No inclusions were observed in the outer regions of the grain where constant low atomic ratios for Mn prevail.

Hollister (1966) has mentioned the possibility of calcium zoning within garnets. This possibility was investigated along with Mn, Fe and Mg and no compositional zoning with respect to Ca was observed.

Thus it is concluded that the compositional zoning of garnets in these rocks is not prevalent and that the variations of garnet compositions within a hand specimen are real. Other factors which lead to this same conclusion are:

1. No optical zoning was evident in any garnets examined.

2. During replicate analyses of the garnets in matrix, no care was taken to "shoot" the same garnet in the same place each time. This had no effect on the precision of the determinations for the various elements within a single grain.
3. If the garnets of specimen 17 I and 17 II had been zoned, spatial equilibration domains as described above would not have been observed as the determinations were not made on the edge of each grain, i.e., within the reacting thermodynamic system.

The domains of equilibration with respect to Fe and Mg in garnets of section 17 II are more extensive although they are still elongated. This elongation is in the direction of the lineation which is defined by trains of sillimanite and garnet.

In summary, the domains of spatial equilibration of Fe and Mg in garnets were found to be quite small, ranging from only a few m.m. to a few centimeters. The shapes of these domains were controlled by the rock structure, i.e., foliation and lineation, and were more extensive along the foliation surfaces and lineation traces than across them. Parallel to the foliation, chemical communication of garnets with respect to Fe and Mg took place over a maximum distance of 4 cm. in the lineation direction and 2 cm across it. Perpendicular to the foliation, chemical equilibrium of garnets was limited to less than 1 cm., i.e., chemical communication across foliation planes was limited to less than a centimeter in most cases. The equilibration domains are possibly roughly ellipsoidal in shape with an axial ratio of close to 4:2:1. It is also interesting to note that in section 17 II spatial equilibration of Fe is more extensive than Mg. Iron shows less distinguishable domains, but these are larger than the Mg domains. The Mg domains of equilibration are much more regular in their orientation in the lineation direction. This is possibly a reflection of the relative mobilities of Fe and Mg under metamorphic conditions.

The spatial equilibration of Mn in the garnets of section 17 is somewhat more extensive than that for Fe and Mg. A distinct structural control is still evident, but equilibration across structural features is more extensive.

In section 17 II (Figure 34, Part Two) cut parallel to the foliation, the domains of Mn equilibration in garnets are at least as extensive as those for Fe, but they are less regular in their orientation according to the lineation direction. The axial ratios of the domains of Mn equilibration, if they are assumed to be roughly ellipsoidal in shape, are about 2:1:1.

The spatial degree of equilibration in the garnets of sample 17 with respect to their Ca content is shown in Figure 31 and 35, Part Two. In Figure 31, looking at the section perpendicular to the foliation, equilibration domains controlled by structure and those having no obvious structural control are both observed. The structurally controlled domains, for the most part, occur at one end of the section and it is proposed that variations in the whole rock Ca content were more prevalent here. This would probably be reflected in the mineral assemblage associated with each of these garnet equilibration domains.

Calcium equilibration in the garnets of section 17 II (Figure 35, Part Two) is more extensive than Fe, Mg or Mn. The domains are usually elongated and extend up to 5 cm. in their longest direction. Although, in some areas of the section, elongation of the equilibration domains is in the lineation direction, there are also regions of garnets having the same Ca content which are distinctly elongated almost perpendicular to the trace of the lineation and some which show no preferred orientation.

Investigation of Possible Correlation of the Parameters Measured

The calculation of correlation and covariance of the physical and chemical measurements on the garnets from specimen 17 was carried out using a computer program described in Biomedical Computer Program, Health Science Computing Facility, Department of Preventative Medicine and

Public Health, School of Medicine, University of California, Los Angeles, and translated into Fortran IV for IBM System/360 by Ralph Wiggins of the M.I.T. Department of Geology and Geophysics.

Tables 13 and 14, Part Two, show the correlation matrix for the size and distance measurements on the garnets of section 17 I and 17 II respectively. As is evident from the correlation coefficients shown in Table 13 and 14, there is a strong correlation between axial diameters and grain volume but this, obviously, is expected.

From the regression analysis, it is evident that for section 17 I only the correlation of lengths of the intermediate axis B and the short axis C is real. Assuming C as the independent variable, 59% of the variance in B may be accounted for. The regression analysis showed also that there is no correlation between any of the axial lengths or grain volumes and the distance to the nearest phase analog.

The regression analyses on the garnet parameters of section 17 II show a strong correlation between A and B. Taking either as the independent variable, 85% of the variance in the dependent variable is due to variance in the independent variable. There is also a strong covariance between the short axis and the volume. 68% of the variance may be accounted for using either C or V as the dependent variable.

Again, in section 17 II, there is no correlation between any axial length or garnet volume and distance to the nearest garnet. Using the chemical data, the correlation matrix was expanded to include all nine parameters which are:

A = Long axis length
 B = Intermediate axis length
 C = Short axis length
 V = Volume

$$\text{Fe} = \text{ratio } \frac{\text{Fe}}{\text{Fe}+\text{Mg}+\text{Mn}}$$

$$\text{Mg} = \text{ratio } \frac{\text{Mg}}{\text{Fe}+\text{Mg}+\text{Mn}}$$

$$\text{Mn} = \text{ratio } \frac{\text{Mn}}{\text{Fe}+\text{Mg}+\text{Mn}}$$

$Ca = \text{ratio } Ca/Fe+Mg+Mn+Ca$

$N = \text{distance to the nearest phase analog}$

The correlation matrix for the above variables in the garnets of section 17I, perpendicular to the foliation, is given in Table 20, Part Two. An analogous matrix for section 17II is given in Table 21, Part Two.

Inspection of these matrices shows very little correlation of any of the chemical parameters among themselves or with the physical variables. However, besides the obvious covariance of Fe and Mg, the other possible correlations were further tested by the application of the step-wise regression analysis to the input data.

From this analysis it was concluded that the Fe and Mn contents of the garnets are correlatable and that they are covariant in that either Fe or Mn may be assumed the dependent variable with no change in the correlation coefficient. The relation of Mg and Mn is similar but only half as strong.

The Ca content of the garnets was found to be strongly dependent on the Mg content. 17 percent of the Ca variance may be accounted for by variation of the Mg content of the same garnets. This is quite significant since only 25 percent of the variance can be accounted for by the parameters measured in this study.

5. CHEMICAL DETERMINATIONS OF BIOTITE AND GARNET FROM A PYROXENE GRANULITE ROCK.

Introduction

As discussed above, it was decided to examine the spatial extent of chemical equilibration in a rock having a different mineral assemblage and possibly a different grade of metamorphism. The rock selected was a garnet-biotite-orthopyroxene gneiss, sample No. 42, described earlier.

The relationship of biotite to hypersthene in this rock is unclear. From thin section analysis, no definite statement can be made as to whether the biotite is retrograde or the hypersthene prograde. The biotite occurs as small discrete grains with only rare association with the pyroxene.

It is suggested that the assemblage observed in sample 42 is indicative ^{of a} pyroxene granulite and represents at least a higher temperature of metamorphism than sample 17 examined earlier.

Method of Separation and Analysis

Sample 42, described above, was trimmed with a diamond saw on those faces exhibiting weathering. A section, 1 cm. thick was then cut parallel to the foliation. This section, from here on referred to as 42II, was cut up in to small cubes measuring roughly 1 cm. on a side.

Selected cubes of 42II were then crushed to -20, +100 mesh in a percussion mortar similar to that described by Wager and Brown (1960). The garnet and biotite were next hand-picked under a binocular microscope and placed in electrodes or stored in gelatine capsules.

Determinations for Fe, Mg, Mn and Ca were made on the garnets separated in the above manner; Fe, Mg and Mn were determined in the biotite. All analyses were performed by emission spectrography according to the parameters in Table 22, Part Two.

Relative line intensities of samples and standards for Fe, Mg and Mn were recalculated to the ratios $Fe/Fe+Mg+Mn$

Mg/Fe+Mg+Mn and Mn/Fe+Mg+Mn. Working curves were made for the various elemental ratios by plotting these intensity ratios against the corresponding concentration ratios of the standards. The coefficient of variation of the method is close to 12 percent for all the elements determined.

Results of the Determinations in Section 42II

Figure 40 and 40A, Part Two show the spatial distribution of Fe in garnet and biotite from section 42II. Figures 41 and 41A, 42 and 42A and 43. Part Two show the spatial distributions of Mg in garnet and biotite, Mn in garnet and biotite and Ca in garnet, respectively. In all the graphic representations, the concentration ratios are rounded off to the nearest $\pm .05$.

A semi-quantitative modal analysis of the section was made while the garnet and biotite were being picked. The results of this are shown Figure 39, Part Two. It should be noted that while biotite is ubiquitous in this section, there is no garnet in the upper right hand corner.

Discussion

From observations on the Figures 40 to 43, it may be said that for Fe, Mg and Mn in garnet, the spatial degree of equilibration is more extensive and measurably larger in this pyroxene garnet gneiss. Variations within a hand specimen may still be seen, however, and these variations are probably due to variation in the whole rock chemistry as reflected in the mineralogical variations. The spatial equilibration of Ca in garnets was found to be no more extensive than in the biotite-cordierite-garnet assemblages. Again the calcium content of the garnet seems to be related to their modal abundance which may be in turn dependent on the CaO content of the rock.

The spatial extent of equilibration of Fe and Mg in biotite is quite extensive, reaching outside the hand specimen-sized sample used, although the domain cannot be much larger than this sample size or it would be highly unlikely to have selected a domain interface on a random basis.

There is a fairly close relationship between the Fe and Mg contents of the biotites and the modal ratio garnet/biotite; the biotite in the area where no garnet occurs has a substantially higher Fe/Mg ratio. The Mn content of the biotite in this specimen is less uniform and the spatial equilibration is not so extensive as it is for Fe and Mg in this phase.

The distribution coefficients $K_{Fe}^{Gar/Bio}$, $K_{Mg}^{Gar/Bio}$ and $K_{Mn}^{Gar/Bio}$ have been calculated for those garnet-biotite pairs determined. Figure 44, Part Two shows the distribution coefficient $K_{Fe}^{Gar/Bio}$ for each cube in the section 42II where both garnet and biotite were measured. A distinct elongated area within the section exhibits a distribution coefficient ≈ 1.0 while the surrounding garnet-biotite pairs show $K_{Fe}^{Gar/Bio} \approx 2.0$. The elongation of this zone is reminiscent of the structural control on the equilibration domains of sample 17, discussed earlier. However, section 42II was cut parallel to the foliation and no lineation direction was apparent.

Areas over which the values $K_{Mg}^{Gar/Bio}$ are equal are much smaller than their Fe counterparts. It is possible that this irregularity is due to the dependence of the atomic ratio $Mg/Fe+Mg+Mn$ in garnet on the whole rock chemistry, the composition of the coexisting hypersthene and its modal concentration in the rock.

The spatial distribution of the values for $K_{Mn}^{Gar/Bio}$ are shown in Figure 45, Part Two. It is obvious from this diagram that the value of the Mn distribution coefficient is constant over very small intervals although the the atomic ratio $Mn/Fe+Mg+Mn$ is nearly constant over sizable areas. The variability must then lie in the Mn content of the biotite.

6. GENERAL SUMMARY AND CONCLUSIONS

The spatial degree of chemical equilibration in the garnets of specimen 17, described above, is in good agreement with the results of other workers (Phinney, 1959, 1963; Brownlow, 1961; Zen, 1961; Harker, 1939; Albee et al., 1965, 1966). The data of this study coupled with the results of these workers give persuasive evidence to the concept of "local" equilibration as discussed by Thompson (1959) or the analogous situation of "mosaic" equilibrium (Korzhinskii, 1959). In each case the rock system as a whole may not be in equilibrium but in each of the small regions thermodynamic equilibrium is attained if definite relationships occur between all the parameters. In other words, the chemical potential of an element must be equal in each phase of the assemblage. The spatial extent of local equilibration of a particular assemblage is, therefore, the volume over which all minerals have equal chemical potentials for each component elements. If the phases exhibit ideal or dilute solution with respect to these components, then the chemical potential is reflected in the phases by their concentrations of that element.

It is germane to note that often the domains of equilibration for the particular elements in the garnets examined in this study do not coincide in shape or size, thus causing the volume in which garnets are of equal composition for all elements determined to be very small.

The examination of equilibration domains in specimen 17 showed ~~distinct~~ distinct structural control on their sizes and shapes. It may be speculated that the domains of equilibration with respect to a certain element are roughly ellipsoidal in shape with their longest axis being parallel to the foliation and lineation, the intermediate axis parallel to the foliation and perpendicular to the lineation. It is interesting to note here that the axial directions and sometimes lengths of the equilibration domains is often

correspondent with the axial ratios of the flattened and elongated garnets positioned on the foliation surfaces. It is thus possible that the structural features largely control the rate and extent of diffusion during metamorphism.

TABLE OF CONTENTS

	Page
Abstract	ii
List of Figures	iii
List of Plates	vi
List of Tables	vii
Acknowledgements	ix
SECTION I. AN EXAMINATION OF CHEMICAL EQUILIBRIUM IN SOME HIGH GRADE METAMORPHIC ROCKS	1
1. INTRODUCTION	2
1.1 Review of Previous Work	2
1.2 Objectives of this Study	4
2. THEORETICAL CONSIDERATIONS	5
2.1 Equilibrium between Coexisting Phases	5
3. AREA STUDIED	11
3.1 General Description	11
3.2 Grade of Metamorphism	14
3.3 Choice of Samples	16
3.4 Petrography of the Samples	18
3.5 Chemical Composition of the Gneisses	20
4. SAMPLE PREPARATION	24
4.1 Separation of the Minerals	24
4.2 Purity of the Mineral Separates	27
4.3 Preparation of Minerals for Analysis	28
5. THE PARTIAL CHEMICAL ANALYSES OF MINERALS	29
5.1 Introduction, Instrumentation and Techniques	29
5.2 Preparation of Standards	32
5.3 Interferences	37
5.4 Precision and Accuracy	38
5.5 Determination of FeO	41
5.6 Analytic Results	42
6. ELEMENT FRACTIONATION BETWEEN COEXISTANT MINERALS	47
6.1 Introduction	47
6.2 The Distribution of Fe, Mg, and Mn between Garnet and Biotite	49
6.3 The Distribution of Cr, Co, Ni and Ca between Garnet and Biotite	55
6.4 Discussion of Results	60
SECTION II. THE SPATIAL EXTENT OF LOCAL EQUILIBRATION	62
7. INTRODUCTION	63
7.1 The Problem	63

7.2 Theoretical Considerations	66
7.3 Proposed Method of Study	70
7.4 Description of the Samples	72
7.5 Morphology of the Garnets	75
8. GRAIN SIZE ANALYSIS AND INTERGRAIN DISTANCE	
DISTANCE MEASUREMENTS	80
8.1 Apparatus and Techniques	80
8.2 Grain Size Distribution of Garnet in Sample 17	83
8.3 Intergrain Distance Measurements	90
8.4 Investigation of Possible Correlation of the Physical Parameters Measured	92
8.5 Discussion of Results with Respect to Rock Texture.	95
9. ANALYSIS OF GARNETS IN MATRIX	98
9.1 The Laser Microprobe	98
9.2 Standardization	101
9.3 Analytic Technique	102
9.4 Precision and Accuracy	108
9.5 Results	110
9.6 An Investigation of Possible Zoning in the Garnets	120
9.7 Results of the Zoning Investigation	122
9.8 Correlation of Results with Grain Size and Intergrain Distances	128
9.9 Discussion	133
10. CHEMICAL DETERMINATIONS IN BIOTITE AND GARNET FROM A PYROXENE GRANULITE FACIES ROCK	137
10.1 Introduction	137
10.2 Method of Separation and Analysis	139
10.3 Results of Determinations in Section 42II	141
10.4 Discussion	149
11. GENERAL SUMMARY AND CONCLUSIONS	157
12. SUGGESTIONS FOR FURTHER RESEARCH	159
APPENDIX I. Sample Locations and Descriptions	160
APPENDIX II. Computer Program for Least Squares Analysis	166
APPENDIX III. Computer Program for Analysis of Grain size, Intergrain Distance and Grain Distribution	166
APPENDIX IV. Computer Program for Correlation and Regression Analysis	170
BIBLIOGRAPHY	
BIOGRAPHICAL SKETCH	

LIST OF FIGURES

Figure		Page
1	Example of Distribution of Mn between Garnet and Hornblende (after Kretz, 1959)	8
2	Example of irregular distribution of V between Biotite and Garnet	9
3	Illustration of the effect of the Calcium content garnet on the distribution of V between Biotite and Garnet	9
4	Geological Map of the Ganonoque Area showing Sample Locations	12
5	Flow Chart for Mineral Separations	25
6	Working Curve for Magnesium	31
7	Working Curve for Calcium	33
8	Working Curve for Manganese	33
9	Working Curve for Iron	34
10	Working Curve for Nickel	36
11	Working Curves for Cobalt and Chromium	36
12	Distribution of Fe between Garnet and Biotite	50
12A	Distribution of FeO/MgO between Garnet and Biotite	51
13	Distribution of Mg between Garnet and Biotite	52
14	Distribution of Mn between Garnet and Biotite	53
15	Distribution of Cr between Garnet and Biotite	56
16	Distribution of Co between Garnet and Biotite	57
16A	Distribution of FeO and MgO between Garnet and Biotite and its relation to the Co content of Biotite	57A
17	Distribution of Ni between Garnet and Biotite	58
18	Distribution of Ca between Garnet and Biotite	60
19	Typical Elongated Garnet from Sample 17	76
20	Distribution of Axial Diameters of Garnets in Section 17I	84
21	Distribution of Volumes of Garnets in Section 17I	85
22	Distribution of Axial Diameters of Garnets in Section 17II	86
23	Distribution of Volumes of Garnets in Section 17II	87
24	Microprobe Working Curve for Iron	104
25	Microprobe Working Curve for Magnesium	105
26	Microprobe Working Curve for Manganese	106
27	Microprobe Working Curve for Calcium	107

Figure		Page
28	Spatial Distribution of Fe in Garnets of Section 17I	112
29	Spatial Distribution of Mg in Garnets of Section 17I	113
30	Spatial Distribution of Mn in Garnets of Section 17I	114
31	Spatial Distribution of Ca in Garnets of Section 17I	115
32	Spatial Distribution of Fe in Garnets of Section 17II	116
33	Spatial Distribution of Mg in Garnets of Section 17II	117
34	Spatial Distribution of Mn in Garnets of Section 17II	118
35	Spatial Distribution of Ca in Garnets of Section 17II	119
36A	Mn Profile Across Garnet in Section 17I	123
36B	Mn Profile Across Garnet in Section 17II	123
37A	Mn Profile Across Garnet in Section 42II	124
37B	Mn Profile Across Garnet in Sample 8	124
38A	Ca Profile Across Garnet in Section 17II	125
38B	Ca Profile Across Garnet in Section 17I	125
39	Distribution of Garnet and Biotite in Section 42II	144
40	Spatial Distribution of Fe in Garnets of Section 42II	145
40A	Spatial Distribution of Fe in Biotites of Section 42II	145
41	Spatial Distribution of Mg in Garnets of Section 42II	146
41A	Spatial Distribution of Mg in Biotites of Section 42II	146
42	Spatial Distribution of Mn in Garnets of Section 42II	147
42A	Spatial Distribution of Mn in Biotites of Section 42II	147
43	Spatial Distribution of Ca in Garnets of Section 42II	148
44	Spatial Distribution of the Distribution Coefficient $K_{\text{Fe}}^{\text{Gar/Bio}}$ in Section 42II	152
44A	Spatial Distribution of the Coefficient $K_{\text{Mg}}^{\text{Gar/Bio}}$ in Section 42II	152

Figure		Page
45	Spatial Distribution of the Coefficient $K_{Mn}^{Gar/Bio}$ in Section 42II	153
A-1	Program for Least Squares Analysis	164
A-2	Program for Analysis of Grain Size and Distribution	168
A-3	Program for Correlation and Regression Analysis	170

LIST OF PLATES

	Page
PLATE IA. Side View of the Micrometer Grinder	81
PLATE IB. Bottom View of the Micrometer Grinder	81
PLATE II. The Laser Microprobe	99

List of Tables

Table		Page
1	Modal analysis of the Gneisses selected for Equilibrium studies	19
2	Operating conditions for Whole-Rock Analysis by the Mutual Standard Method	21
3	Precision and Accuracy of the Mutual Standard Method of Spectrochemical Whole-Rock Analysis	22
4	Chemical Analyses of the Gneisses selected for Equilibration Studies	23
5	Operating Parameters for the Atomic Absorption Spectrophotometric Determinations	30
6	Chemical and Statistical Data on Standard Rocks and Minerals	39
7	Mineral Assemblages of Grenville Gneisses Selected for Mineral Chemical Determinations	43
8	Partial Analyses of Garnet from Grenville Gneisses	44
9	Partial Analyses of Biotite from Grenville Gneisses	45
10	Chemical Data on Coexisting Garnets and Biotites from Wynne-Edwards and Hay (1963)	48
11	Modal Analyses of the Gneisses used for the Study of Equilibration Domains	73
12	Summary of Grain Size Measurement by Garnets in Specimen 17	88
13	Correlation Matrix for the Physical Measurements on Garnets from Section 17 I	94
14	Correlation Matrix for the Physical Measurements on Garnets from Section 17 II	94
15	Chemical Data on Laser Microprobe Standards	101
16	Excitation Parameters for Laser Microprobe Analyses.	102
17	Statistical Data for the Determinations on Garnet Grains with Laser Microprobe	109
18	Statistical Data for replicate Determinations on W-1 using Laser Microprobe	109
19	Operating Parameters used in the Investigation of Zoning in Garnets	121

Table		Page
20	Correlation Matrix for the Measured Physical and Chemical Variables for the Garnets in Section 17I	129
21	Correlation Matrix for the Measured Physical and Chemical Variables for the Garnets in Section 17II	130
22	Excitation Parameters for the Spectrochemical Determination of Fe, Mg, Mn and Ca in Garnet and Biotite from Section 42II	140
23	Concentration Ratios for Garnet and Biotite of Section 42II	142

ACKNOWLEDGEMENTS

The author is indebted to Professor W.H. Dennen, who supervised the thesis, and besides providing encouragement through trying times, devoted much time and labor to its production. Dr. R. Lynn Moxham of the New York State Geological Survey gave advice and information on metamorphic equilibration which is much appreciated. As well as providing the atomic absorption equipment and the facilities of an analytical laboratory, Professor W.H. Pinson gave the author much sound advice pertaining to silicate analysis. Helpful discussions of petrologic matters with fellow graduate students, C.M. Spooner, R.H. Reesman, D.C. Roy and Dr. S.A. Heath are greatly appreciated. The preliminary work on the laser microprobe in the Cabot Spectrographic Laboratory by Y.J.A. Pelletier proved invaluable to the author. Dr. Frederick Brech of the Jarrell-Ash Company provided information on laser-excited spectrography and arranged for time on the Mark II Laser Microprobe.

Others who have contributed time, advice, information or equipment include:

J. Annese	D. Guernsey
D.L. Biggs	K. Harper
W. Burrow	W.C. Luth
W. Correia	E. Mencher
W.S. Dennen	M. Redden
H.W. Fairbairn	L. Walters
P. Fenn	D.R. Wones
N. Griswold	H.R. Wynne-Edwards
T. Griswold	

Mr. R.E. Bruneau performed the gigantic task of keeping track of all the data and did almost all of the computer programming. He also helped with sample preparation and plate reading. Thanks must go to Miss Bernice MacIntyre who typed the final draft, exhibiting great stamina.

Machine computations were performed at the M.I.T. Computation Center. Financial support for the study came under Grant GP-4135 from the National Science Foundation.

Finally, the author wishes to express his gratitude to his wife Geraldine and son Patrick for giving up husband and father, respectively, during the latter stages of the thesis experimentation and writing. Their contribution of love and understanding is gratefully acknowledged.

SECTION I
AN EXAMINATION OF CHEMICAL EQUILIBRIUM IN SOME
HIGH-GRADE METAMORPHIC ROCKS

I INTRODUCTION

1.1 Review of Previous Work

The application of both solid state and chemical thermodynamics to metamorphic petrology has become more popular in recent years with the advances in analytic apparatus and techniques. Previously, rigorous examination of phase equilibria in crystalline rocks was made difficult by the presence of large numbers of components and phases. However, if the rocks in question have approached a state of chemical equilibrium, it should be possible to detect in them conditions which are characteristic of multiphase chemical systems at equilibrium, as discussed by, Ramberg (1952), Fyfe, Turner and Verhoogen (1958), Thompson (1955) and others. These conditions being: (1) Certain phases are not permitted to coexist and will be chemically represented by some chemically equivalent combination of other phases. (2) The chemical composition of a phase may be restricted by the presence of one or more other phases.

Several workers have examined the chemical equilibration of coexisting minerals in metamorphic rocks (Kretz, 1959, 1960, 1961, 1964, Mueller, 1961, 1962. Moxham, 1965, Wynne-Edwards and Hay 1963, O'Hara, 1963, Phinney, 1959, 1963, Krank, 1959, 1961, Moore, 1960) with varying degrees of success.

Attempts to define equilibrium relations in metamorphic rocks must follow two basic assumptions. First it must be assumed or shown that the minerals are in internal equilibrium, i.e., the minerals studied are not chemically or physically zoned although this may be handled in a detailed study (Albee, Chodos and Hollister, 1966, Hollister, 1966). Second, the sample from which the mineral grains are separated must be in local equilibration. The volume of local equilibration being that volume over which free chemical communication has taken place. Kretz (1960) has summed up the second criterion:

"... it is important to consider the size of natural chemical systems (thermodynamic). Spheres of chemical communication may be different in size with reference to different elements depending on their mobility and may vary in size as a function of temperature."

It is obvious that difficulties might arise if sampling does not take place within equilibrated domains, and it is proposed here, that many of the problems found in the analysis of metamorphic minerals are due to sampling without regard to the dimensions of the domain of local equilibration. Phinney's study of the rocks from St. Paul Island and Money Point, Nova Scotia (Phinney, 1959, 1960) is a case in point.

1.2 Objectives of this Study

The primary purpose of this study is to determine the dimensions of the volumes or domains of equilibration with respect to coexisting phases of a specific grade of metamorphism. This is a two stage problem which may be best attacked by first ascertaining the fact of equilibration among coexisting phases in a region where specimens are believed to have undergone the same degree of metamorphism. Next, the dimensions of the equilibrium domains for various element-mineral groups may be worked out.

Chemical analysis of pairs of coexisting minerals, for example, biotite and garnet and examination of the distribution of various component elements of the pairs permits evaluation of the distribution in terms of chemical-phase theory (Kretz, 1959). From a preliminary study such as this, the following questions may be considered:

1. Which elements are regularly distributed and which are randomly distributed?
2. What are the factors, chemical or structural, that account for the regular distribution?
3. What are the factors which may influence the value of the distribution coefficient?
4. Over what range of concentration is equilibrium maintained in these minerals with respect to the various elements?

2 THEORETICAL CONSIDERATIONS

2.1 Equilibrium Between Coexisting Phases

A further condition for chemical equilibrium in rocks is provided by the requirement that, in a multiphase chemical system at equilibrium, the components must be regularly distributed among the phases, i.e., if two phases coexist at equilibrium, the chemical potential of each component contained by both phases must be the same in each phase. At constant temperature and pressure, the chemical potential of a component in a phase is a function of the concentration of the component, and in the case of non-ideal crystals, the chemical potential may also be a function of other chemical conditions within the crystal. If the chemical potential of a component in two coexisting phases is dependent only on concentration, then the component must be regularly partitioned between the two phases, provided that equilibrium conditions exist.

Application of chemical thermodynamic theory to coexisting minerals has been discussed in detail by Kretz (1959, 1960), Mueller (1961, 1962), McIntire (1958, 1963), Moxham (1965) and others. A brief review and discussion is given here.

Consider a chemical system at temperature T and pressure P . In this system two of the phases α and β have formulae $(A,B)Y$ and $(A,B)Z$ respectively where A, B, Y and Z are chemical species. Here we will inquire into the distribution of A and B between α and β . A mineralogical example of this system is olivine $(Mg,Fe)_2Si_2O_6 = \alpha$ and Diopside, $(Mg,Fe)CaSi_2O_6 = \beta$.

The relationship between the chemical potential and concentration of any species in a phase, e.g. A , is

$$\mu_A = \mu_A^* + RT \ln F_A X_A \quad (1)$$

where μ_A is the chemical potential of A in the phase, μ_A^* is the chemical potential of A in some standard state, i.e., in the pure phase AY or AZ at the same temperature and pressure. R is the gas constant, T is the absolute temperature and F_A is the activity coefficient of A . The composition of the phases are indicated by atomic ratios or molecular ratios X_A where $X_A = A/A + B$

$$\begin{aligned} \text{Now } \mu_A^\alpha &= \mu_A^{*\alpha} + RT \ln F_A^\alpha X_A^\alpha \\ \mu_A^\beta &= \mu_A^{*\beta} + RT \ln F_A^\beta X_A^\beta \end{aligned}$$

and at equilibrium

$$\mu_A^\alpha = \mu_A^\beta$$

Therefore
$$X_A^\beta / X_A^\alpha = F_A^\alpha / F_A^\beta \exp (\mu_A^* / RT - \mu_A^* / RT) = K_d \quad (2)$$

Where K_d denotes the distribution coefficient. If α and β are both ideal mixtures within a specified concentration range, or if A is present in dilute concentrations in α and β , then F_A^α / F_A^β is a constant and therefore K_d is constant.

Considering both A and B simultaneously we may use the expression derived by Ramberg and Devore (1951):

$$(X_A^\alpha / 1 - X_A^\alpha) (1 - X_A^\beta / X_A^\beta) = K_f \exp (\Delta G / RT)$$

where K_f is a value depending on the activity coefficients of the chemical species A and B in α and β .

Deriving this type of equation for the general case we may again consider the two phases (AB)Y and (AB)Z where we wish to find a relationship between X_A on phase α and X_A in phase β .

A possible change in the system at equilibrium is the movement of an infinitely small amount (dn_A) of A from α to β and an infinitely small amount of B from β to α at constant T and P.

Now the Hemholtz function for the reaction is $dF = -PdV - PdV - \mu_A^\alpha dn_A + \mu_A^\beta dn_A + \mu_B^\alpha dn_B - \mu_B^\beta dn_B$

but the work done on the system at equilibrium is

$$dF = -PdV - PdV$$

Therefore

$$-\mu_A^\alpha dn_A + \mu_A^\beta dn_A + \mu_B^\alpha dn_B - \mu_B^\beta dn_B = 0 \quad (4)$$

and $dn_A = dn_B$ to maintain charge balance

Therefore
$$\mu_A^\alpha - \mu_B^\alpha = \mu_A^\beta - \mu_B^\beta \quad (5)$$

Substituting equations of type (1) into (5) we obtain

$$X_A^\alpha (1 - X_A^\beta) / (1 - X_A^\alpha) X_A^\beta = f_B^\alpha f_A^\beta / f_A^\alpha f_B^\beta \exp (-\mu_A^* / RT + \mu_B^* / RT - \mu_A^* / RT + \mu_B^* / RT) \quad (6)$$

where $X_A^\alpha (1 - X_A^\beta) / (1 - X_A^\alpha) X_A^\beta = K_d$, the distribution coefficient.

K_f = the term containing the activity coefficients and is a general function of X_A^α , X_A^β , P, T. If both phases are ideal $K_f = 1.0$ and K_d is a function only of P and T. If both phases are ideal mixtures then K_d is constant for all values of X_A^α and X_A^β . Then if X_A^α is plotted against X_A^β for a number of phase

pairs the points will produce a straight line or a smooth curve symmetrical about this line. A plot of $X_A^\alpha / (1 - X_A^\alpha)$ vs. $X_A^\beta / (1 - X_A^\beta)$ produces a straight line of slope K_d .

If one or both phases are not ideal mixtures K_f is not constant but varies with the composition of one or both phases. A plot of X_A^α vs. X_A^β produces an irregular relationship. However, if one or both phases are non-ideal and the concentration of one species, e.g., A, is very small in both phases then within the concentration range in which Henry's Law and Raoult's Law are valid, all activity coefficients must remain constant and

$$X_A^\alpha / X_A^\beta \simeq X_A^\alpha (1 - X_A^\beta) / (1 - X_A^\alpha) X_A^\beta = K_d = \text{Const.}$$

or Nernst's Distribution Law.

Similar relationships may be derived for coexisting phases such as (AB) and (AC); (ABC)Y and (ACB)Z; (AB) (CD)_qY and (AB) (CD)_rZ, etc. following Kretz, (1961). In each case if α and β may be considered to be ideal mixtures with respect to A, B, C and D, then Nernst's Distribution Law is valid.

To illustrate the method employed with respect to the above theoretical considerations an example, namely, the distribution of Mn between coexisting garnet and hornblende may be chosen. First, an attempt is made to find a relationship between $X_{Mn}^{Gar.}$ and $X_{Mn}^{Hb.}$ as expressed by (6). This is accomplished by plotting $X_{Mn}^{Gar.}$ against $X_{Mn}^{Hb.}$ for different mineral pairs of the same metamorphic grade.

An example of such a plot is given in Figure 1, from Kretz's study of amphibolite-grade schists from Southwestern Quebec. The points define a smooth curve so it may be concluded that equilibrium was attained and that the effect of numerous compositional variables has not been great enough to alter the distribution coefficient significantly. If the points produced by the plot were scattered, e.g. Figure 2, the distribution coefficient may have been displaced by the variable concentration of another element in one or both of the phases. A good example of this effect is shown by Figure 3 in which the effect of the calcium content of garnets on the distribution of vanadium between biotite and garnet, Kretz, (1959) is marked. This relationship is best illustrated by plotting the distribution coefficient against

FIGURE 1. DISTRIBUTION OF MANGANESE
BETWEEN GARNET AND HORNBLende
(after Kretz, 1959)

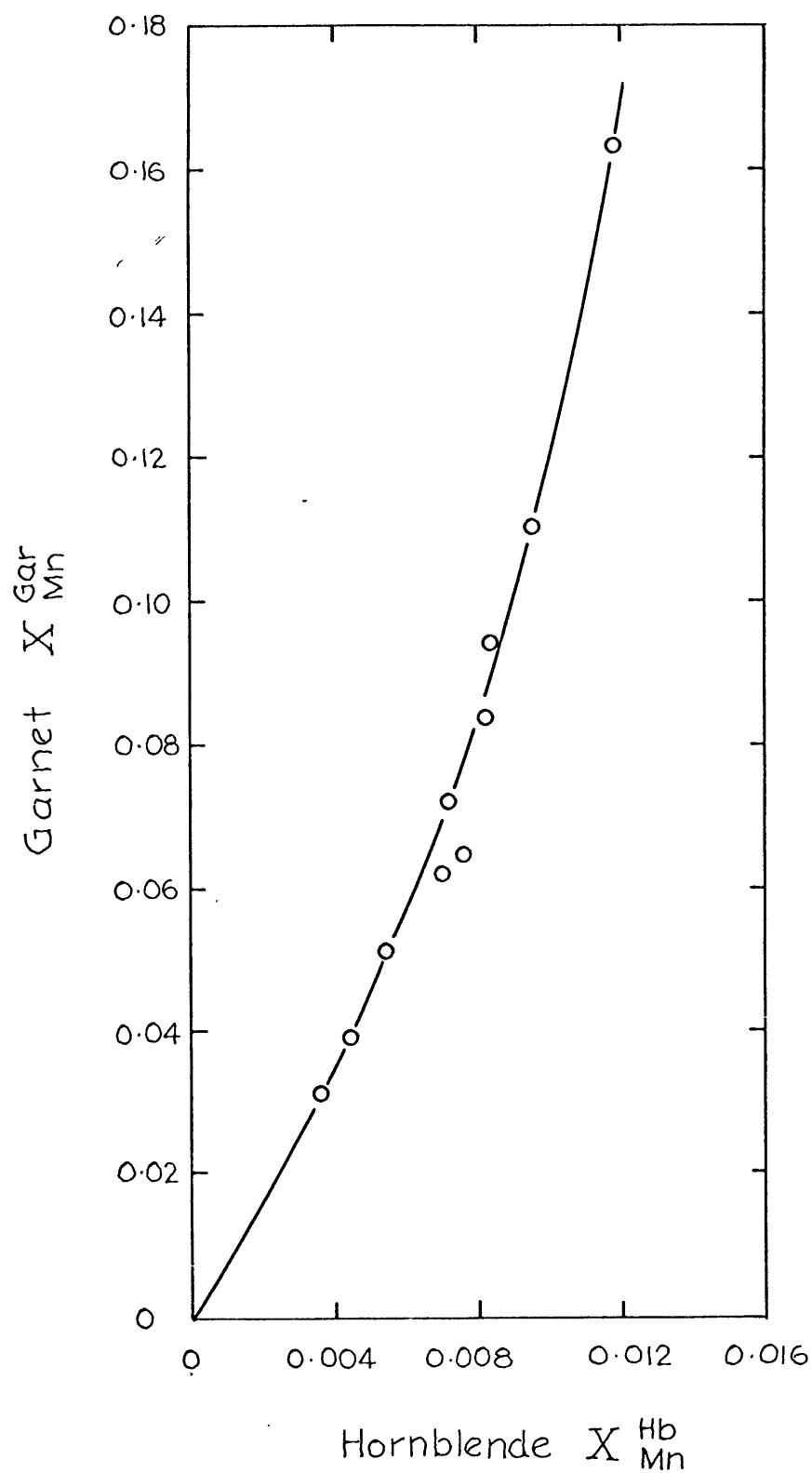


FIGURE 2. DISTRIBUTION OF V_2O_3 BETWEEN
GARNET AND BIOTITE (after Kretz, 1959)

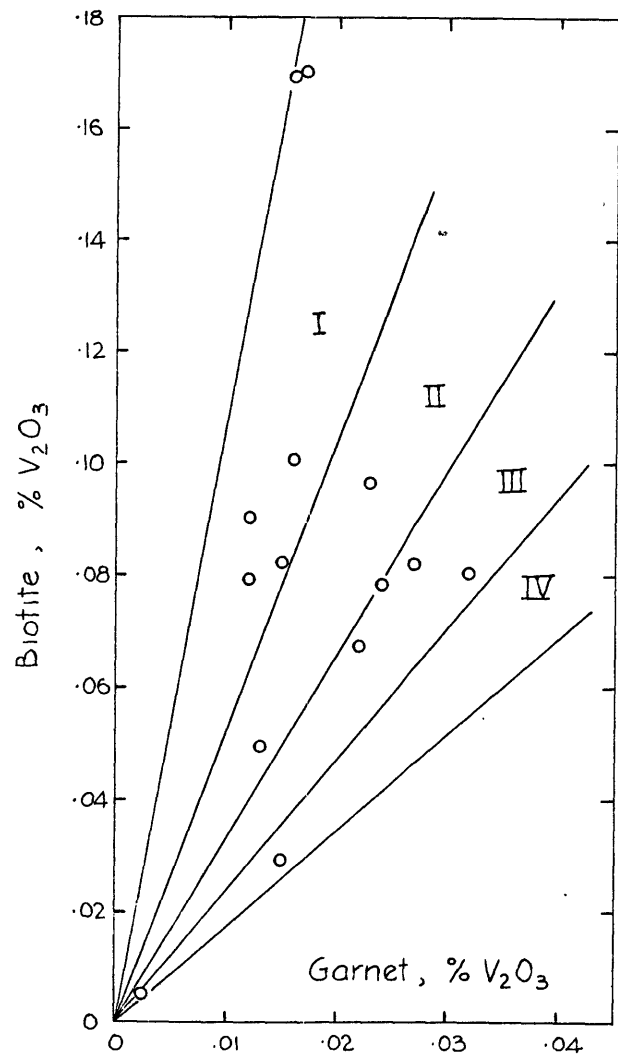
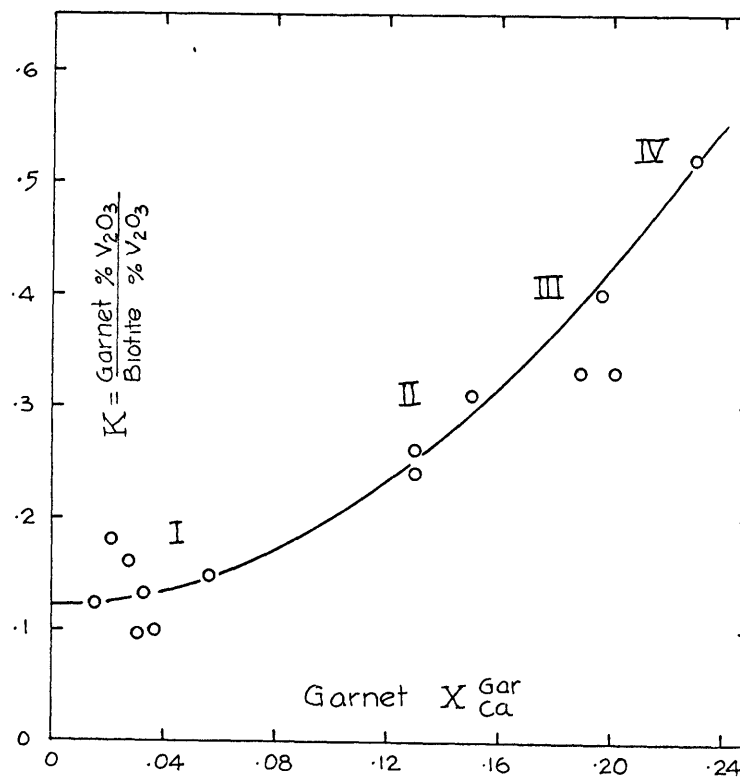


FIGURE 3. EFFECT OF THE CALCIUM CONTENT
OF GARNET ON THE DISTRIBUTION OF
VANADIUM BETWEEN BIOTITE AND GARNET
(after Kretz, 1959)



the concentration of the other element in one of the two minerals.

If no relationship between $x_{Mn}^{Gar.}$ and $x_{Mn}^{Hb.}$ can be found, it must be concluded that one or more of the following possibilities is responsible.

1. The distribution coefficient is a function of many compositional variables and is too complex to be readily seen.
2. The distribution coefficient is a function of an element not determined.
3. Inclusions of submicroscopic phases exist in the minerals and are contaminating the analyses.
4. Variations in the temperature of equilibration exist within the group of minerals.
5. A condition of chemical equilibration with reference to the particular component in question was not established or was not retained in all the specimens.

3 AREA STUDIED

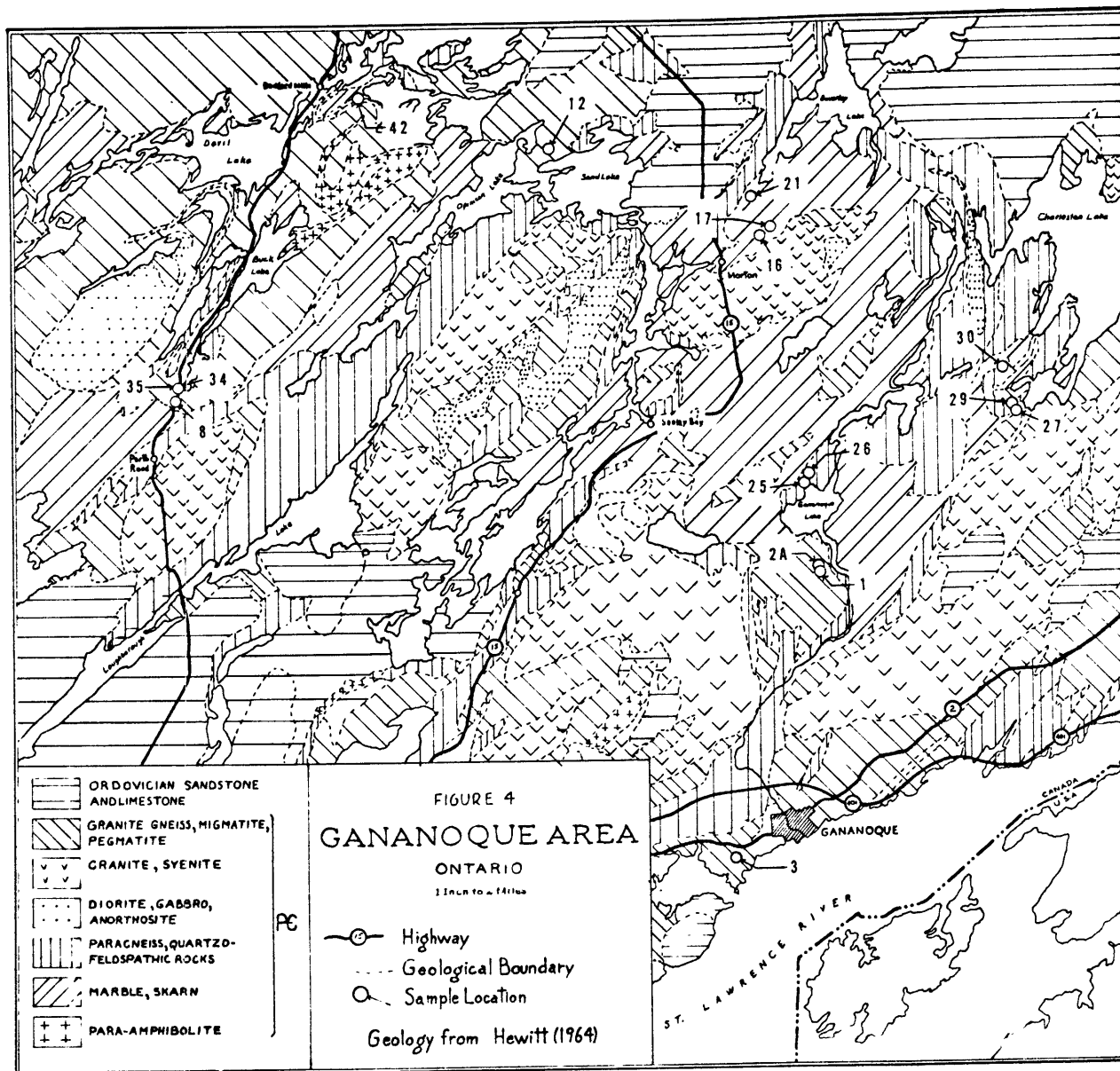
3.1 General Description

In selecting an area for metamorphic equilibration studies, the author has endeavored to find a regionally metamorphosed terrain of great age which has most likely been influenced by more than one regime of metamorphism. This would seem to afford the most favorable conditions for the attainment of chemical equilibrium between coexisting minerals. The area must also meet certain other specifications, these being: Coarse grained assemblages in which the minerals may be recognized in hand specimen; accessibility to fresh samples and sufficient outcrop to allow good sample control. A further criterion was also placed on the area chosen, e.g., that the region had been recently mapped to the extent that sufficient control might be placed on sampling and grade of metamorphism. After searching through the literature, the area selected as being most appropriate for the present study was that of the Ganonoque-Westport region of Ontario. See Figure 4.

The bedrock formations underlying the Ganonoque area are of Precambrian and Paleozoic ages (Wynne-Edwards, 1959, 1962, 1963; Hewitt, 1965). Approximately 80 percent of the area is Precambrian rock consisting of basic and acid volcanics and metasedimentary rocks (mainly marble, amphibolite, paragneiss and quartzite) intruded by basic and acid plutonics. Age determinations indicate that the period of orogeny, the Grenville, affected the whole Precambrian area, Krogh, (1964). Geologically, the region is referred to as the Frontenac Axis; being that belt which joins the Adirondack Highlands to the main Grenville body.

The grade of metamorphism increases westerly from greenschist facies, through epidote-amphibolite and amphibolite to the east, to granulite facies in the Kingston-Ganonoque area Wynne-Edwards, (1959, 1962).

Garnet, garnet-cordierite, and cordierite gneisses form units varying from six inches to several hundred feet in thickness within layered quartz-biotite-feldspar gneisses. The units are continuous and have been used as marker horizons for mapping purposes Wynne-Edwards, (1959). The gneisses are medium to coarse



grained with lepidoblastic to granoblastic texture and pronounced foliation. The major minerals present are garnet, cordierite, biotite, sillimanite, magnetite, quartz, plagioclase, orthoclase or microcline and perthite. Corundum, spinel, zircon, apatite, dumortierite and tourmaline occur locally in small amounts. There is alteration to sericite, chlorite, and epidote in scattered specimens Wynne-Edwards, (1959, 1962, 1963). The mineral assemblages recorded in some of the pelitic rocks of the eastern part of the area are listed below Wynne-Edwards, (1962, 1963). In all of these, quartz and either perthite or plagioclase + potash feldspar are also present:

1. cordierite+sillimanite+biotite
2. cordierite+garnet+sillimanite-biotite
3. cordierite+garnet+biotite
4. cordierite+biotite
5. garnet+sillimanite-biotite
6. garnet+biotite
7. biotite

In the Southwestern part of the area, the rocks contain abundant hypersthene and only minor biotite Wynne-Edwards, (1959) and have attained the pyroxene granulite facies.

3.2 Grade of Metamorphism

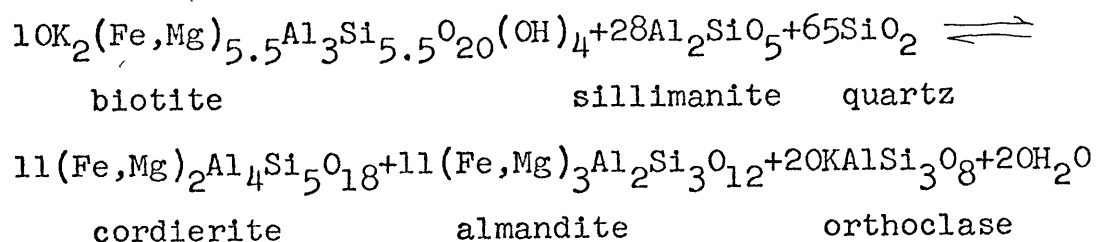
The presence of the assemblage quartz-orthoclase-plagioclase-cordierite-almandine-biotite in the gneisses of the Ganonoque-Westport area is analogous in most respects to the metamorphic facies in the Central Abukuma plateau of Japan as described by Miyashiro, (1958). Here, the presence of cordierite ushers in the amphibolite facies, and in order to differentiate it from Barrovian almandine-amphibolite facies where cordierite is not encountered, the amphibolite facies of the Abukuma-type metamorphism is named the cordierite-amphibolite facies, Winkler, (1965).

The assemblages observed in the present study correspond to Winkler's sillimanite-cordierite-orthoclase subfacies of the cordierite-amphibolite facies. The absence of chloritoid and kyanite and the presence of andalusite or sillimanite denoting a lower pressure environment. The subfacies, as described by Winkler, represents the highest grade of regional metamorphism that is realized under relatively low pressure conditions and is terminated at its high T end by the pyroxene hornfels facies of deep seated contact metamorphism. He proposes a temperature of 700°C and pressure of about 3000 bars, corresponding to a depth of roughly 10 km for this subfacies. Winkler, 1965).

However, the assemblages associated with the garnet-cordierite gneisses of the Ganonoque-Westport area, although biotitic, resemble granulite facies rocks. In the Southwestern part of the Westport area, the rocks contain abundant hypersthene, only minor biotite and no cordierite (Wynne-Edwards, 1959, Wynne-Edwards and Hay, 1963). Metamorphism in this area thus has its upper P and T limit in true pyroxene-granulite facies. Wynne-Edwards and Hay, (1963) proposed that the garnet-cordierite assemblages represent a stage transitional between the high-amphibolite and granulite facies.

It has been proposed by deWaard, (1966) that the assemblages quartz-K-feldspar-plagioclase-sillimanite-cordierite-biotite-almandite and quartz-K-feldspar-plagioclase-cordierite-biotite-almandite-hypersthene associated with hypersthene-bearing granulites and charnokites be established as the biotite-cordierite-almandite subfacies of the hornblende-granulite facies. deWaard states that

the composition of such gneisses fall in the or-co-al field of the AFK portion^{of} an AFKM diagram. However, the mineral assemblages present in these rocks include both biotite and K-feldspar, giving one too many phases for divariant equilibrium. The system then may represent univariant equilibrium for an open system, or divariant equilibrium for a closed, H₂O deficient system (deWaard, 1964, 1965). deWaard (1966), also proposes that the development of coexisting cordierite and almandite is a function P_{load}, T, and FeO/MgO ratio of the rock. The reaction:



then represents the breakdown of biotite in sillimanite bearing, pelitic rocks. The dependence of this reaction on the FeO/MgO ratio of the rock has also been pointed out by Eskola, (1915) and Winkler, (1965). The CaO content has also been found to play an important role in the production of cordierite in pelitic gneisses (Wynne-Edwards and Hay, 1963). In alumina deficient pelites, i.e., those rocks not exhibiting an alumino-silicate, orthopyroxene would occur coexisting with cordierite and almandite.

The subfacies, biotite-cordierite-almandite, as defined by deWaard (1966), occupies the low P_{load} or high T field of the hornblende granulite facies. With higher P_{load} or lower T, it borders on the hornblende-orthopyroxene-plagioclase subfacies, and at lower P_{load} (or higher T) it is transitional into pyroxene hornfels facies Winkler, (1965). At lower P_{H₂O} (or higher T) it adjoins the cordierite-almandite subfacies of the pyroxene granulite facies deWaard, (1965) and at higher P_{H₂O} (or lower T), it borders on the sillimanite-cordierite-orthoclase-almandine subfacies (A2.3) as described by Winkler, (1965) for Abukuma-type metamorphism.

3.3 Choice of Samples

An attempt should be made in a study like this to work with specimens which represent systems with variance one or at most two. That is, the number of phases present should, at least, equal the number of components needed to define the system (considering mobile components) so that the variance in the system is limited to temperature and pressure and the compositions of the phases will remain fixed over a range of compositions at a fixed P and T.

The assemblages, described above, found in the paragneisses of the Ganonoque region may be represented by the major components SiO_2 , Al_2O_3 , FeO , MgO , K_2O and H_2O . Quartz and potash feldspar are present in all samples so that at constant temperature, pressure and water vapor pressure, only MgO , FeO , and Al_2O_3 are variable components. The system allows a maximum of three phases in a P-T field, but in fact the three components are represented by four phases, cordierite, garnet, sillimanite and biotite. Either the assemblage is not stable or there is another variable. Wynne-Edwards and Hay (1963) show that the assemblage is a stable one and that the presence of garnet or cordierite is controlled by the FeO , MgO and CaO content of the host rock. They state that pelitic rocks with low CaO and FeO are cordierite-bearing and garnet-free, and as these components increase, relative to MgO , cordierite-garnet-biotite gneisses appear, followed by garnet-biotite gneisses. This phenomenon has also been noted by Eskola (1915) and Parras (1958). An attempt was therefore made, to collect only samples containing the phases, quartz, potash feldspar, garnet, biotite, plagioclase plus or minus cordierite.

Correct mineral identification and estimate of compositions should be made in the field. However, this is usually difficult and the actual assemblage may only be determined by petrographic analysis in the laboratory. Further, laboratory inspection is often the only way of avoiding specimens which have undergone retrograde or replacement reactions. In order to analyze pure specimens, inclusions within the minerals must be identified microscopically and then separated.

These problems are only solved by collecting many specimens which appear suitable in the field, and after elimination in the

laboratory, those that meet the requirements are kept for further chemical and petrographic study.

3.4 Petrography of the Samples

From the 43 specimens collected, 30 which appeared unaltered and homogeneous were selected for detailed examination. Thin sections were prepared for a close check on the suitability of these samples and examination of the thin sections further limited the number of samples to 23. Figure 4 shows collection locations for the specimens used in this study.

Nearly all of the thin sections showed small amounts of chlorite or sericite replacing various minerals. For the most part, however, alteration was limited to the cordierite with some local alteration of the plagioclase. Retrogression of the other minerals of the assemblages present is essentially negligible in the samples chosen for further study.

The problem of inclusions was examined during the thin section study. The greater part of the garnet grains contain many inclusions of quartz and less commonly sillimanite.

The 23 samples selected for further study were subjected to modal analysis, (See table 1) and the seven best specimens selected for the study of the spacial extent of local equilibrium in these rocks.

Sample locations and brief descriptions are given in Appendix 1.

TABLE 1. Modal Analyses of the Gneisses Selected for Equilibration Studies.

	1	2A	3	8	12	16	21	25	26	27	29	30	34	35
QUARTZ	10.5	27.1	21.1	7.3	30.7	38.2	43.1	25.7	15.6	31.5	16.5	67.2	28.5	8.3
K-FELDSPAR	35.2	17.5	13.6	16.3	3.9	1.1	14.0	24.5	25.8	11.1	32.5	2.2	15.6	49.3
PLAGIOCLASE	21.9	22.3	21.2	48.7	31.9	0.2	1.4	8.4	37.3	15.8	7.8	15.1	13.0	6.6
BIOTITE	15.6	2.7	3.7	12.6	10.5	12.3	23.9	7.6	11.2	19.6	3.5	11.9	9.1	13.1
GARNET	3.4	2.2	3.4	4.8	16.0	27.4	6.7	3.5	1.7	4.7	0.8	1.6	20.0	8.2
SILLIMANITE	-	x	Tr	-	-	1.6	0.2	8.8	0.1	0.2	4.4	x	6.2	5.1
OPAQUES*	2.6	7.1	8.3	5.2	1.7	1.3	0.9	4.5	7.1	4.4	4.3	1.7	2.7	4.8
CORDIERITE	8.5	20.3	28.5	1.8	3.6	9.0	-	16.3	0.4	9.9	26.8	-	3.7	1.8
ZIRCON	Tr	Tr	Tr	Tr	Tr	Tr	0.1	0.1	0.3	x	-	x	x	-
CHLORITE***	-	-	-	1.1	1.8	-	0.9	-	0.1	0.2	0.1	x	0.4	0.2
SPINEL	-	-	-	0.8	-	-	-	0.3	0.4	x	3.1	-	x	-
CARBONATE	-	Tr	-	-	-	0.1	0.1	-	-	-	-	-	-	0.9
CORUNDUM	-	-	-	-	-	-	-	-	0.1	-	-	-	-	-
LEUCOXENE **	-	-	-	-	-	-	-	0.6	-	2.1	0.1	-	-	-
MUSCOVITE	-	-	Tr	0.8	-	-	-	-	-	-	-	-	-	-
APATITE	-	-	-	-	-	-	Tr	-	-	-	-	-	-	-
SERICITE***	-	0.6	-	-	-	7.8	8.9	x	-	0.3	-	-	0.4	1.7
HEMATITE	1.9	-	-	-	-	-	-	-	-	-	-	x	-	-

* Magnetite, ilmenite and pyrite

0.05- x - 0.1

** alteration of ilmenite

Tr \leq 0.05

*** mainly as alteration of cordierite

- = missing

3.5 Chemical Composition of the Gneisses

Whole-rock spectrochemical analyses of the metasediments used in this study were made, Table 4. The analytical procedure employed was a method of mutual standardization as described by (Dennen and Fowler, 1955).

The method is designed as a rapid technique for reconnaissance whole-rock analysis. The 23 samples were analyzed in triplicate with fair precision in ten days. The precision is certainly good enough for comparison of rocks for most petrographic investigations.

The standard rocks G-1 and W-1 (Fairbain and others, 1951, Stevens and others, 1960) along with GR (Roubault et al., 1966) and SR Webber, 1965 were used as standards for the analysis. Both standards and samples (ground to - 200 mesh) were mixed with carbon powder in the ratio, sample: carbon = 1:2 and packed in "specpure" graphite electrodes. Excitation parameters are given in Table 2.

An examination of the precision and accuracy of the method was made by the analysis of rock standards. The data obtained from this study is given in Table 3.

TABLE 2. Operating Conditions for Whole-Rock Spectrographic Analysis by the Mutual Standard Method.

Spectrograph:	Hilger 3m large quartz-glass Littrow-mounted prism spectrograph.
Plates and Development:	Kodak Spectrum Analysis-1 plates developed for 4.5 minutes at 20 C in Kodak D-19 developer in a time controlled tank.
Electrodes:	Sample- National Carbon Co. AGKSP Spec-pure graphite rod with a 6.0 mm. cavity. Counter- National Carbon Co. L1138F Spec-pure carbon rod, pointed.
Excitation:	9 amp. anode to completion (60 sec.) 7mm. analytical gap.
Optical path:	Source focused on masked collimator. Rotating disc sector passing $1/2$, $1/16$, $1/32$, $1/64$ of incident light at slit.
Photometry and Plate Calibration:	Hilger non-recording microphotometer. Calibration by preliminary curve method. All intensities corrected for plate background.
Analytical lines:	Al 2652.5A, Mg2779.8A, Mn2794.8A, Fe 2912.2A, Si2987.6A, Ti3088.0A, Ca3158.9A Na3302.3A, K4044.1A

TABLE 3. Precision and Accuracy of the Mutual Standard Method of Spectrochemical Whole-rock Analysis

Granite GH						Granite GA					
	n	\bar{x}	2s	C	X ¹		n	\bar{x}	2s	C	X ¹
SiO ₂	12	76.5	1.2	1.6	75.6	SiO ₂	4	71.0	3.2	4.5	69.7
TiO ₂	12	0.06	0.007	20.6	0.08	TiO ₂	4	0.30	0.06	20.0	0.37
Al ₂ O ₃	12	12.5	1.4	11.2	12.6	Al ₂ O ₃	4	14.3	2.28	15.9	14.6
Fe ₂ O ₃ *	12	1.2	0.24	19.6	1.3	Fe ₂ O ₃ *	4	2.50	0.35	15.1	2.77
MnO	12	0.05	0.009	19.1	0.05	MnO	4	0.09	0.007	7.4	0.09
MgO	12	0.04	0.011	31.4	0.07	MgO	4	0.88	0.35	39.8	0.97
CaO	12	0.56	0.017	30.4	0.68	CaO	4	3.35	1.22	36.4	2.48
Na ₂ O	12	3.72	0.56	15.5	3.83	Na ₂ O	4	3.42	0.28	8.2	3.57
K ₂ O	12	5.15	0.65	12.6	4.78	K ₂ O	4	4.23	0.55	13.0	4.03
		100.00						100.80			

Basalt BR						Tonalite T-1					
	n	\bar{x}	2s	C	X ¹		n	\bar{x}	2s	C	X ²
SiO ₂	5	41.2	2.3	5.6	38.6	SiO ₂	8	64.6	2.6	4.05	62.5
TiO ₂	5	2.44	0.5	20.9	2.61	TiO ₂	8	0.52	0.08	15.4	0.59
Al ₂ O ₃	5	10.5	1.0	9.5	10.31	Al ₂ O ₃	8	15.6	1.4	9.1	16.5
Fe ₂ O ₃ *	5	14.8	0.96	6.5	12.75	Fe ₂ O ₃	8	5.4	0.3	4.8	4.02
MnO	5	0.25	0.03	12.0	0.20	MnO	8	0.11	0.01	9.1	0.11
MgO	5	13.1	4.4	33.6	13.2	MgO	8	2.96	0.64	21.7	1.89
CaO	5	13.2	1.8	13.6	13.89	CaO	8	6.31	1.24	19.7	5.19
Na ₂ O	5	3.6	0.9	25.0	3.07	Na ₂ O	8	3.42	0.27	7.9	4.39
K ₂ O	5	1.0	0.3	30.0	1.38	K ₂ O	8	1.36	0.40	30.6	1.23
		100.00						100.22			

The standard deviation and the coefficient of variation represent the 95% confidence limit.

* Total Fe as Fe₂O₃

X¹ - Preferred values given by Roubault et al. (1966)

X² - Preferred values given by Thomas (1963)

TABLE 4. Chemical Analyses of the Gneisses Selected for Equilibration Studies.

	1	2A	3	8	12A	12B	16	21	25	26	27	29	30	34	35
SiO ₂	63.8	67.0	55.2	61.3	66.1	68.1	69.6	71.4	65.0	58.0	60.2	66.1	80.4	61.9	59.1
TiO ₂	0.99	1.38	1.64	1.06	0.81	0.82	1.84	1.49	1.40	1.34	1.71	0.91	1.02	1.40	1.83
Al ₂ O ₃	16.8	14.4	20.7	18.1	13.4	13.0	9.62	11.3	17.1	16.1	17.0	17.6	8.08	17.2	18.2
Fe ₂ O ₃ *	6.36	6.74	10.9	8.36	6.49	6.18	11.7	6.45	6.95	7.11	9.91	7.22	5.12	5.56	6.82
MgO	2.51	2.33	3.59	2.43	4.25	3.41	5.85	3.17	2.02	1.49	4.16	2.65	1.49	2.70	2.80
MnO	0.11	0.06	0.09	0.06	0.11	0.13	0.18	0.15	0.03	0.10	0.12	0.05	0.04	0.03	0.06
CaO	2.89	0.66	2.24	0.71	3.40	3.10	0.62	0.85	0.40	5.28	2.94	0.56	1.05	2.00	0.68
Na ₂ O	2.42	1.20	2.11	3.57	2.69	2.74	0.13	0.21	1.64	2.89	1.21	1.42	1.01	2.39	1.88
K ₂ O	4.12	5.65	3.18	3.80	2.44	2.57	1.87	5.10	5.32	6.81	2.71	3.33	1.73	6.61	8.67

* Total Fe as Fe₂O₃

Sample descriptions and locations are given in Appendix 1; modal analyses in Table 1.

4 SAMPLE PREPARATION

4.1 Separation of the Minerals

16 specimens were selected for mineral analysis and were subjected to the following process: Each sample was cut into a cube, about 4.5 cm on a side, which removed any weathered exterior and reduced the sample to a size over which a local equilibrium seems to take place (Kretz, 1959, Moxham, 1965); the sample was then fed through a jaw crusher with the second pass producing a product about one-quarter inch in size; this material was then crushed in a hand percussion mortar of the type described by Smales and Wager (1960), and the screened fractions -60, +100; -100, +200 were then run through the procedure shown in the flow chart of Figure 5.

Initial rough separation of the biotite and garnet was performed on a Frantz isodynamic magnetic separator. Settings of the field strength, feed rate and inclination were determined by trial and error. The non-magnetic portions of these samples were passed on to other workers in the Cabot Spectrographic Laboratory for further study. After heavy liquid separations, the biotite-rich and garnet-rich fractions were recycled several times through the Frantz separator thus reducing the ilmenite and cordierite impurities to minute fraction. Final purification of the biotite samples was accomplished by sliding them back and forth between sheets of paper, the fraction retained on the paper each time being the final concentrate. Garnet samples were purified by removing impurities under a binocular microscope.

Because the garnet fractions may show many inclusions, further processing is necessary. The following steps (after Phinney, 1963) were adequate for the liberation and separation of the inclusions.

1. Grind in agate mortar.
2. Screen, collecting -200, +325; -325, +400 and -400 fractions.
3. Using a liquid close to the index of refraction of the mineral being separated, check each size fraction for liberation of inclusions.
4. If -400 fraction must be used, place small portions of it in a 100 ml. beaker with a wash bottle squirt acetone into the beaker until the sample is well stirred. After five seconds decant the acetone. Continue this procedure until the acetone remains clear after five seconds.

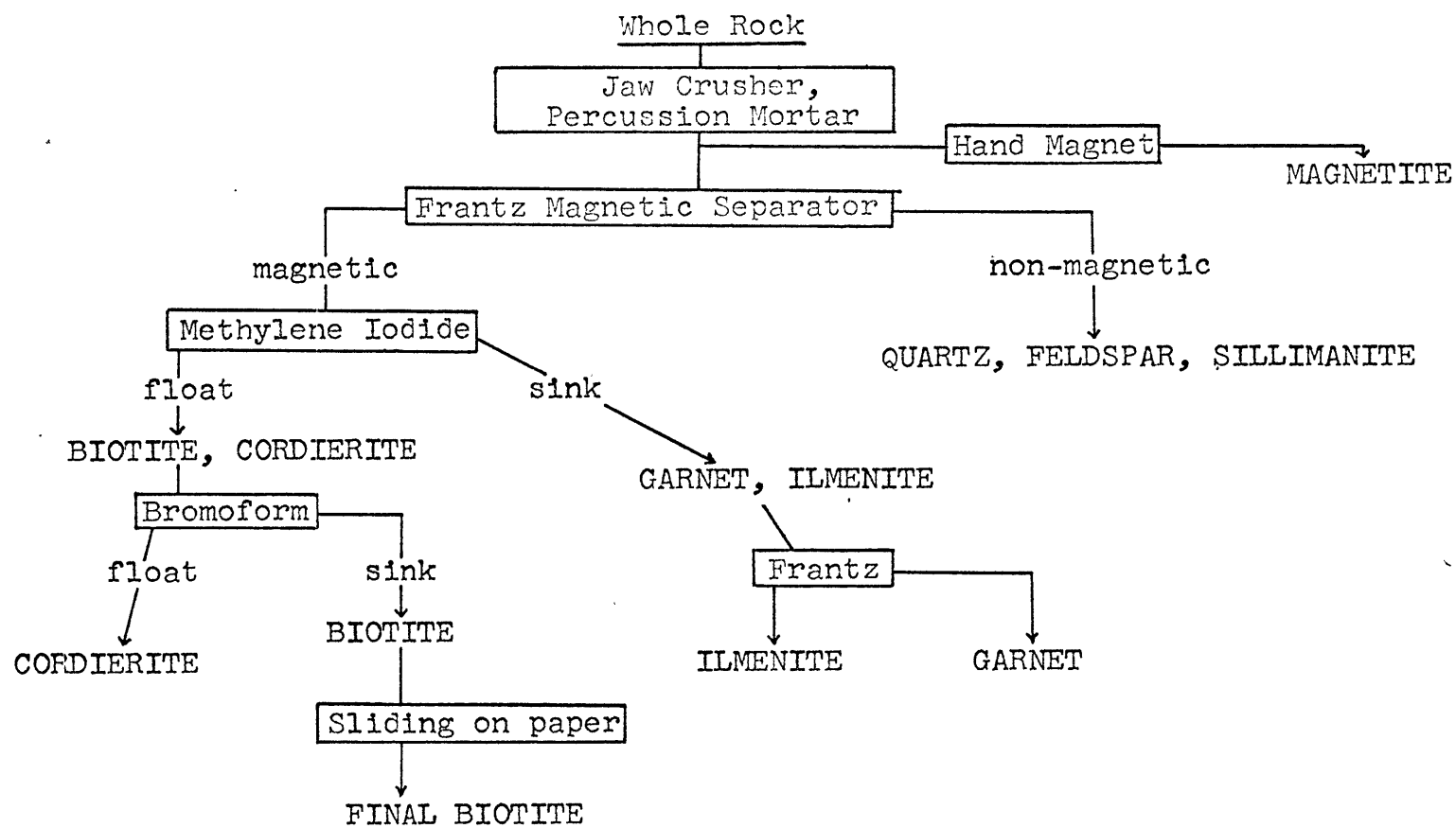


FIGURE 5. Flow Chart for Mineral Separations.

The remaining grains are coarse enough to pass through the Frantz separator.

5. Pass the coarsest fraction in which the inclusions are liberated through the Frantz separator. After several passes, the samples are quite pure.

4.2 Purity of Mineral Separates

All of the separated mineral samples were checked under the petrographic microscope in a liquid whose index of refraction was close to that of the mineral in question. Grain counts of 500 were made on all samples, and samples which were not at least 98% pure were re-run through appropriate steps until the desired purity was attained. Because of the very fine inclusions of quartz and sillimanite in some of the garnets, some of these samples may contain over 2% total quartz and sillimanite. Impurities in the biotite were tiny inclusions of ilmenite, quartz and zircon, their total not exceeding 2% in any sample.

4.3 Preparation of Minerals for Analysis

The biotite samples, after separation, were prepared for chemical analysis by treating about 0.25 grams of sample with vycor-distilled perchloric acid and 48% reagent grade HF. After decomposition, the samples were evaporated to dryness and taken up to 100 ml. in 0.2N HCL.

The garnets were placed into solution using a sodium carbonate fusion technique as described by Kolthoff and Sandell, (1952). Approximately 0.6 grams of garnet, reduced to -325 mesh, was mixed with 3.0 grams of Na_2CO_3 and fused in a platinum crucible. The resulting cake was dissolved in 2N HCL and evaporated to dryness. The evaporate, after dissolution in 0.2N HCL, was filtered into a 100 ml. volumetric flask and brought up to volume.

Suitable dilutions were made from the sample solutions for the various elemental analyses by atomic absorption spectrophotometry. Brief discussions of the procedures used for the analysis of each element determined are given below. In all cases the solutions were in 0.2N HCL. The importance of maintaining dilute solutions of constant normality was pointed out during experiments in the Geochronology Laboratory at M.I.T. It was found that the absorbance for a certain concentration drops off sharply with increasing normality of the acid solution. Aside from the sensitivity of the spectrophotometer, linearity of the working curve is almost non-existent at higher normalities, (P. Kolbe and W.H. Pinson, personal communication, 1966).

5 CHEMICAL ANALYSIS

5.1 Introduction, Instrumentation and Techniques

The garnets and biotites, separated and dissolved as described above were analyzed in at least two replicates by means of atomic absorption spectrophotometry. Partial analyses for Fe, Mg, Mn, Ca, Cr, Co, and Ni were made using, for the most part, standard techniques as described in the literature (Slavin, 1965, Trent and Slavin, 1964).

A Perkin-Elmer model 303 atomic absorption spectrophotometer was used, employing single element hollow-cathode tubes for Fe, Mg and Ca and a multi-element hollow-cathode tube for Mn, Cr, Co and Ni. Instrumental operating parameters are outlined in Table 5.

Standards for Fe, Mg, Ca, Cr, Co and Ni were pure salt solutions made by dissolving high purity compounds of the element in 2N HCL, evaporating to dryness and redissolving in 0.2N HCL. Standards for most elements were prepared in two different ways for cross-checking purposes. As a result of this, matrix effects in atomic absorption spectrophotometry of silicates were found to be negligible, if at all present. For example, magnesium standards were prepared by P. Kolbe by dissolving the standard diabase W-1 (Fairbairn, et al., 1951) by the perchloric acid HF method described above. This primary standard, originally in 2N HCL, was diluted with demineralized water to a normality of 0.2 and a series of standards prepared containing 0.5 to 2.0 $\mu\text{g/ml}$ Mg. Further standards were prepared by the author from a magnesium standard obtained commercially (Will Scientific Company, Lot #W-84212, 1000 $\mu\text{g/ml}$). A portion of the commercial standard was evaporated to dryness in a platinum dish and redissolved on 0.2N HCL. A series of magnesium standards from 2.5 to 5.0 $\mu\text{g/ml}$ was prepared from this primary standard. The resulting working curve for magnesium, incorporating both sets of standards, is shown in Figure 6. Clearly a matrix effect is missing or negligible.

TABLE 5. Operating Parameters for the Atomic Absorption Spectrophotometric Determinations.

ELEMENT	WAVE LENGTH	LAMP	LAMP CURRENT	SLIT WIDTH	FLAME CHARACTER
Fe	2483A	Hollow Cathode	40ma	2A	Oxidizing
Mg	2852A	Hollow Cathode	6ma	20A	Acetylene-rich
Mn	2795A	Hollow Cathode*	30ma	20A	Oxidizing
Ca	4227A	Hollow Cathode	10ma	13A	Acetylene-rich
Cr	3579A	Hollow Cathode*	30ma	2A	Oxidizing
Co	2407A	Hollow Cathode*	30ma	2A	Oxidizing
Ni	2320A	Hollow Cathode*	30ma	2A	Oxidizing

* Multi -element hollow cathode lamp.

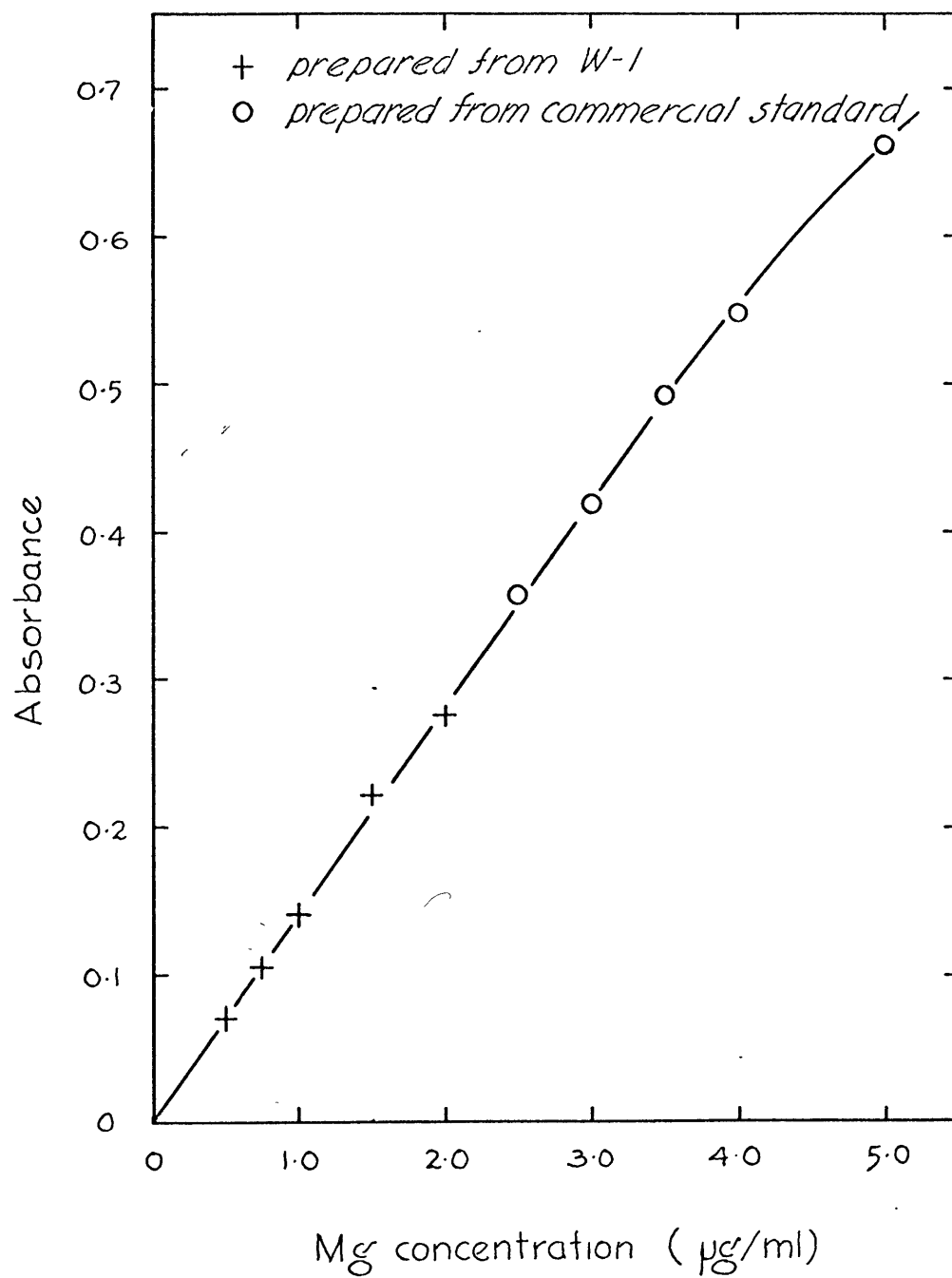


FIGURE 6. WORKING CURVE FOR MAGNESIUM

5.2 Preparation of Standards (See Table 5)

Calcium and Magnesium

Calcium standards were prepared by dissolving CaCO_3 , A.R. grade, in 2N HCL and diluting up to volume making a solution containing $400 \mu\text{g/ml}$ Ca. Further dilution of this primary standard to lower normality of 0.2 was made and a series of standards from 2.0 to 20.0 Ca was made.

Magnesium standards were prepared both from diabase W-1 and Will Scientific Company Atomic Absorption Standard as described above.

All calcium and magnesium standard and sample solutions were made to contain 0.5% La as LaCl_3 . A 10% La solution was prepared by dissolving the required amount of La_2O_3 (City Chemical Corp.) in 2N HCL, evaporating and redissolving in 0.2N HCL.

Figure 6 gives an example of the magnesium working curve. The calcium working curve is shown in Figure 7.

Iron

The primary iron standard was prepared by the dissolution of iron wire, A.R. grade, in HCL and bringing up to volume to make a $514.3 \mu\text{g/ml}$ Fe solution in 2N HCL. Further dilutions with demineralized H_2O gave a series of standards ranging from 5 to $25 \mu\text{g/ml}$ Fe in 0.2N HCL. Chloride complexing at this normality was not noted.

An example of the iron working curve is shown in Figure 9.

Manganese

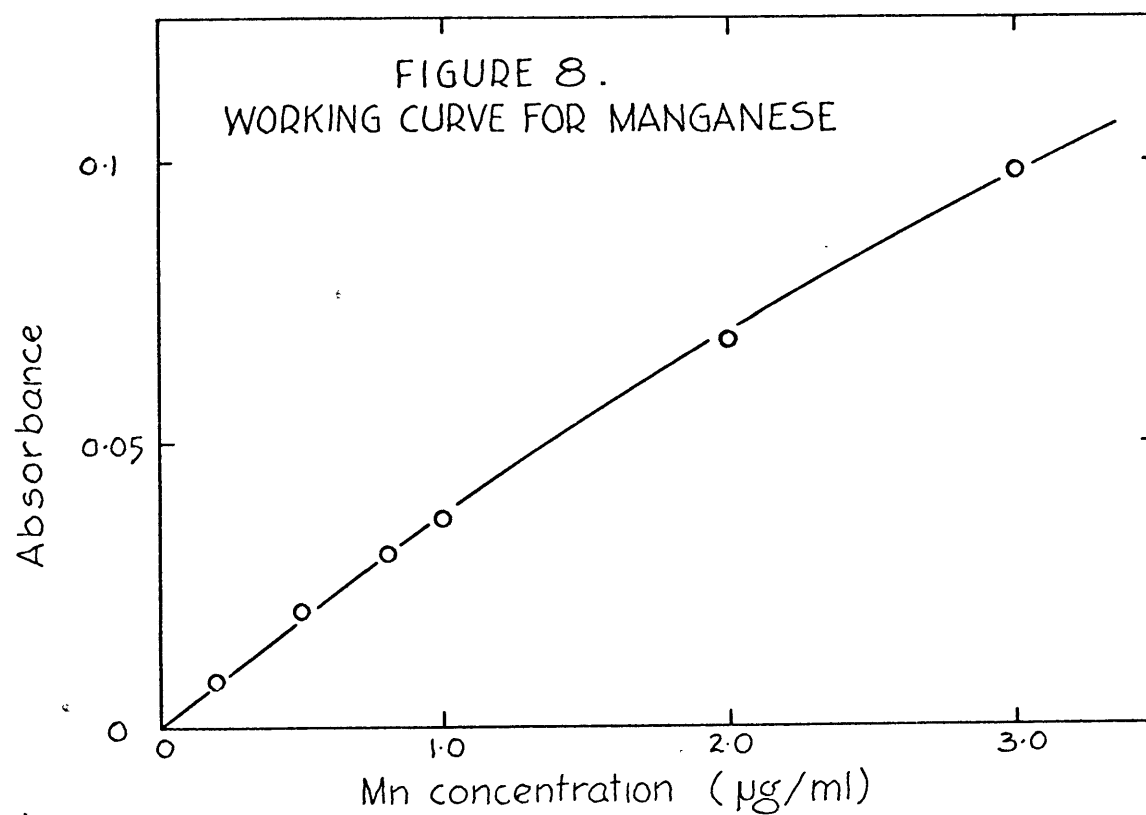
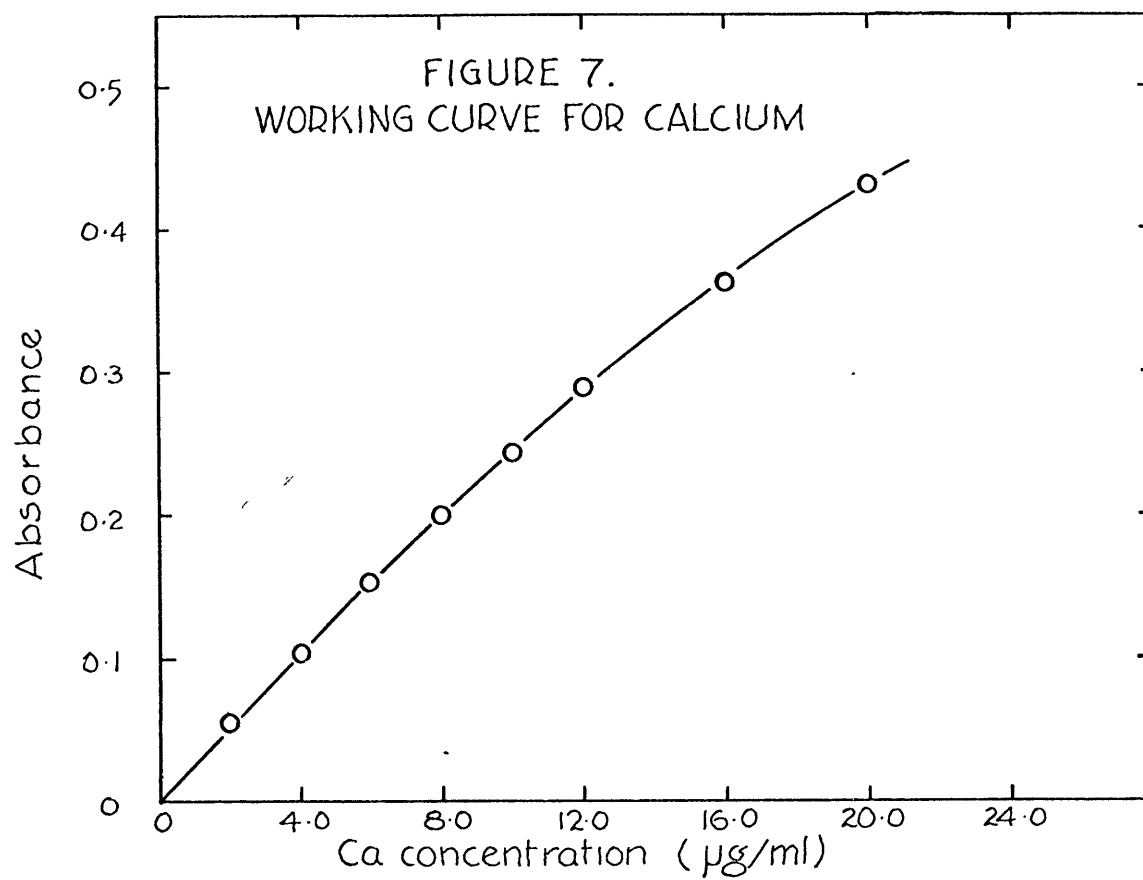
Manganese standards were prepared from the Will Scientific Company Mn Atomic Absorption Standard (Lot #W-84287, $1000 \mu\text{g/ml}$ Mn). A $1000 \mu\text{g/ml}$ primary solution was prepared by evaporating the required amount of the Will Standard in platinum and bringing up to a volume in 0.2N HCL.

A typical manganese working curve is shown in Figure 8.

Cobalt

A 100 ppm cobalt primary standard was made from hydrous cobalt chloride $\text{CoCl}_2 \cdot 6\text{H}_2\text{O}$. A second cobalt standard was prepared from the Fisher Scientific Company Atomic Absorption Co Standard (Lot #762325, $1000 \mu\text{g/ml}$ Co).

Figure 11 shows the cobalt working curve.



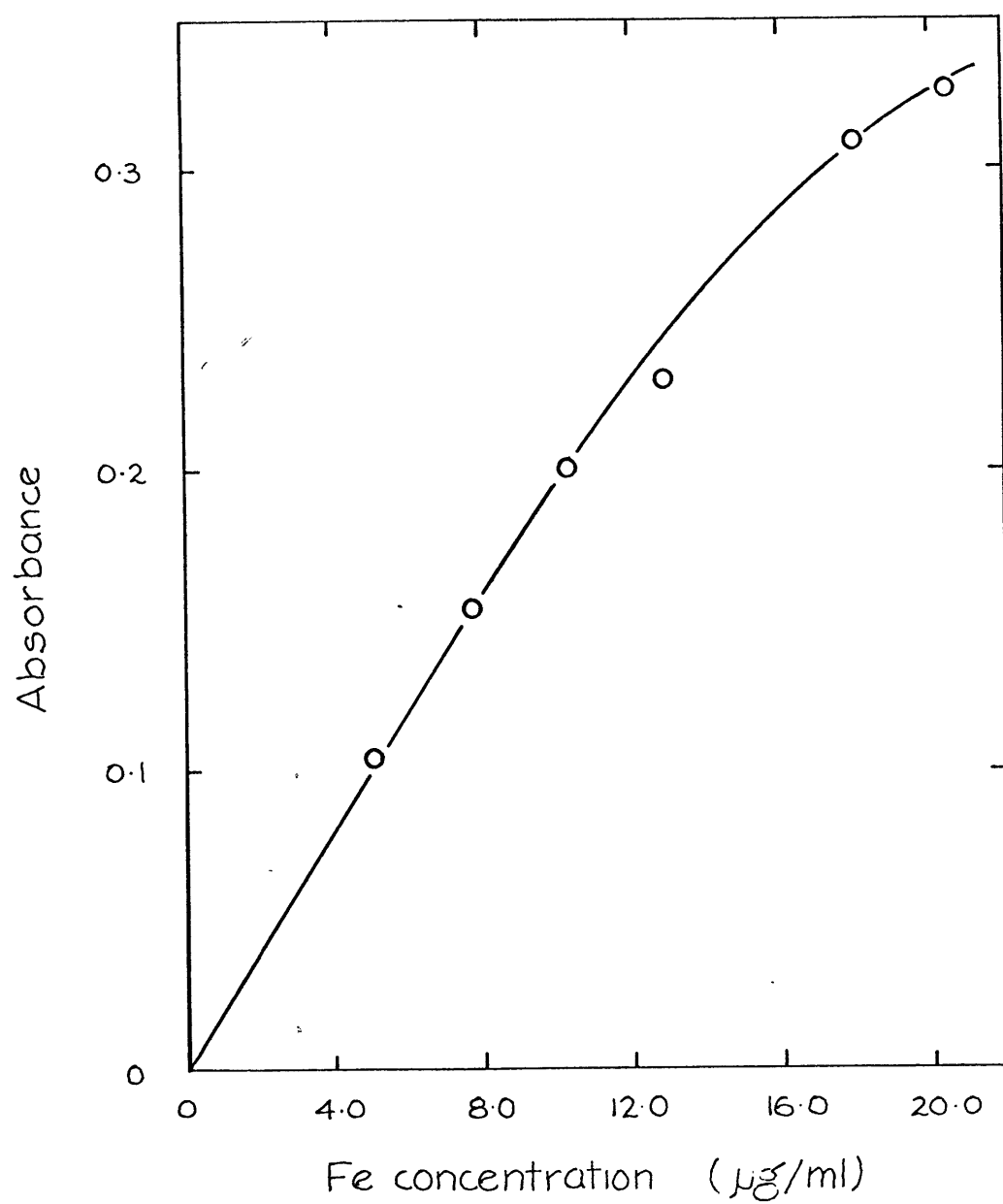


FIGURE 9. WORKING CURVE FOR IRON

Chromium

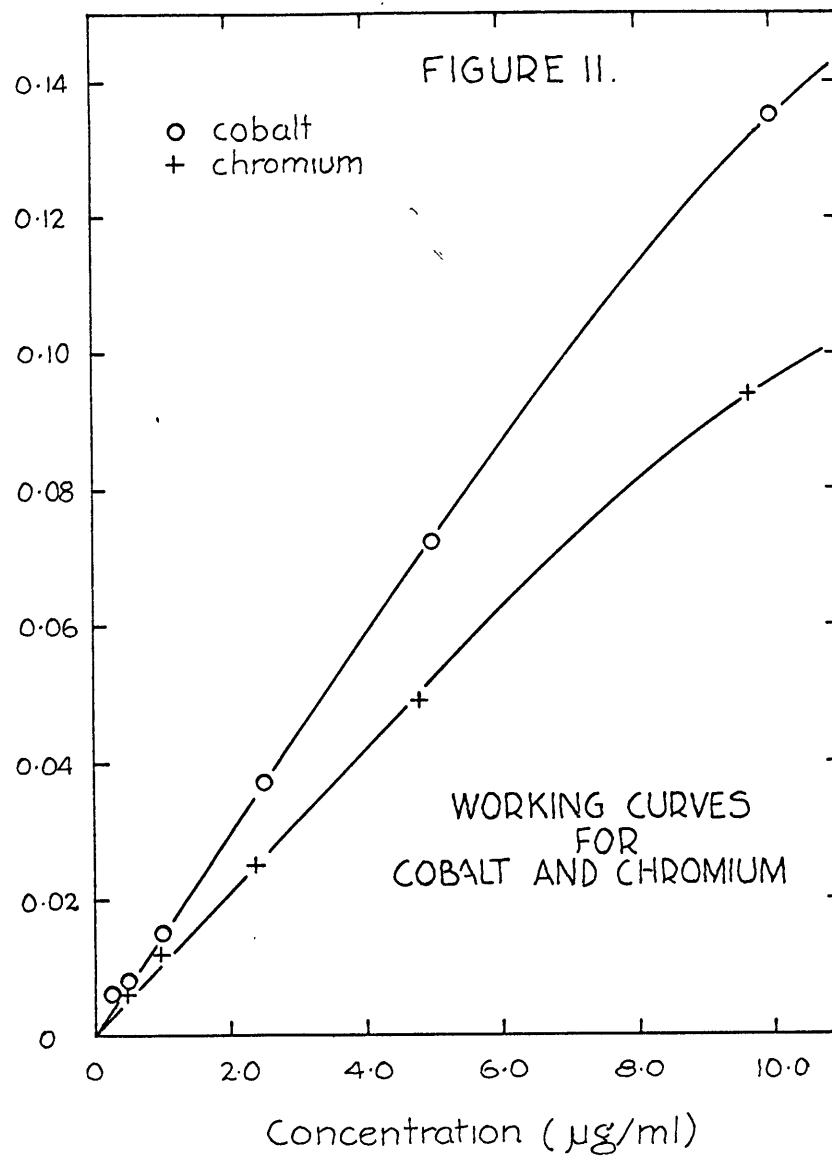
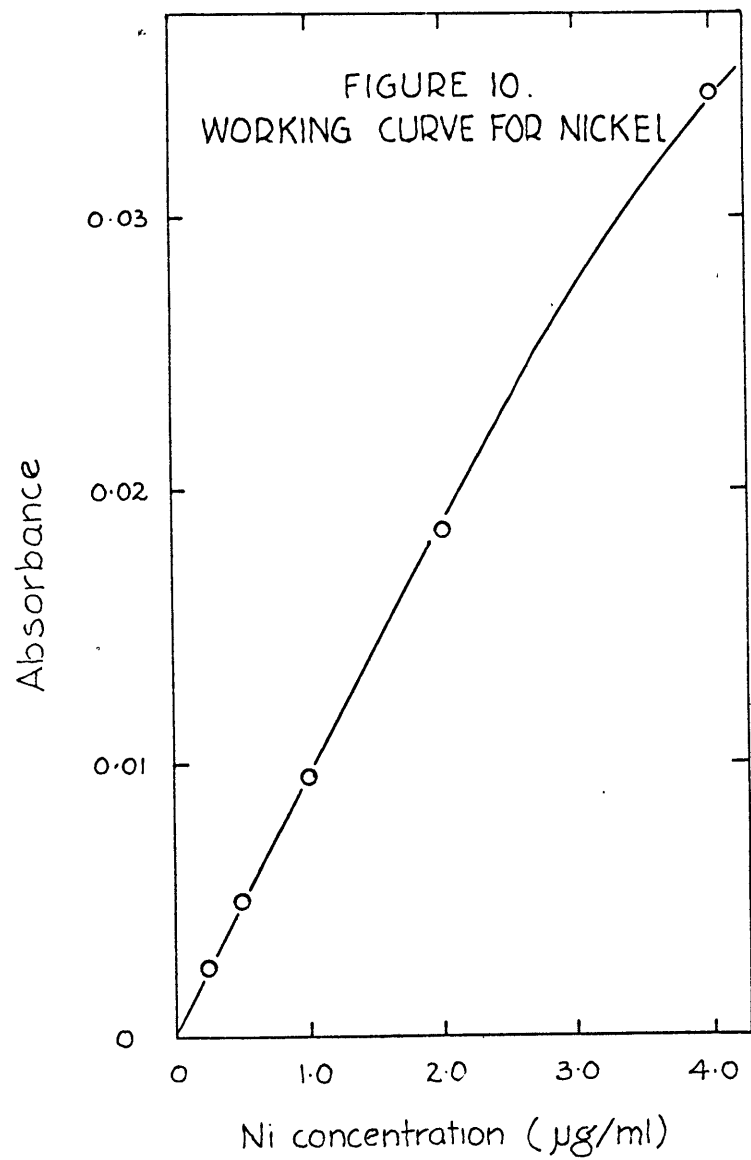
Two chromium standards were prepared from $K_2Cr_2O_7$; one by the author and the other commercially made by the Fisher Scientific Company (Lot #762397, $1000 \mu g/ml$).

Figure 11 shows the chromium working curve.

Nickel

Nickel standards were prepared from the Fisher Scientific Company Atomic Absorption Ni Standard (Lot #751172, $1000 \mu g/ml$).

An example of the nickel working curve is shown in Figure 10.



5.3 Interferences

No interferences were noted in the analysis of the biotites or rock standards. The modulated sharp line source employed by the atomic absorption spectrophotometer eliminates spectral interference. The theoretical reasons for this have been discussed by (Elwell and Gidly, 1962).

A chemical interference due to complexing by silicon, phosphorus and aluminum in the analysis of the alkaline earth metals has been noted, David (1958, 1962). However, silicon is eliminated as SiF_4 during the dissolution of the biotite and rock samples. Following fusion of the garnets, the resulting cake was dissolved in HCL twice, the solution evaporated, the silica gel produced being filtered off after each evaporation. This is part of the usual gravimetric procedure for the determination of SiO_2 .

The concentration of phosphorus was probably too low to interfere with the magnesium and calcium analysis, and the aluminum interference was eliminated by the use of lanthanum buffer.

Light scattering interferences of the type and magnitude as found by Billings, (1965) were not found during the biotite and rock analyses. Billings noted light scattering interference by calcium for the most part but also by sodium and magnesium at high concentrations at the iron, cobalt, manganese and nickel analytic lines. The lack of this effect was probably due to the use of the higher temperature air-acetylene flames and higher fuel and air flows than those used by Billings (Slavin, 1965). A light scattering effect due to the high sodium contents of the garnet solution was, however, noted. It was possible to correct for this by the use of a blank solution prepared in the same manner as the garnet fusions.

The elimination of critical interferences in the analytic ranges may be noted by the linearity of the working curves over a considerable concentration range.

5.4 Precision and Accuracy

The precision and accuracy of routine analysis atomic absorption spectrophotometry has been discussed by Meddings and Kaiser, (1967) and Billings, (1965). [REDACTED] By use of atomic absorption equipment, including the Perkin-Elmer digital readout system DCR-1, Meddings and Kaiser found that the routine analysis of Ni, Co, Ca and Fe shows a coefficient of variation of 0.3 - 0.8%. However, Billings, (1964) found analytic precision somewhat lower. For example, the analysis of a biotite sample gave the following precision data shown as $\pm\%$ of the amount present: Ca, 2, Co, 7, K, 1, Mg, 1, Ni, 7. The precision of the whole rock analysis of G-1 and W-1 by Trent and Slavin, (1964) are quite satisfactory.

Accuracy data given by Trent and Slavin, (1964) on G-1 and W-1 and Billings, (1965) on many varied silicate samples are quite satisfactory for geochemical studies.

Chemical and statistical data derived from this work on standard rocks and minerals are given in Table 6. Except where indicated the following summarizes the statistical terminology used.

- n, number of observations
- \bar{x} , arithmetic mean
- d, deviation of an observation from the mean
- \bar{s} , standard deviation $= \pm \sqrt{\frac{d^2}{n-1}}$
- c, coefficient of variation $= \frac{\bar{s}}{\bar{x}} \times 100$

It is obvious that the precision of silicate analysis by atomic absorption spectrophotometry is not as ^{good} [REDACTED] as gravimetric or most colorimetric techniques. However, its precision may be expected to be an improvement over that obtained in the emission spectrographic techniques usually employed in studies such as these (Kretz, 1959, 1961, Moxham, 1960). The author found that the method of silicate analysis by atomic absorption spectrophotometry combined the speed of quantitative optical emission spectrography with a precision comparable to routine analysis by x-ray fluorescence means.

Statistical data for the biotite and garnet analyses of this paper are given with the analytical results in a following paragraph.

TABLE 6. Chemical and Statistical Data on Standard Rocks and Minerals.

	n	\bar{x}	W-1 s	C	X ¹		n	\bar{x}	G-1 s	C	X ¹
Fe ₂ O ₃ *	7	11.17	0.32	2.9	11.14	Fe ₂ O ₃ *	8	1.89	0.16	8.5	1.96
FeO	3	8.95	0.25	2.8	8.75	FeO	3	0.96	0.11	11.4	0.09
MgO	10	6.41	0.14	2.2	6.64	MgO	5	0.36	0.02	6.2	0.40
CaO	7	10.62	0.19	1.8	10.98	CaO	4	1.16	0.03	2.6	1.39
MnO	5	0.185	0.017	9.2	0.16	MnO	N.D.				
Co	4	56	4	8	51	Co	N.D.				
Cr	4	134	20	15	120	Cr	2	23 ⁺	8	34	22
Ni	4	85	9	11	82	Ni	N.D.				
	n	\bar{x}	SR s	C	X ²		n	\bar{x}	T-1 s	C	X ³
Fe ₂ O ₃ *	9	8.03	0.35	4.4	8.39	Fe ₂ O ₃	7	5.74	0.37	6.4	5.93
FeO	N.D.					FeO	N.D.				
MgO	8	4.00	0.10	2.5	4.06	MgO	4	1.73	0.03	1.7	1.90
CaO	3	10.08	0.17	1.7	10.1	CaO	3	4.85	0.06	1.2	5.18
MnO	5	0.407	0.014	3.4	0.40	MnO	2	0.13	0.026 ⁺	20.0 ⁺	0.10
Co	2	22	7 ⁺	32	19	Co	N.D.				
Cr	3	77	6 ⁺	8	51	Cr	N.D.				
Ni	2	35	9 ⁺	25	37	Ni	N.D.				

N.D.=Not Determined

X¹ = Preferred values from Stevens et al. (1960)X² = Preferred values from Webber (1965)X³ = Preferred Values from Thomas (193)

Biotite 1337B						Biotite 1325A					
	n	\bar{x}	s	C	N [#]		n	\bar{x}	s	C	N [#]
Fe ₂ O ₃	2	23.52	0.19	0.8	25.25		5	16.95	0.99	5.8	16.85
MgO	3	6.84	0.16	2.3	6.95		3	12.05	0.06	0.5	12.22
MnO	N.D.						N.D.				
CaO	2	0.08	0.004	5,2	0.29		N.D.				

TABLE 6. Continued

The biotite samples were obtained from H.C. Liese, U. Conn.

N[#] = Chemical Analysis by Elaine Munson, U.S.G.S., Denver, Colo.

5.5 Determination of FeO

The determination of FeO in the garnet and biotite samples was performed using the titration method of Reichen and Fahey, (1962). The dissolution of the sample took place in the presence of a standard solution of $K_2 Cr_2 O_7$ with the excess dichromate being titrated with standard ferrous ammonium sulphate.

Results of analysis of the standards G-1, W-1 and T-1 are given in Table 6 together with data on precision and accuracy. Somewhat higher values are obtained by this method than by conventional methods, since the Fe^{+2} liberated during dissolution is immediately oxidized by the dichromate in the solution and the source of error by air oxidation found in most conventional methods is eliminated, Reichen and Fahey, (1962). However, it is possible that other elements such as manganese are oxidized along with Fe^{+2} , which would also contribute to ^{high} results.

5.6 Analytic Results

As described above, 16 specimens of Grenville gneiss were selected for mineral analysis. The reference number of each specimen and the minerals observed and analyzed are listed in Table 7. The analysis of the garnets and biotites are listed in Table 8 and 9 respectively.

Although garnet and biotite are chemically complex and cannot be expected to behave ideally with reference to all components, they do closely approximate ideal solutions with respect to the elements in question in this study. Judging from the studies of previous workers, the elements Fe^{+2} , Mg, Mn, Cr, V, Ni and Co seem to equilibrate most easily and correlate very closely to what should be expected from crystal field theory as discussed by Curtis (1964). It was decided then to use atomic ratios as measures of concentration in this study. The calculations of these ratios will be considered briefly at this time.

The 8-coordinated positions of garnet are occupied by Fe^{+2} , Mg^{+2} , Mn^{+2} , and Ca^{+2} . Al^{+3} and Fe^{+3} take up the 6-coordinated positions. The measure of concentration, then, of divalent elements in garnet should be the ratio of the number of atoms of the element divided by the total number of available 8-coordinated positions. However, since Ca-O distances are greater (2.40 Å and 2.36 Å) than the (Fe,Mg,Mn)-O distances (2.40 Å and 2.3 Å), Ca and (Fe,Mg,Mn) probably do not form ideal mixtures. In this study, the measure of concentration of divalent anions in garnet will be as follows: the total number of atoms of the element/total number of 8-coordinated positions minus the number of positions occupied by Ca ions.

The 6-coordinated positions of biotite are occupied by Fe^{+2} , Fe^{+3} , Mg^{+2} and part of the total Al^{+3} Bragg, (1937) and probably also by Mn^{+2} and Ti^{+2} . It was decided to consider only those 6-coordinated positions occupied by the divalent ions Fe^{+2} , Mg^{+2} , Mn^{+2} plus those positions occupied by Fe^{+3} .

Moxham (1965) points out the use of calculating the proportion of atomic sites filled by a minor element, out of the number of sites available to that element. An attempt was originally made to consider only the weight percent of the element dissolved in each phase (after Kretz, 1959) but this produced an extreme scatter.

No.	GARNET	BIOTITE	CORDIERITE	PLAGIOCLASE	K-FELDSPAR	QUARTZ	SILLIMANITE	MUSCOVITE	ZIRCON	MAGNETITE	ILMENITE	SPINEL
1	0	0	X	X	X	0	-	-	X	X	X	-
2A	0	0	X	X	X	0	X	-	X	X	X	-
3	0	0	X	X	X	0	X	X	X	X	X	-
8	0	0	X	X	X	0	-	X	X	X	X	X
12A	0	0	X	X	X	0	-	-	X	X	X	-
12B	0	0	X	X	X	0	-	-	X	X	X	-
16	0	0	X	X	X	X	X	-	X	X	X	-
21	0	0	X	X	X	0	X	-	X	X	X	-
25	0	0	X	X	X	0	X	-	X	X	X	X
26	0	0	X	X	X	0	X	-	X	X	X	X
27	0	0	X	X	X	0	X	X	X	X	X	X
29	0	0	X	X	X	0	X	X	-	X	X	X
30	0	0	-	X	X	X	X	-	X	X	X	-
34	0	0	X	X	X	0	X	X	X	X	X	X
35	0	0	X	X	X	0	X	-	-	X	X	-

TABLE 7.

Mineral Assemblages of Grenville
Gneisses Selected for Chemical De-
terminations on the Coexisting Minerals

0 Mineral analyzed

X Mineral present

- Mineral absent

TABLE 8. Chemical Determinations on Garnet from the Grenville Gneisses.

	1	2A	3	8	12A	12B	16	21	25	26	27	29	30	34	35
Fe ₂ O ₃	1.40	*	*	*	1.72	5.21	*	4.96	4.00	1.39	*	3.76	1.04	3.45	4.22
FeO	29.37	28.76	27.75	28.45	25.87	25.32	33.63	31.42	34.11	32.79	32.06	30.69	31.61	23.56	22 87
MgO	9.36	6.82	5.08	6.04	10.94	10.74	8.67	7.24	5.25	6.11	4.50	5.62	6.24	7.11	6.43
MnO	2.25	1.41	1.31	0.75	2.78	1.94	0.50	2.32	0.43	1.31	1.39	0.91	1.42	0.39	0.40
CaO	1.34	1.42	1.01	1.31	1.62	1.19	1.65	1.79	0.97	1.38	1.26	1.49	1.60	0.95	0.85
Cr ₂ O ₃	0.018	0.017	0.013	0.020	0.017	0.015	0.025	0.026	0.021	0.008	0.020	0.019	0.024	0.032	0.028
CoO	0.008	N.D.	0.008	0.006	0.008	0.008	0.009	0.005	0.006	0.004	0.008	0.007	0.002	0.007	0.006
NiO	0.007	0.011	0.005	0.002	0.007	0.013	0.004	0.010	0.010	0.005	0.007	0.002	0.012	0.009	0.011
Atomic Ratios:															
$\frac{\text{Fe}}{\text{Fe}+\text{Mg}+\text{Mn}}$	0.608	0.679	0.728	0.711	0.537	0.545	0.678	0.673	0.777	0.728	0.772	0.738	0.715	0.644	0.658
$\frac{\text{Mg}}{\text{Fe}+\text{Mg}+\text{Mn}}$	0.345	0.287	0.238	0.269	0.404	0.412	0.312	0.277	0.213	0.243	0.194	0.240	0.252	0.345	0.331
$\frac{\text{Mn}}{\text{Fe}+\text{Mg}+\text{Mn}}$	0.047	0.034	0.035	0.019	0.058	0.042	0.010	0.050	0.010	0.029	0.034	0.022	0.033	0.011	0.012
$\frac{\text{Ca}}{\text{Fe}+\text{Mg}+\text{Mn}+\text{Ca}}$	0.034	0.041	0.033	0.040	0.040	0.032	0.041	0.047	0.028	0.038	0.037	0.044	0.045	0.032	0.030

N.D. = not determined

* = total Fe as FeO

TABLE 9. Chemical Determinations on Biotite from the Grenville Gneisses.

	1	2A	3	8	12A	12B	16	21	25	26	27	29	30	34	35
Fe ₂ O ₃	1.16	*	*	*	1.36	2.09	*	2.36	1.02	1.17	2.06	*	0.30	0.46	1.77
FeO	13.10	15.81	14.62	14.47	12.45	12.42	22.44	14.51	16.93	17.34	14.40	19.10	25.35	12.47	12.45
MgO	13.76	13.35	13.61	13.10	13.73	13.60	14.64	11.11	10.28	10.46	11.37	13.26	9.75	12.90	11.61
MnO	0.065	0.065	0.068	0.042	0.100	0.082	0.022	0.056	0.031	0.051	0.089	0.055	0.045	0.018	0.021
CaO +	0.15	N.D.	N.D.	N.D.	0.10	0.09	N.D.	0.12	0.13	0.08	0.10	N.D.	0.21	0.07	0.08
Cr ₂ O ₃	0.026	0.029	0.030	0.065	0.020	0.022	0.061	0.036	0.051	0.014	0.022	0.023	0.030	0.013	0.049
CoO	0.015	0.018	0.022	0.026	0.014	0.014	0.015	0.004	0.013	0.009	0.020	0.079	0.005	0.011	0.011
NiO	0.023	0.042	0.042	0.063	0.019	0.024	0.041	0.039	0.035	0.011	0.023	0.005	0.014	0.010	0.020
TiO ₂ +	3.79	N.D.	N.D.	N.D.	3.20	3.30	N.D.	2.99	3.40	3.18	N.D.	N.D.	4.18	3.15	3.07

Atomic Ratios:

$\frac{\text{Fe}}{\text{Fe}+\text{Mg}+\text{Mn}}$	0.343	0.399	0.375	0.382	0.330	0.329	0.462	0.411	0.474	0.474	0.403	0.429	0.591	0.350	0.366
$\frac{\text{Mg}}{\text{Fe}+\text{Mg}+\text{Mn}}$	0.642	0.599	0.624	0.617	0.651	0.644	0.538	0.561	0.512	0.510	0.568	0.532	0.405	0.644	0.610
$\frac{\text{Mn}}{\text{Fe}+\text{Mg}+\text{Mn}}$	0.0017	.0016	.0018	.0011	.0027	.0023	.0004	.0016	.0009	.0014	.0026	.0013	.0011	.0005	.0006

N.D. = Not Determined

* = Total Fe as FeO

+ = Determination by emission spectrography

Calculations were then performed producing the atomic ratios of the trace elements in question (Cr,Co,Ni) with the following substitutions in mind:

1. In biotite 6-coordinated positions - Cr, Co, Ni
2. In garnet 8-coordinated positions - Cr, Co, Ni

These data are represented in Tables 8 and 9 and the distributions illustrated and discussed in the following section.

6 ELEMENT FRACTIONATION BETWEEN COEXISTANT MINERALS

6.1 Introduction

Some data relating to the chemistry of the gneisses of the Ganonoque - Westport area has been published (Wynne-Edwards and Hay, 1963). For most elements, however, they had too little information to draw conclusions as to the extent of equilibrium in those rocks. The determinations made on the 15 samples of this study are combined with the data of Wynne-Edwards and Hay and presented graphically in the next section, in some cases, e.g., the distribution of nickel between biotite and garnet, the combined data provides information not available in their study.

The distribution diagrams employed here are similar to those used by Kretz, (1959) and Wynne-Edwards and Hay, (1963) so that a direct comparison may be made. Data taken from their paper is shown in Table 10.

TABLE 10. Chemical Data on Coexisting Garnets and Biotites
from Wynne-Edwards and Hay (1963).

	BIOTITE						GARNET				
	H-29	H-66	H-70	H-126	WE-4	-	H-29	H-66	H-70	H-126	WE-4
Fe ₂ O ₃	4.27	2.81	7.65	4.31	4.39		4.53	5.27	4.62	3.22	4.49
FeO	14.62	15.75	15.10	13.61	16.11		24.68	26.13	23.50	26.36	28.17
MgO	9.70	8.70	8.40	8.20	7.60		6.70	7.10	5.67	7.95	6.54
MnO	0.02	0.05	0.13	0.06	0.08		0.10	0.56	0.80	0.84	0.85
CaO	Tr	Tr	Tr	Tr	Tr		1.50	1.89	1.45	1.64	1.51
Cr ₂ O ₃	0.053	0.034	0.028	0.036	0.016		0.012	0.011	0.009	0.012	0.008
CoO	0.014	0.009	0.012	0.013	0.010		0.006	0.005	0.005	0.006	0.005
NiO	0.026	0.018	0.012	0.016	0.010		0.002	0.005	0.002	0.003	0.011
Atomic Ratios:											
X _{Fe}	0.432	0.484	0.449	0.404	0.509		0.673	0.664	0.684	0.637	0.693
X _{Mg}	0.510	0.477	0.445	0.434	0.427	.	0.325	0.321	0.293	0.342	0.286
X _{Mn}	0.0006	0.0015	0.0038	0.0017	0.0025		0.0027	0.014	0.023	0.021	0.021

6.2 The Distribution of Fe^{+2} , Mg and Mn between Garnet and Biotite

The distribution of Fe^{+2} is shown in Figure 12. Here the atomic ratio $\text{Fe}^{+2} / (\text{Fe}^{+2} + \text{Mg} + \text{Mn})$ for garnet is plotted against the ratio $\text{Fe}^{+2} / (\text{Fe}^{+2} + \text{Fe}^{+3} + \text{Mg} + \text{Mn})$ for biotite. The data, although showing a possible regular distribution, is quite scattered. This is in accordance with the observations of (Kretz, 1959, Wynne-Edwards and Hay, 1963). Kretz observed a correlation between the distribution of Fe and Mg between garnet and biotite and the Mn content of garnet and was able to define the various distribution coefficients on this basis. No such chemical correlation was observed in this study. There is, however, a slight inverse correlation between the distribution coefficient $K_{\text{Fe}}^{\text{Gar/Bio}}$ and the modal ratio cordierite/biotite + garnet + cordierite. The various groupings are more easily recognized by plotting the molecular ratio FeO/MgO for the garnet vs. the molecular ratio $\frac{\text{FeO}}{\text{MgO}}$ for biotite. (Figure 12A). Three reasonable distinct groups of distribution coefficients may then be noted according to amounts of cordierite present. Samples 8 and WE-4-58 are erratic for no obvious reason, although zoning of the garnet of sample 8 has been noted (see Section 9.7).

The distribution of magnesium between garnet and biotite (Figure 13) shows essentially the same scatter as that for iron. This is expected as Fe and Mg form the larger part of the atoms in the group (Fe + Mg + Mn). A closer estimation of the distribution of Fe and Mg would require a more extensive range of iron and magnesium concentrations and Fe/Mg ratios.

The manganese distribution between garnet and biotite is shown in Figure 14. A much greater range of atomic ratio values is exhibited here, and although there is considerable scatter, a regular distribution is obvious. The distribution coefficient $K_{\text{Mn}}^{\text{Bio/Gar}}$ 22 as compared to the value of 30 obtained by Kretz possibly indicating a different grade of metamorphism in the Ganonoque rocks Miyashiro, (1953). Chinner, (1960) however, has shown that the manganese content of garnet may be controlled significantly by the original oxidation state of the rock. Kretz, (1960) also states that the Mn distribution between garnet and biotite in the rocks of southwestern Quebec was controlled by the Fe/Mg ratio of the garnet as well as T and P. This relationship has not been observed in this study.

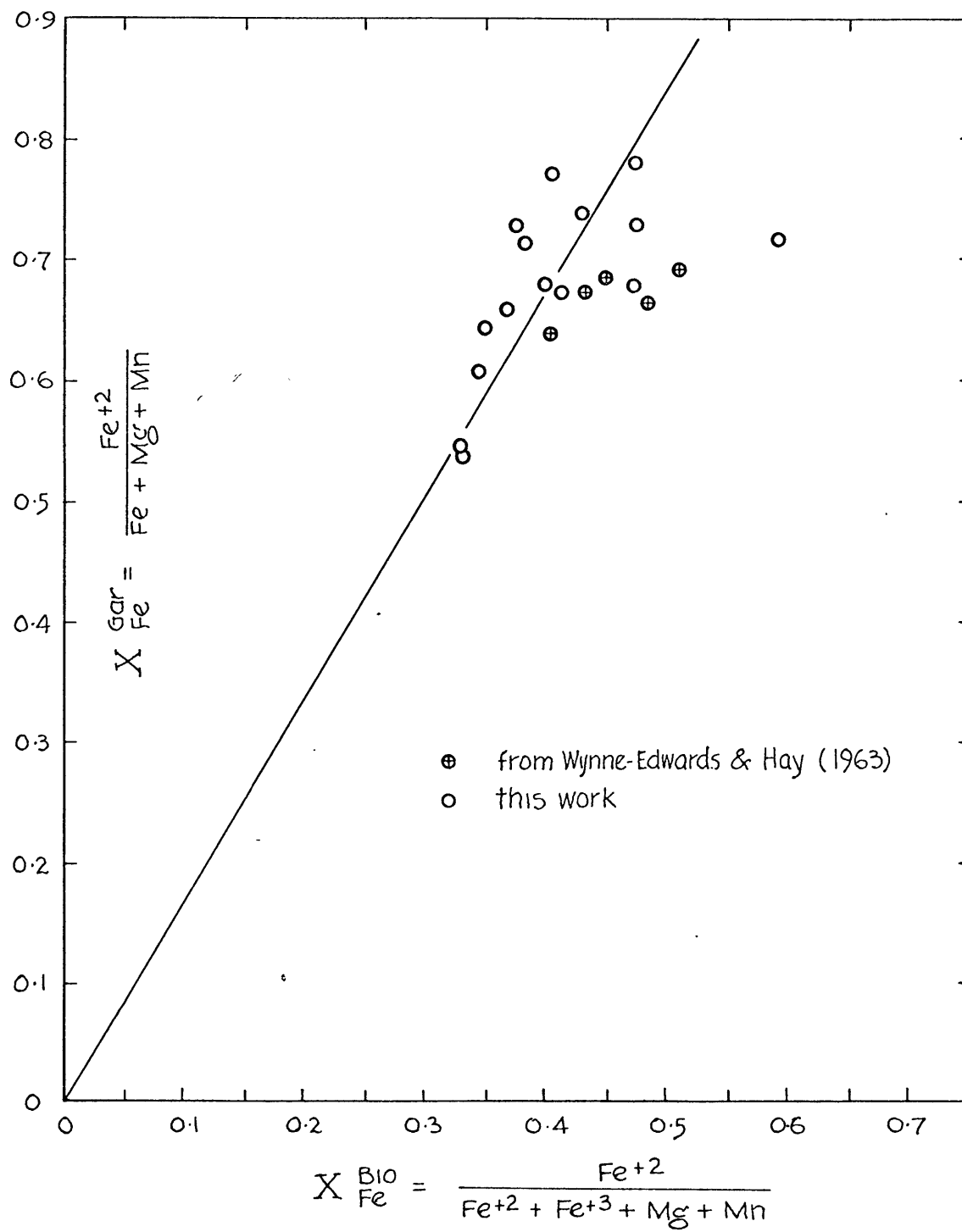


FIGURE 12. DISTRIBUTION OF IRON
BETWEEN GARNET AND BIOTITE

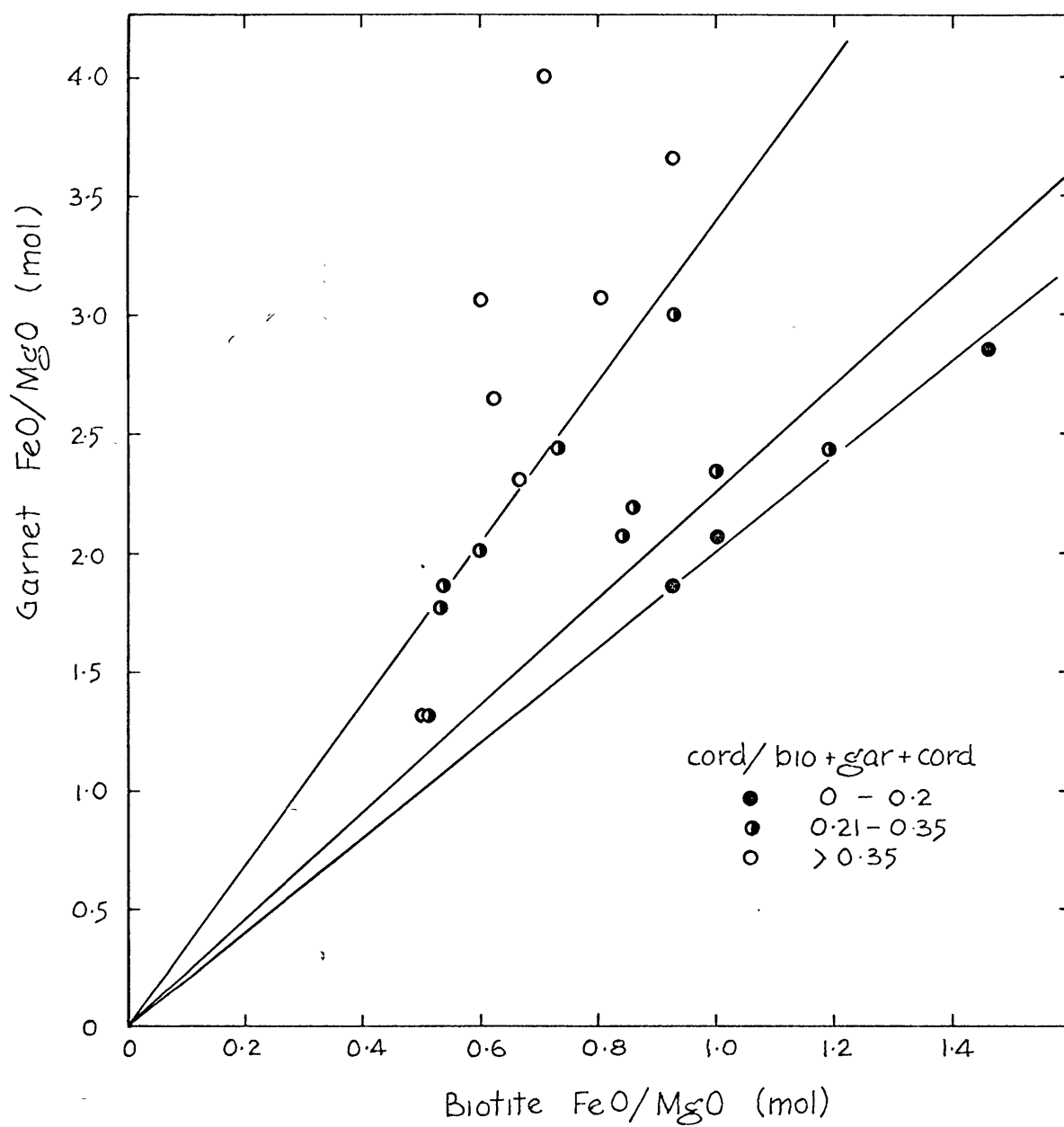


FIGURE 12A. DISTRIBUTION OF Fe AND Mg BETWEEN GARNET AND BIOTITE

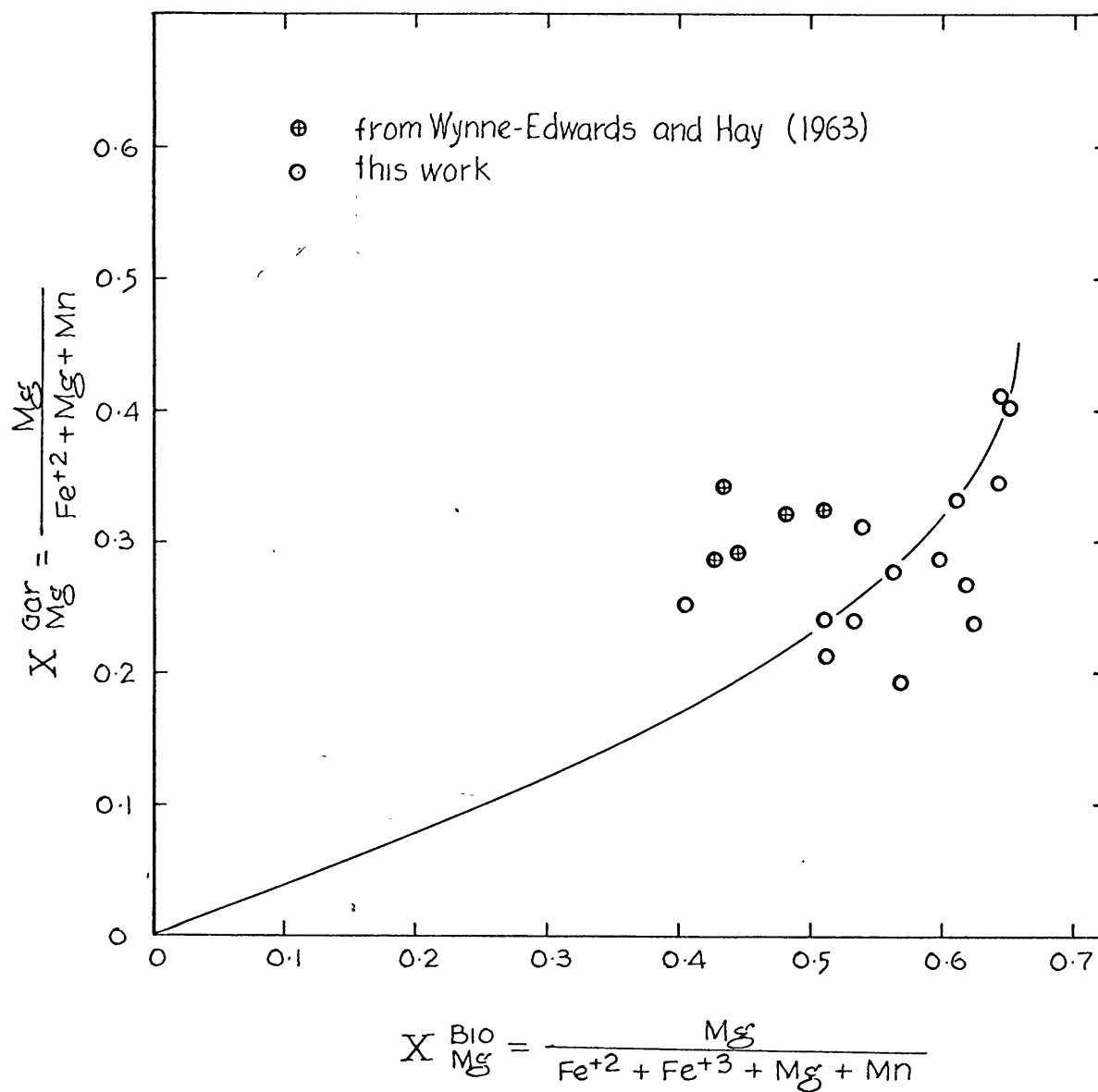


FIGURE 13. DISTRIBUTION OF Mg BETWEEN GARNET AND BIOTITE

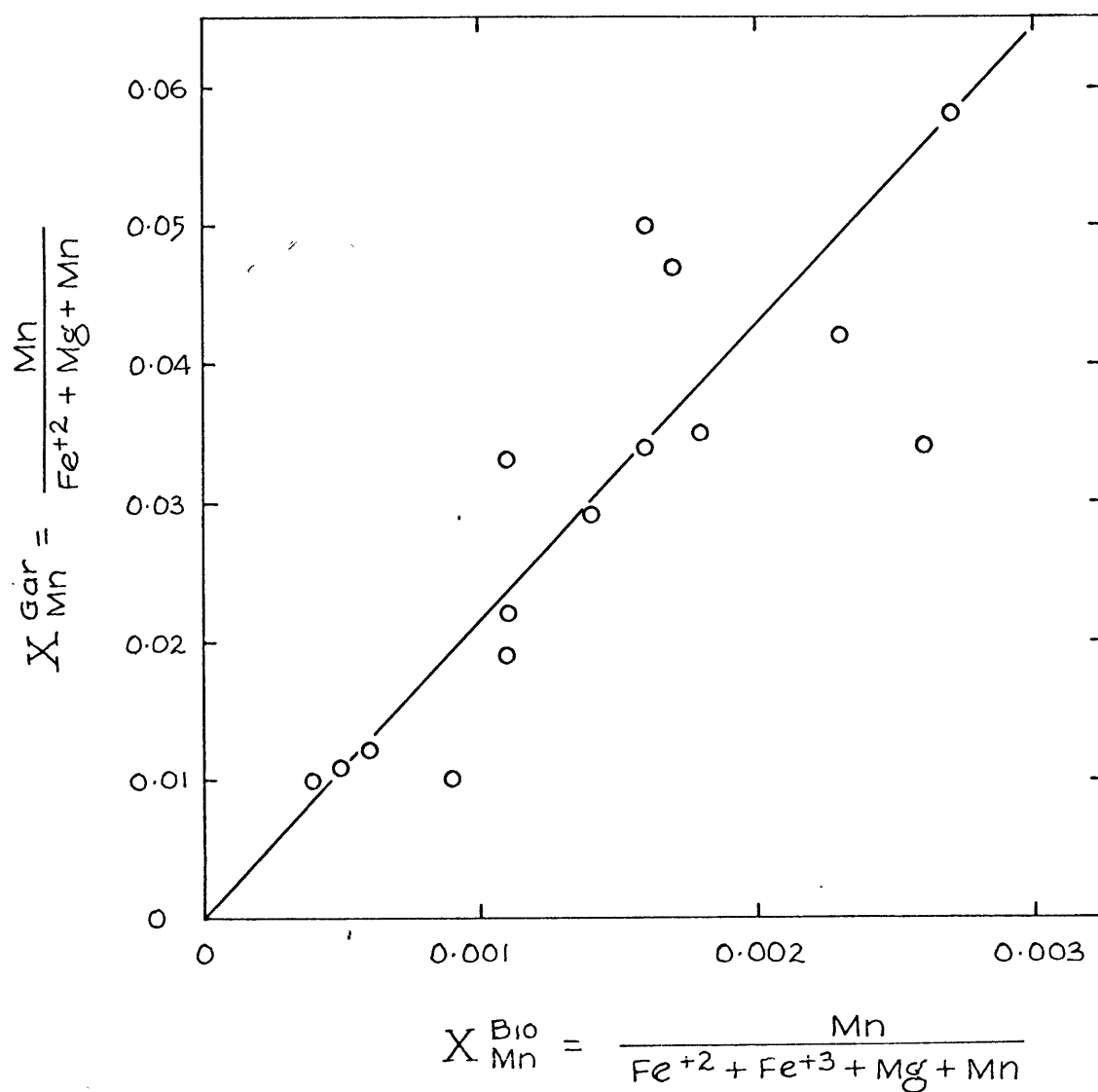


FIGURE 14. DISTRIBUTION OF Mn BETWEEN GARNET AND BIOTITE

It is interesting to note that^{there is} no correlation with the distribution found by Wynne-Edwards and Hay, (1963) who state that, at this grade of metamorphism, garnet reaches saturation with respect to Mn at about 2.3% spessartite molecule. This study finds acceptance of the spessartite molecule in garnet up to at least 5%.

6.3 The Distribution of Cr, Co, Ni and Ca between Garnet and Biotite

The chromium distribution between garnet and biotite is shown in Figure 15. The data points although somewhat scattered, show a fairly regular distribution curve with slope of about 0.60. This would indicate an affinity of Cr for the biotite structure as opposed to garnet. In this light, it is possible that part of the chromium substitutes for aluminum in the 4-fold coordination position. This correlation might be exposed if the Al concentration in biotite and garnet were known. However, Moxham, (1965) finds, in a study of the distribution of Cr between biotite and hornblende, that data scatter is enhanced if Cr is assumed to substitute in the tetrahedral position. The data from Wynne-Edwards and Hay, (1963) shows only one sample, (WE-4-58) with a distribution of Cr similar to that found in this study. The other samples exhibit a much stronger partition of Cr to the biotite phase.

Kretz, (1959) found no regularity of distribution to Cr between garnet and biotite. The reason for this is not clear. There is the possibility, however, that the spectrographic technique employed by Kretz was near the limit of sensitivity for Cr.

The distribution of cobalt between garnet and biotite is illustrated in Figure 16. The distribution is quite regular and the distribution coefficient $K_{Co}^{Bio/Gar} = 0.40$ is in good agreement with data from Wynne-Edwards and Hay, (1963). Carr and Turekian, (1961) noted that while the total amount of Co in a rock or mineral is often closely correlative with the total concentrations of Fe and Mg, its behavior in coexisting minerals seems akin to neither one. However, it is noted in this study that the partitioning of cobalt to biotite is quite strongly dependent on the distribution of molecular FeO/MgO between garnet and biotite as illustrated in Figure 16A. The plot shows that there is an inverse relationship between the cobalt content and the distribution coefficient $K_{FeO/MgO}^{Gar/Bio}$ which may possibly be controlled by the total concentrations of FeO and MgO in the rock

The distribution of nickel between garnet and biotite is shown in Figure 17. Although the greater number of samples show a regular curvilinear distribution, the combination of data from

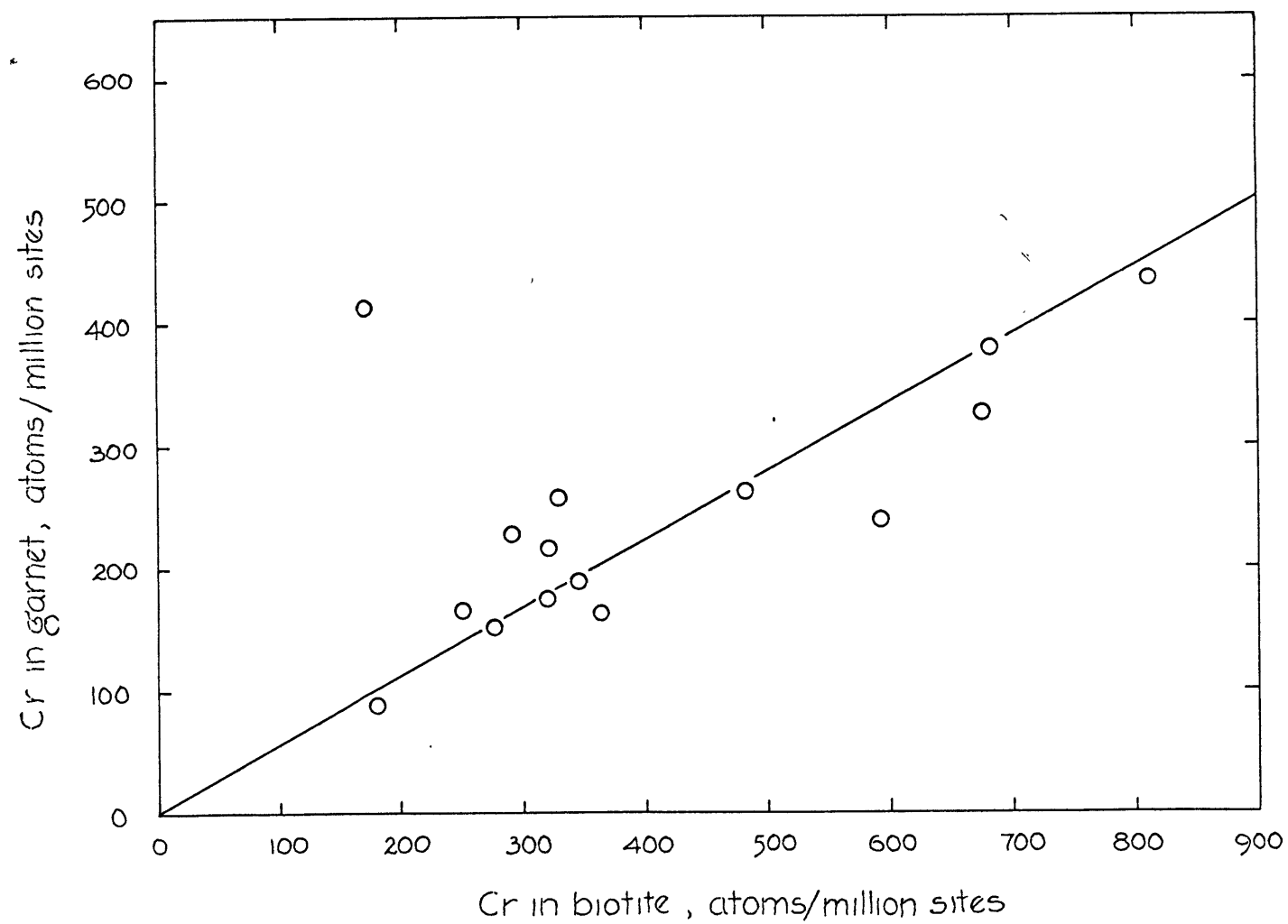


FIGURE 15. DISTRIBUTION OF CHROMIUM BETWEEN GARNET AND BIOTITE

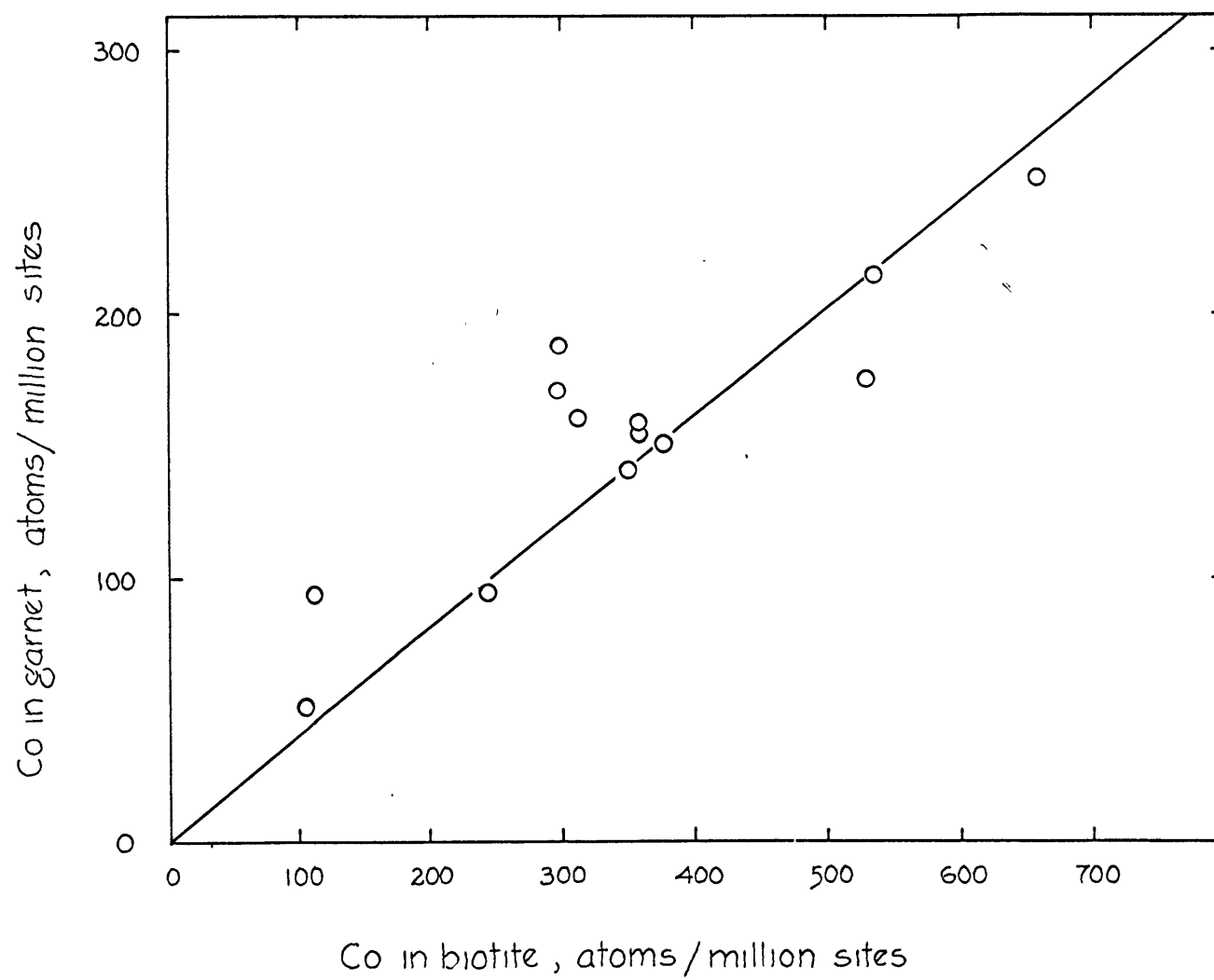


FIGURE 16. DISTRIBUTION OF COBALT BETWEEN GARNET AND BIOTITE

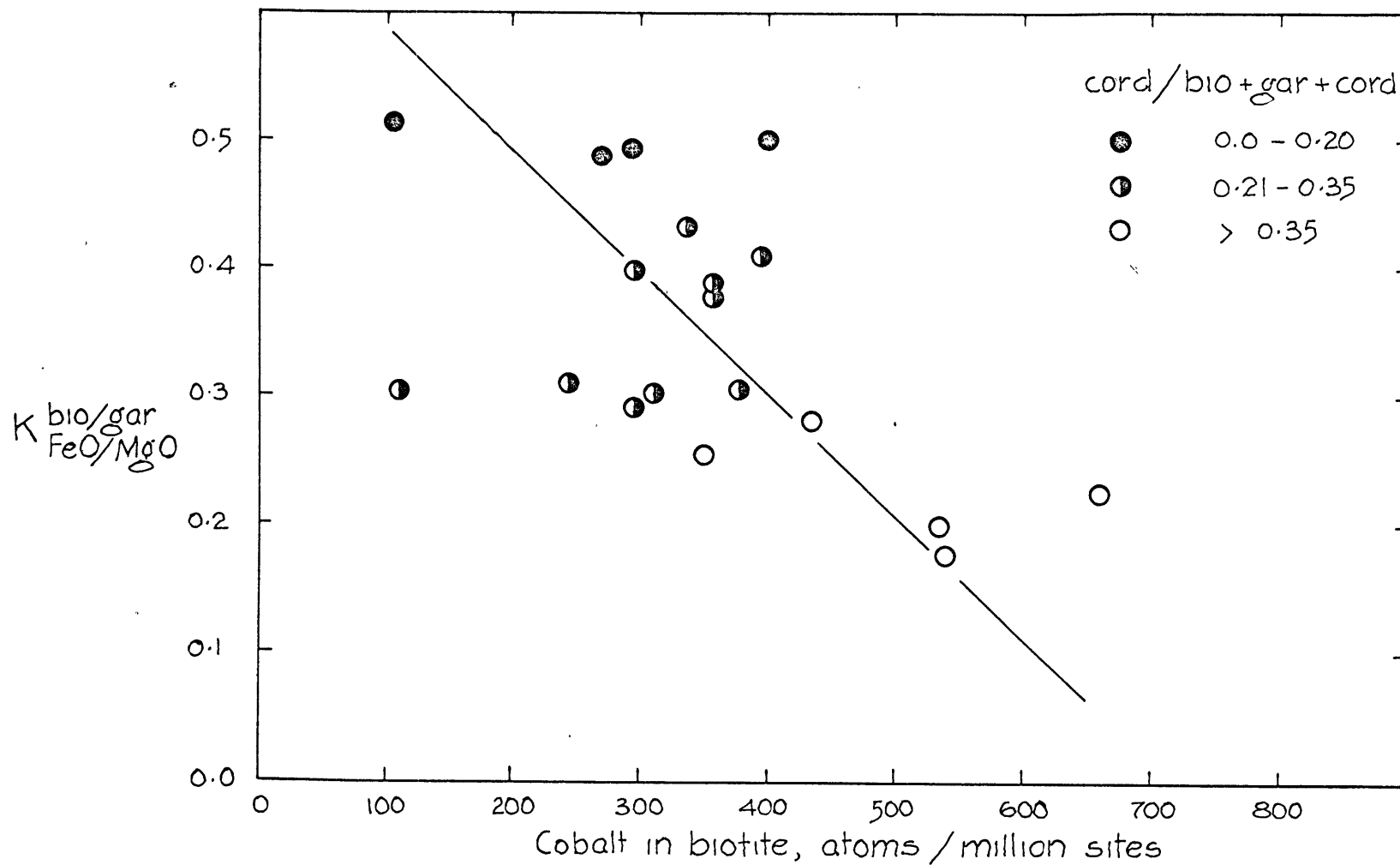


FIGURE 16A. RELATION BETWEEN Co IN BIOTITE AND THE DISTRIBUTION OF FeO AND MgO BETWEEN GARNET AND BIOTITE

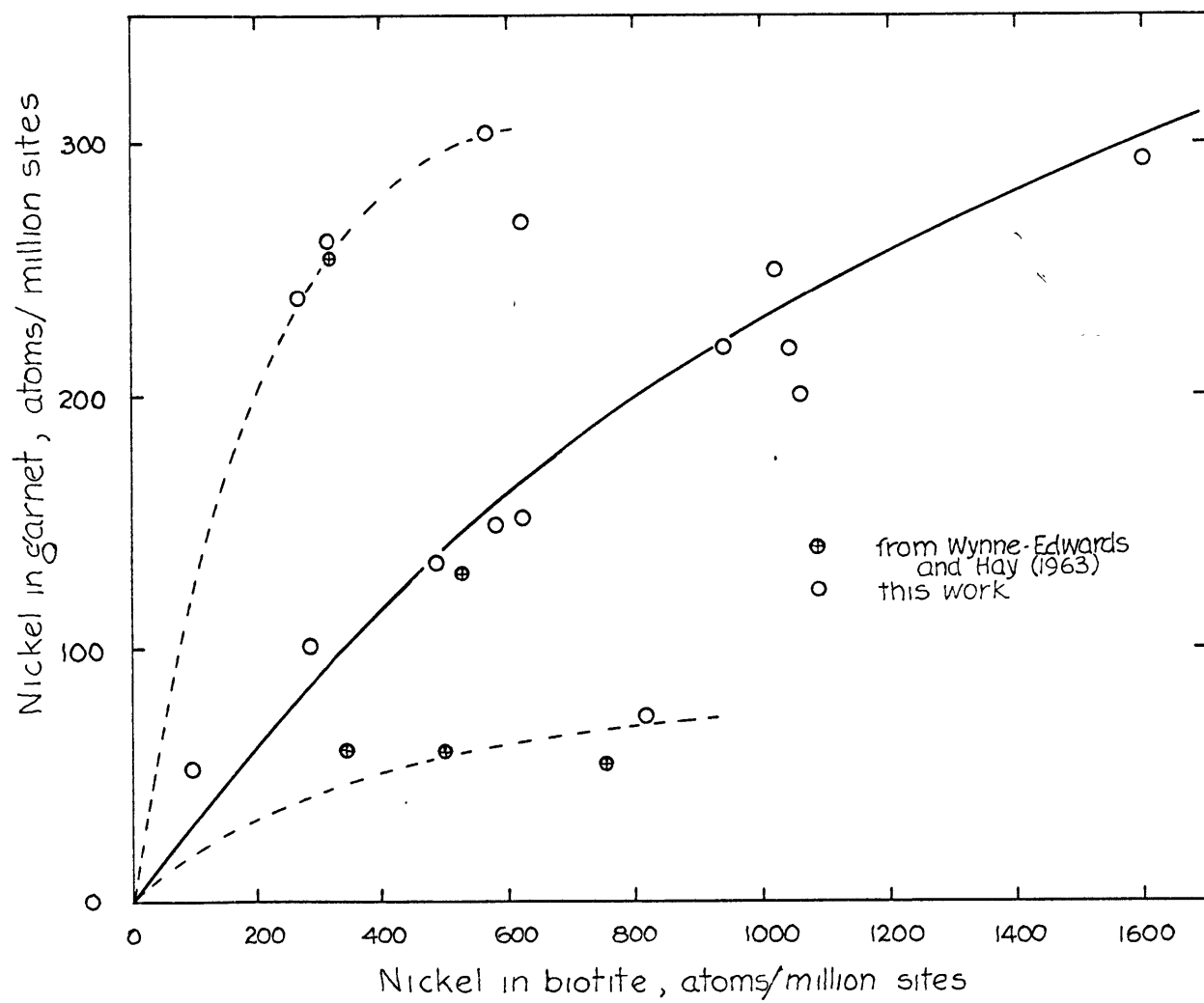


FIGURE 17. DISTRIBUTION OF NICKEL BETWEEN GARNET AND BIOTITE

Wynne-Edwards and Hay, (1963) indicate the possibility of two further distributions indicated by dashed lines in Figure 17. An expected coherence with data for Co, Fe^{+2} and Mg, all of similar size, is not observed and the reason for the various distributions is at present unknown.

One would not expect to find a regular distribution of calcium between garnet and biotite. The distribution would be strongly disproportionate, garnets being able to accept Ca atoms readily in the 8-coordinated position while Ca substitution in biotite is limited to the 12-coordinated K sites, which are more suited to larger singly charged cations. The distribution diagram of the rocks of this study, Figure 18, shows scattered data points but a regular distribution is nevertheless evident. The scatter would be expected to be diminished somewhat if the atomic ratios were used instead of oxide concentrations.

6.4 Discussions of Results

It is evident from the distribution illustrated in the last section that the application of Nernst's Law to the distribution of elements of low concentration is valid. Equilibrium between garnet and biotite is certainly evident for manganese, chromium, cobalt and nickel. In addition, the regular distribution of Mn between biotite and garnet, where Mn is a minor rather than trace component, points to the validity of employing distribution diagrams for the investigation of elements whose concentration precludes dilute solution laws but whose chemical characteristics allow ideal solution in a mineral structure.

Although the diagrams depicting the distribution of Fe and Mg show considerable scatter, it has been shown (Figure 12A) that the distribution of Fe and Mg between garnet and biotite reflects the presence and amount of cordierite in the rock. Wynne-Edwards and Hay, (1963) have previously shown that the presence and amount of cordierite in these gneisses is dependent on the relative amounts of FeO, MgO and CaO in the rock. Thus, the distribution of Fe and Mg between garnet and biotite is dependent on the whole rock chemistry and an approach to equilibrium is apparent with respect to these elements.

Ramberg and DeVore, (1951) have shown that in (Fe, Mg) garnets and biotites, assuming activity coefficients are constant if not unity:

$$K = \frac{\frac{X_{\text{Gar}}^{\text{Mg}}}{1 - X_{\text{Gar}}^{\text{Mg}}}}{\frac{1 - X_{\text{Bio}}^{\text{Mg}}}{X_{\text{Bio}}^{\text{Mg}}}} = \exp -\Delta G^{\circ} / 2RT \quad (1)$$

The distribution coefficient $K_{\text{Mg}}^{\text{Bio/Gar}}$ may vary with temperature and pressure according to the relations after McIntire, (1958, 1963):

$$\left[\frac{\partial \ln K_{\text{Mg}}^{\text{Bio/Gar}}}{\partial T} \right]_P = \left[\frac{(-\Delta G^{\circ}/RT)}{T} \right]_P = \frac{\Delta \bar{H}^{\circ}}{RT^2} \quad (2)$$

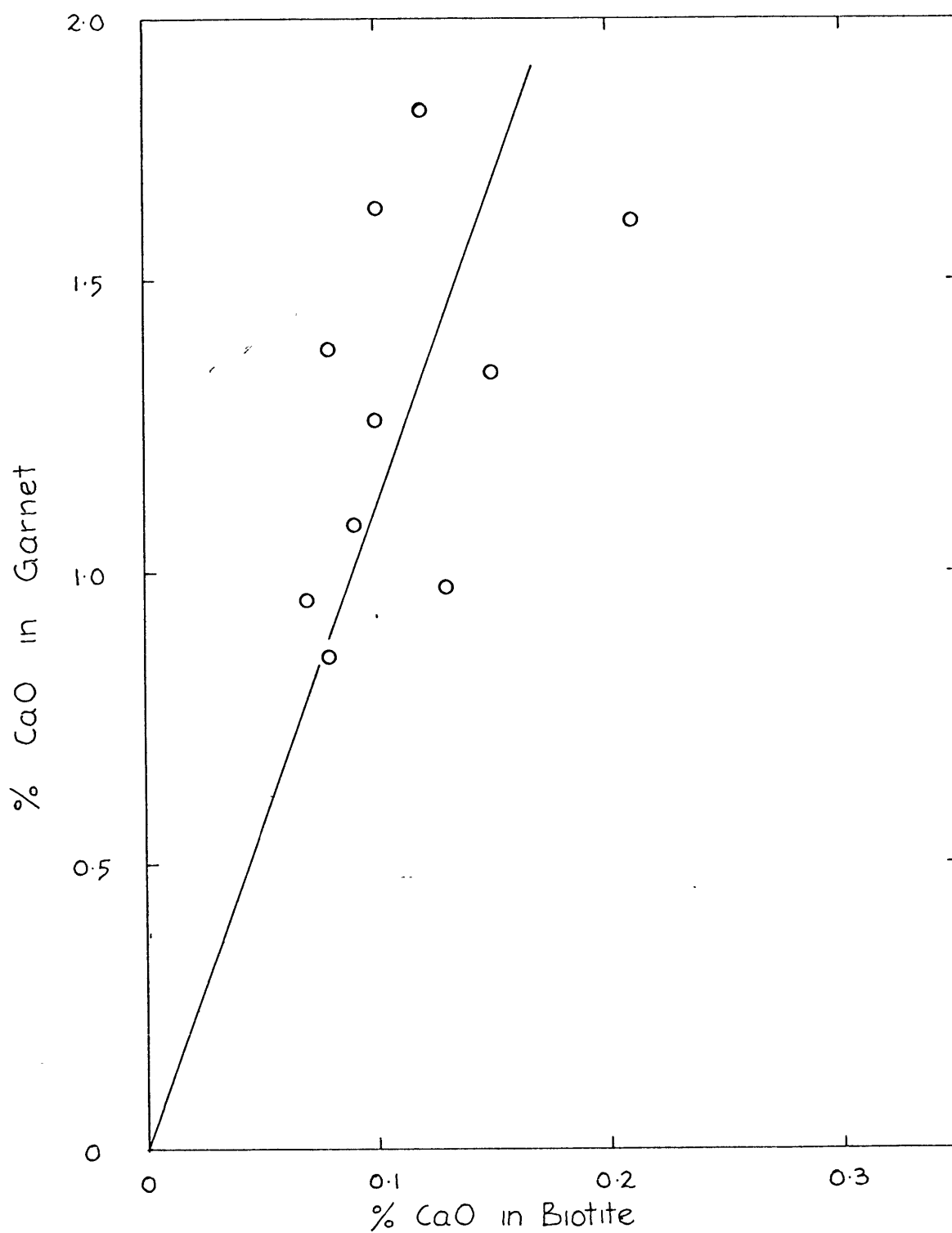


FIGURE 18. DISTRIBUTION OF CALCIUM
BETWEEN GARNET AND BIOTITE

$$\left[\frac{\partial \ln K_{\text{Mg}}^{\text{Bio/Gar}}}{\partial P} \right]_T = \left[\frac{(-\Delta G^\circ / RT)}{P} \right]_T = - \frac{\Delta \bar{V}}{RT}$$

where $\Delta \bar{H}^\circ$ is the change in partial molar enthalpy and $\Delta \bar{V}$ is the change in partial molar volume. Therefore, the distribution coefficient of Fe or Mg could be altered by a change in T and substantially less by a change in P. Thus, the scattered distributions for Fe, and Mg as seen in Figure 12 and 13, respectively, could also be caused by different P, T conditions among samples. This may also be the cause of the scatter around the relatively uniform distribution of Mn as illustrated in Figure 14. However, this is unlikely as some of the samples were taken within 40 feet of each other and these show no less scatter. The same argument holds for the distribution of Co, Cr, and Ni.

The scattering must therefore be attributed to error in the chemical data or small scale disequilibrium, Phinney, (1963). This disequilibrium could reasonably arise ^{because of} metamorphic equilibrium over only very small volumes due to: (1) initial inhomogeneities of the protorock, (2) slowness of diffusion to and from the site of mineral growth (3) low reaction rates (4) zoning of some of the various metamorphic products.

Since much of the previous work done on the equilibrium of metamorphic minerals assumed equilibrium on the local scale and chemical analyses were performed in several different manners, all potentially producing a scatter of points similar to those distributions illustrated in the last section, it was decided to test the assumption of local equilibration by examining possibilities stated above. The results of these tests are given in the following chapters.

SECTION II

THE SPATIAL EXTENT OF LOCAL EQUILIBRATION

7 INTRODUCTION

7.1 The Problem

The data of the previous section and that of Kretz, (1959, 1961), Wynne-Edwards and Hay, (1963), Phinney, (1959) and others who have attempted to define equilibrium distributions for various elements, commonly show a considerable scatter and indication of non-equilibrium. However, Zen, (1963) has shown that even from a textural and mineralogical standpoint, most metamorphic rocks are in equilibrium even at much lower grades than the rocks of this study have undergone. The following possibilities may be the cause of the distribution irregularities:

1. Lack of chemical equilibrium in the rock system
2. Poor precision and accuracy of chemical determinations
3. Lack of knowledge of all the variables in the chemical system
4. Samples taken do not reflect a single region^{or} domain of chemical communication and equilibrium, or a statistically significant number of these domains if they are small.

The first of these possibilities may be eliminated because both texture and mineralogy are consistent with thermodynamic equilibrium in metamorphic rocks as defined by Eskola, (1915), Fyfe, Turner and Verhoogen, (1960) and others.

The second, though still a possibility, is highly unlikely because many workers using different analytic techniques all encounter the same difficulties with respect to the equilibration of major and sometimes minor elements.

The third possibility is a serious problem for equilibration studies. Some of the parameters of metamorphism are cryptic, and to decipher many of the variables in a chemical study of metamorphic rocks, it is necessary to "plot everything against everything." It is usually possible, however, to get good chemical control on the system although this does not eliminate the scatter within the assigned ranges of variability, (Kretz, 1959, this study).

The fundamental problem may be in the fourth possibility listed above. The size of natural chemical systems in rocks is usually an unknown quantity. Local equilibrium is certainly established within a specific rock under the conditions imposed upon it. However, indication of this equilibrium may be lost by irregularities in the

distribution functions if sampling is not performed with this possibility in mind.

Throughout the literature, there has been vague and sketchy mention of the size of the domains of local equilibration (Harker, 1939, Kretz, 1960, Moxham, 1965, Phinney, 1959, 1963). Workers in the field of metamorphic equilibration studies strive to collect and use small samples, 4-5 cm. in each direction, to insure "local equilibrium conditions", (Moxham, 1965). This attitude was taken in the present study and as in Kretz's 1959 paper, the poor quality of the distributions was still evident. In this light, Moxham (1965), in a study of element distributions between coexisting hornblendes and biotites, found that certain elements showed a definite distribution, whereas others just approached an equilibrium distribution and some did not seem to approach equilibrium at all. It may be, however, that in the investigation of the volumes of equilibration, the elements which show very little regularity on a large scale may exhibit a regularity within a small domain.

Phinney(1959,1963) found a correlation between the FeO/MgO ratios and the garnet to staurolite ratios in the rocks from St. Paul Island and Money Point, Nova Scotia. He attributed this to the regularity to the small scale of diffusion of Fe and Mg during metamorphism. Checking his theory, he hand-picked biotite grains from several thin sections noting the position of the grains picked. The grains exhibited a distinctive Fe/Mg ratio when analyzed spectrographically. Phinney found that the samples with a homogeneous texture showed similar compositions for all biotite grains, whereas in the less homogeneous rocks, biotite grains showed similar compositions over only a distance of a few millimeters.

Similar observations have been made by Harker(1893, 1939) in thermally metamorphosed limestones, by Hagner, Leung and Dennison(1965), in mafic silicates of a single pyroxene

amphibolite specimen, by Kretz (1966) in Australian biotite-muscovite-garnet gneisses and by Albee, Chodos and Hollister (1966).

Thus the problem remains of assigning a specific volume of equilibration to a particular phase with respect to a particular element under certain conditions of metamorphism.

7.2 Theoretical Considerations

There are two fundamental requirements which must be fulfilled in order to cause a metamorphic mineral to nucleate and grow. First, all the elements constituting the mineral must be available at the very point at which a nucleus is formed. Second, the elements must be continually supplied to the place of growth for as long as the growth takes place.

At equilibrium, the chemical potential of a component must be the same throughout the chemical system but the probability of forming a nucleus would depend on the energy of nucleation, the concentration of the relevant elements and the mobility of the elements forming the nucleus. As the nucleus is formed it absorbs its component elements from the surroundings and may cause a severe relative drop in the concentrations of some of these components in its immediate proximity. Further growth of the phase, and, therefore, also the stability of the nucleus, is determined now largely by the ease of transferral of these particular elements from surrounding sources. Thus the rate of diffusion of the appropriate substances through the rock to the point of crystallization may influence greatly the size of the resulting crystal and the degree of equilibration which that portion of the rock attains. In the same light, (Harker, 1939) points out that the narrow range of diffusion places a check upon chemical exchange reactions during metamorphism. Thus the equilibrium systems to which the phase rule may be applied may not hold for the rock at large but only for a small equilibration domain in which free diffusion has been operative.

It is evident that one must first investigate the theory of nucleation and growth of metamorphic minerals and the effectiveness of diffusion in silicate rocks in order to establish the dimensions of equilibration domains.

The problem of nucleation and growth of minerals in the solid state has been discussed by Jacobs and Tomkins, (1955), Fyfe, Turner and Verhoogen, (1958), Stone, (1961) and Kretz, (1966). An extensive review of the problems and present knowledge in this subject has been given by Rast, (1965). Generally the work in this field has been done with regard to metallurgical problems, but most of the findings are applicable to geology although there is

a paucity of knowledge of this sort pertaining to silicates.

The nucleation and growth of metamorphic minerals is particularly complex because mineral nucleation and growth need not be contemporaneous with deformation. There is thus a problem of assigning specific conditions to the nucleation and growth stages. The problem of nucleation has been discussed by Smoluchowski, (1951) who states that a nucleus (cluster of atoms) in a homogeneous medium occurs due to statistical fluctuations of concentrations of atoms. Nucleation is a slow process as very small nuclei must reach a certain critical size in order that their volume free energy (negative) may overcome their positive surface free energy. Above this size the nucleus is stable and will continue to grow.

The chemical energy of nucleation is determined by the availability of material on site, the facility of diffusion of material to and from the site, and favorable metamorphic conditions. The rate of nucleation is not known for silicates although it is considered very slow, (Turner and Verhoogen, 1960, Rast, 1965). It is generally considered that for metals, rates of nucleation follow an exponential or linear law, Smoluchowski, (1951) and this is probably true of silicates.

Three different models of nucleation and growth of metamorphic minerals may be considered, (Kretz, 1966, Galwey and Jones, 1963, Jones and Galwey, 1964).

1. All grains nucleate at the same time and extract growth matter from the surrounding volume. Thus the final size of the mineral grains, for example, garnet is determined by the size of this domain, the rate of diffusion to the grain and the proximity of phase analogs.
2. Continuous nucleation followed by constant growth. The size of the crystal is then also dependent on the time of nucleation.
3. All grains nucleate at the same time but certain grains are situated along paths of relatively high diffusivity. These grains may grow at a relatively rapid rate and to a large size.

A combination of all three of these possibilities seems most likely since nucleation has been shown experimentally not to be instantaneous although Rast (1956) described garnets, grown under static conditions in a micaceous quartz-feldspar matrix, that were

of similar size and exhibited haloes of clear quartz. No mica or plagioclase remains in the haloes which were from 2 to 4 m.m. in thickness.

All of these processes involve the diffusion of material to and from the crystallization site. The process of solid diffusion has been investigated experimentally by Jensen, (1965) and others. Jensen finds that the distances over which solid diffusion can be effective is relatively short, being rarely more than a few centimeters. However, he states that transport of substances by relatively rapid movement through rock openings, along fracture zones, around mineral grains and into crystals through flaws and breaks may enhance the diffusion distance substantially.

Solution and consequent diffusion of dissolved material are subject to the primary conditions of metamorphism, i.e., temperature, pressure and chemical gradient. Diffusion itself is not only a slow process but it is also only operative during a finite period of time. Then migration or interchange of material within a rock undergoing metamorphism is confined to narrow limits.

Harker, (1939) states that the mineral formed at any given point depends on the composition of the rock within a very small radius about that point. He shows that the limit of effective diffusion thus indicated is commonly a fraction of an inch as exemplified by the preservation of thin layers different composition in a banded sediment through high grades of metamorphism.

Rast, (1965) proposes, however, that vacancy diffusion under dynamic conditions would be enhanced due to the rapid formation of mineral dislocations. The common homogeneity of matrix materials, the general absence of zoning in the feldspars and the scarcity of solid inclusions in quartz in metamorphic rocks seem to attest to considerable ease of diffusion, although the volume over which free chemical communication takes place may be quite small. According to textural (Rast, 1965) and chemical evidence (Korzhinski, 1959, Thompson, 1959, Phinney, 1963) mosaic equilibrium may be the rule, suggesting that the volume law of Lindgren, (1925) holds for metamorphic reactions on a small scale.

A study of chemical equilibrium in metamorphic rocks should not, then, be placed on a purely petrographic or purely chemical basis. Investigations of chemical equilibration must include strict

petrographic control on mineralogy, grain[✓]size, interphase-analog distances, rock microstructure and, of course, the spatial degree of chemical equilibrium, i.e., that volume over which free diffusion and chemical communication has taken place.

7.3 Proposed Method of Study

The methods of study of the extent of local equilibrium will entail the examination, in great detail, of the chemistry and petrography of a few selected specimens. Examination of a particular specimen will entail true grain size measurements of the coexisting minerals in question and the spatial distribution with respect to grain size of a particular phase. These relationships should give an indication of the nature of nucleation and growth of the particular phase in question, Kretz (1966). An examination of micro-structure at the thin-section level will, most likely, shed light on the ease of diffusion with respect to direction. This may also have a large effect on the size and shape of the equilibration domain.

Finally, an attempt will be made to determine the spatial extent of chemical equilibration between coexisting grains. Since this is essentially a measure of the volume of free diffusion, as discussed above, the distances over which the domains extend may be very small. It may also be that the various minerals are chemically zoned and only the outer portion of a particular grain is in equilibration with its surroundings, (Albee et al., 1966) as found in some of the pelitic schists of Vermont. It is obvious then that analyses of coexisting grains may have to be made at the micro scale and this will be discussed later under analytical methods and the section on zoning in garnets.

At higher metamorphic grades, however, particular grains in a rock may have equilibrated internally and the domains may be measurable by careful handpicking and analysis out of situ. One may expect that this is the case for many of the elements of Kretz's study of the Grenville schists of southern Quebec, Kretz (1959, 1960). It is apparent that for many elements examined, there seemed to be no difficulty in finding regular distributions between coexisting grains picked from samples of small hand-specimen size. One might then expect that, in this case, the domains of local equilibration were much larger than in Albee's Vermont study and that the grains had achieved internal equilibrium.

Those few samples selected for examination of the size of the

domains of local equilibration will be subjected to a rigorous petrographic analysis with respect to grain size and intergranular (same phase) distance measurements. Observations will also be made as to grain shape and micro-structure such as lineation and foliation. These observations will then later be incorporated with the chemical data in the discussion of the sizes of the thermodynamic systems involved.

7.4 Description of the Samples

Two samples were selected for a study of the shape and size of equilibration domains. The selection was made on the basis of:

1. Sufficient garnet and biotite for analytical purposes
2. Lack of retrogression of garnet and biotite
3. Possession of typical assemblages for the gneisses of the Ganonoque-Westport area.
4. Rocks with two different grades of metamorphism were chosen to see the effect of grade on the size of the domains of chemical communication.
5. Possession of distinct micro-structures, since it is possible that diffusion may be largely controlled by structural phenomena such as foliation and lineation.

The samples selected for this intensive study included a strongly foliated biotite-garnet-cordierite gneiss (No. 17) and a pyroxene-garnet gneiss (No. 42) with a less distinct foliation. Modal analyses for these rocks are shown in Table 11.

Sample 17 was collected on Brier Hill Road, 1.6 miles east of the village of Morton, South Crosby Township (See Figure 4). The rock is a medium grained, highly foliated gneiss with quartz, K-feldspar, garnet and biotite as obvious major components in hand specimen. Microscopically, the gneiss exhibits an extremely well-developed foliation with foliation planes populated with biotite, sillimanite, garnet and cordierite grains for the most part. A section perpendicular to the foliation exhibits severely elongated garnets in the plane foliation. Some of these elongated garnets contain sillimanite needles which continue uninterrupted through the garnet. The elongated garnets also have local inclusions of quartz, K-feldspar and biotite. The biotite inclusions, like those of sillimanite retain their orientation with respect to foliation and lineation. The elongated garnets, discussed further in the next section, are mantled by cordierite and K-feldspar.

Cordierite occurs as subhedral grains containing inclusions of quartz and sillimanite. Usually it is altered at grain boundaries and along fractures to waxy, yellow green aggregates (pinite).

The biotite occurs for the very great part in the foliation planes, but is also found scattered throughout the quartz-feldspar layers. Biotite occurs mainly as unaltered, ragged grains, commonly

TABLE 11. Modal Analyses of the Gneisses used for the
Study of Equilibration Domains.

	<u>17</u>	<u>42</u>
Quartz	34.1	17.8
K-Feldspar	22.9	56.9
Plagioclase	2.9	9.7
Biotite	3.5	1.4
Garnet	11.1	5.2
Hypersthene	-	6.9
Cordierite	13.4	-
Sillimanite	9.9	-
*		
Opagues	2.2	1.7
Zircon	Tr	-
Sericite and Chlorite	Tr	0.3

* magnetite, ilmenite and pyrite

Tr ≤ 0.05 percent

- missing

with inclusions of zircon. Magnetite inclusions are uncommon in this specimen.

The feldspars of specimen No. 17 are unaltered; the K-feldspar does not show microcline twinning and the plagioclase is An_{40} .

Sample 42 was collected from a small outcrop on the Wood's Road into Benson Lake, 2 miles east of Bedford Mills, Bedford Township (Figure 4). The rock exhibits a well developed layering in outcrop but foliation is not distinct due to the lack of platy minerals. The major phase constituents are quartz, K-feldspar, plagioclase, orthopyroxene and garnet.

Garnet occurs as small to medium sized, rounded grains with sparse inclusions of quartz. It is unaltered. The orthopyroxene is hypersthene and occurs as scattered subhedral grains. Minor chloritic alteration of the hypersthene is observed at grain boundaries.

Biotite is a minor constituent of the rock and occurs as small ragged, unaltered grains scattered throughout the gneiss and concentrated in pyroxene-garnet-biotite layers.

The K-feldspar present seems to be of the monoclinic variety. The plagioclase is An_{30} . Both K-feldspar and plagioclase are unaltered.

7.5 Morphology of the Garnets

Sample No. 42 exhibits normal rounded garnet grains with no distinguishing features. The garnets of sample 17, along with many of the other gneisses used in the first part of this study (See Appendix I), are strongly elongated, however. They are flattened in the plane of foliation and many, when observed parallel to the foliation surface, are elongated in the direction of lineation.

Foliation in these gneisses is defined by the interface between layers of different composition and it has been proposed that the foliation surfaces are parallel to and coincident with, the original bedding planes Wynne-Edwards, (1959). A lineation is marked by corrugation on the foliation surface and segregation trains of minerals. In sample 17, trains of segregated sillimanite and garnet define the lineation. The lineation direction parallels the adjacent major and minor fold axes Wynne-Edwards, (1959).

The garnets in the foliation planes are usually ellipsoidal in shape with axis lengths commonly in the ratio 4:2:1. The sizes and shapes with regard to their chemistry and position in the gneiss are examined in detail in a later section. It is desirable at this time, however, to consider the mineralogical associations of the flattened garnets and possible origins for them as opposed to the rounded garnets occurring in quartz-feldspar layers.

The rounded garnets of the quartz-feldspar layers are of random size, ranging from about 0.1 to 2.5 m.m. in diameter. They are associated in close proximity with quartz, K-feldspar, plagioclase and sillimanite. Biotite is present in these layers but is scattered and seems to have no definite relationship to garnet.

The garnets located in the plane of foliation are almost always elongated and are closely associated in space with sillimanite, cordierite and K-feldspar. Sillimanite was observed to be very abundant in the plane of foliation where no garnet was present. The modal concentration of sillimanite upon reaching a garnet face, decreased sharply although some grains were still observed to pass directly through the garnet. Biotite was observed to act in the same manner. However, inclusions of biotite within the garnet were



FIGURE 19. Diagram of a Thin Section of Specimen 17. The section is cut perpendicular to the foliation and is shown here as seen in plane polarized light. Magnification is about 100x. A typical elongated garnet is seen in the center of the field of view with the common close association of cordierite, C, and K-feldspar, K. The sillimanite needles passing through the garnet uninterrupted should be noted.

very scarce. The flattened garnets are mantled by cordierite, K-feldspar and quartz. K-feldspar and quartz were also observed as inclusions in the garnet. A diagram of a typical flat garnet is given in Figure 19.

Two possibilities come immediately to mind with respect to the origin of the flattened and often elongated garnets.

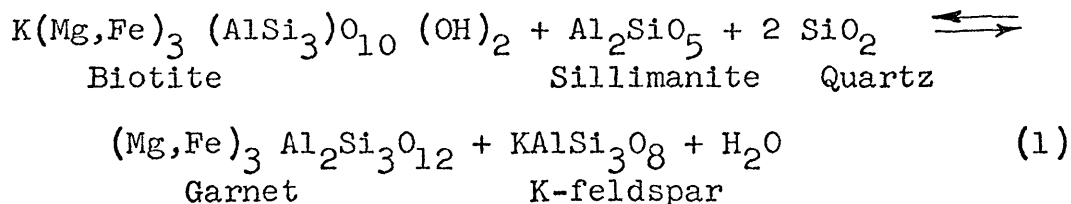
1. The garnets nucleated in the plane of foliation and grew by an exchange reaction with biotite and cordierite as normal spherical to subspherical grains. Later tectonic deformation caused the garnets to assume their present form.
2. The garnets nucleating and growing on the foliation surface grew as pseudomorphs after biotite or had their growth controlled by the foliation surface.

The first possibility may be eliminated on the bases that (1) no fracturing of the garnets was noted. If the garnets had been flattened by tectonic deformation, one would expect fracturing of brittle garnet. Further, (2) none of the elastic effects around inclusions as discussed by (Rosenfeld and Chase, 1961) and Smith, (1953, 1963) have been noted and (3) the garnets in question show no anisotropic effects. It is thus considered that the possibility that these garnets formed in this manner is highly unlikely.

If the second possibility is assumed to be correct, the processes and reactions which have taken place must be investigated carefully since Atherton, (1965) has stated that, in most cases, there is no direct prograde growth of one mineral from another. However, let it be assumed for the moment that biotite existed before the garnet formed, or at the latest was present in its early stages of nucleation. Under these circumstances, the nucleation of garnet would take place at a position in the rock where the garnet components were readily available, probably in, on or very near biotite crystals Rast, (1965). The growth of the new phase, garnet, of fairly restricted composition, results in changes in the composition of the more variable phase, biotite. The initial biotite composition, high in iron, is controlled by the rock composition which is in itself quite variable (Nicholls, 1958, W. H. Dennen, personal communication, 1967). The growth of garnet then results in biotites of increasing magnesium content.

As the garnet grows, it must draw component material from the surrounding biotitic material by an exchange reaction, possibly the

following where the garnet is becoming more iron-rich and the biotite more magnesian.



At a specific temperature, the degree of equilibration will depend on the proximity and abundance of garnet components and the ease of diffusivity of components to and from the site of growth. In this light, one might expect that if nucleation of garnet took place along planes or lines of increased ion mobility, the garnets would grow, if not rapidly, at least to a greater size, and chemical communication between surrounding biotite and garnet grains would be enhanced.

It is suggested then that the flattened, elongated garnets observed in this study nucleated within or on biotite grains on foliation surfaces. The garnets then grew incorporating material from the surrounding biotite. Further growth was enabled by increased mobility of components along the foliation surface and lineation direction resulting in accelerated growth in these directions while growth in the direction perpendicular to the foliation was inhibited because of a lesser diffusivity in this direction. The resulting garnet need not be pseudomorphous after a single biotite grain although in many cases in these rocks this seems a definite possibility.

It should be noted here that the cordierite and K-feldspar closely associated with the garnet grains coupled with the modal concentration changes of biotite, sillimanite and garnet along the foliation surfaces gives supporting evidence for the validity of the reaction (2) given above.


It might be expected then that the domain of chemical equilibration would take on an ellipsoidal shape with its long axis parallel to the foliation and lineation directions, the medium axis parallel to foliation and perpendicular to lineation and the short axis perpendicular to both foliation and lineation. This theory will be tested in a later section.

8 GRAIN SIZE ANALYSIS AND INTERGRAIN DISTANCE MEASUREMENTS

8.1 Apparatus and Techniques

The sizes and distribution of mineral grains in metamorphic rocks are needed for a full understanding of the physico-chemical processes affecting their nucleation and growth. Data on the size distributions of garnet grains has been presented by (Galwey and Jones, 1963, Jones and Galwey, 1964 and Kretz, 1965). The distributions observed here will be compared to those works and an attempt will be made to decipher the growth of garnet grains in the rocks studied.

Sample 17, described above, was chosen for an intensive study of garnet grain sizes and intergarnet distances. Further, the Fe, Mg, Mn and Ca concentrations, were determined on all grains measured.

The original specimen of Sample 17, measuring 9.0 X 7.5 X 7.3 cm. was trimmed with a diamond saw to remove any weathered rind. Surfaces were cut, one parallel to (17 II) and one perpendicular to (17 I) the foliation and these thick slices were in turn cut into slabs of roughly the dimensions of a petrographic slide. The slabs thus formed were cemented to petrographic glass slides and the top surface ground parallel to the glass base.  Grinding was performed on a lap using 400 mesh alumina.

A micrometer grinder, capable of allowing the accurate removal of down to $1/1000$ of an inch, was constructed as an adaptation of one used at Iowa State University for the study of oolites (Donald L. Biggs, personal communication, 1966). Plate I shows photographs of the micrometer grinder with descriptive notes.

With the use of a binocular microscope, the centers of all garnets exposed were traced on a transparent overlay, the coordinates of their centers determined, and the apparent grain size diameter measured by means of an ocular micrometer. Following spectrochemical analyses of the exposed garnets with a laser microprobe as described below, the specimen was ground parallel to the initial surface to remove a layer of determined thickness (average = 0.25 m.m.) and the coordinates and apparent diameters measured again. This process was repeated until enough grains to delimit a significant population,

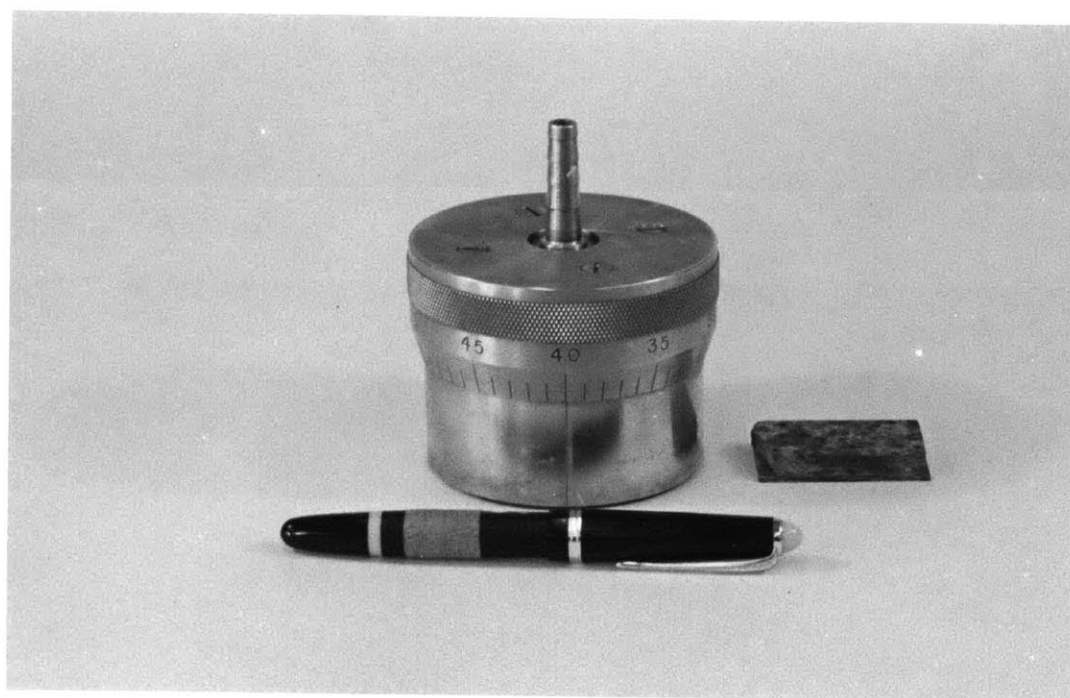


Plate IA The Micrometer Grinder, Side View

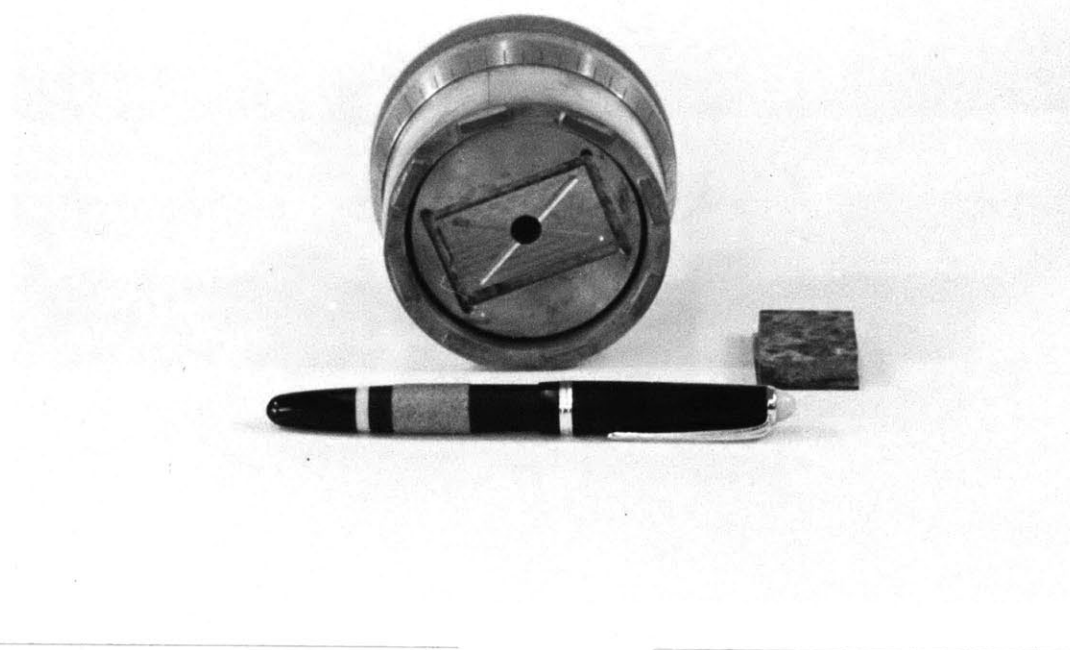


Plate IB The Micrometer Grinder, Bottom View

both chemical and physical, was measured (a total of 9 times). True grain diameters could thus be obtained for most grains intersected at least twice, but due to the odd shape of a great number of the garnets some size parameters has to be estimated. The sizes of about 2% of the garnets measured are by estimates on one or more axes.

8.2 Grain Size Distribution of Garnet in Specimen 17 I

Since many of the garnet grains are approximately ellipsoidal or spheriodal in shape, the distributions, as illustrated in Figure 20 employ the maxium, intermediate and minimum diameter of each grain. The garnet grains range in shape from roughly spherical to ellipsoidal. Hence, it was possible to calculate the grain volume distribution using the equation,

$$\text{Volume} = \pi \frac{d_1 d_2 d_3}{6}$$

thereby converting diameters measured to volume. The volume distribution of garnets in specimen 17 I is shown in Figure 21. A summary of grain size measurements is shown in Table 12.

The diameter of garnet grains in specimen 17 I was found to range from 0.36 to 10.6 m.m. on the long axis, 0.35 to 3.96 m.m. on the intermediate axis and 0.30 to 3.44 m.m. on the short axis. The grain size distribution was found to be bimodal as shown in Figure 20. The volume of the garnet grains in the section perpendicular to the foliation range from 0.024 to 38.59 m.m.³ with a bimodal distribution of volumes as shown in Figure 21. All the distributions show a strong positive skewness. In this light, it should be noted that it is possible that some of the smallest grains were not sectioned during the grinding and measuring sequence. However, this would not be expected to effect the overall distribution of garnet sizes significantly.

The distributions of the long, intermediate and short axes of the garnets in section 17 II cut parallel to the foliation are shown in Figure 22. Although it might be expected, the prominent bimodal character of section 17 I does not show up here. This is possibly explained by the fact that section 17 II exhibits garnets through only one foliation surface while section 17 I affords observation of garnets throughout the complete section of the sample. It is certainly possible that different nucleation and growth rates might have occurred in different foliation laminae.

The distribution of diameter magnitudes of garnets in section 17 II shows a positive skewness although this is not nearly as marked as in the section perpendicular to the foliation. The

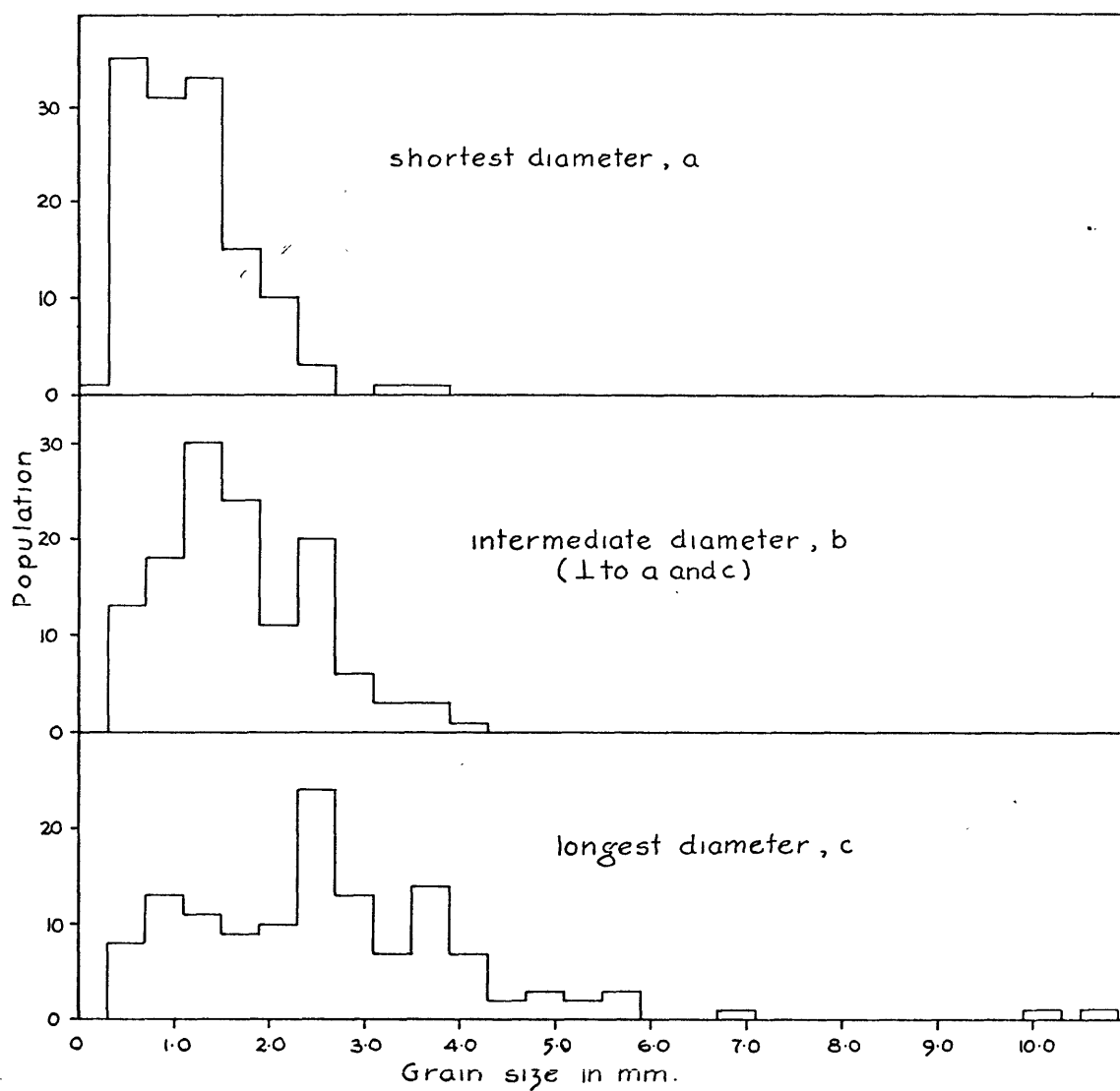
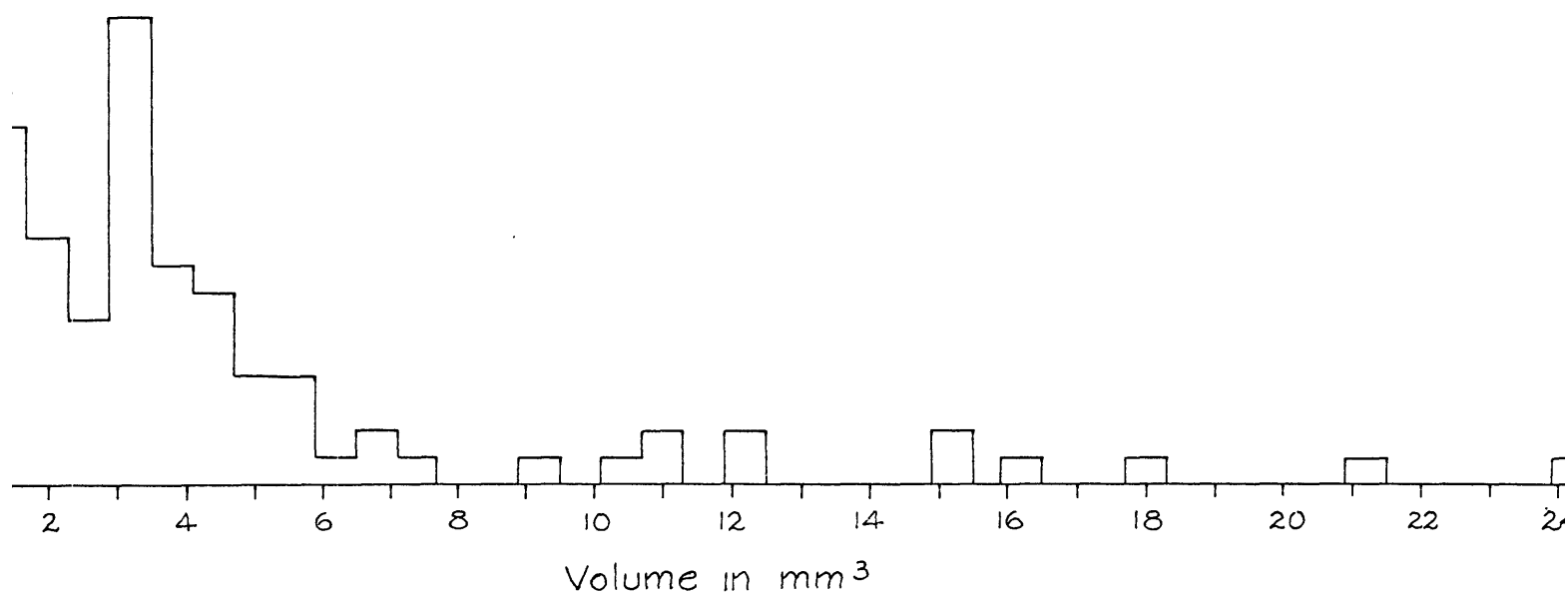


FIGURE 20. DISTRIBUTION OF AXIAL DIAMETERS
OF GARNETS IN SECTION 17 I

FIGURE 21. DISTRIBUTION OF VOLUMES
OF GARNETS IN SECTION 17 I



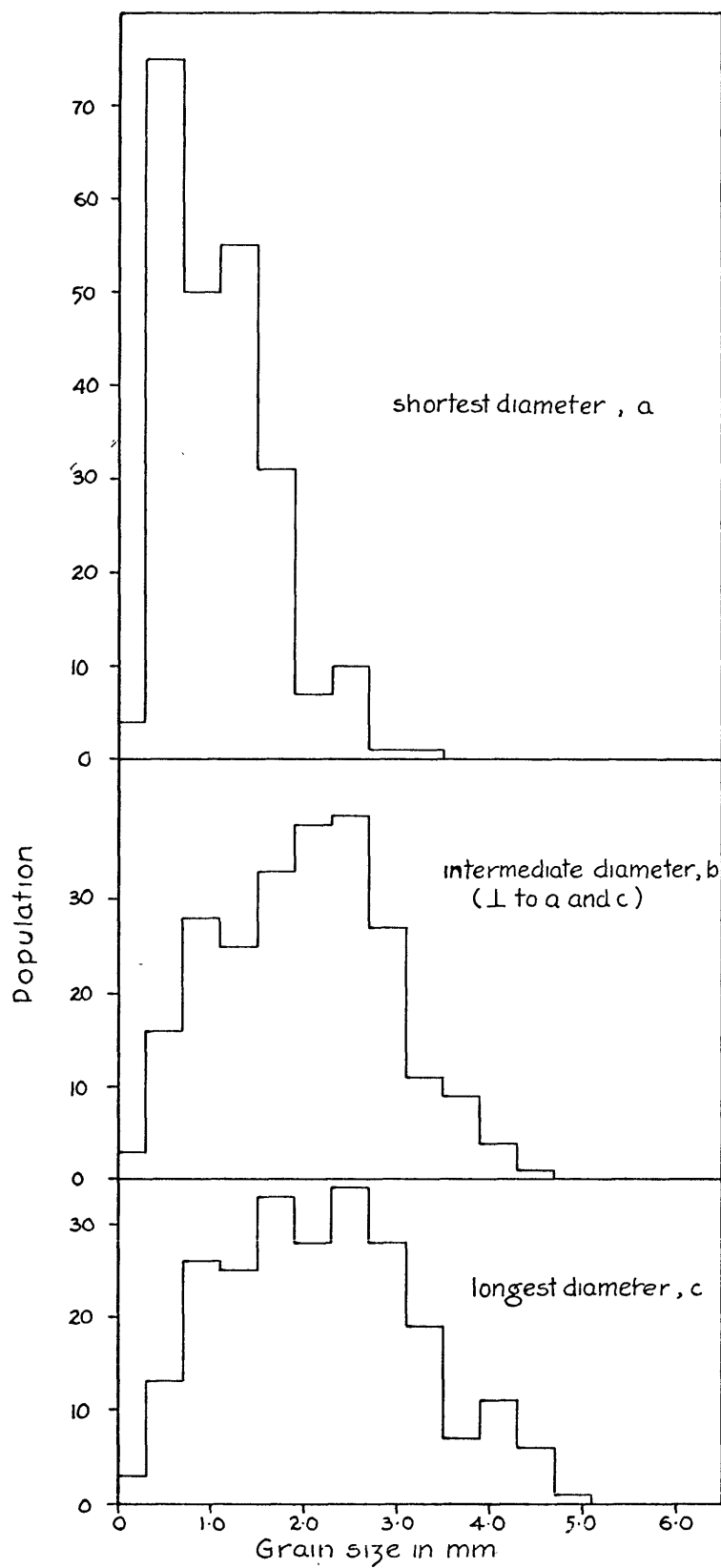


FIGURE 22. DISTRIBUTION OF AXIAL
DIAMETERS OF GARNETS IN
SECTION 17 II

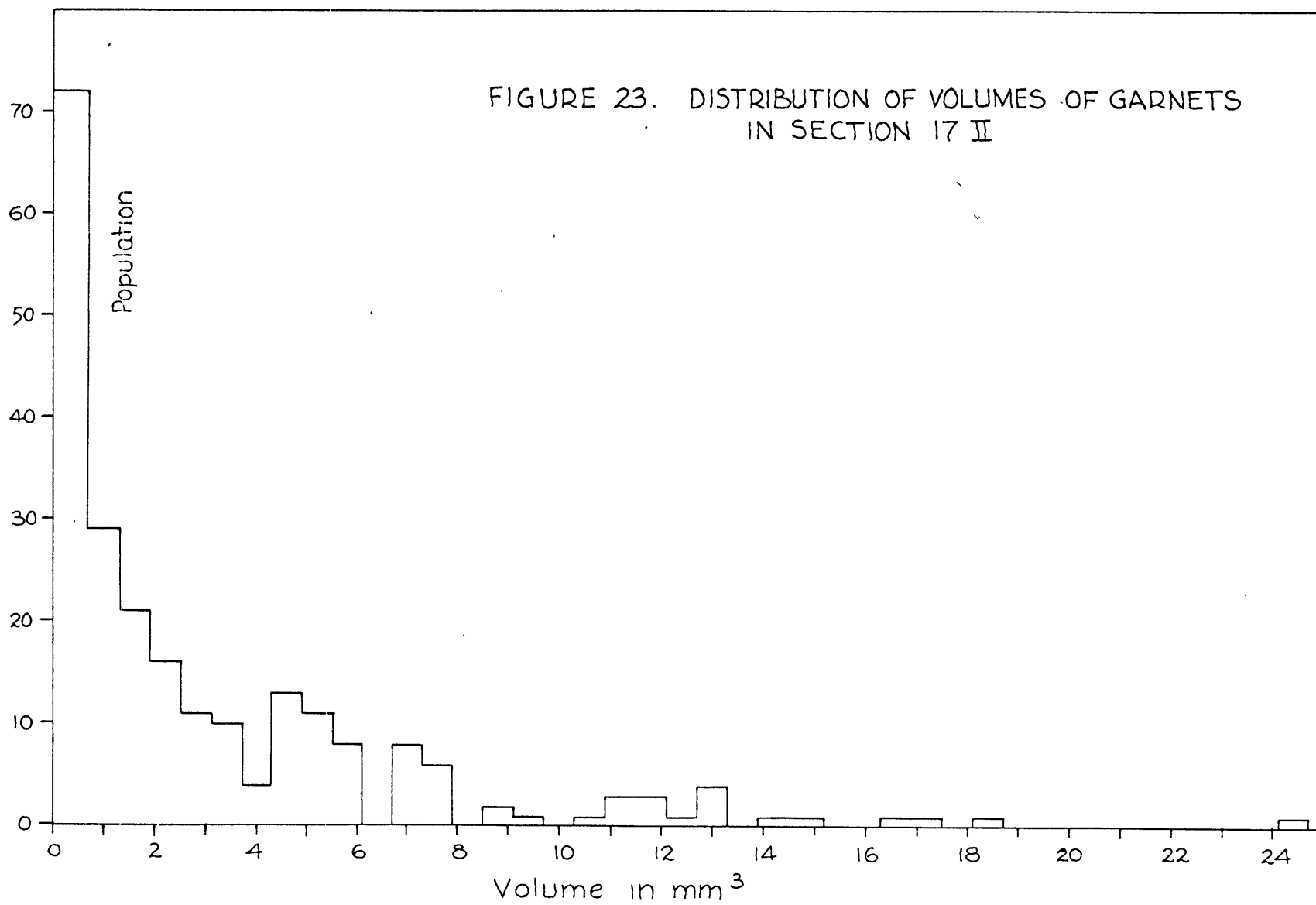


TABLE 12. Summary of Grain Size Measurements of Garnets in
Specimen 17

SECTION	POPULATION	DIMENSION	RANGE (mm)	MODE (mm)	MEAN (mm)	MEDIAN (mm)	STANDARD DEVIATION (mm)
17I	141	Long axis	0.360-10.60	2.30,3.60	2.595	5.120	1.65
		Int. axis	0.350-3.960	1.30, 2.58	1.588	1.805	0.79
		Short axis	0.300-3.440	0.50,1.35	1.058	1.570	0.56
		Volume	0.024-38.59	0.100,3.20	3.573	19.283	5.27
17II	243	Long axis	0.120-4.850	1.700	2.094	2.365	1.05
		Int. axis	0.120-4.370	2.100	1.909	2.125	0.92
		Short axis	0.120-3.000	0.500	0.967	1.440	0.57
		Volume	0.001-24.30	0.100	3.226	12.150	3.97

distribution of garnet volumes in this section, Figure 23, however, does show a similar strong positive skewness as do the garnet volumes of section 17 I

8.3 Intergrain Distance Measurements

The coordinates of the centers of all garnet grains were noted as a routine step in the determinations of apparent diameters. It was then possible to calculate the distance to the nearest grain and test the randomness of distribution of garnets in the two specimens.

The slabs, 17 I and 17 II, measured roughly 78.0 X 36.0 X 1.30 m.m. and 93.0 X 81.0 X 1.20 m.m. respectively. The centers of garnet grains in these slabs may then be considered points in a plane and the departure of the distribution from randomness may then be determined by measuring the distance to the nearest neighbor for each grain (Clark and Evans, 1954).

For slab 17 I, perpendicular to the foliation, the following information was obtained where N = distance to nearest phase analog:

A =	area in $m.m^2$ of slab =2675.5
n =	number of grains measured =141
ρ =	grain density = n/A =0.0527
r =	263.655
r_a =	mean distance to nearest phase analog =2.044
r_e =	mean distance to nearest phase analog expected in a random distribution of the same density = $1/2$ =2.179
R =	measure of departure from randomness of distribution = r_a/r_e =0.938

The value of R may range from 0 for a distribution with maximum aggregation to unity for a random distribution, to 2.1491 for a distribution as evenly and widely spaced as possible.

For slab 17 II, parallel to the foliation, the values found were as follows:

A =6328.1
n =243
ρ =0.03840
r =555.336
r_a =2.373
r_e =2.552
R =0.930

All calculations of distances to the nearest neighbor and of the distribution factor R were carried out using IBM System/360 and the Fortran IV program described in Appendix 3.

The values R , computed both for the grain distribution, parallel to an perpendicular to the foliation, are only slightly less than unity (~ 0.93). We may then infer that the distribution of garnets in specimen 17 is very nearly random with a possible slight aggregation. This is in good agreement with macroscopic observation of these sections in which the garnets appear to locally aggregate in trains in the lineation direction.

8.4 Investigation of Possible Correlation of the Physical Parameters Measured

As discussed above, the coordinates of the center of all the grains, whose dimensions were measured, were recorded and the distance to the nearest phase analog calculated. This data, along with the size measurements, allowed investigation of possible correlations between them for further understanding of the nucleation and growth habits of the garnets in these gneisses.

The calculation of correlation and covariance of the physical measurements on the garnets from specimen 17 was carried out using a computer program described in Biomedical Computer Programs, Health Science Computing Facility, Department of Preventative Medicine and Public Health, School of Medicine, University of California, Los Angeles, and translated into Fortran IV for IBM System/360 by Ralph Wiggins of the M.I.T. Department of Geology and Geophysics. The program and a brief discussion of its capabilities are given in Appendix 4. In this case the variables examined were, for each garnet; (1) long axis diameter A, (2) intermediate axis diameter B, (3) short axis diameter C, (4) volume and (5) nearest neighbor distance. Output included a listing of data cases for each variable, the covariance matrix, the correlation matrix and a step-wise regression on each parameter as the dependent variable.

Tables 13 and 14 show the correlation matrix for the size and distance measurements on the garnets of section 17 I and 17 II respectively. As is evident from the correlation coefficients shown in Table 13 and Table 14, there is a strong correlation between axial diameters and grain volume but this, obviously, is expected. More interesting are the correlations between the length of the garnet axes. A very strong correlation between the long axis diameter A and the intermediate counterpart B in section 17 II is apparent. ~~Less~~ Less obvious, although quite strong according to the correlation coefficients, ^{are} correlations between A and C and B and C. These correlations may be tested further by examining the regression analysis which assumes, step-wise, each parameter as the dependent variable and allows the computation of the dependency of the parameter on the variation of each of the other parameters as independent

variables. For example, taking A, the long axis as the dependent variable, it was found that 55% of its variance was due to variance of the independent variable V, the volume.

From the regression analysis, it is evident that for section 17 I only the correlation of lengths of the intermediate axis B and the short axis C is real. Assuming C as the independent variable 59% of the variance in B may be accounted for. The regression analysis showed also that there is no correlation between any of the axial lengths on the grain volume and the distance to the nearest phase analog.

The regression analyses on the garnet parameters of section 17 II show a strong correlation between A and B. Taking either as the independent variable, 85% of the variance in the dependent variable is due to variance in the independent variable. There is also a strong covariance between the short axis and the volume. 68% of the variance may be accounted for using either C or V as the dependent variable.

Again, in section 17 II, there is no correlation between any axial length or garnet volume and distance to the nearest garnet.

The matter of correlation of parameters measured on the garnets of specimen 17 will be brought up again later when chemical data is available.

TABLE 13. Correlation Matrix for the Physical Measurements on Garnets from Section 17I

Number of Variables		5				
Number of Cases		95				
	A	B	C	V	N	
	1.000	0.562	0.511	0.739	0.165	A
		1.000	0.768	0.733	0.208	B
			1.000	0.792	0.220	C
				1.000	0.180	V
					1.000	N
A	Long axis diameter					
B	Intermediate axis diameter					
C	Short axis diameter					
V	Grain volume					
N	Distance to the nearest garnet					

TABLE 14. Correlation Matrix for the Physical Measurements on Garnets from Section 17II.

Number of Variables		5				
Number of Cases		195				
	A	B	C	V	N	
	1.000	0.924	0.598	0.780	-0.074	A
		1.000	0.616	0.789	-0.066	B
			1.000	0.826	-0.069	C
				1.000	-0.042	V
					1.000	N

8.5 Discussion of Results with respect to Rock Texture

A brief summary of results obtained during the measurements made during this chapter is as follows:

1. Many of the garnets are flattened and elongated. They are flattened in the plane of the foliation, and often elongated in the direction of lineation. In many cases, a pseudomorphic or, at least, a close association with biotite is evident. It was proposed that nucleation took place on or in grains of biotite.
2. Looking at a section cut perpendicular to the plane of foliation, i.e., section 17 I, a bimodal distribution of axial diameters and volumes of garnets was observed. A similar, although less distinct, distribution was noted for the axial diameters on the section cut parallel to the foliation (section 17 II). The volume distribution on section 17 II was analogous to that of section 17 I. All distributions, especially the volume distributions, were positively skewed.
3. The distributions of grains in section 17 I and 17 II were found to be close to random with a possible slight aggregation. Macroscopic observation deems this valid as there is a small inclination of garnet grains to form in trains in the foliation surfaces and lineation directions.
4. Correlation computations of possible covariance between the various parameters showed strong correlation between the length of the intermediate axis and the length of the short axis. Good correlations were also observed between the length of the long axis and the length of the intermediate axis; the short axis length and the volume V.

There was no correlation between any of the measured axial lengths or computed volumes and the distance to the nearest garnet.

In the last chapter, a discussion of the various aspects of nucleation and growth of mineral grains in metamorphic rocks mentioned the possibility of three models of nucleation and growth. The first of these, i.e., that all grains nucleate at the same time (Galway and Jones, 1963) involves the random distribution of nucleation sites. Material for growth is extracted from the volumes surrounding the nuclei. The dimensions and shape of these volumes are thus determined by the proximity of nearest phase analogs and a distinct correlation between grain size and nearest neighbor distance should occur. The lack of such a correlation in the garnets of specimen 17 eliminates this model.

A second model proposed nucleation to be an instantaneous process but certain grains being situated along paths of relatively great diffusivity grow at a relatively rapid rate. The possibility of variations in the rate of diffusivity seems likely enough in specimen

17 where garnets grown in the plane of nucleation are of an uncommon shape and usually larger than their normal-shaped counterparts in the quartz-feldspar-biotite layers. Mehl and Dube, 1951, Jacobs and Tomkins, 1955 and Stone, 1961 have discussed nucleation in solids and find that nucleation is not an instantaneous process. Kretz, (1966) worked on the problem of nucleation and growth of several different silicate minerals in metamorphic rocks supports this conclusion. He finds that the nucleation of these minerals followed a linear or power law depending on the stage of metamorphism and growth of the particular grain.

The third possibility, i.e., that all grains grow at the same rate but nucleation is a continuing process while conditions are appropriate (Galwey and Jones, 1963) is probably not valid with respect to a uniform growth rate. The growth rates of minerals are a direct measure of the reaction kinetics taking place during metamorphism. The kinetics of metamorphic reactions are certainly dependent on temperature, pressure, the availability of the necessary components and diffusion to and from the site of crystal growth. Although temperature and pressure are most likely constant over the hand specimen-sized area of observation, the latter two are probably variable. Changes in the nucleation rate (Mehl and Dube, 1951) and the growth rate may be brought about by changes in the temperature or changes in the rate of increase in temperature. The bimodal distribution of garnet sizes observed in this work was thus possibly caused by one or more of the following:

1. Two stages of metamorphism causing two stages of nucleation and growth of garnet.
2. Nucleation in regions of different whole rock chemistry causing variability in the amount of material available for garnet growth.
3. Nucleation in regions exhibiting structural and textural variations, possibly causing a variability in diffusivity.
4. Variation in the temperature or the rate of temperature increase during garnet growth.

As discussed in the last chapter, the observations on garnet shapes with respect to their mineralogical and textural environments seems to indicate that the variables 2 and 3 were operative in these rocks and others as well. Kretz, (1965) describes the grain distribution of garnets in two schists from the same metamorphic aureole in the Yellowknife-Beaulieu region of Canada. One schist exhibits

a bimodal distribution of garnet sizes while the other is unimodal. Kretz cannot believe that this is due to changes in temperature or in the rate of increase of temperature. He therefore, proposed that the chemical and /or textural environment was uniform throughout the sample displaying the unimodal distribution but not in the sample with the bimodal distribution of garnet sizes.

In the next chapter, the chemistry of the garnets in sections 17I and 17II will be investigated. The possibility of relations between the data of this chapter and the chemistry of the grains seems most likely judging from the mineralogical associations of the garnets.

9 ANALYSIS OF GARNETS IN MATRIX

9.1 The Laser Microprobe

The selection of an analytic system for the investigation of the chemistry of many garnets distributed over a sizable area was of fundamental concern for this study. The electron micro-analyzer is, for many elements, a precise and accurate tool but handles only very small samples which would not be satisfactory in a program such as this where the garnets were studied with respect to size and distribution as well as chemistry. Further, an electron probe was not readily available to the author.

It was decided that the most practical tool for the job was the laser microprobe (Brech, 1962,1963,1965,1967, Goldman et al., 1964). This instrument, manufactured by the Jarrell-Ash Company, has an enormous potential as a petrographic tool.

The Jarrell-Ash Laser Microprobe, Plate III, is a spectrochemical source unit of wide applicability and is used to excite samples of microgram size for emission spectroscopy. It may be operated in conjunction with any fast and efficient spectrograph.

A laser is a device for producing a powerful monochromatic beam of light which the waves are coherent. The term "laser" is an acronym for "light amplification by simulated emission of radiation." The essential component in the unit used is a single crystal of ruby, containing 0.05% Cr, machined into a rod 4 cm. long and 0.5 cm. in diameter. A powerful electronic flash tube is coiled about the polished ruby to provide an intense source of "pumping" light. The light raises the chromium atoms in the ruby to an excited state, from which they drop back, in two steps, to the ground state, Lengyel (1962). In the first drop to a metastable state, some of the energy is given to the crystal structure, with no light emission. In the subsequent second drop, there is an emission of energy in the form of photons, or quanta of light, with a wave length of 6943\AA . The time required for a return to the stable state occurs at 1 to 2 milliseconds. When properly focused, the high intensity light beam emitted provides such a high photon density that it can weld, melt or vaporize a small amount of any substance.

The laser microprobe employs a pulsed ruby laser to vaporize



Plate II The Laser Microprobe

minute amounts of sample. The vapor temperature of approximately 5000°K, however, is not sufficient to achieve excitation adequate for spectrographic analysis. The sample vapor is, therefore, further excited as it passes between two auxiliary graphite electrodes positioned above the sample and in front of the entrance slit of the associated spectrograph. The vapor breaks down the high-potential gap producing emission energies sufficient to provide photographic recording of the spectrum.

9.2 Standardization

The problem of standardization for laser spectrography is analogous in many respects to those of electron microanalyzer. The problem of finding chemically analyzed substances which are homogeneous and of a similar composition to the unknown substance is a challenging one. Fortunately, the matrix problems that are so prevalent in analytical work using the electron microanalyzer are not so disturbing in spectrographic analyses. In fact, there is very little matrix effect if one employs silicate standards for the analysis of silicates.

In this study, chemically analyzed samples of silicates, already powdered and homogenized, were fused to a glass in alumina boats at 1400°C in a combustion furnace. Chemical data on the standards used are given in Table 15.

TABLE 15

	<u>A-50*</u>	<u>A-12D*</u>	<u>G12A⁺</u>	<u>G25⁺</u>	<u>G1⁺</u>	<u>R-1**</u>
Fe as FeO	26.5 %	4.9 %	27.4 %	37.7 %	30.8 %	8.21 %
MgO	1.8	16.8	10.9	5.3	9.4	14.24
CaO	15.3	22.8	1.6	0.97	1.3	20.46
MnO	2.0	0.11	2.8	0.43	2.2	
<u>Fe</u>	0.89	0.28	0.71	0.89	0.76	0.36
<u>Fe+Mg+Mn</u>						
<u>Mg</u>	0.046	0.72	0.22	0.097	0.18	0.64
<u>Fe+Mg+Mn</u>						
<u>Mn</u>	0.068	0.006	0.072	0.010	0.056	
<u>Fe+Mg+Mn</u>						
<u>Ca</u>	0.32	0.54	0.037	0.026	0.030	0.43
<u>Fe+Mg+Mn+Ca</u>						

* = analyses by S. Krank, (1959)

+ = this work, section I

** = analyses by G. Beall, (1962)

9.3 Analytic Technique

Excitation parameters for the analyses of garnets in specimen 17 are given in Table 16. All photometry was performed on a Hilger non-recording microphotometer.

TABLE 16

Spectrograph - Bausch and Lomb Large Quartz Littrow-Mounted spectrograph.
 Electrodes - 1/8" National Carbon Co. AGKSP graphite rods, pointed pencil sharp.
 Photographic Plates - Eastman Kodak 103-0
 Analytic gap - 2 m.m.
 Position of electrodes - 2 m.m. above sample
 Cross excitation voltage - 1825 volts
 Plate calibration - preliminary curve method. Neutral step filter with steps of approximately 2.5
 Wave length region - 2600Å - 4200Å
 Plate Development - 3'50" at 22°C in Kodak D-19 developer. Fixed for 25 minutes in Kodak Acid Fixer.

After grinding the slabs of sample 17 and measuring the garnet apparent diameters and the coordinates of their centers, a slab was placed on the microscope stage of the laser microprobe. Each garnet exposed on the slab was then "shot" with the laser beam. The routine for spectrographic analysis of each garnet grain was as follows:

1. Locate the grain
2. Focus on surface of the grain
3. Flip in laser beam deflection prism
4. Pull out viewing mirror
5. Turn on flash-tube power
6. Raise stage 75 microns
7. Trigger laser and shoot garnet
8. Lower stage to focus and check crater
9. Change electrodes, rack plate and move on to next garnet

The electrodes were changed after shooting each garnet in order to prevent contamination by carry-over of sublimates from the former shot.

Since the power output of a ruby laser is very temperature dependent, a strict time routine between shots was imposed on the analysis. An interval of two minutes between each shot has been recommended (Y. Pelletier, personal communication, 1967) and was found entirely satisfactory in this study.

After each garnet was analyzed ^(in duplicate) in section 17 I (perpendicular to the foliation) and 17 II (parallel to the foliation), the slabs were ground again to remove 0.25 m.m. as described above, ^{and} the apparent diameters measured ~~the apparent diameters measured~~. Standard glasses were shot on every plate.

After measurement of line densities on a microphotometer, and transformation of these densities to relative line intensities by means of the photographic calibration curve, the following intensity ratios were calculated:

$$\frac{I_{\text{Fe } 2740}}{I_{\text{Fe } 2740} + I_{\text{Mg } 2852} + I_{\text{Mn } 4030}}$$

$$\frac{I_{\text{Mg } 2852}}{I_{\text{Fe } 2740} + I_{\text{Mg } 2852} + I_{\text{Mn } 4030}}$$

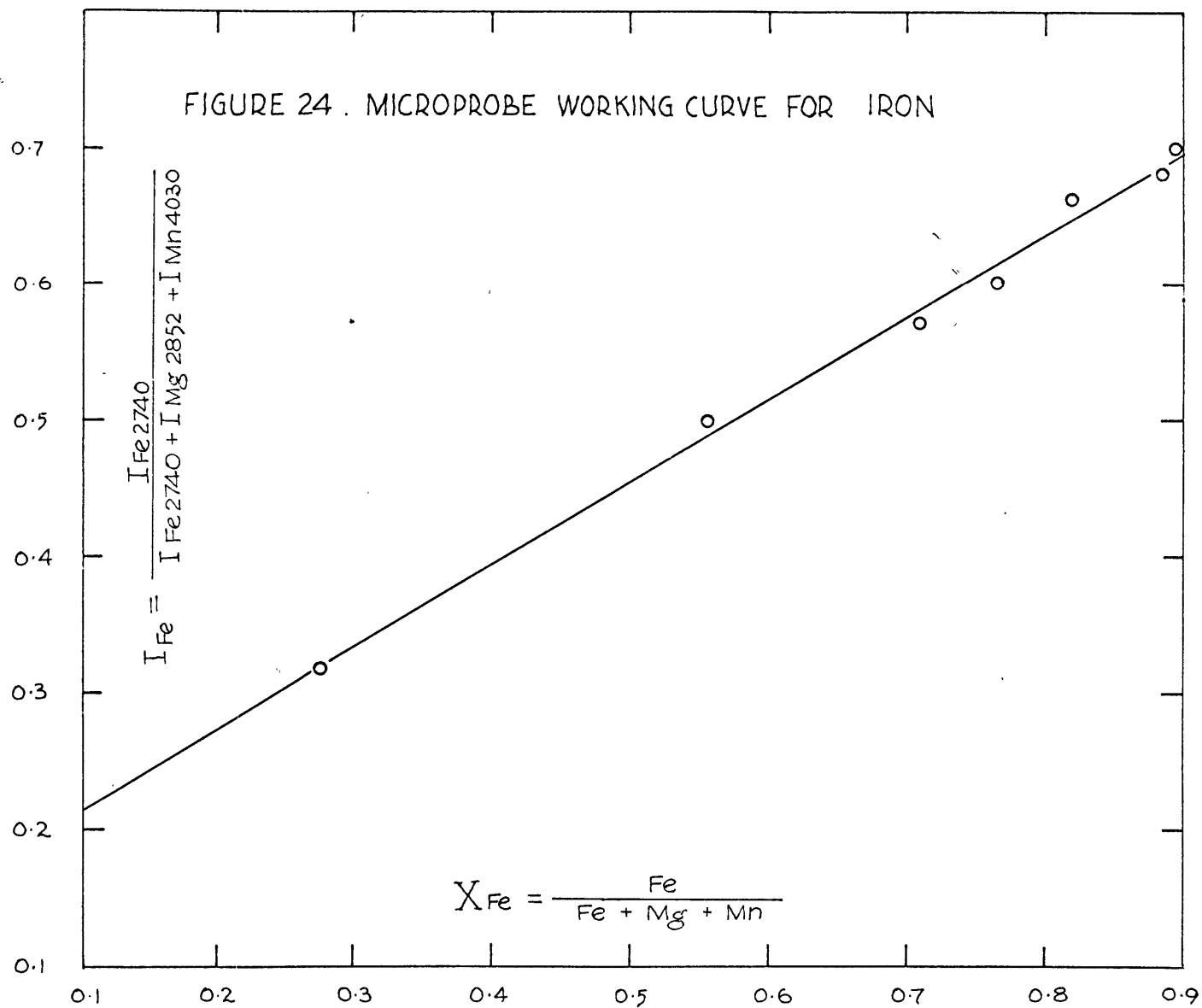
$$\frac{I_{\text{Mn } 4030}}{I_{\text{Fe } 2740} + I_{\text{Mg } 2852} + I_{\text{Mn } 4030}}$$

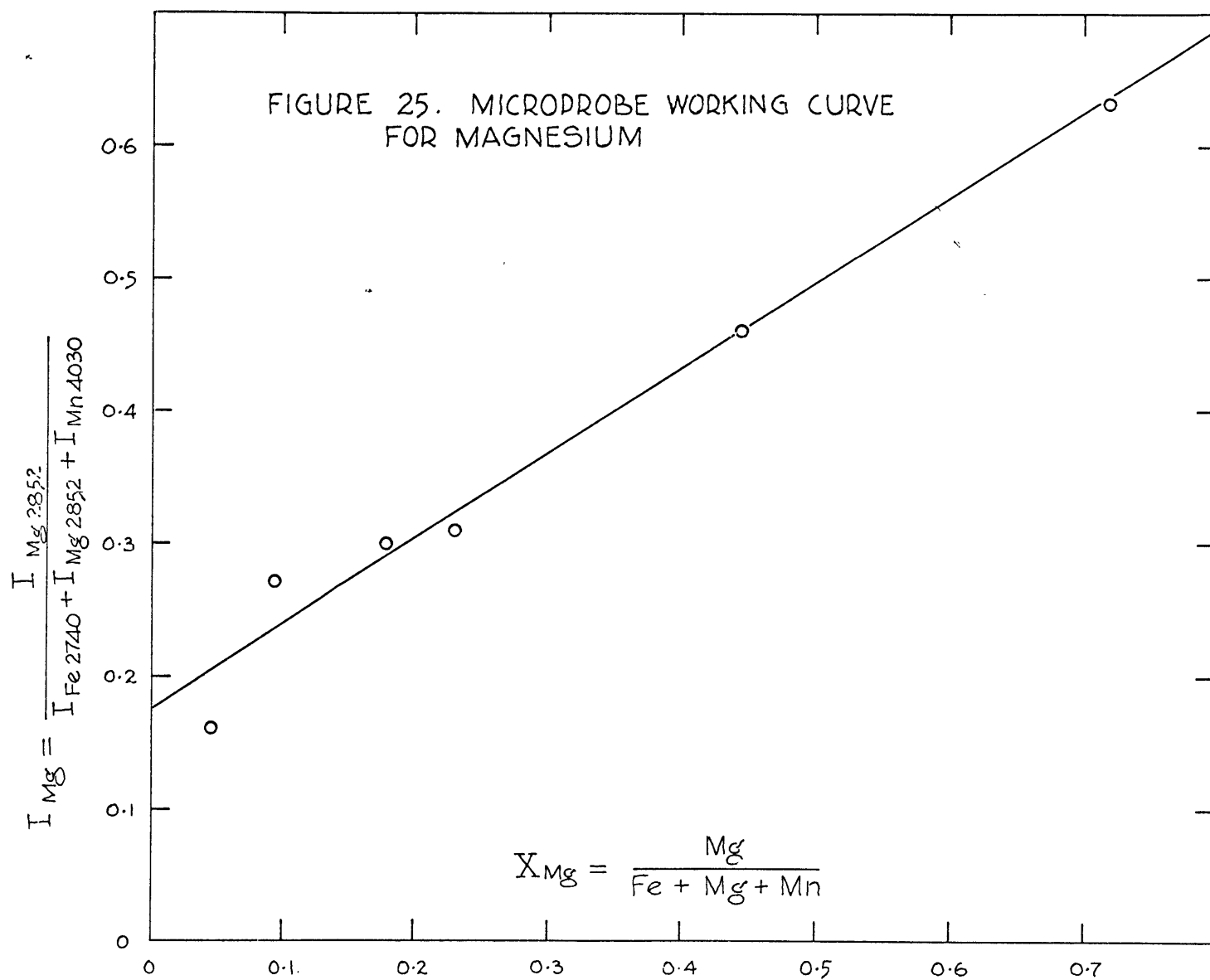
$$\frac{I_{\text{Ca } 3158}}{I_{\text{Fe } 2740} + I_{\text{Mg } 2852} + I_{\text{Mn } 4030} + I_{\text{Ca } 3158}}$$

All intensity ratio data, for both garnets and standards was converted to concentration data by means a Fortran IV program of a least squares analysis for the IBM/360 adapted from Shaw and Bankier (1954). The program, given in Appendix 2, allows a least squares regression analysis of the standard data and gives average concentration values for replicate analyses plus the standard deviation and coefficient of variation for each analysis. The standard deviations of both the slope of the analytic line and its Y intercept are also calculated.

Figures 24, 25, 26, and 27 show the resulting working curves for Fe, Mg, Mn, and Ca respectively.

Analytic results for the garnets of section 17 I and 17 II plus data on the precision and accuracy of the analyses are given in the following sections.





$$I_{Mn} = \frac{I_{Mn\ 4030}}{I_{Fe\ 2740} + I_{Mg\ 2852} + I_{Mn\ 4030}}$$

FIGURE 26. MICROPROBE WORKING CURVE FOR MANGANESE

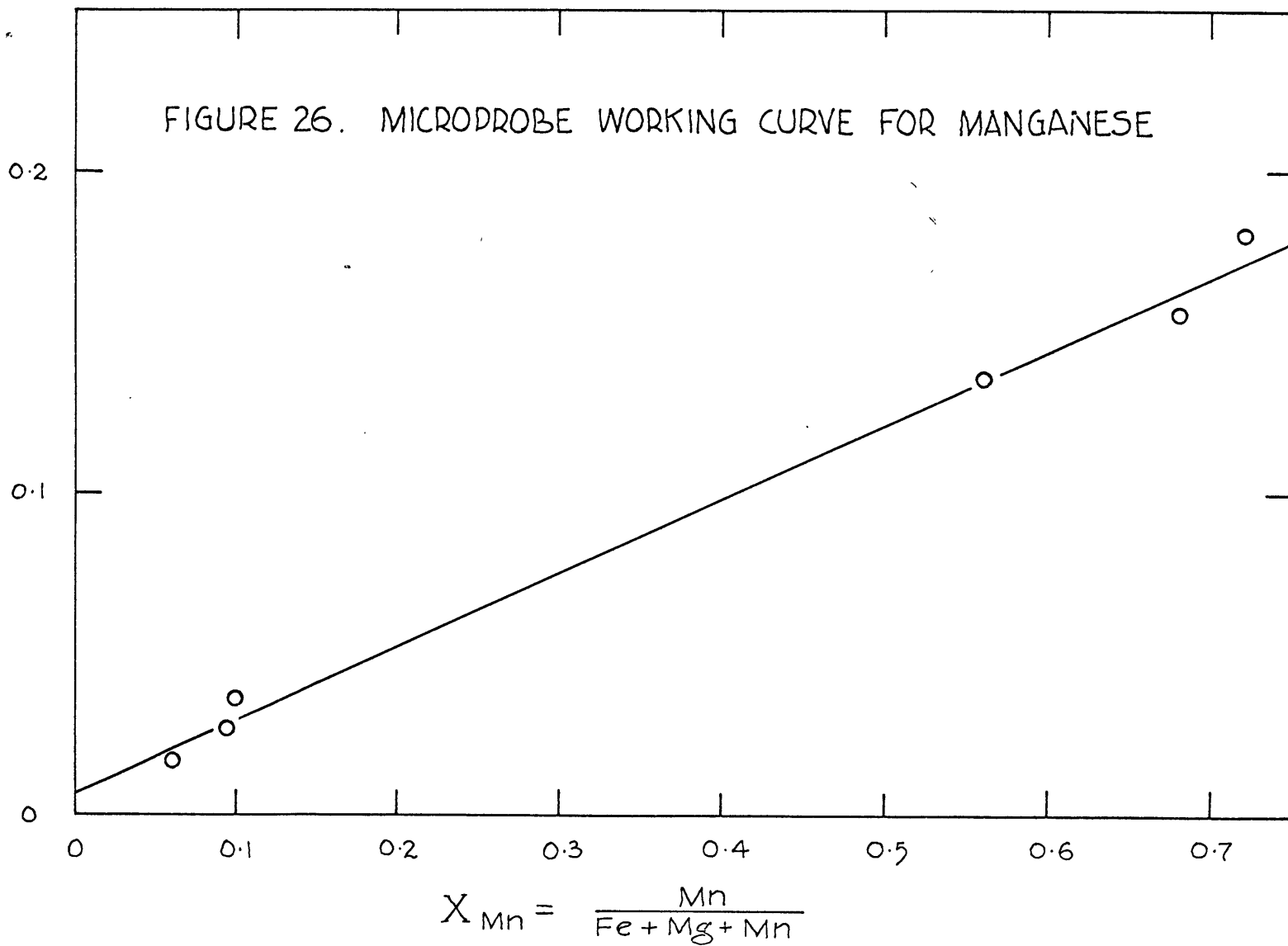
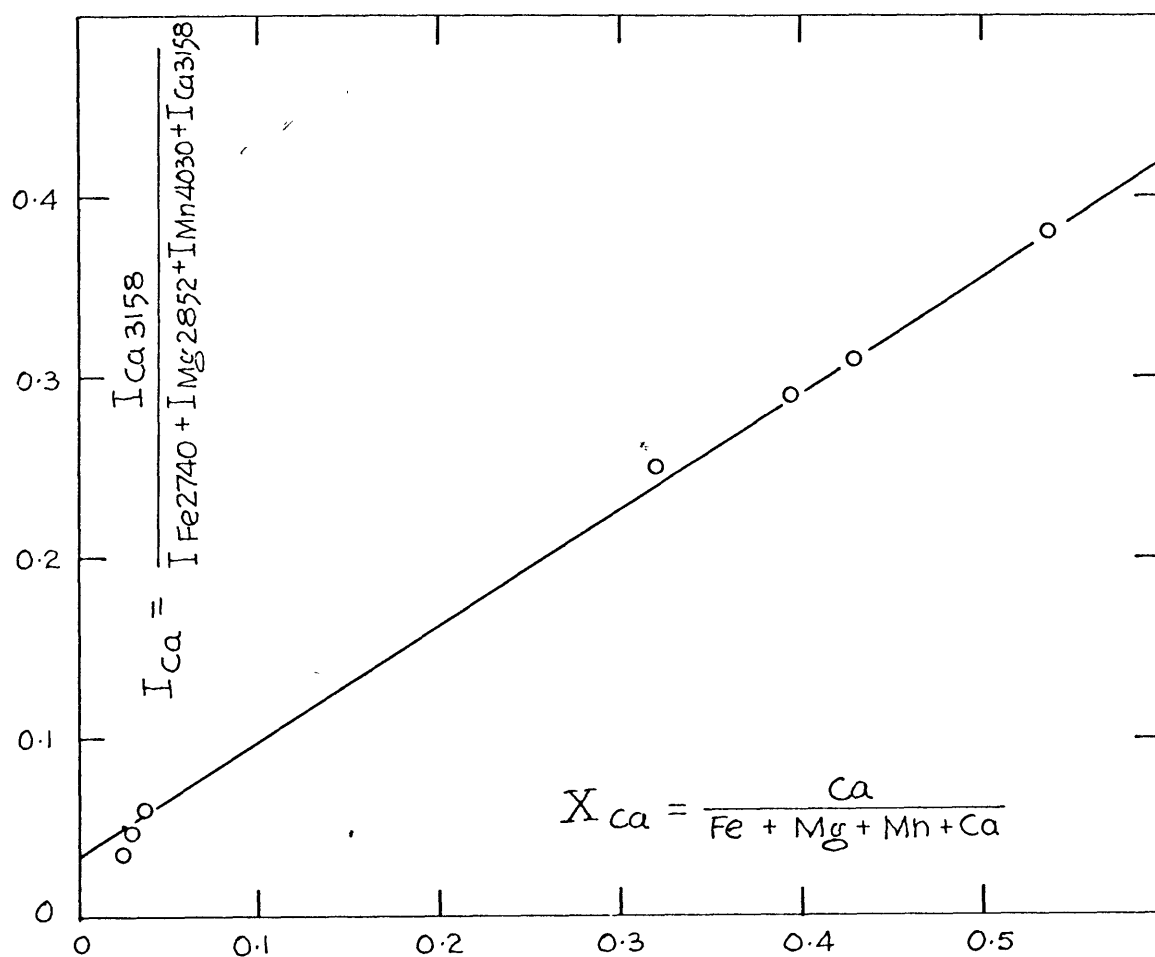


FIGURE 27. MICROPROBE WORKING CURVE FOR
CALCIUM



9.4 Precision and Accuracy

The least squares analysis of standard data (Shaw and Bankier, 1954) programmed for the IBM/360 (See Appendix 1) afforded output that included the slope of the working curve, the Y intercept of the working curve and the standard deviation of the points around the working curve. Also given in the output were the mean of replicate determinations, \bar{x} , for each unknown, the standard deviation of each mean value, s , and the corresponding coefficient of variation, C .

Table 17 presents the statistical data for the various working curves and the average of the coefficients of variation for all the grains measured in each section.

In order to evaluate the statistical data, a sample of the standard diabase W-1 (Fairbairn et al., 1951) was fused to a glass in the same manner as the standards described above. During the course of the routine analyses of the garnets, the W-1 glass was periodically "shot" following the same procedure as for garnets. This operation was performed 5 times and the resulting mean values and statistical data are presented in Table 18.

A further check may be made on the accuracy of the garnet determinations by seeing whether or not the concentration ratios $Fe/Fe+Mg+Mn$, $Mg/Fe+Mg+Mn$ and $Mn/Fe+Mg+Mn$ add up to unity. Of the 222 garnets measured in this manner, only 21 or less than 10 percent gave values significantly different than 1.00, i.e., without the precision of the analytic method. These determinations were discarded, and since the garnets which were represented by these unacceptable analyses were scattered randomly throughout the samples, no significant change in the overall results are likely.

As may be seen from the data of Tables 17 and 18, the precision and accuracy of silicate analysis by this technique is entirely satisfactory for most petrologic investigations.

TABLE 17. Statistical Data from the Chemical Determinations on Garnet Grains with the Laser Microprobe.

*	Slope of Working Curve	Y Intercept of Working Curve	S.D. of points around line	Average C for grains
X_{Fe}	0.60	0.154	0.035	6.65
X_{Mg}	0.64	0.174	0.042	12.8
X_{Mn}	2.22	0.0065	0.017	0.83
X_{Ca}	0.66	0.033	0.023	10.8

$$X_{Fe} = Fe/Fe+Mg+Mn, \text{ etc.}$$

TABLE 18. Statistical Data for Replicate Determinations on W-1 using the Laser Microprobe.

	n	\bar{x}	s	C	Preferred Value
X_{Fe}	5	0.65	0.0066	1.01	0.65
X_{Mg}	5	0.34	0.0038	1.13	0.35
X_{Mn}	5	0.014	0.00005	0.37	0.11
X_{Ca}	5	0.44	0.0098	2.24	0.40

$$X_{Fe} = Fe/Fe+Mg+Mn, \text{ etc.}$$

* Computed from preferred values of the oxides given by Stevens et al. (1960).

9.5 Results

In total, 365 garnet grains were measured in the above manner for Fe, Mg, Mn, and Ca. Presenting an amount of data such as this in an illustrative manner is in itself a problem. It is desirable to present the data in the context of the rock, showing the concentration of an element in a grain with respect to its position in the rock section. Since tabular notation is obviously useless, it was decided that a diagram^matic presentation showing the position of each garnet grain along with the concentration of the element in question would be most lucid.

Figures 28 to 31 show the spatial distribution of Fe, Mg, Mn, and Ca in the garnets of section 17I, which is cut perpendicular to the foliation. A standard error of 10 percent is assumed for the analyses of all the grains and for all elements. Thus, various symbols are used to illustrate the concentration value of an element rounded off to the nearest decimal place. It is felt that this procedure is certainly a liberal estimate of the concentration since only magnesium, with a coefficient of variation of 12.8 percent,^{is} significantly higher than 10 percent.

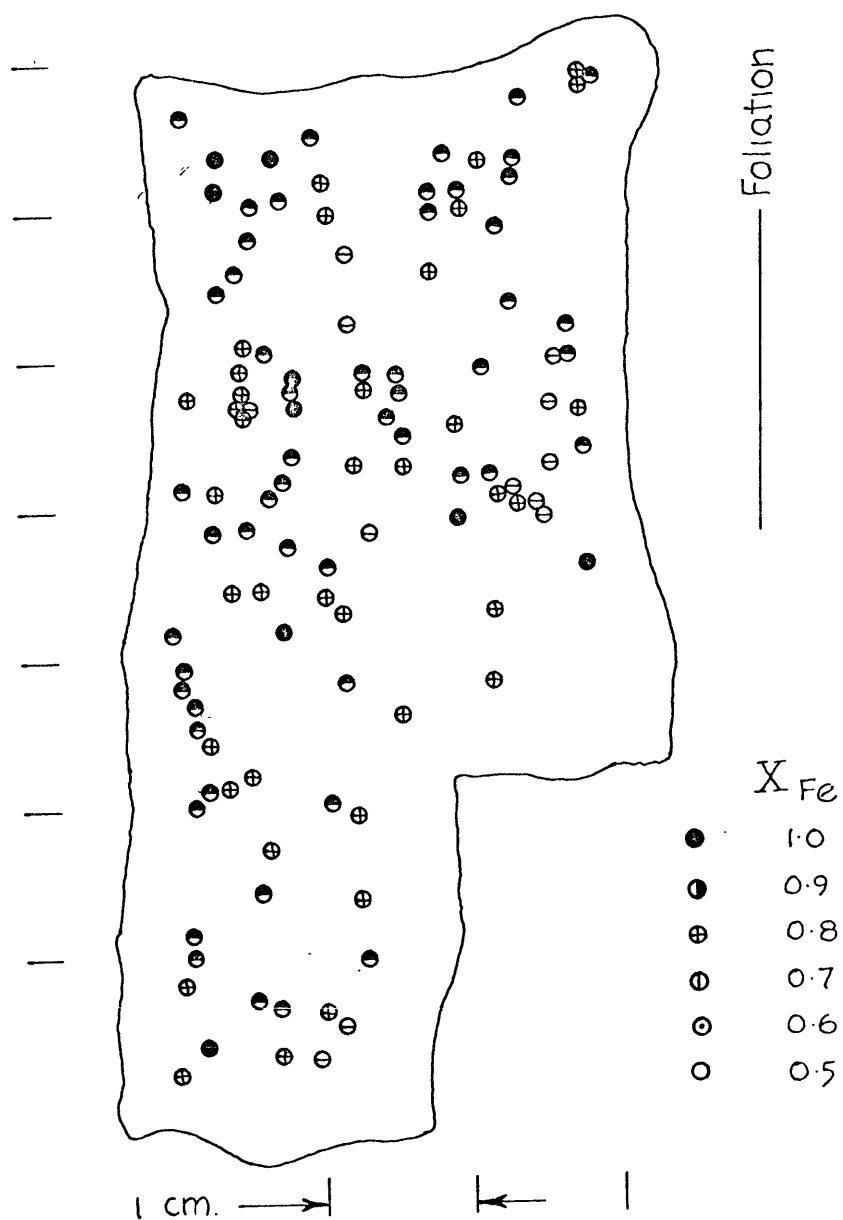
Figures 32, 33, 34 and 35 show the spatial distribution of Fe, Mg, Mn, and Ca, respectively, in section 17II cut parallel to the foliation. The same method of data presentation is employed here.

As the diagrams of the sections indicate, the composition of the garnets with respect to Fe, Mg, Mn, and Ca is quite variable. Groups of garnets with the same concentration of a particular element are quite small, indicating small volumes of equilibration with respect to that element. These volumes, on the average, measure only a few centimeters in their longest direction.

Looking at the figures illustrating the spatial distribution of various elements in garnets of section 17I, it may be seen that the equilibration volumes are very small, usually measuring only a few mm. across the foliation. However, they are more extensive in the foliation direction. Section 17II shows more extensive domains of equilibration, and these are usually elongated in the direction of lineation.

The particular domains of equilibration will be discussed further in a later section. Information gleaned from this aspect of the study will be compared to grain size measurements, inter-garnet distances and rock microstructure for possible correlations.

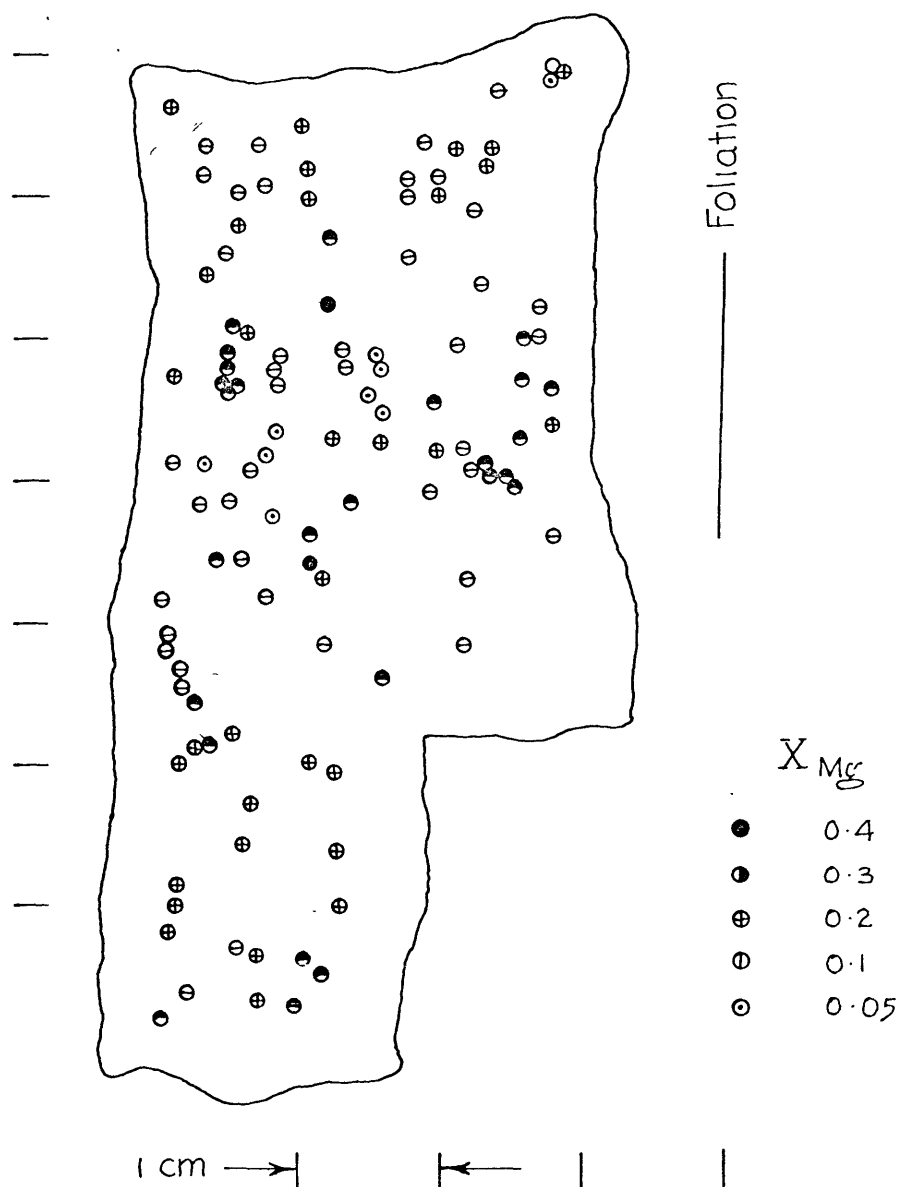
FIGURE 28.



SPATIAL DISTRIBUTION OF IRON IN GARNETS

SECTION 17I, \perp TO FOLIATION

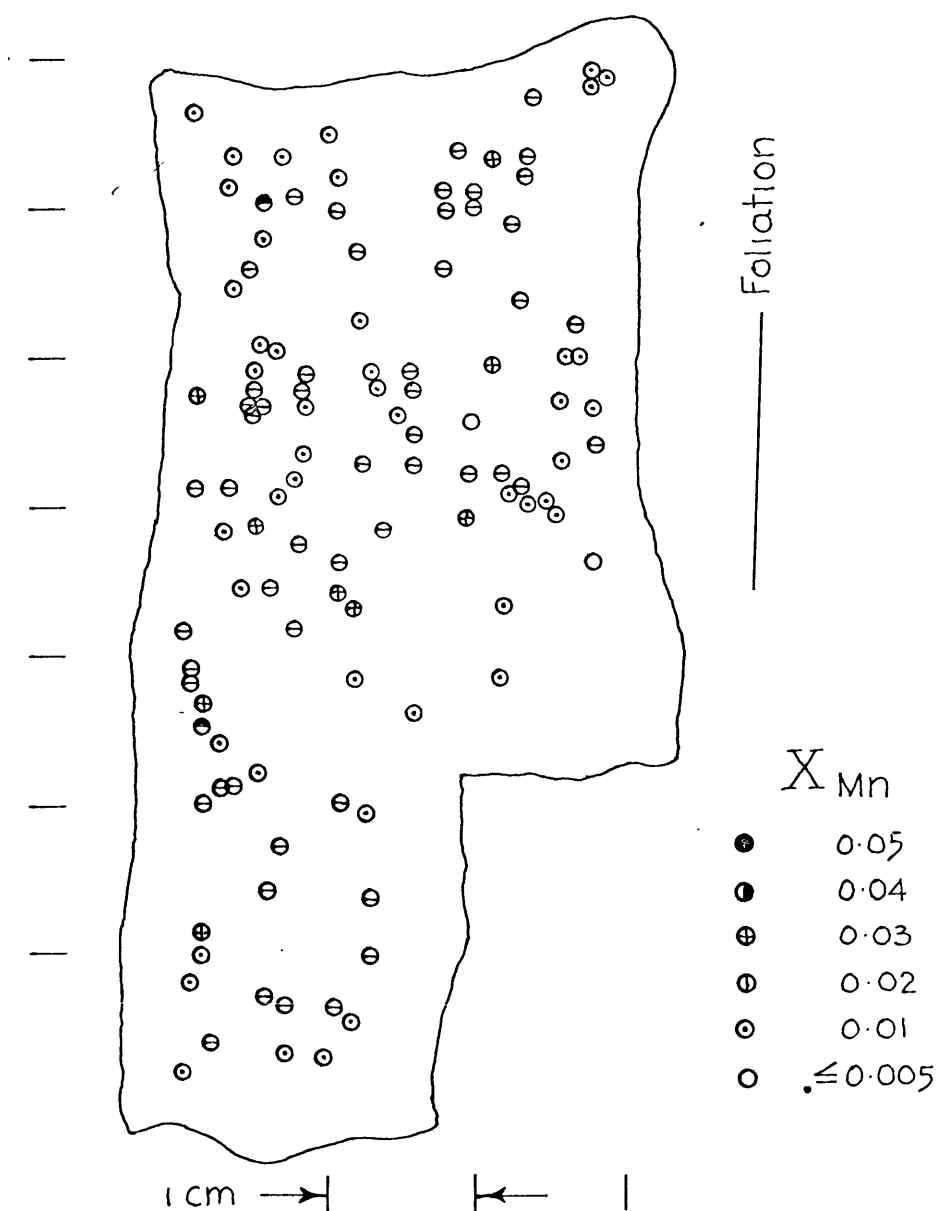
FIGURE 29.



SPATIAL DISTRIBUTION OF MAGNESIUM IN GARNETS

SECTION 171, \perp TO FOLIATION

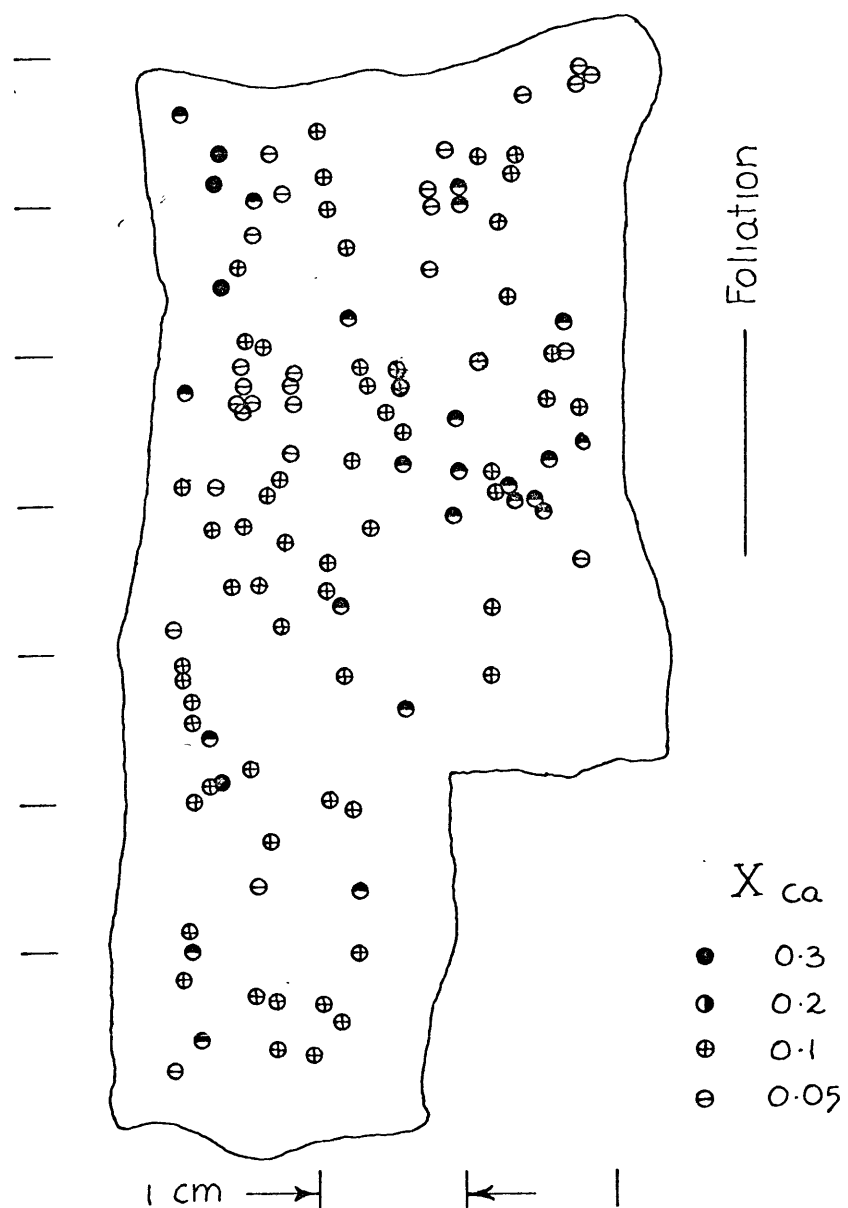
FIGURE 30.



SPATIAL DISTRIBUTION OF MANGANESE IN GARNETS

SECTION 17I, \perp TO FOLIATION

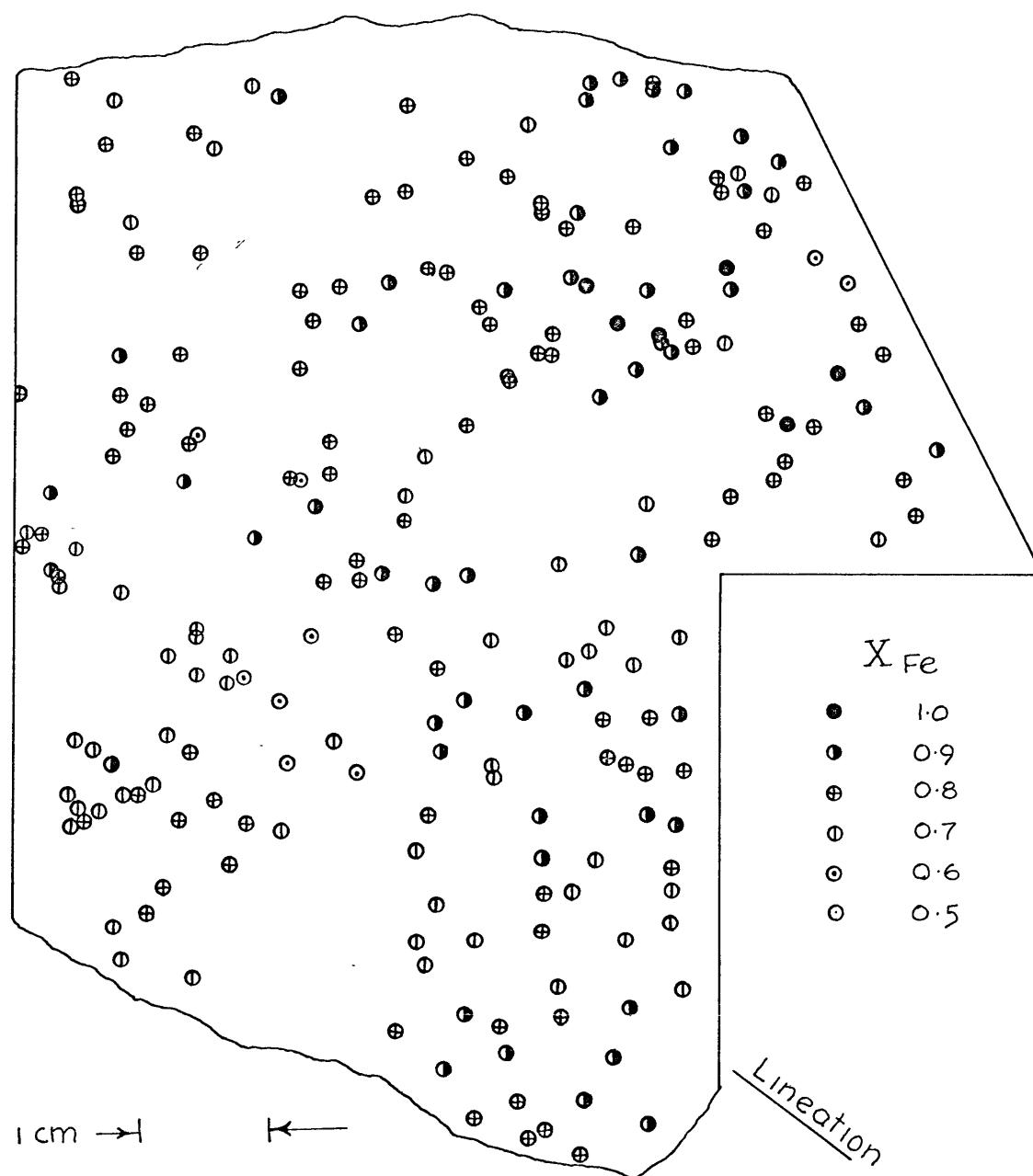
FIGURE 31.



SPATIAL DISTRIBUTION OF CALCIUM IN GARNETS

SECTION 171 , \perp TO FOLIATION

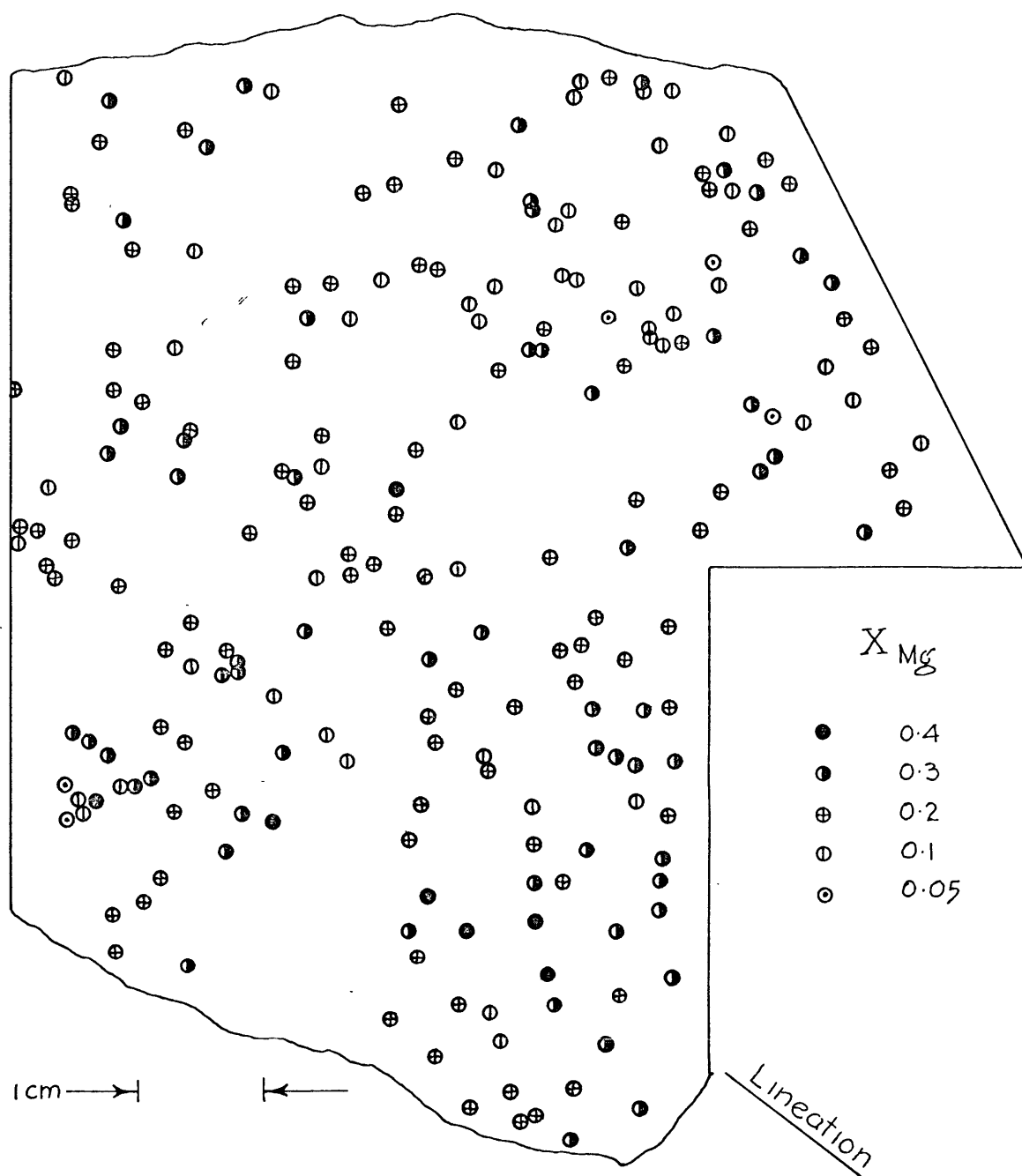
FIGURE 32.



SPATIAL DISTRIBUTION OF IRON IN GARNETS

SECTION 17II, PARALLEL TO FOLIATION

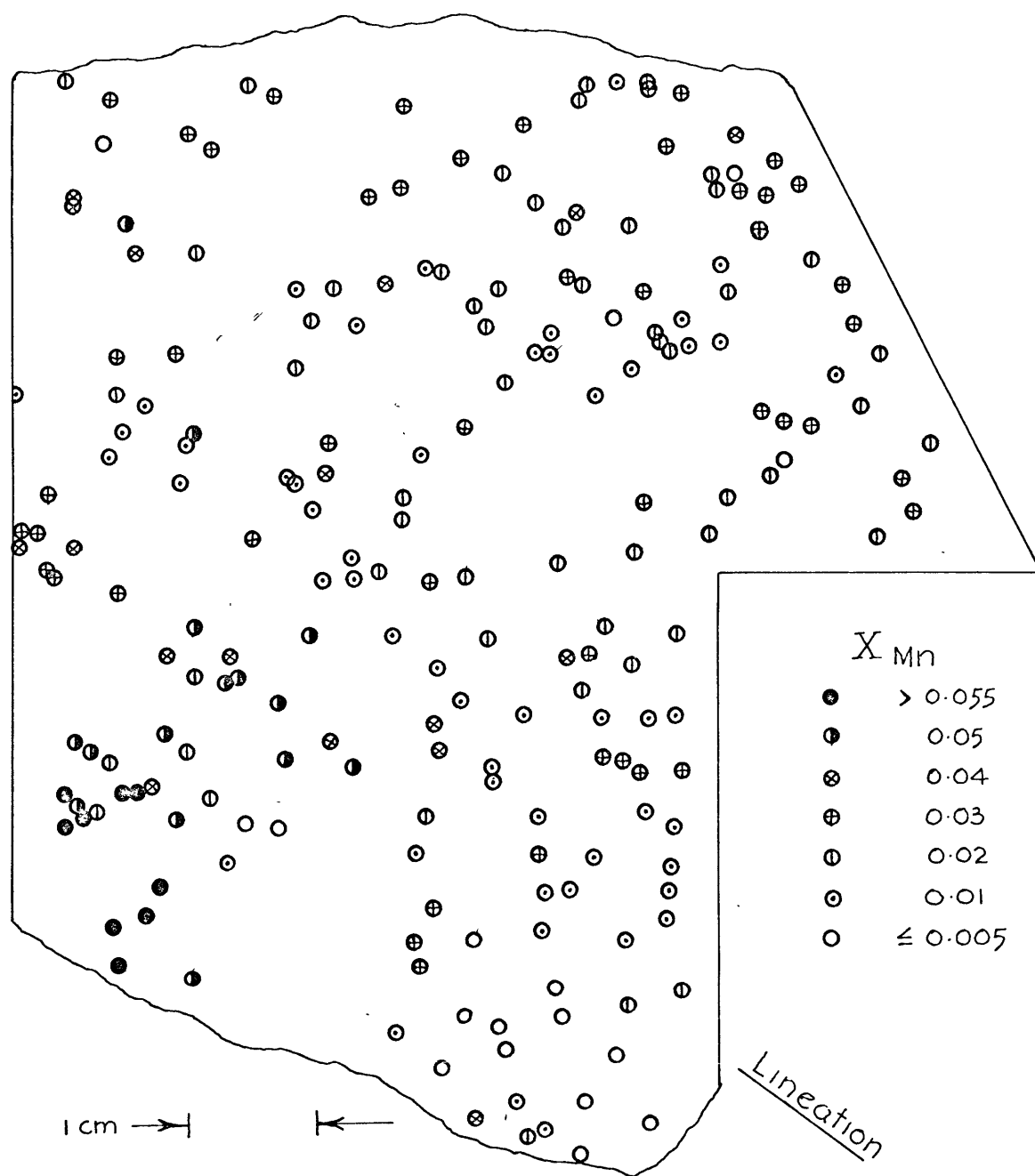
FIGURE 33.



SPATIAL DISTRIBUTION OF MAGNESIUM IN GARNETS

SECTION 17II, PARALLEL TO FOLIATION

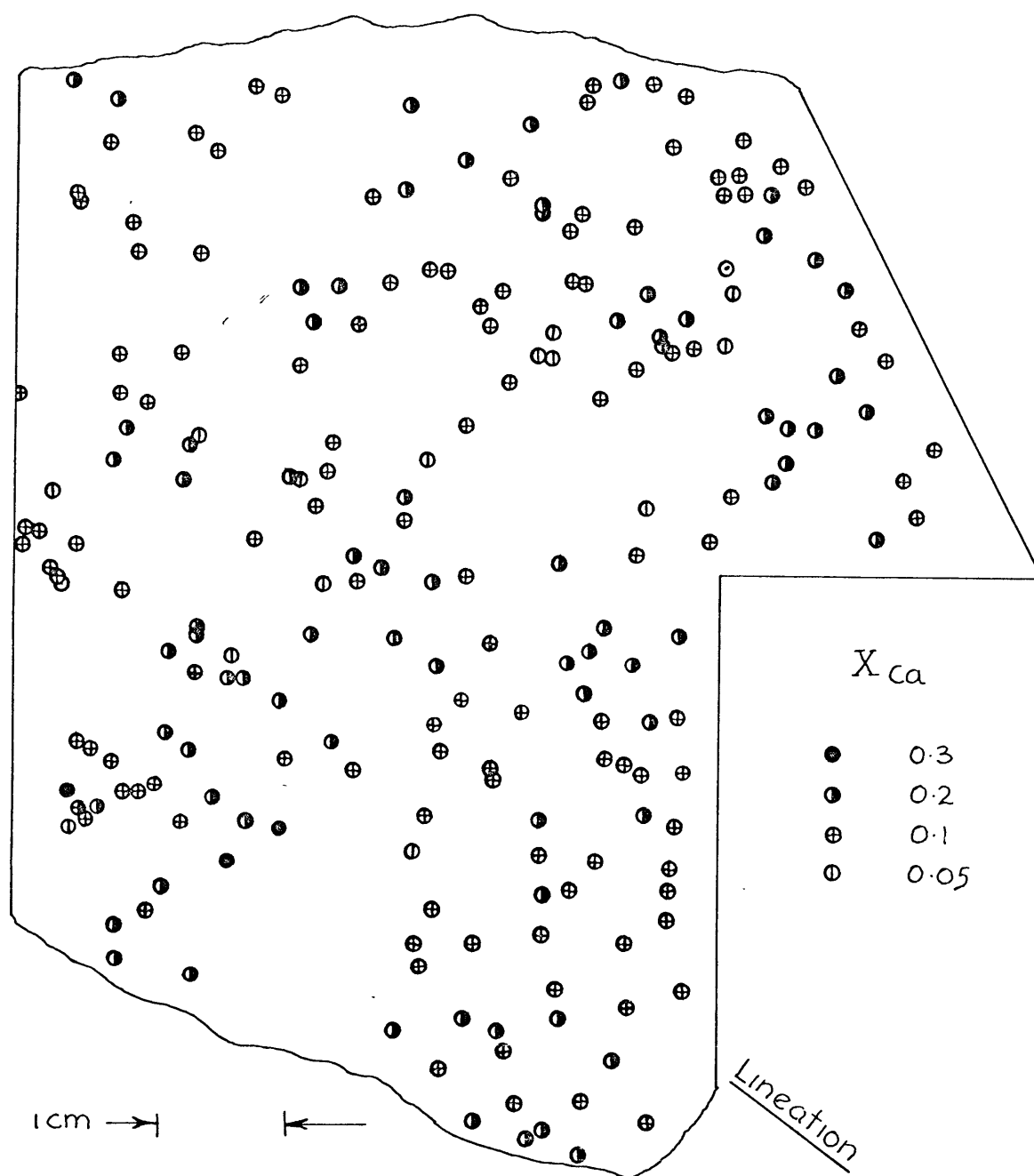
FIGURE 34.



SPATIAL DISTRIBUTION OF MANGANESE IN GARNETS

SECTION 17 II , PARALLEL TO FOLIATION

FIGURE 35.



SPATIAL DISTRIBUTION OF CALCIUM IN GARNETS

SECTION 17II, PARALLEL TO FOLIATION

9.6 An Investigation of Possible Zoning in the Garnets

A recent discussion of zoning in garnets by Hollister (1966) points out the problems of equilibration studies if zoning of one or more of the minerals present is observed. Hollister finds that the compositional variations in zoned garnets follows a Rayleigh fractionation model (Rayleigh, 1902) where only the extreme outermost layer of the garnet is part of the reacting chemical system at any stage of garnet growth. The garnets from the Kwoiek area of British Columbia (Hollister, 1966) and those described by Albee et al. (1966) from kyanite-zone schists from central Vermont show a strong systematic variation of Mn decreasing outwards from the center with contradistinct Fe and Mg variation.

It is obvious that if the garnets of the present study are zoned, most of the variation observed is probably due to poor precision of the point of analysis on each garnet. Thus, it was imperative that the garnets be inspected for compositional zoning.

Compositional variations in the garnets of this study were investigated on a Mark II Laser Microprobe at the Jarrell-Ash Company in Waltham, Massachusetts. The Mark II is the newest model of the laser microprobe and features a non-temperature sensitive neodymium laser with controlled output energy and a much improved optical system. Reproducibility of laser energy output and, therefore, crater dimensions are greatly improved over the model used throughout the rest of this study (S. Targonski, personal communication, 1966). Operating parameters used in the zoning investigation are given in Table 19.

Four garnets were traversed at approximately 25 micron intervals and intensity ratios obtained in the same manner as discussed above. Two of the garnets examined were from sample 17 showing minor inclusions of sillimanite. One garnet was from sample 42 where inclusions in the garnets are rare and the last was from sample 8 and exhibited quartz inclusions located in a clump in the center of the garnet.

TABLE 19. Operating Parameters used in the Investigation
of Zoning in the Garnets.

Source:	Jarrell-Ash Co. Mark II Laser Microprobe.
Spectrograph:	1 m. Czerny-Turner mounted spectro- graph. Jarrell-Ash Co.
Electrodes:	1/8th inch National Carbon Co. AGKSP graphite rods, pointed pencil sharp
Photographic Plates:	Eastman Kodak Type 103-0.
Analytic gap:	2 mm. above the sample.
Cross Excitation voltage:	2000 volts.
Wave length region:	2600 A - 4200 A
Plate develop- ment:	4 minutes at 20 C in Kodak D-19 developer.

9.7 Results of Zoning Investigation

Figure 36A shows the Mn/Fe+Mg+Mn profile across a garnet exposed on section 17 I which is cut perpendicular to the foliation. The traverse is in the short axis direction of one of the garnets which is elongated as described above. As is evident from Figure 36A, no zoning with respect to manganese is apparent within the limits of analytic error. Further, there was no zoning of the garnet with respect to Fe and Mg.

A traverse across a garnet cut parallel to the foliation (section 17 II) showed no compositional zoning with respect to Mn, Fe or Mg. The profile of the compositional ratio Mn/Fe+Mg+Mn in this grain is shown in Figure 36B. The profile shows a semblance of a oscillatory zoning with respect to Mn. However, this variation is within the limits of analytic error and a proposed zoning in this grain would be purely conjectural.

Figure 37A illustrates the Mn profile across a garnet from section 42 II cut parallel to the foliation. No significant inhomogeneity is noted. The traverse across this grain found it homogeneous with respect to Fe and Mg as well.

The only zoning observed was along a traverse across a garnet from sample No. 8 (see Table 8, section I) which showed a distinct rise in the ratio Mn/Fe+Mg+Mn from about 0.020 at the edges to 0.070 near the center. The area in which the high Mn values are located corresponds exactly with the clump of small quartz inclusions. No inclusions were observed in the outer regions of the grain where constant low atomic ratios for Mn prevail.

Hollister, (1966) has mentioned the possibility of calcium zoning within garnets. This possibility was investigated along with Mn, Fe and Mg and no compositional zoning with respect to Ca was observed. Figures 38A and 38B show Ca profiles across sections 17II and 17I, respectively. All variations are within the standard deviation of analysis.

Thus it is concluded that the compositional zoning of garnets in these rocks is not prevalent and that the variations of garnet compositions within a hand specimen are real. Other factors

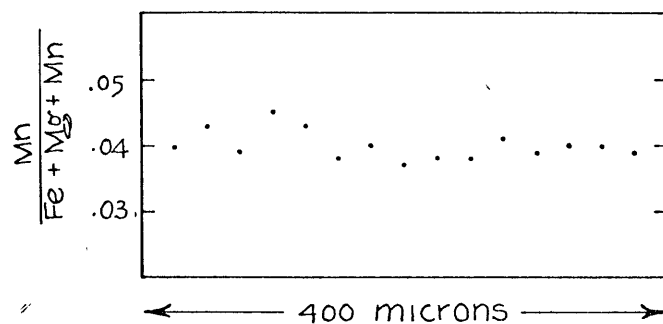


FIGURE 36A. Mn PROFILE ACROSS GARNET
IN SECTION 17 I

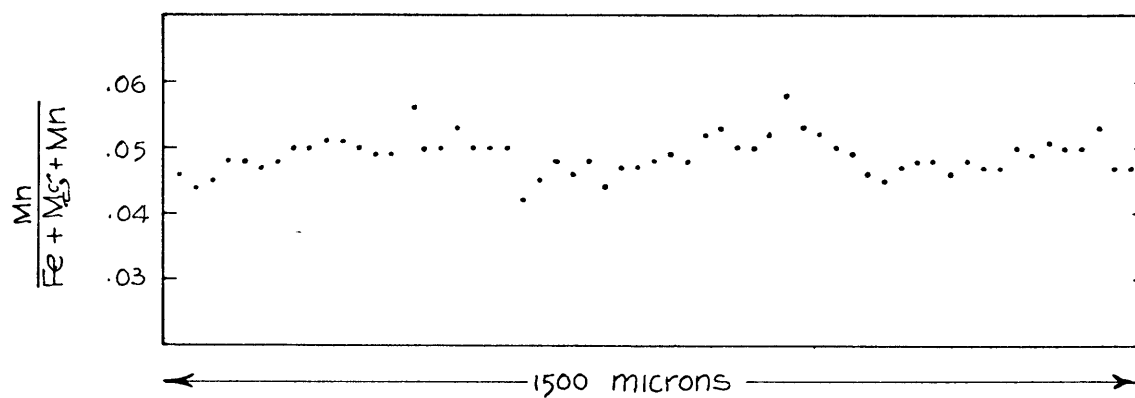


FIGURE 36 B. Mn PROFILE ACROSS GARNET
IN SECTION 17 II

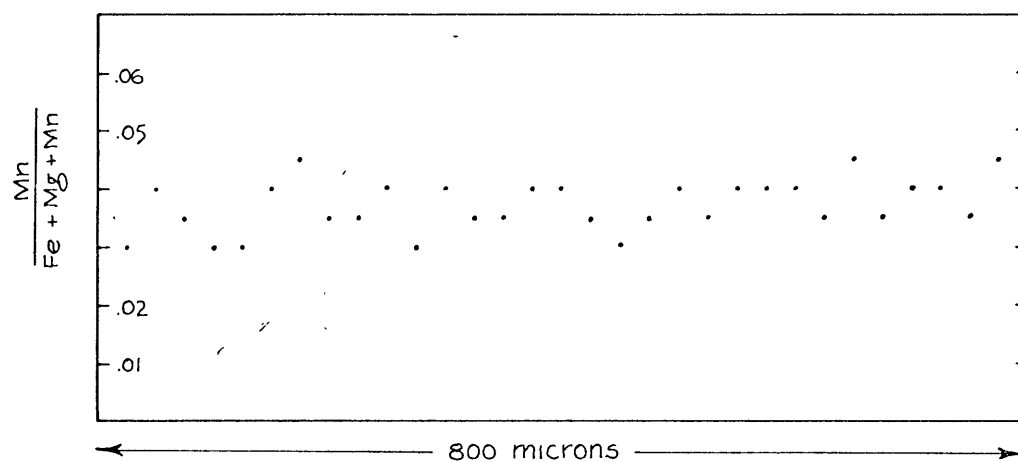


FIGURE 37 A. Mn PROFILE ACROSS GARNET
IN SECTION 42 II

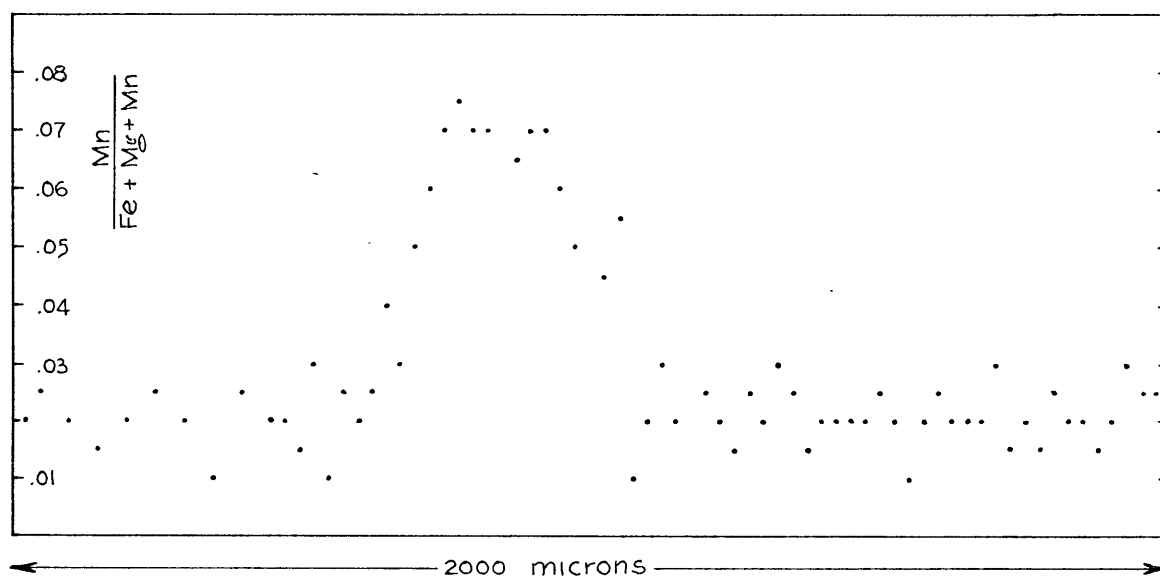


FIGURE 37 B. Mn PROFILE ACROSS GARNET
IN SECTION 8

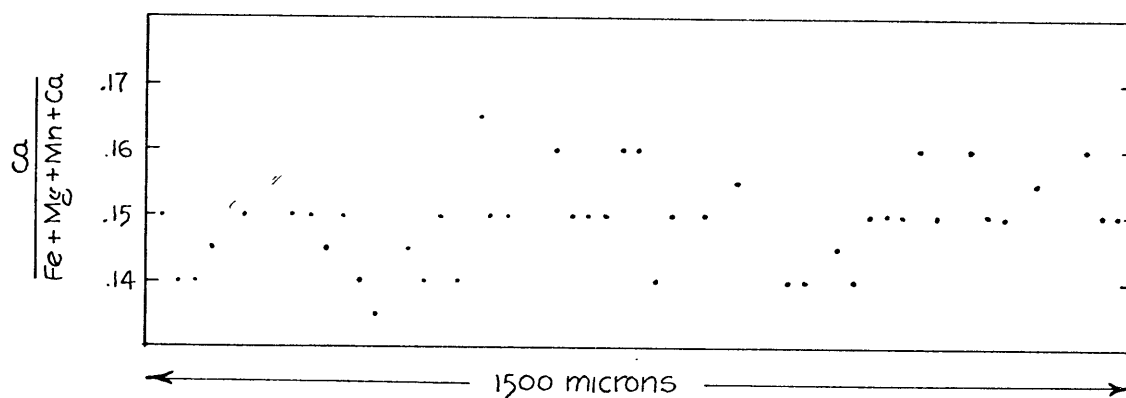


FIGURE 38A. Ca PROFILE ACROSS GARNET
IN SECTION 17 II

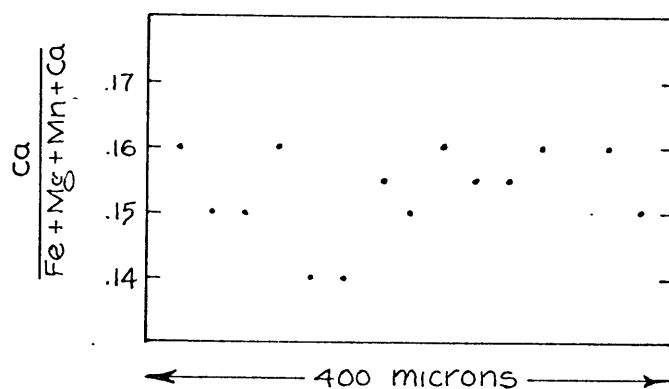


FIGURE 38 B. Ca PROFILE ACROSS GARNET
IN SECTION 17 I

which lead to this same conclusion are:

1. No optical zoning was evident in any garnets examined.
2. During replicate analyses of the garnets in matrix, no care was taken to "shoot" the same garnet in the same place each time. This had no effect on the precision of the determinations for the various elements within a single grain.
3. If the garnets of specimen 17 I and 17 II had been zoned, spatial equilibration domains as described above would not have been observed as the determinations were not made on the edge of each grain, i.e., within the reacting thermodynamic system.

Zoning, or the lack of it, in minerals is a reflection of the velocity of growth since zoning implies that the internal equilibration of the mineral has not had time to take place. Rast, (1965) suggests that the presence of inclusions in minerals of metamorphic rocks represents a higher velocity of growth, and that this higher velocity of growth reflects the chemical state of the immediate neighborhood of the point of mineral nucleation. Sturt and Harris, (1961) cite an example of replacement of amphibole by garnet where the quartz interstitial to the garnet remains unaffected. This may also be the case in many of the elongated garnets of specimen 17 where local inclusions of sillimanite continue uninterrupted through the garnet along the foliation surface. Although zoning is not evident at present in the garnets of this study, the unusual clumping of quartz inclusions in the garnet from sample No. 8 coupled with the higher Mn values of the garnet in the region of this clumping suggests that the garnets of these gneisses did indeed grow quickly and were at one time zoned, at least with respect to Mn. It is proposed that the garnets have later equilibrated internally expelling non-stoichiometric included material and thus eliminated compositional zoning. (Yoder, 1952, and Buddington, 1965) have proposed that the formation of garnet is dependent on a sufficient reaction time for the minerals to nucleate and grow. Buddington further suggests that temperatures above the equilibrium temperature will be required to facilitate reaction. It is thus possible that zoned garnets have grown quickly under temperature conditions higher than that needed for garnet production. A subsequent rapid decline in temperature would leave garnets with only their extreme edges in the reaction system. This is

possibly the case in the Kwoi^eck area of British Columbia Hollister, (1966) and the Lincoln Mountain Quadrangle, Vermont occurrence, Albee et al., (1966). However, if temperatures leveled off for an extended period of time, or if there was a later metamorphic event with temperatures near the almandine stability region, redistribution of stoichometric and non-stoichometric material within the garnet might take place as in specimens 17 and 42 or in part as in specimen 8.

Since the Grenville is most likely an area of both regional and deep seated contact metamorphism, Wynne-Edwards, (1959, 1962) and polymetmorphism (Krogh 1964, 1966, Silver, 1966), the above scheme for the formation of zoning and its later destruction is entirely possible.

9.8 Correlation of Results with Grain Sizes and Intergrain Distances

In the last chapter, an attempt was made to uncover possible correlations between the physical parameters measured. Using the chemical data of this chapter the correlation matrix was expanded to include all nine parameters which are:

- A = Long axis length
- B = Intermediate axis length
- C = Short axis length
- V = Volume
- Fe = ratio $\frac{\text{Fe}}{\text{Fe}+\text{Mg}+\text{Mn}}$
- Mg = ratio $\text{Mg}/\text{Fe}+\text{Mg}+\text{Mn}$
- Mn = ratio $\text{Mn}/\text{Fe}+\text{Mg}+\text{Mn}$
- Ca = ratio $\text{Ca}/\text{Fe}+\text{Mg}+\text{Mn}$
- N = distance to the nearest phase analog

The Fortran IV program described above (see Chapter 8.4) and (Appendix 4) which determined the covariance and correlation of above parameters also applied a step-wise regression analysis to all parameters which possessed an F-ratio exceeding the critical value for the population. The correlation matrix for the above variables in the garnets of section 17 I, perpendicular to the foliation, is given in Table 20. An analogous matrix for section 17 II, cut parallel to the foliation is given in Table 21.

Possible correlation between physical parameters will not be discussed ^{here} as it has already been covered in Chapter 8.4. Inspection of Tables 20 and 21 show very little correlation of any of the chemical parameters among themselves and with the physical variables. However, besides the obvious covariance of Fe and Mg, there are possible correlations between the following:

- A - Fe and Mg in 17 I
- C - Fe in 17 II
- Fe - Mn in 17 I and 17 II
- Mg - Mn in 17 I
- Ca - Fe, Mg, in 17 I
- Ca - Fe, Mg and Mn in 17 II
- Ca - Distance to nearest garnet in 17 II

TABLE 20. Correlation Marix for the Measured Physical and Chemical Variables
for the Garnets of Section 17I.

A	B	C	V	Fe	Mg	Mn	Ca	N	*
1.000	0.562	0.511	0.739	-0.149	0.139	0.015	0.029	0.165	A
	1.000	0.768	0.733	0.082	-0.074	-0.018	0.009	0.208	B
		1.000	0.792	0.085	-0.048	0.064	0.063	0.220	C
			1.000	0.077	-0.046	0.020	0.012	0.180	V
				1.000	-0.859	-0.170	-0.232	0.050	Fe
					1.000	-0.189	0.254	-0.005	Mg
						1.000	0.000	-0.005	Mn
							1.000	0.018	Ca
								1.000	N

Number of Variables 9

Number of Cases 95

* variable code given in text.

TABLE 21. Correlation Matrix for the Measured Physical and Chemical Variables
for the Garnets of Section 17II

[illegible]

These possibilities were further tested by the ^{application} ~~of~~ of the step-wise regression analysis to the input data. From this analysis, it was shown that there is a high negative correlation of Fe and Mg values but this is expected since Fe and Mg are the dominant bivalent elements in the garnets. If the Fe concentration of the garnet is assumed to be the independent variable and the length of the long axis as the dependent variable, only 5% of the variance of the long axis length may be accounted for by variance in the Fe content. This is probably not significant but may possibly give support to the reasoning that garnets will nucleate and grow faster in regions where the component materials are more plentiful. The correlation of the length of the short axis and the Fe content in section 17 II was found to be insignificant. The correlation of the Ca content of garnet in section 17 I to the distance from the nearest neighbor may likewise be eliminated. However, in section 17 II, taking the Ca content as the dependent variable we may account for 3% of its variance by the distance to the nearest neighbor. The opposite assumption of nearest neighbor distance as the dependent variable gives the same answer. In each case, this 3% dependency is a significant amount of the total accounted for.

The correlation between the contents of Ca and Mg in the garnets of this rock are real. This same conclusion is applicable to the correlation of the Fe and Mn contents. The correlation of the garnet Mg and Mn contents is real although only about half as strong as the Fe-Mn covariance. There is no significant correlation between Fe and Ca in the garnets of specimen 17

It may be concluded that the Fe and Mn contents are correlatable and that their concentrations are covariant in that either Fe or Mn may be assumed the dependent variable with no change in the correlation coefficient. The relationship of Mg and Mn in these garnets is similar although only half as strong.

The Ca content of the garnets was found to be strongly dependent on the Mg content. Seventeen per cent of the variation of the Ca content of the garnets is due to variation of the Mg contents of the same garnets. This is quite significant since

only 25% of the Ca variance can be accounted for by the parameters measured in this study. Taking Mg as the dependent variable and Ca as the independent, very little of the Mg variance may be accounted for and this possibility was eliminated.

9.9 Discussion

As noted above, the spatial degree of garnet equilibration in sample 17 is quite limited. The domains of equilibration for Fe and Mg are limited to less than 4 cm. in the longest direction. The garnets of section 17 I, cut perpendicular to the plane of foliation show a distinct structural control of the shape and size of the equilibration domain. The areas over which garnets are of the same composition are elongated in the plane of the foliation to such an extent that in some cases chemical communication has been in effect over a distance of about 3 cm. along a foliation surface, but garnets in the adjacent layer are of a different composition with respect to Fe and Mg.

An examination of Figures 32 and 33 gives the spatial relations of Fe and Mg in the garnets of section 17 II, cut parallel to the foliation. Here the domains of equilibration with respect to Fe and Mg are more extensive although they are still elongated. This elongation is in the direction of the lineation which is defined by trains of sillimanite and garnet.

In summary, the domains of spatial equilibration of Fe and Mg in garnets were found to be quite small, ranging from only a few m.m. to a few centimeters. The shapes of these domains were controlled by the rock structure, i.e., foliation and lineation, and were more extensive along the foliation surfaces and lineation traces than across them. Parallel to the foliation, chemical communication of garnets with respect to Fe and Mg took place over a maximum distance of 4 cm. in the lineation direction and 2 cm. across it. Perpendicular to the foliation, chemical equilibrium of garnets was limited to less than 1 cm. ~~_____~~. Chemical communication across foliation planes was limited to less than a centimeter in most cases. The equilibration domains are possibly roughly ellipsoidal in shape with an axial ratio of close to 4:2:1. It is also interesting to note that in section 17 II spatial equilibration of Fe is more extensive than Mg. Iron shows less distinguishable domains, but these are larger than the Mg domains ~~_____~~. The Mg domains of equilibration are much more regular in their orientation in the lineation

direction. This is possibly a reflection of the relative mobilities of Fe and Mg under metamorphic conditions. This relationship is not so easily recognized in section 17 I.

The spatial equilibration of Ca in garnets in sample 17 was found to be somewhat more extensive than that for Fe or Mg and the domains of analogous Mn concentration are more irregular in shape than their Fe and Mg counterparts. A distinct structural control is still evident, but equilibration across structural features is more extensive. For example, in section 17 I (Figure 30) equilibration domains measuring up to 1.5 cm. across the foliation can be distinguished. The elongation in the foliation surface still persists, however. In section 17 II (Figure 34) cut parallel to the foliation, the domains of Mn equilibration in garnets are at least as extensive as those for Fe, but they are less regular in their orientation according to the lineation direction. The axial ratios of the domains of Mn equilibration, if they are assumed to be roughly ellipsoidal in shape, are about 2:1:1.

The spatial degree of equilibration in the garnets of sample 17 with respect to their Ca content is shown in Figure 31 and 35. In Figure 31, looking at the section perpendicular to the foliation, equilibration domains controlled by structure and those having no obvious structural control are both observed. The structurally controlled domains, for the most part, occur at one end of the section and it is proposed that variations in the whole rock Ca content were more prevalent here. This would probably be reflected in the mineral assemblage associated with each of these garnet equilibration domains

Calcium equilibration in the garnets of section 17 II (Figure 35) is more extensive than Fe, Mg or Mn. The domains are usually elongated and extend up to 5 cm. in their longest direction. Although, in some areas of the section, elongation of the equilibration domains is in the lineation direction, there are also regions of garnets having the same Ca content which are distinctly elongated almost perpendicular to the trace of the lineation and some which show no preferred orientation.

The spatial degree of chemical equilibration in the garnets of specimen 17, as described above for Fe, Mg, Mn and Ca is in good agreement with the results of other workers. Phinney, (1959, 1963) found that the $^{Fe}/Mg$ ratios of the biotites picked from thin sections showed significant change over a few millimeters. It is interesting to note, however, that biotites from sections, which exhibited the same assemblage throughout and were essentially mineralogically homogeneous, gave nearly identical $^{Fe}/Mg$ ratios. Brownlow, (1961) describes a similar phenomenon where the compositions of coexisting biotite-actinolite pairs from a contact zone show significant differences within the distance of a few inches. Zen, (1961) has discussed the petrology of pyrophyllite deposits in North Carolina. He finds that the coexisting minerals are in equilibrium but only on a small scale and within a particular assemblage which is controlled by the relative concentrations of Al_2O_3 , SiO_2 and H_2O .

Harker, (1939) describes metasediments in which bands of different composition are preserved into high grades of metamorphism. The bands are only a few millimeters thick. Finally Albee et al. (1965, 1966) have shown that although the schists of the Mt. Grant area of Vermont have reached wide-spread equilibrium with respect to the $^{18}O/^{16}O$ ratio, the presence of different mineral assemblages in adjacent bands of the schist point out that equilibration of cations has taken place only very locally.

The data of this study coupled with the examples above give persuasive evidence to the concept of "local" equilibration, Thompson (1959) or the analogous situation of "mosaic" equilibrium discussed by Korzhinskii (1959). In each case, the rock system as a whole may not be in equilibrium but in each of the small regions thermodynamic equilibrium is attained if definite relationship occur between all the parameters. In other words, the chemical potential of an element must be equal in each phase of the assemblage. If the phase exhibits ideal or dilute solution with respect to the element, the chemical potential is reflected in the phase by its concentration of that element. The spatial extent of

local equilibration of the assemblage is thus the volume over which all minerals have equal chemical potentials for each component element. The definition of the local extent of chemical equilibrium for one of the phases of an assemblage thus defines the maximum extent of the equilibration domain of the assemblage. For example, the garnet bearing assemblages of specimen 17 are as follows:

cordierite+garnet+biotite
cordierite+garnet
garnet+biotite

If the spatial extent of local equilibration is defined for garnet, then this places an upper limit on the volume of local equilibration with respect to a specific element in a particular assemblage. In this case, the assemblage is possibly controlled by the whole rock chemistry (Wynne-Edwards and Hay, 1963).

It is germane to note that often the domains of equilibration for the particular elements, as described earlier in this chapter, do not coincide in shape or size thus causing the volumes in which the garnets are of the same concentration for all elements determined to be very small.

It may be concluded that, in agreement with Phinney (1963), the author finds that the chemically analyzed minerals from a normal hand specimen really represent the average compositions, different parts of which are in equilibrium with different assemblages.

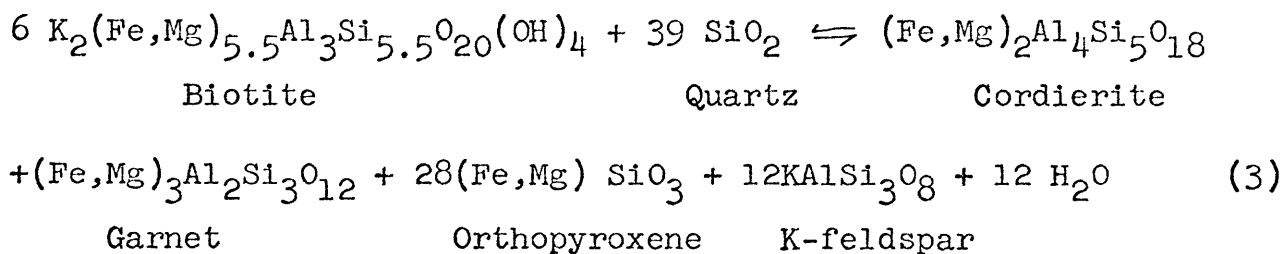
10 CHEMICAL DETERMINATIONS IN BIOTITE AND GARNET FROM A PYROXENE GRANULITE FACIES ROCK

10.1 Introduction

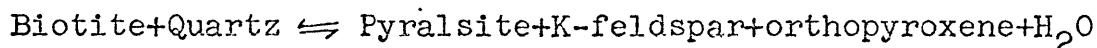
As discussed above, it was decided to examine the spatial extent of chemical equilibration in a rock having a different mineral assemblage and possibly a different grade of metamorphism. The rock selected was a garnet-biotite-orthopyroxene gneiss, sample No. 42, described in the last chapter.

Wynne-Edwards, (1959) and Wynne-Edwards and Hay, (1963) have proposed that the assemblage which sample No. 42 represents belongs to the pyroxene granulite facies. However, there are some differences from normal pyroxene granulites observed in these rocks: (1) The quartz and feldspar have not taken on a platy aspect. (2) Rutile is not seen although ilmenite, if present, is scarce and the TiO_2 content of the rock may be low. (3) The garnets are lower in pyrope content than is expected in these assemblages although it is higher on the average than the garnets studied elsewhere in this work. No aluminosilicate was observed in any of the garnet-hypersthene gneisses collected. In many respects the rocks resemble charnockites (Subramanian, 1959).

No cordierite was observed in the garnet-orthopyroxene gneisses. Therefore, the reaction for alumina deficient rocks,



given by deWaard (1965) is not applicable. A reaction of the type,



seems to ^{be} in operation here, the lack of cordierite being due both to an alumina deficiency and to excess CaO (Wynne-Edwards and Hay, 1963).

The relationship of biotite and hypersthene in this rock are unclear. From thin section analysis, no definite statement can be made as to whether the biotite is retrograde or the hypersthene prograde. The biotite occurs as small discrete grains with only rare association with the orthopyroxene. In some cases, however, textural relations indicate that hypersthene is replacing garnet.

It is suggested that the assemblage observed in sample 42 is indicative of pyroxene granulite facies and represents at least a higher temperature of metamorphism than sample 17 examined in the last chapter.

The examination of sample 42 will allow evaluation of the volumes of chemical equilibration under a different set of chemical, physical and mineralogical conditions. It might be expected that the volumes of chemical communication and thus, free diffusion, would be more extensive at higher grades of metamorphism. If both the biotite and garnet are subjected to chemical determinations, the distribution coefficients for various elements may also be examined with respect to distance between specific grains. In Chapter 9 the garnet grains were found to be of the same composition only over a volume of about 3 X 2 X 1 cm. If this is true for biotite, then the samples taken for equilibration studies as that of Section I of this work should be on the order of 2 cm. on a side.

It may be found that the volume over which garnet and biotite equilibrate at a higher temperature is larger due to increased mobility of elements and a more prolonged period of metamorphism. Foliation is not nearly so marked in this rock and a lineation was not observed. It is also possible that the volume of chemical equilibration in rock such as this will be more nearly spherical due to the lack of preferred diffusion direction as proposed in the last chapter.

10.2 Method of Separation and Analysis

Sample 42, described above, was trimmed with a diamond saw on those faces exhibiting weathering. A section 1 cm. thick was then cut parallel to the foliation. This section, from here on referred to as section 42 II, was cut up into small cubes measuring roughly 1 cm. on a side. For reference, each of these cubes was lettered sequentially as A,B,C....Z,A',B',C'....Z', etc.

Selected cubes of 42 II were then crushed to $-20 + 100$ mesh, in a percussion mortar as described by Wager and Brown, (1960). The biotite and garnet were next hand-picked under a binocular microscope and placed in electrodes or stored in gelatine capsules until analysis.

Determinations for Fe, Mg, Mn and Ca were made on the garnets separated in the above manner; Fe, Mg and Mn were determined in biotite. All analysis were performed by emission spectrography according to the parameters in Table 22.

The samples of biotite and garnet were placed in prearced electrodes and arced neat as the anode. Standards were neat samples of biotite and garnet, B12B, B21, B26 and G12B, G21 and G26 respectively whose Fe, Mg, Mn and Ca values had been determined by atomic absorption spectrophotometry (see Table 8 and 9).

Relative line intensities of samples and standards for Fe, Mg and Mn were recalculated to the ratios $\text{Fe}/\text{Fe}+\text{Mg}+\text{Mn}$, $\text{Mg}/\text{Fe}+\text{Mg}+\text{Mn}$, $\text{Mn}/\text{Fe}+\text{Mg}+\text{Mn}$. Working curves were made for the various elements by plotting these intensity ratios against the corresponding concentration ratios. The coefficient of variation of the method is close to 12% for all the elements determined.

TABLE 22. Excitation Parameters for the Spectrochemical Determination of Fe, Mg, Mn and Ca in Garnet and Biotite from Section 42II.

Spectrograph:	3m. Littrow-mounted quartz prism (Adam Hilger. Co., Ltd. No. E-478); source focused on masked collimator.
Excitation:	9 amp. anode for 40 sec.; 25 Ω ; 7mm. analytic gap.
Electrodes:	Sample- National Carbon Co. AGKSP Spec-pure graphite with a cavity measuring 0.5 x 3.0 mm. Counter- National Carbon Co. L1138F Spec-pure carbon, pointed.
Plates and Development:	Kodak Spectrum Analysis-1, developed for 4.5 minutes at 20° C in Kodak D-19 developer.
Plate calibration and Photometry:	Calibration by the preliminary curve method; photometry with a Hilger non-recording micro- photometer.
Analytic Lines:	Fe $_{2912.2\text{\AA}}$, Mg $_{2779.8\text{\AA}}$, Mn $_{2794.8\text{\AA}}$, Ca $_{3158.9\text{\AA}}$

10.3 Results of Determinations in Section 42 II

The results of determinations for Fe, Mg, Mn and Ca in the garnets of section 42 II are shown in Table 23 as concentration ratios.

Figure 40 and 40A shows the spatial distribution of Fe in garnet and biotite. Figure 41 and 41A, 42 and 42A and 43 show the spatial distributions of Mg in garnet and biotite, Mn in garnet and biotite and Ca in garnet respectively. In all graphic representations, the concentration ratios, although determined to the second decimal place are rounded off to the nearest $\pm .05$.

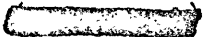
A semi-quantitative modal analysis of the section was made while the garnet and biotite was being picked. The results of this are shown in Figure 39. Figure 39 shows the relative amounts of garnet from cube to cube while Figure 39A shows the relative amounts of biotite. It should be noted that while biotite is found throughout the section, there is no garnet in the upper right hand corner .

TABLE 23. Concentration Ratios for Garnet and Biotite of Sample 42II.

Cube	GARNET				BIOTITE				$K_D^{\text{Gar/Bio}}$	
	X_{Fe}	X_{Mg}	X_{Mn}	X_{Ca}	X_{Fe}	X_{Mg}	X_{Mn}	K_{Fe}	K_{Mg}	K_{Mn}
A	0.74	0.33	0.020	0.005	0.39	0.60	0.0032	1.90	0.55	6.25
B	0.48	0.53	0.0037
C	0.41	0.60	0.0031
D	0.41	0.59	0.0016
E	0.39	0.61	0.0028
F	0.71	0.23	0.061	0.04	0.43	0.56	0.0019	1.65	0.65	32.10
G	0.66	0.37	0.031	0.022	0.40	0.57	0.0037	1.65	0.65	8.38
H	0.56	0.35	0.043	0.040	0.44	0.55	0.0021	1.27	0.64	20.50
I	0.48	0.53	0.0031
J	0.40	0.56	0.0021
K	0.50	0.50	0.0027
L	0.44	0.55	0.0020
M	0.60	0.45	0.029	0.005	0.42	0.58	0.0025	1.43	0.77	11.20
N	0.54	0.40	0.042	0.020	0.36	0.62	0.0003	1.54	0.65	140.0
O	0.57	0.35	0.043	0.036	0.42	0.58	0.0016	1.36	0.60	26.8
P	0.63	0.33	0.050	0.019	0.37	0.60	0.0012	1.70	0.55	41.7
Q	0.40	0.61	0.0022
R	0.43	0.56	0.0023
S	0.44	0.55	0.0034
T	0.63	0.37	0.036	0.033	0.40	0.60	0.0011	1.57	0.62	32.7
U	0.39	0.67	0.032	***	0.42	0.58	0.0040	0.93	1.16	8.00
V	0.59	0.36	0.041	0.049	0.45	0.54	0.0016	1.31	0.67	25.6
W	0.40	0.60	0.036	0.016	0.33	0.67	0.0001	1.21	0.89	360.0
X	0.39	0.60	0.0016
Y	0.41	0.60	0.0022
Z	0.46	0.54	0.0019
A'	0.47	0.52	0.0023
B'	0.48	0.53	0.0025
C'	0.71	0.23	0.061	0.060	0.44	0.55	0.0029	1.61	0.42	21.00
D'
E'
F'
G'
H'

TABLE 23. Continued.

Cube	GARNET				BIOTITE				K ^{Gar/Bio}	
	X _{Fe}	X _{Mg}	X _{Mn}	X _{Ca}	X _{Fe}	X _{Mg}	X _{Mn}	K _{Fe}	K _{Mg}	K _{Mn}
I'	0.75	0.25	0.033	0.005
J'	0.59	0.39	0.037	0.039	0.39	0.61	0.0011	1.51	0.64	33.60
K'	0.58	0.40	0.031	0.020	0.43	0.61	0.0026	1.35	0.66	11.90
L'
M'	0.40	0.61	0.0033
N'	0.38	0.69	0.029	***	0.38	0.60	0.0018	1.00	1.15	16.1
O'	0.44	0.55	0.0032
P'
Q'	0.66	0.36	0.032	0.028	0.40	0.57	0.0019	1.65	0.63	16.8
R'
S'	0.55	0.43	0.038	0.029
T'	0.63	0.40	0.032	0.039
U'	0.65	0.39	0.032	0.022
V'
W'	0.61	0.37	0.038	0.036	0.48	0.52	***	1.27	0.71	...
X'
Y'	0.44	0.55	0.0022
Z'	0.59	0.37	0.040	***	0.40	0.59	0.0014	1.31	0.67	...
A"	0.59	0.40	0.037	0.032	0.38	0.60	0.0011	1.55	0.67	33.6
B"	0.62	0.35	0.038	0.033	0.40	0.60	0.0040	1.55	0.58	9.5
C"	0.61	0.42	0.032	0.032	0.38	0.60	0.0013	1.60	0.70	24.6
D"	0.59	0.40	0.038	0.036	0.60	0.40	***	0.98	1.00	...
E"	0.61	0.42	0.033	0.036	0.41	0.58	0.0013	1.50	0.72	25.4
F"
G"	0.62	0.36	0.036	0.037	0.37	0.60	0.0012	1.70	0.70	30.8

... = not determined

*** = not detected

Analyst: W.H. Dennen

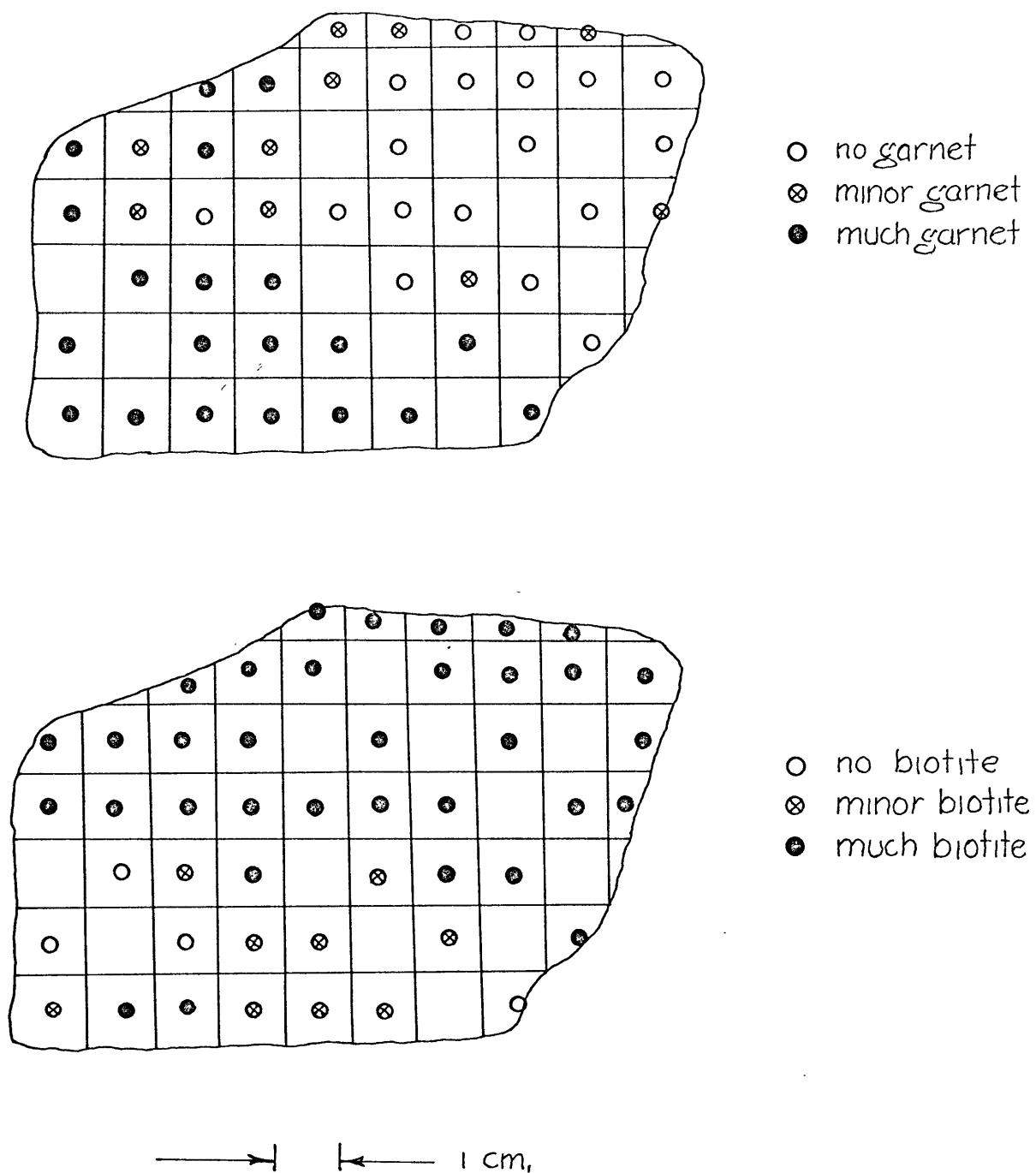


FIGURE 39. DISTRIBUTION OF GARNET
AND BIOTITE IN SECTION 42 II

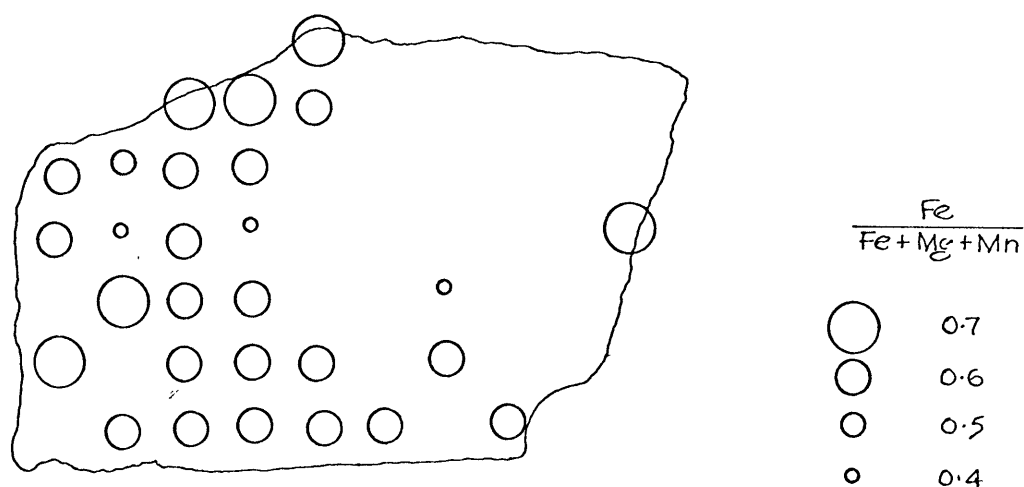


FIGURE 40. SPATIAL DISTRIBUTION OF IRON
IN GARNETS OF SECTION 42 II

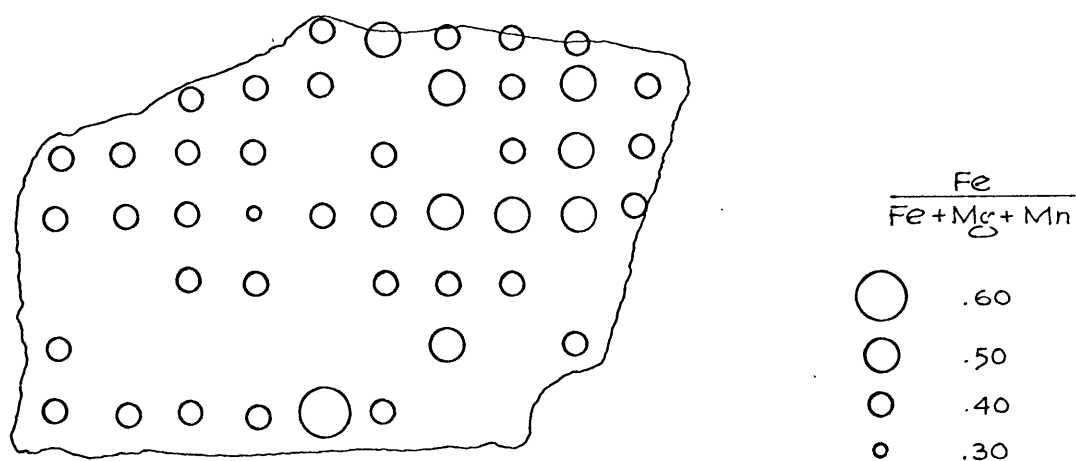


FIGURE 40A. SPATIAL DISTRIBUTION OF IRON
IN BIOTITES OF SECTION 42 II

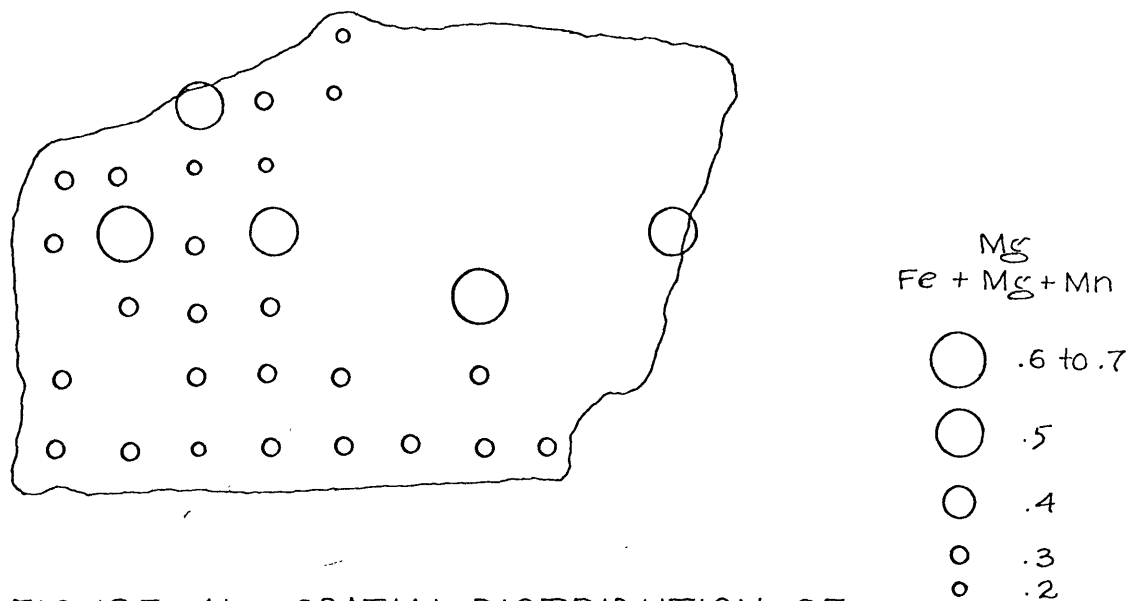


FIGURE 41. SPATIAL DISTRIBUTION OF
MAGNESIUM IN GARNETS OF SECTION 42 II

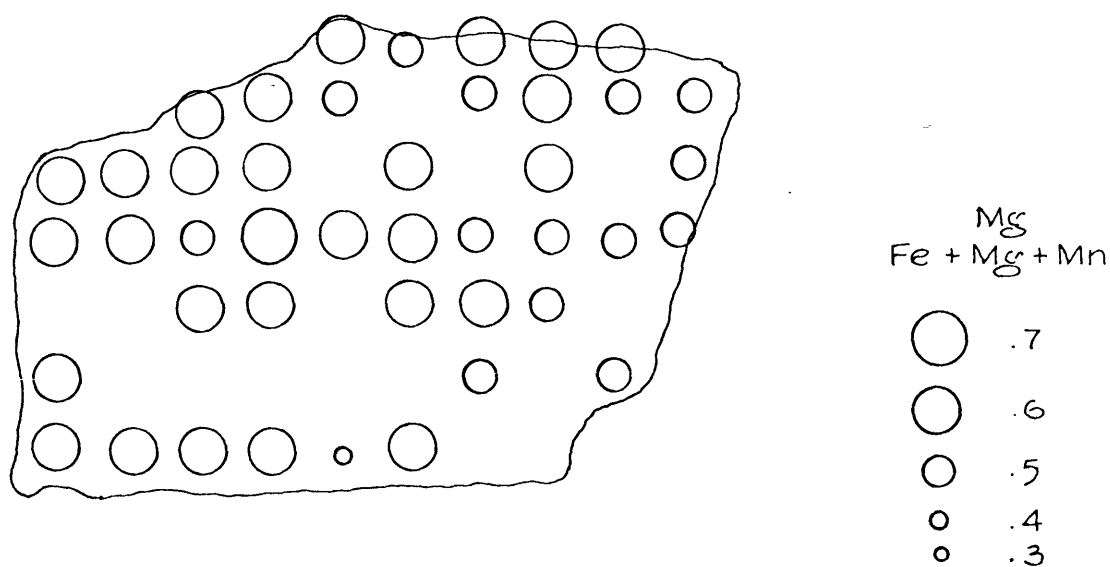


FIGURE 41A. SPATIAL DISTRIBUTION OF
MAGNESIUM IN BIOTITES OF SECTION 42 II

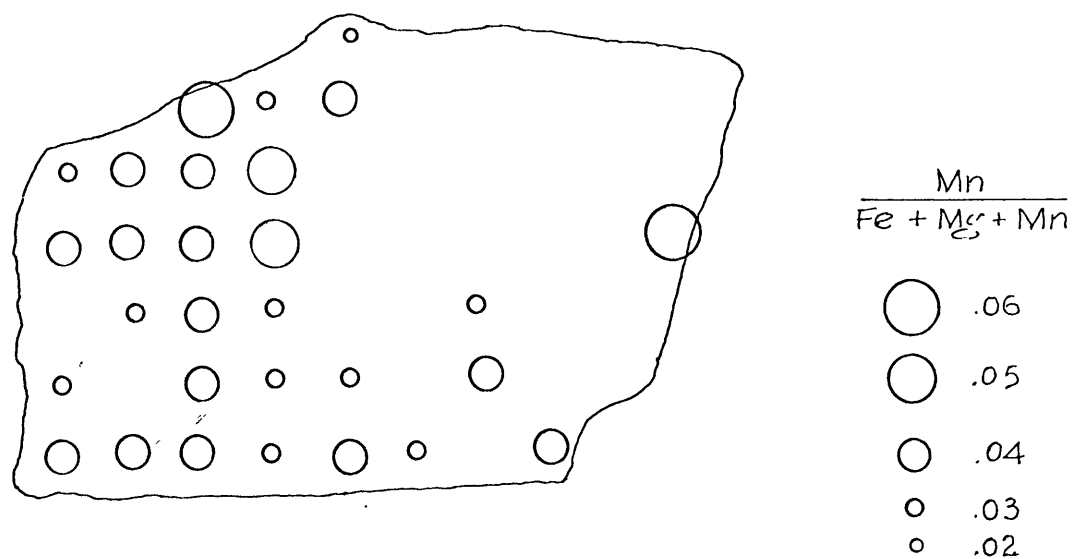


FIGURE 42. SPATIAL DISTRIBUTION OF MANGANESE
IN GARNETS OF SECTION 42 II

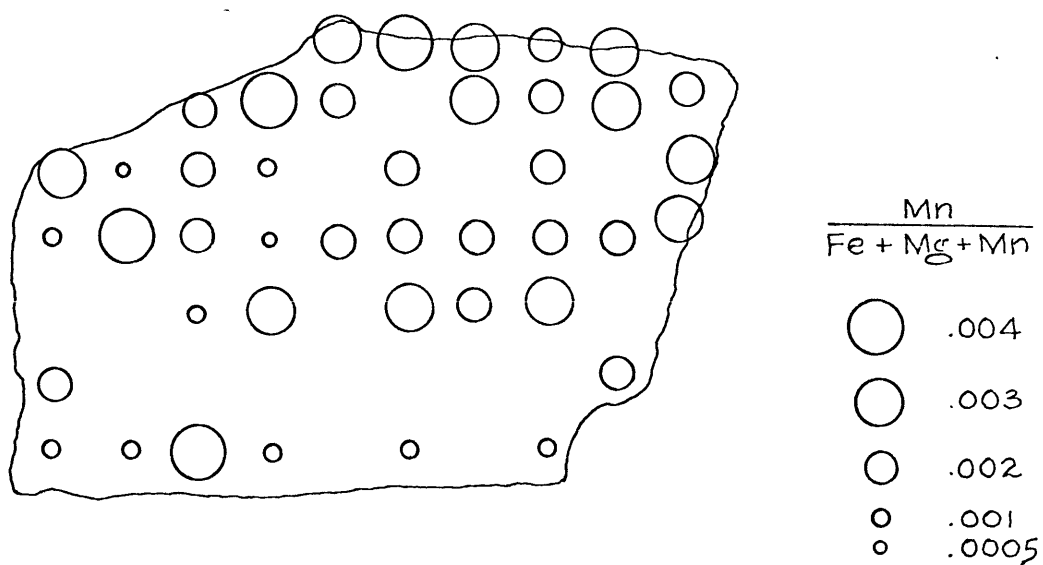


FIGURE 42 A. SPATIAL DISTRIBUTION OF MANGANESE
IN BIOTITES OF SECTION 42 II

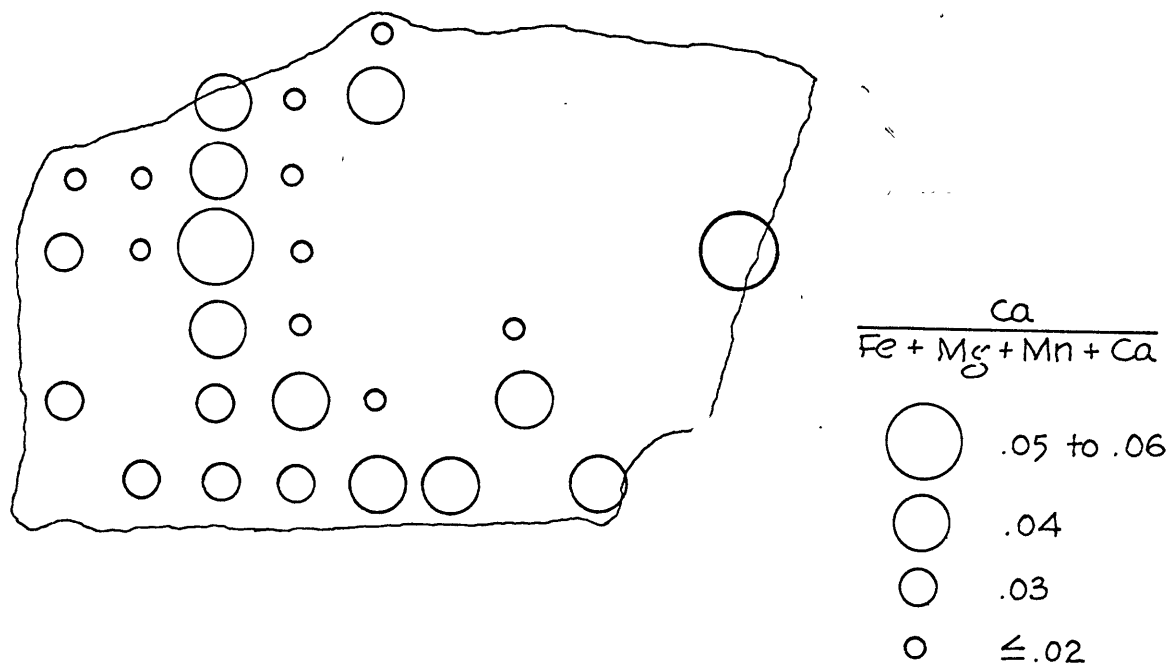


FIGURE 43. SPATIAL DISTRIBUTION OF
CALCIUM IN GARNETS OF SECTION 42 II

10.4 Discussion

IRON

Examination of Figure 40 and 40A show the spatial distribution of Fe in garnet and biotite of section 42II. The spatial distribution of Fe in garnet seems to be more regular than in section 17 II which was also parallel to the foliation. The greater part of the section shows garnets with $^{Fe}/Fe+Mg+Mn$ close to 0.6. Comparison of this diagram to Figure 39 shows that the cubes showing low Fe values are also those cubes which have very little garnet and are on the border of the "no garnet" zone. Both the modal and compositional differences are possibly due to a decrease in the rock $^{FeO}/MgO$ ratio in the upper right hand corner of the section.

The spatial distribution of Fe in biotite, shown in Figure 40A shows a uniform distribution of Fe values throughout this section. The area in the section in which there is little or no garnet exhibits biotite Fe values somewhat higher than in the rest of the section. The absence of the iron-rich garnet phase in this area is probably the cause of the increased Fe substitution in the biotite as hypersthene is ubiquitous in the section and most likely acts as an Fe-Mg buffer in the system.

MAGNESIUM

The distributions of magnesium in garnet and biotite of section 42 II is shown in Figure 41 and 41A. Many of the arguments proposed while discussing the distribution of Fe also apply here. Most of the garnets in the section have a $^{Mg}/Fe+Mg+Mn$ ratio of 0.4. Those garnets from cubes bordering on or in the garnet free area are higher in Mg, the ratio being 0.6 to 0.7.

The magnesium content of the biotite is quite uniform throughout the section at a value of 0.6. Lower values are found in the non-garnet-bearing area.

MANGANESE

The spatial distribution of the value x_{Mn}^{Gar} in the section 42II is quite uniform. Out of the 28 cubes in which manganese was determined in the garnet, only 6 had garnets in which the ratio $^{Mn}/Fe+Mg+Mn$ was outside of the range 0.03 to 0.04. These

irregular values were scattered and no correlation between the modal ratio garnet/biotite is apparent. The accuracy of these irregular results might be questioned although there is no reason to discard these values due to analytic reasons.

It is obvious from Figure 42 that the equilibration domain with respect to Mn in garnet is much larger than those observed in sample 17. It may be said that the garnets of this specimen, No. 42 II, have close to the same Mn content throughout the section and possibly beyond.

The spatial distribution of $\text{Mn}/\text{Fe}+\text{Mg}+\text{Mn}$ in the biotite of specimen 42 II is less regular than distributions of Fe and Mg. There seems to be an increase in the Mn content of the biotite going from the lower left hand corner to the upper right hand corner or towards the garnet deficient zone. This is not a regular increase however, and may be due only to an increase in the MnO content of the rock in this region and have nothing to do with the modal concentrations of biotite and garnet. It is interesting to note that the cube exhibiting garnet at the right hand side of the slab has a high Mn content as does the biotite of the same cube.

CALCIUM

The calcium content of the garnets in this section varies from 0.02 to 0.06 as the ratio $\text{Ca}/\text{Fe}+\text{Mg}+\text{Mn}+\text{Ca}$. Quite definite relationships to the zone of garnet deficiency and to the Ca content of the garnet surrounding this zone may be seen. The garnet closest to this zone has a very low Ca content ranging from $X_{\text{Ca}}^{\text{Gar}} = 0.02$ down to undetectable Ca. The next zone outwards contains garnets in which $X_{\text{Ca}}^{\text{Gar}}$ groups around the value 0.04. Moving farther outwards, i.e. to the lower left hand corner, the atomic ratio for Ca drops again to 0.03. The relationship here is unclear and the Ca contents of the gneiss and of the orthopyroxene would have to be taken into consideration before a meaningful evaluation could be made. Wynne-Edwards and Hay point out that in the biotite-cordierite-garnet gneisses discussed above, a low CaO content prohibits the growth of garnet and biotite-cordierite gneisses are formed. If the pyroxene-garnet gneiss under question

here is a prograde product of a biotite-garnet cordierite gneiss, it is possible that the hypersthene displaced cordierite and part of the biotite as part of the ferromagnesian assemblage, and the area now deficient in garnet was originally a biotite-cordierite assemblage deficient in CaO.

In summary, it may be said that for Fe, Mg and Mn in garnet, the spatial degree of equilibration was measurably larger in this pyroxene garnet gneiss. Variations within a hand specimen may still be seen, however, and these variations are probably due to variations in whole rock chemistry as reflected in the mineralogical variations. The spatial equilibration Ca in garnets was found to be no more extensive than in the biotite-cordierite-garnet assemblages. Again the calcium content of the garnet seems to be related to their modal abundance which may in turn be dependent on the CaO content of the rock.

The spatial degree of equilibration of Fe and Mg in biotite is quite extensive extending outside the hand specimen-sized sample used, (See Figure 40A and 41A), although the domain cannot be much larger than hand specimen-size or it would be highly unlikely to have selected a domain interface on a random basis. There is fairly close relationship between the Fe and Mg contents of the biotite and the modal ratio garnet/biotite; the biotite in the area where no garnet occurs has a substantially higher Fe/Mg ratio. The Mn content of the biotite in the specimen is less uniform and the spatial equilibration is not so extensive as it is for Fe and Mg in this phase. There is a possible correlation of the Mn content of the biotite and the modal variation of garnet/biotite and therefore a possible control by the FeO/MgO ratio.

The distribution coefficients $K_{\text{Fe}}^{\text{Gar/Bio}}$, $K_{\text{Mg}}^{\text{Gar/Bio}}$ and $K_{\text{Mn}}^{\text{Gar/Bio}}$ have been calculated for those garnet-biotite pairs determined for these elements. These values are given in Table 23. Figure 44 shows the distribution coefficient $K_{\text{Fe}}^{\text{Gar/Bio}}$ for each cube in the section 42 II where garnet and biotite were both measured. A distinct elongated area within the section exhibits a distribution coefficient $K_{\text{Fe}}^{\text{Gar/Bio}} \approx 1.0$ while the surrounding garnet-biotite

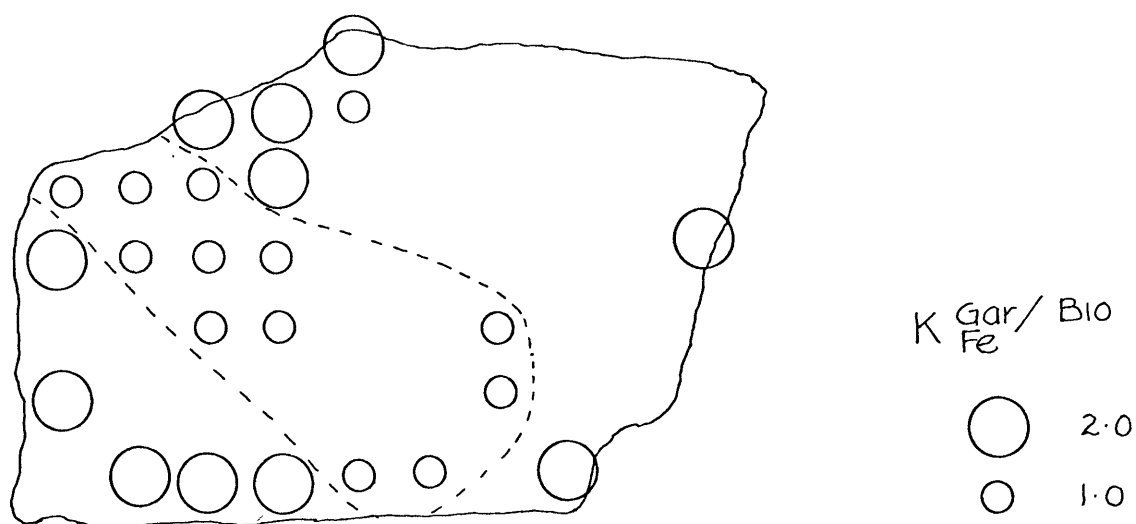


FIGURE 44. SPATIAL DISTRIBUTION OF THE DISTRIBUTION COEFFICIENT $K_{Fe}^{Gar/Bio}$ IN SECTION 42 II

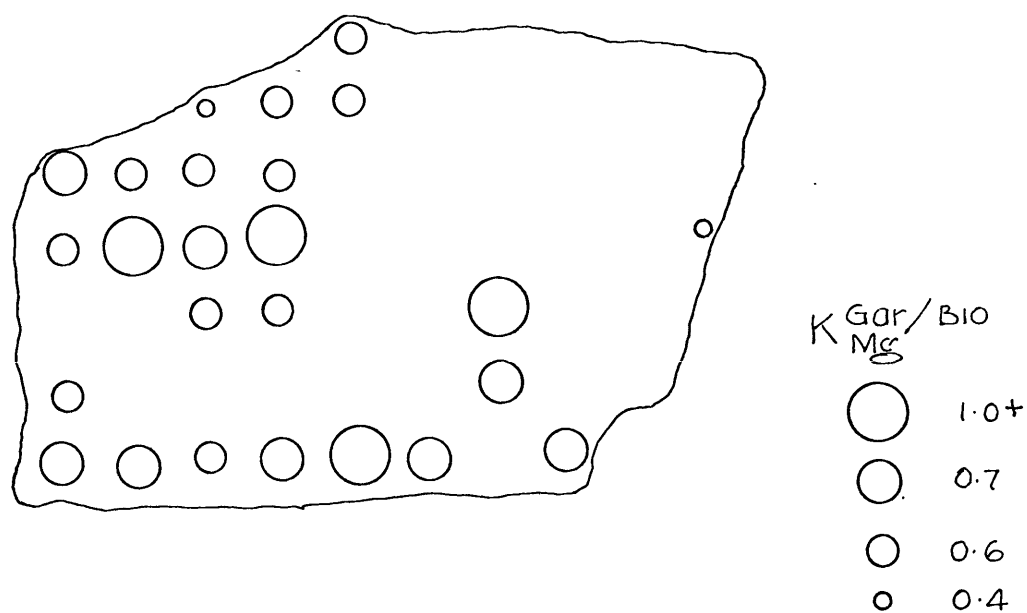


FIGURE 44A. SPATIAL DISTRIBUTION OF THE DISTRIBUTION COEFFICIENT $K_{Mg}^{Gar/Bio}$ IN SECTION 42 II

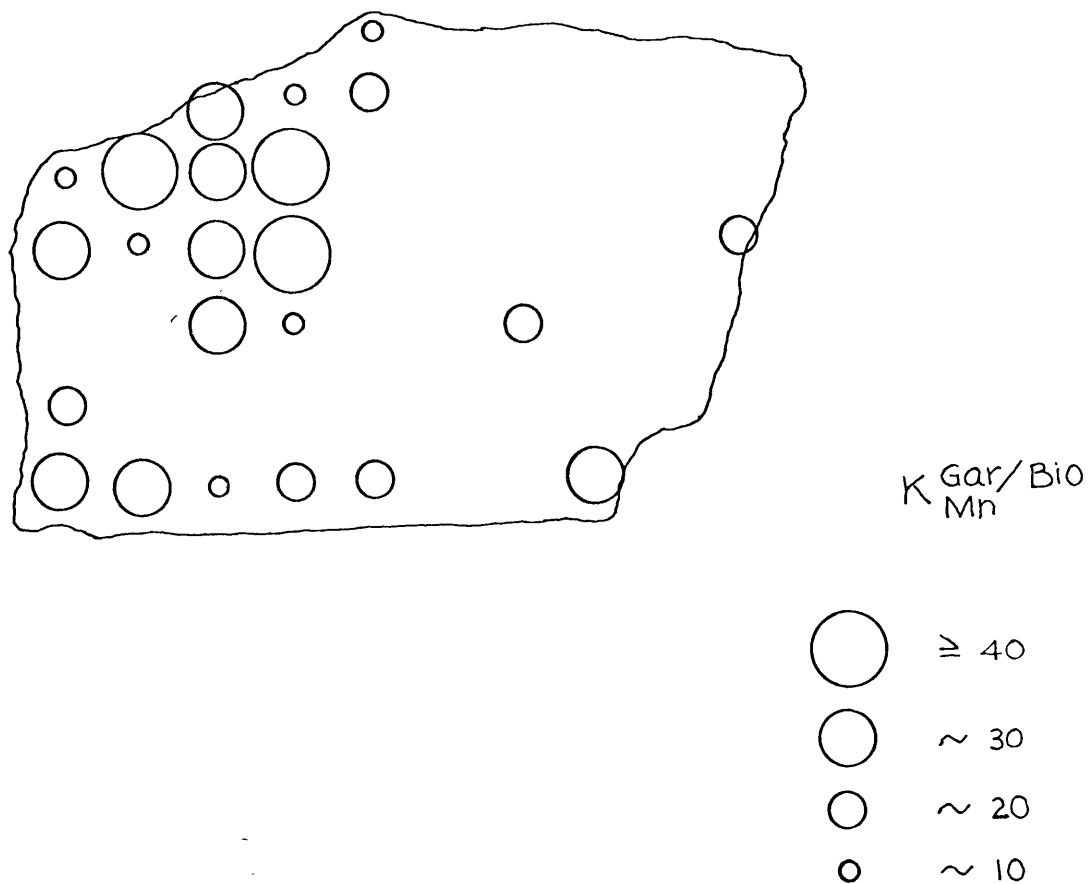


FIGURE 45. SPATIAL DISTRIBUTION OF THE
DISTRIBUTION COEFFICIENT $K_{Mn}^{Gar/Bio}$
IN SECTION 42 II

pairs show $K_{Fe}^{Gar/Bio} \approx 2.0$. The elongation of this zone of $K_{Fe}^{Gar/Bio} \approx 1.0$ is reminiscent of the structural control on the equilibration domains exhibited in specimen 17 discussed earlier. However, section 42 II was cut parallel to the foliation and no lineation direction was apparent. There is no obvious macroscopic reason for the elongation of the equilibration domain as shown in Figure 44. The zone measures about 4 cm. across at its widest point and has an apparent length of close to 8 cm. although it probably extends past the edge of the section.

The spatial distribution of the distribution coefficient $K_{Mg}^{Gar/Bio}$ is not nearly so regular as that for Fe. Four distinct groups of values for $K_{Mg}^{Gar/Bio}$ appear, these being 0.4, 0.6, 0.7 and 1.1. These values are shown diagrammatically in Figure 44A. It should be noted by comparing Figure 39 to Figure 44 A that the value $K_{Mg}^{Gar/Bio} = 1.1$ in all but one case is correspondent with a low garnet/biotite ratio. The exception shows just the opposite and is unexplained at present.

Areas over which the values $K_{Mg}^{Gar/Bio}$ are equal are much smaller than the equivalent distribution for Fe. It is possible that this irregularity is due to the dependence of the atomic ratio $Mg/Fe+Mg+Mn$ in garnet on whole rock chemistry, the composition of the coexisting hypersthene and its modal concentration in the rock. It is germane to note here the variability of the ratio $Mg/Fe+Mg+Mn$ in garnet as opposed to the equivalent ratio in biotite which is quite constant.

The values of the distribution coefficient $K_{Mn}^{Gar/Bio}$ may be broken down into groups as follows:

$K_{Mn}^{Gar/Bio} = 10$	population = 6
20	= 6
30	= 7
40	= 1
100	$\frac{= 2}{22}$

The spatial distribution of these values is shown in Figure 45. It is obvious from this diagram that the value of $K_{Mn}^{Gar/Bio}$ is

constant over very small intervals although the atomic ratio $\text{Mn}/\text{Fe}+\text{Mg}+\text{Mn}$ in garnets is nearly constant over sizable areas. The variability must then lie in the Mn content of the biotite which is somewhat more irregularly distributed.

11 GENERAL SUMMARY AND CONCLUSIONS

This work has been a preliminary investigation into the spatial degree of equilibration in high-grade metamorphic rocks. There is obviously much more work to be done in this direction both with lower grade rocks and higher grades and beyond the point of anatexis.

The hypothesis that the domain of chemical equilibrium will increase in size with increased grade of metamorphism seems to hold true. Phinney (1959, 1963) found Fe/Mg equilibration in biotites from staurolite bearing schists on the order of only a few m.m. Specimen 17 of this study showed equilibration of Fe and Mg over distances of about 3 cm. in the longest direction. a pyroxene granulite, Sample No. 42 II, showed equilibration, parallel to foliation, over areas of almost hand specimen dimensions.

The examination of equilibration domains in specimen 17 showed that the distinct structural control on their sizes and shapes. It may be speculated that the domains of equilibration with respect to a certain element are roughly ellipsoidal in shape and possess an axial ratio, at least for Fe and Mg, of about 4:2:1. The longest axis is almost always parallel to the foliation and lineation, the intermediate axis being parallel to the foliation and perpendicular to the lineation. It is interesting to note here that the axial ratio for the shape of the equilibrium volumes is very often correspondent with the axial ratio of the flattened, elongated garnets positioned on the foliation surfaces. It is thus possible that the structural features largely control the rate and extent of diffusion during metamorphism.

In ^{this} light, the size of the volume of chemical equilibrium with respect to a certain element is a direct measure of the volume of free diffusivity and chemical communication. The small volumes encountered in this study indicate that diffusion in metamorphic rocks of high grade is very limited and the origin of seemingly homogeneous granites without the intervention of a liquid phase, as proposed by Perrin and Roubault, (1937, 1939), Perrin, (1952) and Reynolds, (1946) is deemed virtually impossible.

Further, the results given here add complications to the sampling of metamorphic rocks for chemical analysis. An analysis, if used to define the chemical system to which the rock belongs, should be representative of the assemblage present in thermodynamic equilibrium. The common practice of assuming a closed system over the size of a hand specimen for rocks of medium grain size (or a thousand grains) is not sufficient. The specimen taken should, strictly speaking, be the size of one domain of equilibration or better still a volume sufficiently large to include 1000 domains.

With respect to techniques for petrochemical analysis, the laser microprobe has proved to be an exceeding valuable tool. Sample preparation is simple, time for replicate determinations is short and the precision and accuracy certainly good enough for most petrographic purposes.

12 SUGGESTIONS FOR FURTHER RESEARCH

With respect to studies on the distribution of elements between coexisting phases, preliminary work on the oxide minerals from the rocks of this study (not reported here) are quite encouraging and this line of effort should certainly be followed. Further, the compositions of the other ferro-magnesian silicates of the assemblages noted above, i.e., cordierite and hypersthene should be determined. The effects of the presence of these minerals is probably important on both the distribution of garnet and biotite and their compositions. There has been very little work published on the relationship of small scale differences in rock composition and the modal abundance and composition of assemblage minerals. This is possibly where equilibrium studies of metamorphic rocks should start.

Certainly, the results obtained to date in the study of the spatial extent of chemical equilibration of garnet and biotite are encouraging. This work should be carried on with special regard to rock and mineral fabric and the mineral assemblages in close proximity to each grain measured. This would essentially involve a separate modal analysis over each small increment of the rock containing the mineral or minerals in question.

Investigations on the effect of zoning in metamorphic minerals with regard to the spatial degree of equilibrium should be carried out. It should be possible to trace the growth history of the equilibration domain by correlating zones of the same composition.

The morphology of the flattened and elongated garnets should be investigated by crystallographic techniques. If they are pseudomorphous after biotite grains, it is possible that the structural orientation will reflect this.

With regard to analytic techniques, the laser microprobe has proved to be a valuable petrochemical instrument. Further exploratory work should certainly be carried out to evaluate other mineralogical applications of laser-excited spectrochemistry.

APPENDIX I

Sample Locations and Descriptions *

NO. 1 is from a fresh roadcut 0.6 miles west of the Ganonoque River on the road running north from the hamlet of Marble Rock. The rock is a layered gneiss with well developed foliation. Quartz, feldspar, biotite and pink garnet are the dominant minerals with the garnet and biotite segregated in adjacent bands. No cordierite is obvious in hand specimen. Under the microscope, both potash feldspar and plagioclase are fresh with very little included material. The garnets are rounded and mainly associated with potash feldspar and cordierite. No retrogression of the garnet is noted and local inclusions of quartz are sparse. Cordierite is present only in association with garnet. Biotite occurring mainly as ragged plates, is fresh with rare zircon inclusions.

NO. 2A is from the north end of the roadcut from which No. 1 was taken and about 75 feet separate the two samples. The rock is a well layered gneiss containing quartz, feldspar, garnet, biotite and cordierite. In hand specimen, a distinct relationship between garnet size and inter-garnet distance is evident. Groups of small garnets are clustered while the larger garnets are more dispersed.

On microscopic examination, the plagioclase is observed to have local sericitic and carbonate alteration. The garnets are large, rounded and contain many inclusions of quartz and sillimanite. However, some garnets are quite free of inclusions. The garnets are mantled by quartz, potash feldspar and cordierite grains. Biotite is scattered as small grains with some magnetite inclusions

NO. 3 is a specimen from a large roadcut on the road to Howe Island, west of Ganonoque, and 0.25 miles south of Route 2. The rock is a medium-grained, well foliated, garnet-biotite gneiss with abundant quartz and feldspar. Garnet grains are of similar size and randomly scattered. The potash feldspar and plagioclase are both fresh, with the potash feldspar showing a microcline twinning. Myrmekitic intergrowth of plagioclase and quartz is abundant. The garnets are rounded and locally contain inclusions of quartz and sillimanite. Most garnets are mantled with cordierite. Biotite is sparse and ragged but shows no sign of retrogression.

NO. 8 is from a large roadcut on the Bedford Mills Road, 0.75 miles north of the hamlet of Perth Road. The sample is a coarse-grained quartz-feldspar-garnet-biotite gneiss with well developed foliation. Both the microcline and plagioclase are fresh with rare alteration of the plagioclase to carbonate. Garnet occurs as small rounded and elongated grains which are quite free of inclusions. Garnet is associated with cordierite, magnetite and green spinel. Biotite is ragged and possibly altered to chlorite locally but for the most part fresh. The biotite contains inclusions of biotite and zircon.

NO. 12 (samples 12A and 12B are from the same outcrop, about 10 feet apart) is from an outcrop in a field just north of West Bay, Sand Lake in South Crosby Township. The rock is fresh, highly foliated and very coarse grained. Major minerals include quartz, feldspar, garnet and biotite. The potash feldspar shows no twinning and plagioclase occurs both as discrete grains and as myrmekite. Both feldspars are unaltered. Garnet occurs both as rounded and flattened grains, is unaltered and quite free of inclusions. Where inclusions occur they are quartz, potash feldspar and biotite with their long axes parallel to the foliation. The long axes of the flattened garnet grains also parallel the foliation. The garnet is mantled with highly altered cordierite (pinite). Biotite occurs as distinct grains, with no alteration and local zircon inclusions.

NO. 16 is a coarse grained foliated gneiss with quartz, biotite, cordierite, feldspar and a great abundance of garnet. The sample is from a large outcrop on the Brier Hill Road, 0.6 miles east of the village of Morton. Garnet occurs mainly as grains elongated in the foliation direction. Many inclusions of quartz and sillimanite are present in the garnet with their long axes following the foliation direction. The garnet is surrounded by cordierite which is almost completely altered to pinite. Potash feldspar, where present, is associated with the garnet and cordierite. Biotite is ragged but unaltered and contains local inclusions of magnetite and zircon.

NO. 21 is from a large outcrop beside the road, 0.26 miles north of Morton Creek, on the concession road from Morton to Elgin. The outcrop shows a distinct banding and foliation although the

hand specimen looks massive. Quartz, feldspar, biotite and garnet are the dominant minerals. Both potash feldspars are present, and the plagioclase is highly altered. Garnet occurs in rounded grains of variable size. It is fresh with sparse inclusions of quartz and sillimanite. Biotite is very fresh and contains rare inclusions of magnetite and zircon.

NO. 25 is from an outcrop in a field 0.2 miles north of the north-western end of Ganonoque Lake. The rock has a distinct layering and foliation, is medium grained and has quartz, feldspar, cordierite and biotite as its dominant minerals. Both plagioclase and potash feldspar are very fresh. The garnet is unaltered and contains many needles of sillimanite. The garnets are almost all slightly elongated in the direction of foliation and mantled by cordierite which is only slightly altered. Sillimanite is very abundant.

Most of the garnet is located in the foliation planes where it is associated with cordierite, quartz, sillimanite and potash-feldspar but never biotite.

NO. 26 is from a very large outcrop in a wooded area about 0.25 miles north-east of Ganonoque Lake. The rock is a medium to coarse grained, highly foliated gneiss with distinct feldspathic bands. Quartz, potash feldspar, plagioclase and biotite are the dominant phases. The garnet occurs as small rounded grains which are free of inclusions. The biotite is fresh and locally contains zircon inclusions.

NO. 27 is a well foliated gneiss with abundant quartz plus feldspar, biotite, garnet and cordierite. The sample is from a large new roadcut at the southern end of Charleston Lake just north of the village of Outlet. The feldspars are for the most part fresh with local alteration of the plagioclase. Garnets occur as very large, very irregular grains in the planes of foliation. They contain many large inclusions of quartz, potash feldspar, cordierite. The garnet grains are mantled with unaltered cordierite. Biotite occurs in large fresh grains with sparse inclusions of zircon.

NO. 29 is from a large new roadcut at the southern end of Charleston Lake, taken about 300 feet north of No. 27. The rock is a medium grained quartz, feldspar, garnet, cordierite gneiss with no obvious foliation. Microscopically, the potash feldspar and plagioclase are quite fresh and very abundant. Biotite is unaltered

and occurs in small distinct grains showing no preferred orientation. The garnet is almost completely free of inclusions and occurs in very irregular grains associated with unaltered cordierite, quartz and potash feldspar.

NO. 30 was taken from an outcrop beside the road between Charleston Lake and Killenback Lake about 0.2 miles from Killenback Lake. The rock is a well-foliated gneiss with quartz, feldspar and biotite as major phases. Potash feldspar and garnet occur in minor amounts. The garnet occurs in small rounded grains, is free of inclusions, and shows no regular mineralogical associations. Biotite occurs in large fresh grains with rare zircon inclusions. Plagioclase is very abundant, occurring both as distinct grains and as myrmekitic intergrowths.

NO. 34 is from a roadcut just to the south of South Bay, Buck Lake on the perth Road. It is a well foliated gneiss showing quartz, potash feldspar, plagioclase, biotite and garnet as major constituents. Microscopically, the garnet occurs both in round and elongated forms. Where the garnet is rounded it is free of inclusions and is associated with quartz, biotite and cordierite. Associated minerals with the elongated garnets are cordierite, sillimanite and potash feldspar. Biotite is always removed. Alteration of the minerals in this sample is almost non-existent.

NO. 35 taken from a roadcut about 200 feet north of that which No. 34 was taken. The rock is massive coarse grained gneiss with quartz, garnet, biotite and dominant feldspar. There is no obvious foliation in hand specimen. Under the microscope, the abundant potash feldspar shows microcline twinning and is unaltered. Plagioclase shows alteration to carbonate locally. Garnet occurs both as small round grains and large elongated grains with no obvious mineralogical associations with either morphology except that cordierite, where present, is always associated with the garnet.

NO. 17 and NO. 42 are described in other sections of the text. (See Section II, Chapter 7, and 10.)

* Modal Analyses given in Section I, Chapter 3.

APPENDIX 2

Computer Program for Least Squares Analysis

These computations and the ones described below in Appendices 3 and 4 were performed on an I.B.M. System/360, model 65 computer at the M.I.T. Computation Center. Source decks were prepared on an I.B.M. 029 key punch; data decks on both I.B.M. 029 and 026 key punches. Source decks were coded in Fortran IV G.

The purposes of the least squares program, from here on referred to as LSQ was to read points (X,Y), produce a least squares linear fit to the data points and compute unknown X' values from known Y' values. The program also computes the standard deviation of the calibration points around the least squares line and the standard deviation and coefficient of variation of the X' values. The mathematical operations used in these computations are from Shaw and Bankier, (1954) and will not be described here.

Inputs

1. Number of standard points
2. X, Y values of standard points
3. Number of unknowns
4. Y' values of unknowns

Output

1. Y intercept of least squares line
2. Slope of least squares line
3. Standard deviation of standard points around the line
4. List of X' values for the unknowns, the standard deviations of these X' values and the corresponding coefficients of variation.

A print out of the compiled program is shown as Figure A-1

References

Shaw, D. M. and Bankier, J. D. (1954): Statistical methods applied to geochemistry, *Geochim. et Cosmochim. Acta*, 5, pp. 111-123

A-1

```

//LSQ JOB. JM5807,5710,2,500,0*,'R.E. BRUNEAU',MSGLEVEL=1
//STEP1 EXEC FORCLG,PARM.C='EBCDIC'
//C.SYSIN DD *
C LEAST SQUARES CURVE FIT
C
  DIMENSION X(500*),Y(500*),YPRIME(50*)
  1 FORMAT (1X,I3*
  2 FORMAT (2)1X,F10.5**
  3 FORMAT (3)1X,F10.5**
  4 FORMAT (1) SLOPE OF LEAST SQUARES LINE EQUALS.....',F10.5,/**
  5 FORMAT (1) Y INTERCEPT OF LEAST SQUARES LINE EQUALS.....',F10.5LSQ 09
  1,/**
  6 FORMAT (1) STANDARD DEVIATION OF POINTS AROUND LINE EQUALS...',F8.6LSQ 11
  1,/**
  7 FORMAT (1) STANDARD DEVIATION OF Y PRIME EQUALS.....',F8.6LSQ 13
  1,/**
  8 FORMAT (1) STANDARD DEVIATION OF Y EQUALS.....',F8.6LSQ 15
  1,/**
  9 FORMAT (1) STANDARD DEVIATION OF X(10)* EQUALS.....',F8.6LSQ 17
  1,/**
  14 FORMAT (1) X(10)* EQUALS.....',F10.5LSQ 19
  1,/**
  15 FORMAT (1)H1,' TRIAL NUMBER',3X,I2,/**
  10 FORMAT (1) COEFFICIENT OF VARIATION EQUALS',3X,F8.6,2X,' PERCENT'* LSQ 21A
  17 FORMAT (1X,' SAMPLE =' ,1X,I3,T20,' X0 =' ,1X,F10.5,T40,' STANDARD D
  EVIATION =' ,1X,F10.6,10X,' VARIATION =' ,3X,F9.6,/*
  18 FORMAT (1)H1*
  21 FORMAT (1X,' SAMPLE =' ,1X,I3,5X,' NO DATA GIVEN',/*
  L=1
  READ (5,1* N
  READ (5,2* (X(I),Y(I)),I=1,N*
  SUMX=0.0
  SUMY=0.0
  DO 11 I=1,N
  SUMX=SUMX+X(I)*
  SUMY=SUMY+Y(I)*
  XBAR=SUMX/N
  YBAR=SUMY/N
  A1=0.0
  A2=0.0
  A3=0.0
  B1=0.0
  B2=0.0
  DO 12 I=1,N
  A1=A1+X(I)**Y(I)*
  A2=A2+X(I)*
  A3=A3+Y(I)*
  B1=B1+X(I)**X(I)*
  B2=B2+Y(I)**Y(I)*
  BETA=(A1-A2*A3/N)/(B1-A2*A2/N*
  ALPHA=YBAR-BETA*XBAR
  C=B2-A3*A3/N-BETA*BETA*(B1-A2*A2/N*
  S12=C/(N-2*
  IF (S12.LT.0.* S12=-S12
  S1=SQRT(S12*
  WRITE (6,18*
  WRITE (6,15* L
  WRITE (6,4* BETA
  WRITE (6,5* ALPHA
  WRITE (6,6* S1
  WRITE (6,18*
  L=0
  M=3

```

```

16  READ )5,3* )YPRIME)I*,I=1,M*
    L=L.1
    IF )YPRIME)1*.EQ.0..AND.YPRIME)2*.EQ.0..AND.YPRIME)3*.EQ.0.**GO TO 63
1  20
    IF )YPRIME)1*.EQ.0..AND.YPRIME)2*.EQ.0..OR.YPRIME)1*.EQ.0..AND.YPR
1IME)3*.EQ.0..OR.YPRIME)2*.EQ.0..AND.YPRIME)3*.EQ.0.* M=1      *
    IF )YPRIME)1*.EQ.0..AND.YPRIME)2*.NE.0..AND.YPRIME)3*.NE.0..OR.YPR
1IME)2*.EQ.0..AND.YPRIME)1*.NE.0..AND.YPRIME)3*.NE.0..OR.YPRIME)3*.
2EQ.0..AND.YPRIME)1*.NE.0..AND.YPRIME)2*.NE.0.* M=2
    SUM=0.0
    SUM2=0.0
    DO 13 I=1,M
    SUM=SUM.YPRIME)I*
13  SUM2=SUM2.YPRIME)I***2
    D=SUM2-SUM*SUM/M
    S22=D/ )M-1*
    IF )S22.LT.0.* S22=-S22
    S2=SQRT)S22*
    SY2= )C.D*/ )N.M-3*
    IF )SY2.LT.0.* SY2=-SY2
    SY=SQRT)SY2*
    SX2= )SY**2/BETA**2** )1/M.1/N.)SUM/M-YBAR***2/BETA**2*)B1-A2**2*/N*
    IF )SX2.LT.0.* SX2=-SX2
    SX=SQRT)SX2*
    X0= )SUM/M-ALPHA*/BETA
    VAR=SX*100./X0
    WRITE )6,17* L,X0,SX,VAR
    GO TO 16
20  WRITE )6,21* L
    GO TO 16
    END
/*
//G.SYSIN DD *

```

LSQ 63

LSQ 50

LSQ 51

LSQ 53

LSQ 55

LSQ 56

LSQ 57

LSQ 58

LSQ 58A

LSQ 58B

LSQ 59

LSQ 59A

LSQ 59B

LSQ 60

LSQ 60A

LSQ 61

LSQ 62

LSQ 62A

LSQ 72

LSQ 73

APPENDIX 3

Computer Program for Analysis of Grain Size, Intergrain Distance and Grain Distribution

The program designated as GRD was designed to compute the distance between each grain whose coordinates have been measured and every other phase analog in the sample. Using Function Min, the program will find the distance to the nearest phase analog only. The randomness of the distribution of a specific mineral within a rock is computed if the following are known:

- (a) distance to nearest neighbor for each grain
- (b) total number of grains
- (c) volume of the sample

The program is also designed for computing the volumes of each grain from its axial lengths and punches out on cards the following data: length of measured axes and the volume of each grain:

Inputs

- 1. Reference number for each grain
- 2. 3-dimensional coordinates of the center of each grain
- 3. Measured lengths of the axes of each grain
- 4. Total number of grains

Computation

- Step 1: Distance from each grain to every other grain measured is calculated by

$$(X_1 - X_2)^2 + (Y_1 - Y_2)^2 + (Z_1 - Z_2)^2$$

- Step 2: The answers from Step 1 are stored in an array at the end of calculations. The array is passed to a subprogram, which returns for each grain the distance to the nearest grain measured. This distance is then placed in an array called M DIST.

- Step 3: The array M DIST, along with the volume of the sample and the total number of grains is subject to an analysis of randomness of grain distribution as given by Clark and Evans, (1954). The mathematics involved here are given in Chapter 8, Part Two.

- Step 4: Using the axial length, the volume of each grain is computed by the formula

$$V = \frac{A B C}{6}$$

In this study, grains measured ranged in shape from spherical to ellipsoidal so the above formula is applicable. Other suitable equations for the calculation of volumes may replace this one.

Output

1. From Step 2: The array called M DIST is listed.

The Format is:

Grain Numbers=... Nearest Distance=...

The nearest neighbor distance for all grains measured is listed.

2. From Step 3: The following are printed:

- (a) Grain density
- (b) Sum of the nearest neighbor distances
- (c) Arithmetical mean distance from grains to their nearest neighbor
- (d) Expected mean distance if the distribution were random
- (e) The ratio of actual mean distance to the expected random mean distance

3. From Step 4: A listing of all the volumes calculated is given as follows:

Grain Number A B C Volume

4. From Step 5: Punched cards giving for each grain:

A B C Volume

A print out of the program GRD is given as Figure A-2

References

Clark, P.J. and Evans, F.C., (1954): Distance to nearest neighbor as a measure of spatial relationships in populations, *Ecology*, 35, pp. 445-453.

A-2

```

//GRAIN JOB JM5807,5710,4,500,500*, 'R.E. BRUNEAU', MSGLEVEL=1
//STEP1 EXEC FORCLG,PARM.C='EBCDIC'
//C.SYSIN DD *
C GRAIN SIZE/DISTRIBUTION
C
C DIMENSION X)500*,Y)500*,Z)500*,A)500*,B)500*,C)500*,DIST)500*,
1MDIST)500*,V)500*,NUM)500*
REAL MDIST,MAX,MIN
1 FORMAT )I3,F10.3*
2 FORMAT )I3,3F9.3,3F7.3*
3 FORMAT )I GRAIN NUMBER = ,I3,T25, NEAREST DISTANCE = ,F7.3,/**
4 FORMAT )6X,I3,T20,F9.3*
5 FORMAT )1H1, GRAIN DENSITY',5X,F9.5,/**
6 FORMAT )I SUM OF NEAREST NEIGHBOR DISTANCES',5X,F9.3,/**
7 FORMAT )I MEAN DISTANCE TO NEAREST NEIGHBOR',5X,F6.3,/**
8 FORMAT )I RANDOM DISTRIBUTION MEAN DISTANCE',5X,F6.3,/**
9 FORMAT )I DEGREE OF DEPARTURE FROM RANDOM MEAN DISTANCE',5X,F5.3*
10 FORMAT )1H1, GRAIN NUMBER',T15, A AXIS',T30, B AXIS',T45, C AXIS',T60, VOLUME',****/*
11 FORMAT )1X,T5,I3,T15,F7.3,T30,F7.3,T45,F7.3,T60,F11.5*
12 FORMAT )1X,F6.3*
13 FORMAT )1X,3F7.3,F11.5*
READ )5,1* N,VOL
READ )5,2* )NUM)I*,X)I*,Y)I*,Z)I*,A)I*,B)I*,C)I**,I=1,N*
DO 15 J=1,N
DO 14 I=1,N
IF )I.EQ.J* GO TO 16
DIST)I*=SQRT)X)J*-X)I****2, Y)J*-Y)I****2, Z)J*-Z)I****2*
14 CONTINUE
MDIST)J*=MIN)N,DIST*
15 CONTINUE
GO TO 17
16 DIST)I*=10000.
GO TO 14
17 CONTINUE
WRITE )6,3* )NUM)I*,MDIST)I**,I=1,N*
RHO=N/VOL
SIGMAR=0.0
DO 18 I=1,N
18 SIGMAR=SIGMAR,MDIST)I*
ACDIST=SIGMAR/N
EXDIST=1./)2.*SQRT)RHO**
DEPART=ACDIST/EXDIST
WRITE )6,5* RHO
WRITE )6,6* SIGMAR
WRITE )6,7* ACDIST
WRITE )6,8* EXDIST
WRITE )6,9* DEPART
DO 19 I=1,N
19 V)I*=4.18877*A)I*B)I*C)I*/8.
WRITE )7,13* )A)I*,B)I*,C)I*,V)I**,I=1,N*
WRITE )6,10*
WRITE )6,11* )NUM)I*,A)I*,B)I*,C)I*,V)I**,I=1,N*
END
REAL FUNCTION MIN)N,X*
DIMENSION X)250*
MIN=X)1*
DO 1 I=1,N
IF )X)I*.LT.MIN* MIN=X)I*
1 CONTINUE
RETURN
END

REAL FUNCTION MAX)N,X*
DIMENSION X)250*
MAX=X)1*
DO 1 I=1,N
IF )X)I*.GT.MAX* MAX=X)I*
1 CONTINUE
RETURN
END
/*
//G.SYSIN DD *

```

APPENDIX IV

Computer Program for Correlation and Regression Analysis

This program computes a sequence of multiple linear regression equations in a stepwise manner. The variable added at each step is the one which makes the greatest reduction in the error of the sum of squares. Besides performing the regression analysis, the program also has optional output which includes:

1. Means and standard deviation
2. Covariance matrix
3. Correlation matrix

Figure A-3 shows the printout of the program compiled for IBM/360.

The program is discussed in detail in the reference given and no more will be said here.

Reference

Biomedical Computer Programs, Health Science Computing Facility, Dept. of Preventative Medicine and Public Health, School of Medicine, University of California, Los Angeles

```

C8002R  MAIN PROGRAM - STEPWISE REGRESSION      JUNE  2, 1964      0030
C                                              0040
C  . PROBLEM CARD FORMAT (NAMELIST NAME = PROBLM)
C
C  . NAME
C
C  . CODE      ALPHANUMERIC PROBLEM NAME
C  . N          NUMBER OF CASES
C  . NOV        NUMBER OF ORIGINAL VARIABLES
C  . NAIT       ALTERNATE INPUT TAPE NUMBER
C  . PVAR       .TRUE. IF INPUT VARIABLES ARE TO BE PRINTED
C  . SDAM       .TRUE. IF ST.DEV. AND MEANS TO BE PRINTED
C  . COVP       .TRUE. IF COVARIANCE MATRIX TO BE PRINTED
C  . CORP       .TRUE. IF CORRELATION MATRIX TO BE PRINTED
C  . ZEROI      .TRUE. IF ZERO REGRESSION INTERCEPT DESIRED
C  . FMTR(40)   FORMAT TO READ VARIABLES BY
C  . ALBEL(100) LABELS FOR VARIABLES (UP TO 8 LETTERS)
C
C  . SUB-PROBLEM CARD FORMAT (NAMELIST NAME = SUBPRO)
C
C  . NAME
C
C  . KDEP       DEPENDENT VARIABLE NUMBER
C  . MAXSTP     MAXIMUM NUMBER OF STEPS
C  . FINC       F FOR INCLUSION
C  . FOOT       F FOR DELETION
C  . TOL        TOLERANCE
C  . NVIP       NUMBER OF VARIABLES TO BE PLOTTED
C  . IVPT(100)  INDECS OF VARIABLES TO BE PLOTTED
C  . C(100)     CONTROL DELETE PARAMETERS
C  . RESID      .TRUE. IF RESIDUALS ARE TO BE PRINTED
C  . SUMTAB     .TRUE. IF SUMMARY TABLE DESIRED
C
C
0001  COMMON/PARA/ N,DF,IP,XN,LKL,TOL,FINC,FOOT,KDEP,NVIP,RMAX,RMIN
0002  COMMON/PARA/ ALPHA,ZEROI,MAXSTP,ITP1,ITP2,NMAX,SUMTAB
0003  LOGICAL      ZEROI,SUMTAB
C
0004  COMMON      ALBEL(100), ANAME(100),BNAME(100)
0005  REAL*8      ALBEL,ANAME,BNAME
0006  COMMON      A(100,100), XMEAN(100), STDEV(100), IVPT(100)
0007  COMMON      B(100), C(100), X(100), XMAX(100)
0008  COMMON      XMIN(100), IQ(50,50), KP(50,50), COL(11), PINT(11)
0009  COMMON      QINT(11), RES(5000)
C
0010  REAL*8      CODE/' '/
0011  LOGICAL      PVAK/.TRUE./,SDAM/.TRUE./,COVP/.TRUE./,CORP/.TRUE./
0012  LOGICAL      RESID/.TRUE./, LSTCRD
0013  INTEGER      FMTR(40)

```

A-3

0014	C	ZERUI = .FALSE.	0590
0015		SUMTAB = .TRUE.	
0016		ITP1 = 7	
0017		ITP2 = 8	
0018		NAIT = 5	
0019		NMAX = 100	
0020		IPDIM= NMAX	
	C		
	C	SETUP DISK	
	C		
0021		DEFINE FILE 7(6,200,U,IRR1)	
0022		DEFINE FILE 8(400,100,U,IRP2)	
0023		CALL WRTIME(.FALSE...TRUE...FALSE...FALSE.,*RUNTM ',TIME)	
	C		0640
	C	READ PROBLEM CARD	0650
	C		0660
0024		20 CALL WRTIME(.FALSE...FALSE...TRUE...TRUE.,*RUNTM ',TIME)	
0025		NAMLIST /PKOBLM/ CODE,N,NOV,NAIT,PVAR,SDAM,COVP,	
		1 CORP,ZERUI,FMTR,ALBEL	
0026		READ (5,PROBLM,END=400)	
	C		0700
	C	CHECK PROBLEM CARD FOR VALID PARAMETERS	0710
	C		0720
0027		IP = NOV	
0028		WRITE (6,2090)	
0029		2090 FORMAT('1')	
0030		CALL WRTIME(.FALSE...FALSE...FALSE...TRUE.,DUM,DUM)	
0031		WRITE (6,3000)CODE,N,IP	
0032		3000 FORMAT(' BMD02R - STEPWISE REGRESSION - VERSION OF FEBRUARY, 1967	
		1'2X40HHEALTH SCIENCES COMPUTING FACILITY, UCLA//2X12HPROBLEM CODE	0760
		215X8/2X15HNUMBER OF CASES16X14/' TOTAL NUMBER OF VARIABLES'8X12)	
0033		IF (IP.LT.2.OR.IP.GT.NMAX) GO TO 430	
	C		
0034		CALL WRTIME(.FALSE...TRUE...FALSE...FALSE.,*GET VAR ',TIME1)	
0035		IF (PVAR) WRITE (6,3010) (ALBEL(I),I=1,IP)	
0036		3010 FORMAT('0 INPUT VARIABLES'//2X'CASE'4X10A12/(10X10A12))	
	C		1240
	C	INITIALIZE ACCUMULATORS AND MATRIX A	1250
	C		1260
0037		XN=N	1270
0038		DO 90 I=1,IP	1280
0039		XMEAN(I)=0.0	1290
0040		DO 90 J=1,IP	1300
0041		90 A(I,J)=0.0	1310
	C		1320
	C	READ THE INPUT MATRIX X ONE ROW AT A TIME AND CONSTRUCT A	1330
	C		1340

FORTRAN IV G LEVEL 0, MOD 0		MAIN	DATE = 67216	17/10/30	PAGE 0003
0042		FIND (ITP2*1)			
0043		XK = 0.		1360	
0044		XM = XN		1370	
0045		IF (.NOT.ZEROI) XM = XM - 1.		1380	
0046		TIMEA = 0.			
0047		TIMEB = 0.			
0048		DO 170 K=1,N		1400	
0049		NINCS=K		1410	
0050		CALL WRTIME(.TRUE...TRUE...FALSE...FALSE..DUM,TIMEA)			
0051		READ (NAIT,FMTR,END=400) (X(L),L=1,NOV)			
0052		IF (PVAR) WRITE (6,3020) K,(X(L),L=1,IP)			
0053	3020	FORMAT(1X15,10G12.5/(6X10G12.5))			
0054		CALL WRTIME(.TRUE...FALSE...FALSE...FALSE..DUM,TIMEA)			
0055	C	IF (.NOT.ZEROI) GO TO 110		1440	
	C			1450	
	C	ZERO INTERCEPT		1460	
	C			1470	
0056		DO 100 I=1,IP		1480	
0057		XMEAN(I)=XMEAN(I)+X(I)		1490	
0058		DO 100 J=1,IP		1500	
0059	100	A(I,J)=A(I,J)+X(I)*X(J)		1510	
0060		GO TO 140		1520	
	C			1530	
	C	NO ZERO INTERCEPT		1540	
	C			1550	
0061		110 XK = XK + 1.		1560	
0062		DO 120 I=1,IP		1570	
0063		XMEAN(I)=XMEAN(I)+X(I)		1580	
0064		IF (K.EQ.1) GO TO 140			
0065		DO 130 I=1,IP		1590	
0066		DO 130 J=1,IP		1600	
0067		130 A(I,J)=A(I,J)+(X(I)*(XK*X(J)-XMEAN(J)) +		1610	
		1 XMEAN(I)*((XMEAN(J)/XK)-X(J)))/(XK-1.0)		1620	
	C			1630	
	C	WRITE THE X MATRIX ON UNIT ITP2			
	C			1650	
0068		140 CONTINUE			
0069		CALL WRTIME(.TRUE...TRUE...FALSE...FALSE..DUM,TIMEB)			
0070		WRITE (ITP2*K) (X(I),I=1,IP)			
0071		FIND (ITP2*K+1)			
0072		CALL WRTIME(.TRUE...FALSE...FALSE...FALSE..DUM,TIMEB)			
	C			1720	
	C	END OF DATA ACQUISITION LOOP		1730	
	C			1740	
0073		170 CONTINUE		1750	
	C			1800	
	C	REPLACE XMEAN WITH MEAN VECTOR, A WITH COVARIANCE MATRIX,AND		1810	

	C	COMPUTE STANDARD DEVIATIONS	1820
	C		1830
0074		DO 180 I=1,IP	1840
0075		XMEAN(I)=XMEAN(I)/XN	1850
0076		DO 180 J=I,IP	1860
0077		A(I,J)=A(I,J)/XM	1870
0078	180	A(J,I)=A(I,J)	1880
0079		DO 190 I=1,IP	1890
0080	190	STDEV(I)=SQRT(A(I,I))	1900
	C		1910
	C	WRITE OUT MEANS AND STANDARD DEVIATIONS IF REQUESTED	1920
	C		1930
0081		IF (.NOT.SDAM) GO TO 200	1940
0082		WRITE (6,3050)	1950
0083	3050	FORMAT(///// 4X,8HVARIALE,8X,4HMEAN,7X,18HSTANDARD DEVIATION)	1960
0084		WRITE (6,3060) (ALBEL(I),I,XMEAN(I),STDEV(I),I=1,IP)	1970
0085	3060	FORMAT(3X,A6,I3,2X,G14.6,4X,G14.6)	1980
0086		CALL WRTIME(.FALSE...FALSE...TRUE...TRUE...GET VAR ',TIME1)	
0087		CALL WRTIME(.FALSE...FALSE...TRUE...TRUE...WRITE A ',TIMEA)	
0088		CALL WRTIME(.FALSE...FALSE...TRUE...TRUE...WRITE B ',TIMEB)	
	C		1990
	C	PRINT COVARIANCE MATRIX IF REQUESTED	2000
	C		2010
0089	200	IF (.NOT.COVF) GO TO 210	2020
0090		WRITE (6,3070)	2030
0091	3070	FORMAT(19H1 COVARIANCE MATRIX)	2040
0092		CALL WRTIME(.FALSE...FALSE...FALSE...TRUE...DUM,DUM)	
0093		CALL MOUT (6,1,A,'A ', '(1X10G13.6)',IP,IPDIM,IP,IPDIM,1,0)	2050
	C		2060
	C	CONVERT A TO CORRELATION MATRIX	2070
	C		2080
0094	210	DO 220 I=1,IP	2090
0095		DO 220 J=I,IP	2100
0096		A(I,J)= A(I,J)/(STDEV(I)*STDEV(J))	2110
0097	220	A(J,I)=A(I,J)	2120
	C		2130
	C	PRINT CORRELATION MATRIX IF REQUESTED	2140
	C		2150
0098		IF (.NOT.CORF) GO TO 230	2160
0099		WRITE (6,3080)	2170
0100	3080	FORMAT(20H1 CORRELATION MATRIX)	2180
0101		CALL WRTIME(.FALSE...FALSE...FALSE...TRUE...DUM,DUM)	
0102		CALL MOUT (6,1,A,'A ', '(1X10G13.5)',IP,IPDIM,IP,IPDIM,1,0)	2190
0103	230	IF (.NOT.ZERO1) XN = XN-1.	2200
	C		2210
	C		2220
	C	READ SUBPROBLEM CARD AND LOOP ON RESULT	2230
	C		2240

0104	C	LSTCRD = .FALSE.	2250
0105		M = 0	
0106	235	M = M+1	
0107		IF (M.GT. NOV) GO TO 20	
	C		2270
	C	RESTORE THE CORRELATION MATRIX	2280
	C		2290
0108		DO 240 I=1,IP	2300
0109		A(I,I)=1.0	2310
0110		C(I) = 0.0	
0111		K=I+1	2320
0112		DO 240 J=K,IP	2330
0113	240	A(I,J)=A(J,I)	2340
	C		2350
	C	READ SUB PROBLEM CARD	2360
	C		2370
	C		
	C	SET VALUES FOR SUB PROBLEM	
	C		
0114		KDEP=M	
0115		MAXSTP=6	
0116		FINC=.5	
0117		FOUT=.3	
0118		TOL=0.	
0119		NVIP=0	
0120		SUMTAB=.TRUE.	
0121		RESID=.FALSE.	
0122		LSTCRD=.FALSE.	
	C		2400
	C	INSERT DEFAULT VALUES	2410
	C		2420
0123		IF (FINC.LE.0.) FINC = 0.01	2430
0124		IF (FOUT.LE.0.) FOUT = 0.005	2440
0125		IF (TOL.LE.0.) TOL = 0.001	2450
0126		IF (MAXSTP.LE.0) MAXSTP = IP+IP	2460
	C		2470
	C	WRITE THE CONTROL PARAMETERS	2480
	C		2490
0127		WRITE (6,2090)	
0128		CALL WRTIME(.FALSE.,.FALSE.,.FALSE.,.TRUE.,DUM,DUM)	
0129		WRITE (6,3090)M,KDEP,MAXSTP,FINC,FOUT,TOL	2500
0130	3090	FORMAT(3X 10H SUB-PROBLEM,15/3X,18H DEPENDENT VARIABLE,11X,12/3X,	
		123H MAXIMUM NUMBER OF STEPS,6X,12/3X,21H LEVEL FOR INCLUSION,4X,	2520
		2F8.6/3X,20H LEVEL FOR DELETION,5X,F8.6/3X,15H TOLERANCE LEVEL,10X,	2530
		3F8.6)	2540
0131		CALL WRTIME(.FALSE.,.TRUE.,.FALSE.,.FALSE.,'REGRES ',TIME2)	
	C		2550

	C SET THE CONTROL DELETE PARAMETER.	
	C C = 1. DEPENDENT OR DELETE	2570
	C C = 2. FREE	2580
	C C = 3. LOW-LEVEL FORCED VARIABLE	2590
	C ...	2600
	C C = 4. HIGH-LEVEL FORCED VARIABLE.	2610
	C	2620
0132	DO 260 I=1,IP	2690
0133	260 IF (C(I).LE.0.) C(I) = 2.0	2700
0134	C(KDEP)=1.0	2710
	C	2720
	C PERFORM THE REGRESSION	2730
	C	2740
0135	FIND (ITP1'I)	
0136	CALL REGRES	2750
	C	
0137	CALL WRTIME(.FALSE...FALSE...TRUE...FALSE., 'REGRES ', TIME2)	
	C	2760
	C TERMINATE THIS SUBPROBLEM	2770
	C	2780
0138	IF (.NOT.SUMTAB) GO TO 290	2830
0139	FIND (ITP1'I)	
	C	2840
	C WRITE SUMMARY TABLE IF PRESENT.	2850
	C	2860
0140	IF (LKL.GT.0) GO TO 270	2870
0141	WRITE (6,3120)	2880
0142	3120 FORMAT(///49HOSUMMARY TABLE OMITTED DUE TO LACK OF INFORMATION)	2890
0143	GO TO 290	2900
	C	2910
0144	270 WRITE (6,2090)	
0145	CALL WRTIME(.FALSE...TRUE...FALSE...TRUE., 'SUMTAB ', TIME3)	
0146	WRITE (6,3130)	
0147	3130 FORMAT(' SUMMARY TABLE' //	
	1 5X'STEP'16X'VARIABLE'16X'MULTIPLE'16X'INCREASE'11X'F VALUE TO'	
	2 5X'NUMBER OF INDEPENDENT' / 4X'NUMBER'8X'ENTERED'6X'REMOVED'	
	3 9X'R'10X'RSQ'13X'IN RSQ'10X'ENTER OR REMOVE'	
	4 4X'VARIABLES INCLUDED' //	
	C	
0148	RISQ = 0.0	
0149	DO 280 I=1,LKL	2980
0150	READ (ITP1'I) LMN,KAY,FLAG,XMULTR,FKAY,NVI	
0151	RSQ = XMULTR*XMULTR	
0152	RSQI = RSQ-RISQ	
0153	RISQ = RSQ	
0154	IF (FLAG.GT.0.)	3030
	1 WRITE (6,3140)LMN,ALBEL(KAY),KAY,XMULTR,RSQ,RSQI,FKAY, NVI	3040
0155	3140 FORMAT(6X12,7XAB,1X13,14XF9.4,F13.4,6XF11.4,4XG13.6,18XI3)	

FORTRAN IV G LEVEL 0, MOD 0			MAIN	DATE = 67216	17/10/30	PAGE 0007
0156		IF (FLAG.LT.0.)				3060
0157		1 WRITE (6,3150)LMN,ALBEL(KAY),KAY,XMULTR,RSQ,RSQI,FKAY,NVI				3070
0158		3150 FORMAT(6X12,20XA8,1X13,F9.4,F13.4,6XF11.4,4XG13.6,18X13)				3090
	C	280 CONTINUE				
0159		FIND (ITP2*1)				
0160		CALL WRTIME(.FALSE...FALSE...TRUE...TRUE., 'SUMTAB ', TIME3)				
	C					3110
	C	PRINT AND/OR PLOT THE RESIDUALS IF REQUESTED				3120
	C					3130
0161		290 IF (NVIP.GT.0) GO TO 300				3140
0162		IF (RESID) GO TO 320				3150
0163		GO TO 390				3160
	C					3220
	C	CHECK LEGALITIES				3230
	C					3240
0164		300 IF (NVIP.GT.IP) GO TO 470				3250
0165		DO 310 K=1,NVIP				3260
0166		IF (IVPT(K).GT.IP) GO TO 490				
0167		310 CONTINUE				
0168		320 DO 330 J=1,NVIP				3280
0169		XMIN(J)=+999999.9				3290
0170		330 XMAX(J)=-999999.9				3300
0171		RMIN=+999999.9				3310
0172		KMAX=-999999.9				3320
0173		CALL WRTIME(.FALSE...TRUE...FALSE...FALSE., 'RESID ', TIME4)				
	C					3330
	C	COMPUTE RESIDUALS				3340
	C					3350
0174		DO 380 I=1,N				3390
	C					3400
	C	READ THE RAW DATA FROM UNIT ITP2				
	C					3420
0175		READ (ITP2*1) (X(J),J=1,IP)				
	C					3510
	C	COMPUTE THE RESIDUALS				3520
	C					3530
0176		SUMB=0.0				3540
0177		NVI=0				3550
0178		DO 360 J=1,IP				3560
0179		IF (C(J).GT.0) GO TO 360				3570
0180		NVI=NVI+1				3580
0181		SUMB=SUMB+B(NVI)*X(J)				3590
0182		360 CONTINUE				3600
	C					3610
0183		DO 370 L=1,NVIP				3620
0184		MM=IVPT(L)				3630
0185		XMIN(L) = AMIN1(XMIN(L),X(MM))				3640

```

0186      370 XMAX(C) = AMAX1(XMAX(L),X(MM))          3650
0187      RES(I)=X(KUEP)-ALPHA-SUMB                    3660
0188      RMIN = AMIN1(RMIN,RES(I))                    3670
0189      RMAX = AMAX1(RMAX,RES(I))                    3680
0190      380 CONTINUE                                3690
C                                                3700
0191      IF (.NOT.RESID) GO TO 390                    3720
C                                                3730
C PRINT THE RESIDUALS                                3740
C                                                3750
0192      WRITE (6,3160)                               3760
0193      3160 FORMAT('1 LIST OF RESIDUALS' ///
1 4X4('CASE'3X'RESIDUAL'11X),'CASE'3X'RESIDUAL' )
0194      NS = (N+4)/5                                  3780
0195      DO 385 I=1,NS
0196      385 WRITE (6,3170) (J,RES(J),J=I,N,NS)
0197      3170 FORMAT(1X5(1X16,1XG15.6,2X))
C                                                3800
C PLOT THE RESIDUALS                                3810
C                                                3820
0198      390 IF (NVIP.GT.0) CALL PLTRES                3830
0199      CALL WRTIME(.FALSE...FALSE...TRUE...TRUE...RESID ',TIME4) 3840
C                                                3850
C GO GET NEXT CARD                                  3860
C                                                3870
0200      IF (.NOT.LSTCRD) GO TO 235
0201      GO TO 20
C                                                3900
C TERMINATION PROCEDURE                            3910
C                                                3920
0202      400 WRITE (6,3180)                            3930
0203      3180 FORMAT(///24H FINISH CARD ENCOUNTERED) 3940
0204      410 WRITE (6,3190)                            3950
0205      3190 FORMAT(10H PROGRAM TERMINATED)          3960
0206      STOP                                          3990
C                                                4000
C ERROR MESSAGES                                    4010
C                                                4020
0207      430 WRITE (6,3200)                            4030
0208      3200 FORMAT(50HNUMBER OF VARIABLES, P OR PQ, OUTSIDE OF LIMITS.) 4040
0209      GO TO 410
0210      450 WRITE (6,3220)                            4100
0211      3220 FORMAT(37H CARD INCORRECTLY PUNCHED OR MISSING.) 4110
0212      GO TO 410
0213      470 WRITE (6,3240)                            4120
0214      3240 FORMAT('USUB=PROBLEM')                  4160
0215      GO TO 450
0216      490 WRITE (6,3260)                            4170

```

```

0217      3260 FORMAT('0INDEX=PLOT')                  4230
0218      GO TO 450                                    4240
0219      END                                          4250

```

BIBLIOGRAPHY

- Albee, A.L.(1965): Phase equilibria in three assemblages of kyanite-zone pelitic schists, Lincoln Mountain Quadrangle, Central Vermont, J. of Pet., 6, pp. 246-301
- , Chodos, A.A. and Hollister, L.S.(1966): Equilibration volumes for different species in three assemblages of kyanite-zone schists, Lincoln Mountain, Vermont, (Abstract) A.G.U. Transactions, 47, pp. 213
- Atherton, M.P.(1965): The chemical significance of isograds, in Controls of Metamorphism, W.S. Pitcher and G.W. Flinn, eds., John Wiley & Sons, Inc., New York, 368 p.
- Billings, G.K.(1965): Light scattering in trace element analysis by Atomic Absorption, A.A. Newsletter, Perkin-Elmer Corp., 4, pp.357-363
- (1965): The analysis of geological materials by Atomic Absorption Spectrometry: II Accuracy Tests, A.A. Newsletter, Perkin-Elmer Corp., 4, pp.312-316
- , and Adams, J.A.S., (1964); The analysis of geological materials by atomic absorption spectrometry, A.A. Newsletter, Perkin-Elmer Corp., 23, pp.1-7
- Bragg, W.L. (1937): The Atomic Structure of Minerals; Ithaca, New York
- Brech, F. (1962): International Colloquium for Spectroscopy, College Park, Md.
- (1963): Pittsburgh Conference on Analytical Chemistry and Applied Spectroscopy.
- (1965): Current status and the potentials of laser excited spectrochemical analysis, 4th Meeting of Spectroscopy, Perth, Australia
- (1967): A review of achievements in laser-excited spectrochemistry, XIII Colloquium Spectroscopium Internationale, Ottawa, Canada
- Brownlow, A.H. (1961): Variation in composition of biotite and actinolite from monomineralic contact bands near Westfield, Massachusetts, Am. J. Sc., 259, pp. 353-370
- Buddington, A.F. (1965): The origin of three garnet isograds in Adirondack gneisses, Min. Mag., 34, pp. 71-81
- Carr, M.H. and Turekian, K. (1961): The geochemistry of cobalt, Geochim. et. Cosmochim. Acta., 26, pp. 1-29

- Chinner, G.A. (1960): Pelitic gneisses with varying ferrous/ferric ratios from Glen Clova, Angus, Scotland, *J. Petrology*, 1, 178
- Clark, P.J. and Evans, F.C. (1954): Distance to nearest neighbour as a measure of spatial relationships in populations, *Ecology*, 35, pp. 445-453
- Curtis, C.D. (1964): Applications of the crystal-field theory to the inclusion of trace transition elements in minerals during magmatic differentiation, *Geochim. et Cosmochim. Acta*, 28, p.389.
- David, D.J. (1958): The determination of zinc and other elements in plants by Atomic Absorption Spectroscopy, *Analyst*, 83, p.655.
- (1962): The determination of Sr in biological materials and exchangeable Sr in soils by Atomic Absorption Spectrophotometry, *Analyst*, 87, p.576.
- Dennen, W.H. and Fowler, W.C., (1955): Spectrographic analysis by use of mutual standard method, *Bull. G.S.A.*, 66, pp. 655-662.
- de Waard, D. (1966): The biotite-cordierite-almandite subfacies of the hornblende-granulite facies, *Canadian Mineralogist*, 8, pp.481-492.
- (1965): The occurrence of garnet in the granulite-facies terrane of the Adirondack highlands, *Jour. of Pet.*, 6, pp. 165-191.
- (1965): A proposed subdivision of the granulite facies, *Am. J. of Science*, 263, pp. 455-461.
- Elwell, W.T. and Gidley, J.A.F., (1961): Atomic Absorption Spectrophotometry, Pergamon Press.
- Eskola, P. (1915): On the relations between the chemical and mineralogical composition in the metamorphic rocks of the Orijarvi region, *Bull. Comm. Geol. Finlande*, 44, pp.109-143.
- Fairbairn, H.W. and others (1951): A Cooperative Investigation of Precision and Accuracy in Chemical, Spectrochemical and Modal Analysis of Silicate Rocks, U.S. Geological Survey Bulletin 980.
- Fyfe, W.S., Turner, F.J. and Verhoogen, J. (1958): Metamorphic Reactions and Metamorphic Facies, *Geol. Soc. of America Mem.* 73.

- Galwey, A.K., and Jones, K.A. (1963): An attempt to determine the mechanism of a natural mineral-forming reaction from examination of the products, J.Chem. Soc., 5681.
- Goldman, H.M., Ruben, M.P. and Sherman, D. (1964): The application of laser spectroscopy for the qualitative and quantitative analyses of inorganic components of calcified tissues, Oral Surgery, Oral Medicine and Oral Pathology, 17, pp.102-103.
- Hagner, A.F., Leung, S.S. and Dennison, J.M. (1965): Optical and chemical variations in minerals from a single rock specimen, Am. Miner., 50, pp.341-355.
- Harker, A. (1939): Metamorphism, second edition, Methuen & Co., London.
- (1893): On the migration of material during the metamorphism of rock masses, Jour. of Geology, 1, pp.574-578.
- Hewitt, D.F. (1965): The Madoc-Ganonoque Area, Ontario Dept. of Mines Circ. No. 12.
- Hollister, L.S. (1961): Garnet zoning: an interpretation based on the Rayleigh fractionation model, Science, December, pp.1647-1651.
- Jacobs, P.M. and Tomkins, F.C. (1955): Classification and theory of solid reactions, in Garner, W.E., Chemistry of the Solid State, Butterworth, London.
- Jones, K.A. and Galwey, A.K. (1964): A study of possible factors concerning garnet formation in rocks from Ardara, Co. Donegal, Ireland, Geol. Mag., 101, p.76.
- Kolthoff, I.M. and Sandell, E.B. (1952): Textbook of Quantitative Inorganic Analysis, MacMillan Company, New York, 759 p.
- Korzhinski, D.S. (1959): Physicochemical Basis of the Analysis of the Paragenesis of Minerals, Consultants Bureau, New York.
- Krank, S.H. (1959): Chemical petrology of metamorphic iron formations and associated rocks in the Mount Reed area in Northern Quebec, Ph.D. Thesis, Mass. Inst. of Tech., 145 p.
- (1961): A study of phase equilibria in a metamorphic iron formation, Journ. of Pet., 2, pp.137-184.

- Kretz, Ralph (1959): Chemical study of garnet, biotite and hornblende from gneisses of southwestern Quebec, with emphasis on the distribution of elements in coexisting minerals, *Journ. of Geol.*, vol. 67, pp.371-402.
- (1960): The distribution of certain elements among coexisting calcic pyroxenes, calcic amphiboles and biotites in skarns, *Geochim. et Cosmochim. Acta*, vol. 20, pp. 161-191.
- (1961): Some application of thermodynamics to coexisting minerals of variable composition, *Journ. of Geol.*, vol. 69, pp.361-387.
- (1966): Grain size distribution for certain metamorphic minerals in relation to nucleation and growth, *Journ. of Geol.*, vol. 74, pp. 147-174.
- Krogh, T.E. (1964): Strontium isotope variation and whole-rock isochron studies in the Grenville Province of Ontario, Ph.D. thesis, Mass. Inst. of Tech.
- (1966): Whole-rock Rb-Sr studies in the northwest Grenville area of Ontario, *A.G.U. Transactions*, 47, p.208.
- Lengyel, B.A. (1962): *Lasers*, John Wiley and Sons, New York, 125 pages.
- Lindgren, W. (1925): Metasomatism, *Bull. G.S.A.*, 36, p.247.
- Meddings, B. and Kaiser, H. (1967): Precision of routine Atomic Absorption Analysis, *Atomic Absorption Newsletter*, Perkin-Elmer Corp., 6, pp.28-32.
- Mehl, R.F., and Dube, A. (1951): The eutectoid reaction, in Smoluchowski, R., ed., *Phase Transitions in Solids*, John Wiley and Sons, New York.
- McIntire, W.L. (1958): A thermodynamic treatment of trace element distribution in geologic systems with application to geologic thermometry, Ph.D. thesis, Mass. Inst. of Tech.
- (1963): Trace element partition coefficients - a review of theory and applications to geology, *Geochim. et Cosmochim. Acta*, vol. 27, pp. 1209-1263.
- Miyashiro, A. (1958): Regional metamorphism of the Gosaiasyo-Takanuki District in the Central Abukuma Plateau, *J. Fac. Sci., Univ. Tokyo, Sec.II*, 2, p.219.
- Moore, J.M. (1960): Phase relations in the contact aureole of Onawa pluton, Maine, Ph.D. thesis, Mass. Inst. of Tech., 187 pages.

- Moxham, R.L. (1960): Minor element distribution in some metamorphic pyroxenes, *Canadian Mineralogist*, 6, pp.522-545.
- (1965): Distribution of minor elements in coexisting hornblendes and biotites, *Canadian Mineralogist*, 8, pp.204-240.
- Mueller, R.E. (1961): Analysis of relations among Mg, Fe and Mn in certain metamorphic minerals, *Geochim. et Cosmochim. Acta*, vol. 25, pp. 267-296.
- (1962): Energetics of certain silicate solid solutions, *Geochim. et Cosmochim. Acta*, vol. 26, pp. 581-598.
- O'hara, M.J. (1963): Distribution of iron between coexisting olivines and calcium-poor pyroxenes in peridotites, gabbros and other magnesian environments, *Am. Jour. of Science*, 261, p.32.
- Nicholls, G.D. (1958): Sedimentary geochemistry, *Petroleum*, Sept., p.416.
- Parras, K. (1958): On the charnockites in the light of a highly metamorphic rock complex in southwestern Finland, *Bull. Comm. Geol. Finlande*, 181, pp.1-137.
- Perrin, R. and Roubault, M. (1937): Les réactions a l'état solide et la géologie, *Bull. Serv. Carte géol. Algerie*, ser. 5, *Petrographie*, No. 1.
- (1939): Le granite et les réactions a l'état solide, *Bull. Serv. Carte géol. Algerie*, ser. 5, *Petrographie*, No. 4.
- Perrin, R. (1952): Long range solid diffusions in geology, answer to objections, *Int. Geol. Cong., Algiers*, pp.43-56.
- Phinney, W.C. (1959): Phase equilibria in the metamorphic rocks of St. Paul Island and Cape North, Nova Scotia, Ph.D. thesis, Mass. Inst. of Tech.
- (1963): Phase equilibria in the rocks of St. Paul Island and Cape North, Nova Scotia, *Journ. of Pet.*, vol. 4, pp.90-130.
- Ramberg, Hans (1952): *The Origin of Metamorphic and Metasomatic Rocks*, Univ. of Chicago Press, Chicago.
- , and Devore, G. (1951): The distribution of Fe^{++} and Mg^{++} in coexisting olivines and pyroxenes, *Journ. of Geol.*, vol. 59, pp.193-210.

- Rast, Nicholas (1965): Nucleation and growth of metamorphic minerals, in Controls of Metamorphism, Pitcher, W.S. and Flinn, G.W., eds., John Wiley and Sons, Inc., New York, 368 p.
- Reichen, L.E. and Fahey, J.J. (1962): An Improved Method for the Determination of FeO in Rocks and Minerals Including Garnet, U.S. Geological Survey Bulletin 1144-B.
- Reynolds, D.L. (1946): The sequence of geochemical changes leading to granitization, Quart. Journ. Geol. Soc. London, 52, pp.389-446.
- Roubault, M., de la Roche, H. and Govindaraju, K. (1966): Rapport sur quatre roches étalon géochimiques; Granites GR, GA, GH et Basalt BR, Sciences de la Terre, 11, pp.105-121.
- Silver, L.T. (1966): Geochronologic investigations of the Adirondack Anorthosite Complex, Symposium on the Origin of Anorthosite, October, 1966, Plattsburgh, N.Y.
- Shaw, D.M., and Bankier, J.D. (1954): Statistical methods applied to geochemistry, Geochim. et Cosmochim. Acta, vol. 5, pp.111-123.
- Slavin, Walter (1966): Atomic Absorption Spectroscopy - A Critical Review, Applied Spectroscopy, 20, pp.281-288.
- Smith, F.G. (1953): Historical Development of Inclusion Thermometry, University of Toronto Press, Toronto, 149 p.
- (1963): Physical Geochemistry, Addison-Wesley Publishing Co., Inc., Reading, Mass., 624 p.
- Smoluchowski, R. (1951): Nucleation theory, in Phase Transformations in Solids, ed. Smoluchowski, R., New York, p.149.
- Stevens, R.E., et al (1960): Second Report on a Cooperative Investigation of Two Silicate Rocks, U.S. Geological Survey Bulletin 1113.
- Stone, F.S. (1961): The kinetics and mechanisms of the reactions of solids, in DeBoer, J.A., Reactivity of Solids, Elsevier, Amsterdam.
- Sturt, B.A. and Harris, A.L. (1961): The metamorphic history of the Loch Tummel area, Central Perthshire, Scotland, Liverpool-Manchester Geological Journal, 2, p.689.
- Subramaniam, A.P. (1959): Charnokites of the type area near Madras - a reinterpretation, Amer. J. of Sci., 257, pp.321-353.

- Thomas, W.K.L. (1963): Supplement No.1, Standard Geochemical Sample T-1, Tanganyika Geol. Survey.
- Thompson, J.B. (1955): The thermodynamic basis for the mineral facies concept, *Am. Journ. of Sci.*, vol. 253, pp.65-103.
- (1959): Local equilibrium in metasomatic processes, in *Researches in Geochemistry*, P.H. Ableson, ed., p.247.
- Trent, D. and Slavin, W. (1964): Determination of the major metals in granitic and diabasic rocks by Atomic Absorption Spectrophotometry, *Atomic Absorption Newsletter*, Perkin-Elmer Corp, No. 19, pp.1-6.
- Wager, L.R. and Brown, G.M. (1960): Collection and preparation of material for analysis, in *Methods in Geochemistry*, A.A. Smales and L.R. Wager, eds., Interscience Publishers Inc., New York.
- Webber, G.R. (1965): Second report of analytical data for CAAS syenite and sulphide standards, *Geochim. et Cosmochim. Acta*, 29, pp.229-248.
- Winkler, H.G.F. (1965): *Petrogenesis of Metamorphic Rocks*, Springer-Verlag, New York, 220 p.
- Yoder, H.S. (1955): Role of water in metamorphism, *Spec. Pap. Geol. Soc. America*, 62, p.505.
- Zen, E-an (1963): Components, phases and criteria of chemical equilibrium in rocks, *Am. J. of Sci.*, 261, p.929.
- Wynne-Edwards, H.R. and Hay, P.W. (1963): Coexisting cordierite and garnet in regionally metamorphosed rocks from the Westport Area, Ontario, *Canadian Mineralogist*, 1, pp.453-478.
- Wynne-Edwards, H.R. (1962): Ganonoque map-area, Geol Surv. Canada, Map 27-1962.
- (1959): Westport map-area, Geol. Surv. Canada, Map 28-1959.
- Jensen, M.L. (1965): The rational and geological aspects of solid diffusion, *Can. Mineral.*, vol. 8, pt.3, pp.271-290.
- Rayleigh, L. (1902): *Phil. Mag.* (6th series), 4, 521.

BIOGRAPHICAL SKETCH

The author was born in Ottawa, Ontario on July 30, 1941. He was educated in the public school system of Ottawa and graduated from Lisgar Collegiate Institute in 1960 with an Ontario Senior Matriculation Certificate.

Undergraduate training leading to the degree of B.Sc. (Honors) was received at St. Francis Xavier University in Antigonish, Nova Scotia between September, 1961 and May, 1964. At St. Francis Xavier, the author was placed on the Deans List for Science in 1961, 1962, 1963 and 1964. He was awarded St. Francis Xavier University Fellowships in 1963 and 1964. Upon graduation, the author was the recipient of the Mining Society of Nova Scotia Prize for 1964.

The author has been a graduate student at M.I.T. since September, 1964 at which time he was awarded a Canadian M.I.T. Alumni Trust Fund Scholarship. During his years at M.I.T., he spent one semester as a teaching assistant in the Department of Geology and Geophysics. He was a research assistant in the Cabot Spectrographic Laboratory in the same department during the rest of his tenure at M.I.T.

The author spent one summer each with the Consolidated Mining and Smelting Company of Canada Ltd. and Gunnar Mines Ltd. doing heavy metal exploration in Nova Scotia. He was employed two summers by the Geological Survey of Canada: one spent on a gold exploration research team in northern Ontario and the other mapping in southern Newfoundland.

The author was nominated to associate membership in the Society of Sigma Xi in 1966. He is also a member of the Geological Society of America, the Geological Association of Canada and the Mineralogical Society of America.

He was married to Geraldine MacIntyre of Sydney, Nova Scotia in September, 1964 and at present has one son, Patrick William, born May 1966.

Upon graduation, the author will join the faculty of the Department of Geology at the University of Kentucky.